

**UNIVERSITY OF KWAZULU – NATAL**

**AN INVESTIGATION INTO THE EFFECTS OF  
SUTHERLANDIA FRUTESCENS, L-CANAVANINE AND  
AFLATOXIN B<sub>1</sub> IN THE HEPG<sub>2</sub> HUMAN  
HEPATOCAARCINOMA CELL LINE**

**2008**

**EVASHIN PILLAY**

**AN INVESTIGATION INTO THE EFFECTS OF  
SUTHERLANDIA FRUTESCENS, L-CANAVANINE AND  
AFLATOXIN B<sub>1</sub> IN THE HEPG<sub>2</sub> HUMAN  
HEPATOCELL CARCINOMA CELL LINE**

**By**

**Evashin Pillay**

**BMedSci (Hons), University of KwaZulu-Natal**

**Submitted in partial fulfilment of the requirements for the degree of Masters in Medical  
Science in the Discipline of Medical Biochemistry, Faculty of Health Sciences, Nelson R.  
Mandela School of Medicine, University of KwaZulu-Natal, Durban.**

**2008**

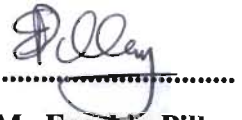
## ABSTRACT

Aflatoxin B<sub>1</sub> (AFB<sub>1</sub>), a potent hepatotoxic and hepatocarcinogenic mycotoxin synthesised by toxigenic fungi (*Aspergillus flavus* and *Aspergillus parasiticus*), is a common contaminant of many cereal commodities consequently posing a major threat to human and animal health. *Sutherlandia frutescens* (SF), a traditional medicinal plant endemic to Southern Africa, is commonly used by many cultures as a tonic for various health-related conditions. Incidentally, the present study aimed at investigating the potential hepatoprotective capacity of SF and L-canavanine (L-can, a major constituent of SF) against AFB<sub>1</sub>-induced cytotoxicity in human HepG<sub>2</sub> cells and used a standard treatment procedure of 24 h. Cell viability was evaluated using the methyl thiazol tetrazolium (MTT) assay, which effectively demonstrated the ability of SF, when administered individually and in combination with AFB<sub>1</sub>, to be significantly cytotoxic to HepG<sub>2</sub> cells in a dose-dependant manner. Reactive oxygen species (ROS) and consequent peroxidative damage caused by AFB<sub>1</sub> are considered to be the main mechanisms leading to hepatotoxicity and was confirmed by the thiobarbituric acid reactive substances (TBARS) assay which revealed that AFB<sub>1</sub> mediated a significant increase in lipid peroxidation. Additionally, comet assay analysis demonstrated the most pronounced effect to be observed following administration of AFB<sub>1</sub>. In contrast, AFB<sub>1</sub>-mediated genotoxicity was significantly reduced by SF and L-can. Such amelioration can be attributed to the marked increases in glutathione (GSH) levels observed after the co-administration of SF and L-can with AFB<sub>1</sub>. Cytoprotection by SF and L-can against AFB<sub>1</sub>-induced toxicity was further substantiated by the significant increases in heat shock protein 70 expression. Moreover, when SF and L-can were co-administered along with AFB<sub>1</sub>, analysis by flow cytometry revealed that AFB<sub>1</sub>-induced increases in apoptosis and necrosis were reduced. The findings of this study propose that SF and L-can may be selectively effective in alleviating AFB<sub>1</sub>-induced cytotoxicity and lends pharmacological credibility to the suggested ethnomedical uses of SF. However, the exact mechanism of action and the extracts efficacy in humans requires further authentication.

## **PREFACE**

This study represents the original work by the author and has not been submitted in any form to another University. The use of work by others has been duly acknowledged in the text.

The research described in this study was conducted during March 2008 to December 2008 under the supervision of Professor A. A. Chuturgoon in the Discipline of Medical Biochemistry, Faculty of Health Sciences, Nelson R. Mandela School of Medicine, University of KwaZulu-Natal, Durban.

A handwritten signature in black ink, appearing to read 'E. Pillay', is written over a horizontal dotted line.

**Mr Evashin Pillay**

## ACKNOWLEDGEMENTS

Several people have assisted in various ways toward the completion of this project. I am grateful to those who offered encouragement or who contributed in effort and time.

- First and foremost, my parents and sister, Ugeshni Pillay, have always been supportive, encouraging and understanding. To them I am eternally grateful.
- To my supervisor, Professor Anil A. Chuturgoon, thank you for all your encouragement, guidance and technical expertise. Your constructive criticism during the preparation of this manuscript is greatly appreciated.
- My friend Alisa Phulukdaree has played a significant role in this project. Her priceless assistance during many aspects of this study was overwhelming and will always be appreciated.
- To Mr. Leshern Karamchand, Mr. Devan Moodley and Miss. Kristina Naidoo, thank you for the invaluable support, suggestions and advice.
- I am also grateful to Ms. Rene Myburg and Mrs. Narisha Needhi for their technical guidance and cooperation throughout the project.
- To the National Research Foundation and UKZN, I express my appreciation for the scholarships that provided financial assistance which enabled completion of the degree.
- Lastly, I would like to express my sincere gratitude to all academic staff and postgraduate students of the Mycotoxins Research Laboratory for their encouragement and support.

# TABLE OF CONTENTS

|  | <b>page</b> |
|--|-------------|
| <b>TITLE PAGE</b>  | <b>i</b>    |
| <b>ABSTRACT</b>  | <b>ii</b>   |
| <b>PREFACE</b>   | <b>iii</b>  |
| <b>ACKNOWLEDGEMENTS</b>                                  | <b>iv</b>   |
| <b>TABLE OF CONTENTS</b>                                 | <b>v</b>    |
| <b>LIST OF FIGURES</b>                                   | <b>xii</b>  |
| <b>LIST OF TABLES</b>                                    | <b>xiv</b>  |
| <b>LIST OF ABBREVIATIONS</b>                             | <b>xv</b>   |
| <br>   |             |
| <b>Chapter 1 INTRODUCTION</b>                            | <b>1</b>    |
| <b>1.1 Toxicology</b>                                    | <b>1</b>    |
| <b>1.2 Objectives</b>                                    | <b>3</b>    |
| <br>   |             |
| <b>Chapter 2 LITERATURE REVIEW</b>                       | <b>4</b>    |
| <b>2.1 Introduction</b>                                  | <b>4</b>    |
| 2.1.1 Mycotoxins   | <b>4</b>    |
| 2.1.2 Aflatoxins and aflatoxicosis                       | <b>4</b>    |
| <b>2.2 Cellular Metabolism</b>                           | <b>5</b>    |
| 2.2.1 Activation   | <b>5</b>    |
| 2.2.2 Detoxification                                     | <b>7</b>    |
| 2.2.3 Interaction with biomolecules                      | <b>8</b>    |
| 2.2.3.1 Nucleic acids                                    | <b>8</b>    |
| 2.2.3.1.1 Aflatoxin B <sub>1</sub> -DNA adduct formation | <b>8</b>    |
| 2.2.3.2 Proteins   | <b>10</b>   |
| 2.2.3.3 Effects on the mitochondrion                     | <b>11</b>   |

|             |  |           |
|-------------|--|-----------|
| <b>2.3</b>  | <b>Effects on Macromolecular Biosynthesis</b>                            | <b>12</b> |
| 2.3.1       | DNA  | 12        |
| 2.3.2       | RNA  | 13        |
| 2.3.3       | Protein  | 13        |
| <b>2.4.</b> | <b>Specific Effects</b>  | <b>14</b> |
| 2.4.1       | Oxidative damage   | 14        |
| 2.4.2       | Repair of Aflatoxin B <sub>1</sub> -induced DNA damage                   | 15        |
| <b>2.5</b>  | <b><i>Sutherlandia frutescens</i></b>                                    | <b>16</b> |
| 2.5.1       | Toxicity   | 16        |
| 2.5.2       | Chemistry  | 17        |
| 2.5.3       | Pharmacology   | 18        |
| 2.5.3.1     | Diabetes   | 18        |
| 2.5.3.2     | HIV  | 18        |
| 2.5.3.3     | Antioxidant properties   | 19        |
| 2.5.3.4     | Anticonvulsant properties  | 19        |
| 2.5.3.5     | Anti-inflammatory properties   | 19        |
| 2.5.3.6     | Stress   | 19        |
| 2.5.3.7     | Antimutagenic, antimetabolic and pro-apoptotic<br>properties             | 20        |
| <b>2.6</b>  | <b>L-canavanine</b>  | <b>22</b> |
| 2.6.1       | Natural sources and functions of L-canavanine                            | 22        |
| 2.6.2       | Physicochemical properties of L-canavanine                               | 22        |
| 2.6.3       | Mechanism of action of L-canavanine                                      | 23        |
| 2.6.3.1     | L-canavanine is loaded to arginyl-tRNA                                   | 24        |
| 2.6.3.2     | L-canavanine is incorporated into proteins in place<br>of L-arginine     | 24        |
| 2.6.3.3     | Incorporation of L-canavanine results in altered<br>protein conformation | 25        |
| 2.6.3.4     | Incorporation of L-canavanine alters protein function                    | 25        |
| 2.6.4       | Anticancer properties of L-canavanine                                    | 26        |
| 2.6.5       | Mechanisms of L-canaline toxicity  | 27        |

|                  |   |           |
|------------------|---|-----------|
| <b>2.7</b>       | <b>Apoptosis</b>  | <b>28</b> |
| 2.7.1            | Mechanisms of apoptosis   | 29        |
| 2.7.1.1          | Extrinsic cell death signalling                                   | 30        |
| 2.7.1.2          | Intrinsic cell death signalling                                   | 33        |
| 2.7.2            | Caspases  | 35        |
| 2.7.3            | The role of p53 in apoptosis                                      | 37        |
| 2.7.4            | The modulation of apoptosis by different heat shock gene products | 39        |
| 2.7.4.1          | Heat shock protein 70   | 41        |
| 2.7.4.2          | Heat shock protein 90   | 42        |
| <b>Chapter 3</b> | <b>CELL CULTURE AND CYTOTOXICITY</b>                              | <b>44</b> |
| <b>3.1</b>       | <b>Introduction</b>   | <b>44</b> |
| <b>3.2</b>       | <b>The cell and its environment</b>                               | <b>44</b> |
| 3.2.1            | Temperature and pH  | 44        |
| 3.2.2            | Gas phases  | 45        |
| 3.2.3            | Substrate   | 45        |
| 3.2.4            | Medium  | 45        |
| <b>3.3</b>       | <b>The HepG<sub>2</sub> cell line</b>                             | <b>46</b> |
| <b>3.4</b>       | <b>Cytotoxicity testing</b>                                       | <b>47</b> |
| <b>3.5</b>       | <b>Materials and Methods</b>                                      | <b>48</b> |
| 3.5.1            | Ethical approval  | 48        |
| 3.5.2            | Materials   | 48        |
| 3.5.3            | Methodology   | 48        |
| 3.5.3.1          | Cell culture environment  | 48        |
| 3.5.3.2          | Preparation of cell culture media and freezing medium             | 48        |
| 3.5.3.3          | Trypsinisation  | 49        |
| 3.5.3.4          | Cell counting by dye exclusion using a haemocytometer             | 49        |
| 3.5.3.5          | Preparation of the <i>Sutherlandia frutescens</i> aqueous extract | 51        |
| 3.5.3.6          | Preparation of stock solutions                                    | 51        |



|  |           |
|--|-----------|
| 3.5.3.7 Treatment, isolation and harvesting of HepG <sub>2</sub> cells                           | 52        |
| 3.5.3.8 The methyl thiazol tetrazolium bioassay on cultured<br>HepG <sub>2</sub> cells           | 52        |
| 3.5.3.9 Data analysis and statistics   | 53        |
| <b>3.6 Results and Discussion</b>  | <b>54</b> |
| <b>3.7 Conclusion</b>  | <b>58</b> |
| <br>   |           |
| <b>Chapter 4 CELLULAR REDOX STATE</b>  | <b>59</b> |
| <b>4.1 Introduction</b>  | <b>59</b> |
| <b>4.2 Reactive oxygen species and oxidative stress</b>  | <b>59</b> |
| <b>4.3 The role of glutathione</b>   | <b>61</b> |
| <b>4.4 The GSH-Glo™ Glutathione assay</b>  | <b>62</b> |
| 4.4.1 Principle and applications   | 62        |
| <b>4.5 The thiobarbituric acid reactive substances assay</b>                                     | <b>63</b> |
| 4.5.1 Principle of the assay   | 63        |
| <b>4.6 Materials and methods</b>   | <b>64</b> |
| 4.6.1 Materials  | 64        |
| 4.6.2 Methodology  | 64        |
| 4.6.2.1 Treatment, isolation and harvesting of HepG <sub>2</sub> cells                           | 64        |
| 4.6.2.2 Preparation of the GSH-Glo™ Reagent 2X and<br>Luciferin Detection Reagent                | 65        |
| 4.6.2.3 The GSH-Glo™ Glutathione assay on cultured HepG <sub>2</sub><br>cells                    | 65        |
| 4.6.2.4 The thiobarbituric acid reactive substances assay on<br>cultured HepG <sub>2</sub> cells | 66        |
| 4.6.2.5 Data analysis and statistics   | 67        |
| <b>4.7 Results and Discussion</b>  | <b>67</b> |
| <b>4.8 Conclusion</b>  | <b>79</b> |

|                  |  |            |
|------------------|--|------------|
| <b>Chapter 5</b> | <b>GENOMIC INTEGRITY</b>   | <b>80</b>  |
| <b>5.1</b>       | <b>Introduction</b>  | <b>80</b>  |
| <b>5.2</b>       | <b>Fluorescence Microscopy</b>   | <b>80</b>  |
| 5.2.1            | Fluorescent nucleic acid stains utilised for the analysis of genomic integrity     | 82         |
| <b>5.3</b>       | <b>The comet assay</b>   | <b>83</b>  |
| 5.3.1            | Principle and applications   | 83         |
| <b>5.4</b>       | <b>Materials and Methods</b>   | <b>84</b>  |
| 5.4.1            | Materials  | 84         |
| 5.4.2            | Methodology  | 84         |
| 5.4.2.1          | Treatment, isolation and harvesting of HepG <sub>2</sub> cells for the comet assay | 84         |
| 5.4.2.2          | The comet assay on cultured HepG <sub>2</sub> cells                                | 85         |
| 5.4.2.3          | Treatment of HepG <sub>2</sub> cells for Hoechst staining                          | 86         |
| 5.4.2.4          | Preparation of 10% paraformaldehyde and Hoechst 33342 stock solutions              | 86         |
| 5.4.2.5          | Hoechst 33342 staining   | 87         |
| 5.4.2.6          | Instrumentation and analysis of samples  | 87         |
| 5.4.2.7          | Data analysis and statistics   | 87         |
| <b>5.5</b>       | <b>Results and Discussion</b>  | <b>88</b>  |
| <b>5.6</b>       | <b>Conclusion</b>  | <b>97</b>  |
| <br>             |  |            |
| <b>Chapter 6</b> | <b>PROTEIN INTEGRITY</b>   | <b>98</b>  |
| <b>6.1</b>       | <b>Introduction</b>  | <b>98</b>  |
| <b>6.2</b>       | <b>Sodium dodecyl sulphate-polyacrylamide gel electrophoresis</b>                  | <b>100</b> |
| 6.2.1            | Principle of the technique   | 100        |
| <b>6.3</b>       | <b>Western Blotting</b>  | <b>101</b> |
| 6.3.1            | Principle of the technique   | 101        |
| <b>6.4</b>       | <b>Materials and methods</b>   | <b>103</b> |
| 6.4.1            | Materials  | 103        |

|                  |  |            |
|------------------|--|------------|
| 6.4.2            | Methodology  | 103        |
| 6.4.2.1          | Treatment, isolation and harvesting of HepG <sub>2</sub> cells | 103        |
| 6.4.2.2          | Protein isolation  | 103        |
| 6.4.2.3          | Protein quantification and standardisation                     | 104        |
| 6.4.2.4          | Sodium dodecyl sulphate-polyacrylamide gel<br>electrophoresis  | 104        |
| 6.4.2.5          | Silver staining  | 105        |
| 6.4.2.6          | Western blotting   | 106        |
| 6.4.2.7          | Instrumentation and analysis of samples                        | 107        |
| 6.4.2.8          | Data analysis and statistics                                   | 107        |
| <b>6.5.</b>      | <b>Results and Discussion</b>                                  | <b>108</b> |
| <b>6.6</b>       | <b>Conclusion</b>  | <b>116</b> |
| <b>Chapter 7</b> | <b>CELLULAR DEATH</b>  | <b>117</b> |
| <b>7.1</b>       | <b>Introduction</b>  | <b>117</b> |
| <b>7.2</b>       | <b>Flow cytometry</b>  | <b>118</b> |
| 7.2.1            | Fluidics   | 118        |
| 7.2.2            | Optics   | 119        |
| 7.2.3            | Electronics  | 119        |
| 7.2.4            | Data collection and display                                    | 120        |
| <b>7.3</b>       | <b>Flow cytometric detection of apoptosis/necrosis</b>         | <b>120</b> |
| <b>7.4</b>       | <b>Materials and methods</b>                                   | <b>122</b> |
| 7.4.1            | Materials  | 122        |
| 7.4.2            | Methodology  | 122        |
| 7.4.2.1          | Treatment, isolation and harvesting of HepG <sub>2</sub> cells | 122        |
| 7.4.2.2          | Preparation of Annexin-V-Fluos labelling solution              | 122        |
| 7.4.2.3          | Staining procedure of cultured HepG <sub>2</sub> cells         | 122        |
| 7.4.2.4          | Instrumentation and analysis of samples                        | 122        |
| 7.4.2.5          | Data analysis and statistics                                   | 123        |

|                  |                                 |            |
|------------------|---------------------------------|------------|
| <b>7.5</b>       | <b>Results and Discussion</b>   | <b>123</b> |
| <b>7.6</b>       | <b>Conclusion</b>               | <b>135</b> |
| <b>Chapter 8</b> | <b>CONCLUSION</b>               | <b>137</b> |
|                  | <b>REFERENCES</b>               | <b>139</b> |
|                  | <b>APPENDICES</b>               | <b>166</b> |
|                  | <b>PRESENTATIONS AND PAPERS</b> | <b>169</b> |

## LIST OF FIGURES

|                   | <b>page</b>  |
|-------------------|--|
| <b>Figure 2.1</b> | Glutathione <i>S</i> -transferase-catalysed conjugation of aflatoxin B <sub>1</sub> exo- and endo-epoxide with glutathione. <span style="float: right;">6</span>                                       |
| <b>Figure 2.2</b> | Aflatoxin B <sub>1</sub> -DNA adduct formation. <span style="float: right;">9</span>   |
| <b>Figure 2.3</b> | L-canavanine and L-arginine. <span style="float: right;">22</span>   |
| <b>Figure 2.4</b> | Tumour necrosis factor- $\alpha$ signalling. <span style="float: right;">30</span>   |
| <b>Figure 2.5</b> | Multiple pathways of caspase activation. <span style="float: right;">31</span>   |
| <b>Figure 2.6</b> | Regulation of p53 stability and function in response to genotoxic stress. <span style="float: right;">38</span>  |
| <b>Figure 2.7</b> | The mechanism of heat shock protein 70 production. <span style="float: right;">41</span>   |
| <b>Figure 3.1</b> | Diagram of a haemocytometer. <span style="float: right;">50</span>   |
| <b>Figure 3.2</b> | Schematic diagram of the treatment of cells for the MTT assay. <span style="float: right;">52</span>   |
| <b>Figure 3.3</b> | The effect of SF, AFB <sub>1</sub> and SF-AFB <sub>1</sub> combination treatments on cell viability of the HepG <sub>2</sub> cell line. <span style="float: right;">55</span>                          |
| <b>Figure 4.1</b> | The GSH-Glo <sup>TM</sup> and Luciferin Detection reactions of the GSH-Glo <sup>TM</sup> Glutathione assay. <span style="float: right;">63</span>  |
| <b>Figure 4.2</b> | Reaction between thiobarbituric acid and malondialdehyde to form the thiobarbituric acid pigment. <span style="float: right;">64</span>  |
| <b>Figure 4.3</b> | The effect of SF, L-can, AFB <sub>1</sub> , SF-AFB <sub>1</sub> and L-can-AFB <sub>1</sub> treatments on intracellular levels of GSH in HepG <sub>2</sub> cells. <span style="float: right;">68</span> |
| <b>Figure 4.4</b> | The effect of SF, L-can, AFB <sub>1</sub> , SF-AFB <sub>1</sub> and L-can-AFB <sub>1</sub> treatments on intracellular levels of MDA in HepG <sub>2</sub> cells. <span style="float: right;">70</span> |
| <b>Figure 5.1</b> | Typical filter setup of a fluorescence microscope. <span style="float: right;">81</span>   |
| <b>Figure 5.2</b> | Chemical structure of Hoechst 33342. <span style="float: right;">82</span>   |
| <b>Figure 5.3</b> | Chemical structure of ethidium bromide. <span style="float: right;">83</span>  |
| <b>Figure 5.4</b> | Ethidium bromide staining of HepG <sub>2</sub> cells. <span style="float: right;">89</span>  |

|                   |  |            |
|-------------------|--|------------|
| <b>Figure 5.5</b> | Induction of DNA migration by SF, L-can, AFB <sub>1</sub> , SF-AFB <sub>1</sub> and L-can-AFB <sub>1</sub> in HepG <sub>2</sub> cells.                               | <b>90</b>  |
| <b>Figure 5.6</b> | Hoechst 33342 staining of HepG <sub>2</sub> cells.   | <b>92</b>  |
| <b>Figure 6.1</b> | Chemiluminescent detection in western blotting.  | <b>102</b> |
| <b>Figure 6.2</b> | Silver staining of crude HepG <sub>2</sub> cellular proteins resolved by SDS-PAGE.   | <b>108</b> |
| <b>Figure 6.3</b> | Western blot analysis of Hsp70 protein levels in HepG <sub>2</sub> cells treated with SF, L-can, AFB <sub>1</sub> , SF-AFB <sub>1</sub> and L-can-AFB <sub>1</sub> . | <b>109</b> |
| <b>Figure 6.4</b> | Western blot analysis of Hsp90 protein levels in HepG <sub>2</sub> cells treated with SF, L-can, AFB <sub>1</sub> , SF-AFB <sub>1</sub> and L-can-AFB <sub>1</sub> . | <b>110</b> |
| <b>Figure 6.5</b> | Western blot analysis of p53 protein levels in HepG <sub>2</sub> cells treated with SF, L-can, AFB <sub>1</sub> , SF-AFB <sub>1</sub> and L-can-AFB <sub>1</sub> .   | <b>112</b> |
| <b>Figure 7.1</b> | Principle of Annexin-V-FITC and PI staining.   | <b>121</b> |
| <b>Figure 7.2</b> | Dot-plots showing Annexin-V-FITC versus propidium iodide fluorescence of HepG <sub>2</sub> cells (control).  | <b>130</b> |
| <b>Figure 7.3</b> | Dot-plots showing Annexin-V-FITC versus propidium iodide fluorescence of HepG <sub>2</sub> cells (AFB <sub>1</sub> ).  | <b>131</b> |
| <b>Figure 7.4</b> | Dot-plots showing Annexin-V-FITC versus propidium iodide fluorescence of HepG <sub>2</sub> cells (SF-AFB <sub>1</sub> ).   | <b>132</b> |
| <b>Figure 7.5</b> | Dot-plots showing Annexin-V-FITC versus propidium iodide fluorescence of HepG <sub>2</sub> cells (L-can-AFB <sub>1</sub> ).  | <b>134</b> |
| <b>Figure A1</b>  | BSA protein concentration versus average absorbance.   | <b>167</b> |

## LIST OF TABLES

|                  |  | <b>page</b> |
|------------------|--|-------------|
| <b>Table 3.1</b> | Mean cell viability as a percentage of the control $\pm$ SD following exposure of HepG <sub>2</sub> cells to SF only and SF-AFB <sub>1</sub> combination treatments. | <b>56</b>   |
| <b>Table 4.1</b> | Preparation of samples.  | <b>65</b>   |
| <b>Table 5.1</b> | Preparation of samples.  | <b>86</b>   |
| <b>Table 7.1</b> | The percentage of viable, apoptotic and necrotic cells determined using flow cytometry.  | <b>124</b>  |
| <b>Table A1</b>  | Components present in EMEM.  | <b>166</b>  |
| <b>Table A2</b>  | Absorbance's and concentrations of standards.  | <b>167</b>  |
| <b>Table A3</b>  | Absorbance's and concentrations of samples.  | <b>168</b>  |
| <b>Table A4</b>  | Standardisation of proteins to 1mg/ml (200 $\mu$ l) using storage buffer.  | <b>168</b>  |

## LIST OF ABBREVIATIONS

|                         |  |
|-------------------------|--|
| <b>ABS:</b>             | Absorbance                             |
| <b>ADC:</b>             | Analog-to-Digital converter            |
| <b>AFB<sub>1</sub>:</b> | Aflatoxin B <sub>1</sub>               |
| <b>AFM<sub>1</sub>:</b> | Aflatoxin M <sub>1</sub>               |
| <b>AFP<sub>1</sub>:</b> | Aflatoxin P <sub>1</sub>               |
| <b>AFQ<sub>1</sub>:</b> | Aflatoxin Q <sub>1</sub>               |
| <b>AIDS:</b>            | Acquired immune deficiency syndrome    |
| <b>AIF:</b>             | Apoptosis inducing factor              |
| <b>ALA:</b>             | Aminolevulinic acid                    |
| <b>ANOVA:</b>           | Analysis of variance                   |
| <b>AP:</b>              | Apurinic                               |
| <b>Apaf-1:</b>          | Apoptosis protease activating factor-1 |
| <b>APS:</b>             | Ammonium persulphate                   |
| <b>ASK1:</b>            | Apoptosis signal-regulated kinase-1    |
| <b>asp:</b>             | Aspartate                              |
| <b>ATM:</b>             | Ataxia telangiectasia mutated protein  |
| <b>ATP:</b>             | Adenosine triphosphate                 |
| <b>ATR:</b>             | ATM-related                            |
| <b>Avg:</b>             | Average                                |
| <b>BCA:</b>             | Bicinchoninic acid                     |
| <b>Bcl-2:</b>           | B cell lymphoma-2                      |
| <b>BH:</b>              | Bcl-2 homology                         |
| <b>BHT:</b>             | Butylated hydroxytoluene               |
| <b>BSA:</b>             | Bovine serum albumin                   |
| <b>Ca:</b>              | Calcium                                |
| <b>CAD:</b>             | Caspase-activated deoxyribonuclease    |
| <b>CARD:</b>            | Caspase recruitment domain             |
| <b>Caspase:</b>         | Aspartate-specific cysteine protease   |
| <b>CAT:</b>             | Catalase                               |



|                           |   |
|---------------------------|---|
| <b>CCD:</b>               | Charge coupled device                   |
| <b>CCM:</b>               | Complete culture medium                 |
| <b>cDNA:</b>              | Complementary DNA                       |
| <b>cFLIP:</b>             | FLICE inhibitory protein                |
| <b>CHO:</b>               | Chinese hamster ovary                   |
| <b>CL:</b>                | Chemiluminescent                        |
| <b>CO<sub>2</sub>:</b>    | Carbon dioxide                          |
| <b>COX:</b>               | Cyclooxygenase                          |
| <b>Cu:</b>                | Copper                                  |
| <b>CuSO<sub>4</sub>:</b>  | Copper (II) sulphate                    |
| <b>CYP<sub>450</sub>:</b> | Cytochrome P <sub>450</sub>             |
| <b>DCFH-DA:</b>           | 2',7'-dichlorofluorescein diacetate     |
| <b>DD:</b>                | Death domain                            |
| <b>DED:</b>               | Death effector domain                   |
| <b>DFO:</b>               | Desferral                               |
| <b>dH<sub>2</sub>O:</b>   | Deionised water                         |
| <b>DISC:</b>              | Death inducing signalling complex       |
| <b>DMSO:</b>              | Dimethyl sulfoxide                      |
| <b>DNA:</b>               | Deoxyribonucleic acid                   |
| <b>DNA-PK:</b>            | DNA-dependant protein kinase            |
| <b>DNase:</b>             | Deoxyribonuclease                       |
| <b>DR:</b>                | Death receptor                          |
| <b>DTT:</b>               | Dithiothreitol                          |
| <b>EDTA:</b>              | Ethylene diamine tetraacetic acid       |
| <b>ELISA:</b>             | Enzyme-linked immunosorbent assay       |
| <b>EMEM:</b>              | Eagles minimum essential medium         |
| <b>EOR:</b>               | Endoplasmic reticulum overload response |
| <b>EPR:</b>               | Electron paramagnetic resonance         |
| <b>ER:</b>                | Endoplasmic reticulum                   |
| <b>EtBr:</b>              | Ethidium bromide                        |
| <b>ETC:</b>               | Electron transport chain                |

|                                     |   |
|-------------------------------------|---|
| <b>F-2,6-BP:</b>                    | Fructose-2,6-bisphosphate                                 |
| <b>FACS:</b>                        | Fluorescence activated cell sorting                       |
| <b>FADD:</b>                        | Fas-associated death domain                               |
| <b>FAPY:</b>                        | Formamidopyrimidine                                       |
| <b>FCS:</b>                         | Foetal calf serum   |
| <b>Fe:</b>                          | Iron  |
| <b>FITC:</b>                        | Fluorescein isothiocyanate                                |
| <b>FLICE:</b>                       | Fas activated protein like IL-1 $\beta$ converting enzyme |
| <b>FSC:</b>                         | Forward scattered light                                   |
| <b>GABA:</b>                        | Gamma-amino-butyric-acid                                  |
| <b>GC:</b>                          | Guanine-Cytosine  |
| <b>GCS:</b>                         | $\gamma$ -glutamyl-cysteine synthase                      |
| <b>GGR:</b>                         | Global genome repair                                      |
| <b>GMP:</b>                         | Guanosine monophosphate                                   |
| <b>GPX:</b>                         | Glutathione peroxidase                                    |
| <b>GSH:</b>                         | Glutathione   |
| <b>GSSG:</b>                        | Glutathione disulphide                                    |
| <b>GST:</b>                         | Glutathione S-transferase                                 |
| <b>GTP:</b>                         | Guanosine triphosphate                                    |
| <b>Gua:</b>                         | Guanine   |
| <b>H:</b>                           | Hydrogen  |
| <b>H<sub>2</sub>O<sub>2</sub>:</b>  | Hydrogen peroxide   |
| <b>H<sub>3</sub>PO<sub>4</sub>:</b> | Phosphoric acid   |
| <b>HAT:</b>                         | Histone acetyl transferase                                |
| <b>HCl:</b>                         | Hydrochloric acid   |
| <b>HIV:</b>                         | Human immunodeficiency virus                              |
| <b>HRP:</b>                         | Horseradish peroxidase                                    |
| <b>Hsf:</b>                         | Heat shock factor   |
| <b>Hsp:</b>                         | Heat shock protein  |
| <b>HSR:</b>                         | Heat shock response                                       |
| <b>i.p:</b>                         | Intraperitoneal   |

|                                      |   |
|--------------------------------------|---|
| <b>IAP:</b>                          | Inhibitor of apoptosis protein                |
| <b>IgG:</b>                          | Immunoglobulin G                              |
| <b>IKK:</b>                          | I $\kappa$ B kinase                           |
| <b>IL:</b>                           | Interleukin                                   |
| <b>JNK:</b>                          | Jun NH <sub>2</sub> -terminal kinase          |
| <b>K<sub>2</sub>EDTA:</b>            | Dipotassium ethylene diamine tetraacetic acid |
| <b>KH<sub>2</sub>PO<sub>4</sub>:</b> | Potassium dihydrogen phosphate                |
| <b>L-arg:</b>                        | L-arginine                                    |
| <b>L-can:</b>                        | L-canavanine                                  |
| <b>LMPA:</b>                         | Low-melting-point-agarose                     |
| <b>MAP:</b>                          | Mitogen activated protein                     |
| <b>MDA:</b>                          | Malondialdehyde                               |
| <b>MDBK:</b>                         | Mardin-Darby bovine kidney                    |
| <b>MDCK:</b>                         | Mardin-Darby canine kidney                    |
| <b>Mdm-2:</b>                        | Mouse double minute-2                         |
| <b>MGE:</b>                          | Microgel electrophoresis                      |
| <b>mRNA:</b>                         | Messenger RNA                                 |
| <b>MTT:</b>                          | Methyl thiazol tetrazolium                    |
| <b>Mwt:</b>                          | Molecular weight marker                       |
| <b>Na<sub>2</sub>EDTA:</b>           | Disodium ethylene diamine tetraacetic acid    |
| <b>NaCl:</b>                         | Sodium chloride                               |
| <b>NADP:</b>                         | Nicotinamide adenine dinucleotide phosphate   |
| <b>NaOH:</b>                         | Sodium hydroxide                              |
| <b>NER:</b>                          | Nucleotide excision repair                    |
| <b>NF-<math>\kappa</math>B:</b>      | Nuclear factor- $\kappa$ B                    |
| <b>NO:</b>                           | Nitric oxide                                  |
| <b>NOS:</b>                          | Nitric oxide synthase                         |
| <b>O<sub>2</sub>:</b>                | Oxygen  |
| <b>O<sub>2</sub><sup>·-</sup>:</b>   | Superoxide                                    |
| <b>OH<sup>-</sup>:</b>               | Hydroxide                                     |
| <b>p53:</b>                          | Tumour suppressor protein p53                 |

|                  |   |
|------------------|---|
| <b>PBS:</b>      | Phosphate buffered saline   |
| <b>PFA:</b>      | Paraformaldehyde  |
| <b>PG:</b>       | Prostaglandin   |
| <b>PI:</b>       | Propidium iodide  |
| <b>PKC:</b>      | Protein kinase C  |
| <b>PMT:</b>      | Photomultiplier tube  |
| <b>PPP:</b>      | Pentose phosphate pathway   |
| <b>pRb:</b>      | Retinoblastoma protein  |
| <b>PS:</b>       | Phosphatidylserine  |
| <b>PUFA:</b>     | Polyunsaturated fatty acid  |
| <b>PUMA:</b>     | p53 upregulated modulator of apoptosis                              |
| <b>RAIDD:</b>    | RIP-associated ICH-1 / CED-3 homologous protein with a death domain |
| <b>RIP:</b>      | Receptor-interacting protein  |
| <b>RLU:</b>      | Relative light unit   |
| <b>RNA:</b>      | Ribonucleic acid  |
| <b>RNase:</b>    | Ribonuclease  |
| <b>ROH:</b>      | Alcohol   |
| <b>ROOH:</b>     | Lipid hydroperoxide   |
| <b>ROS:</b>      | Reactive oxygen species   |
| <b>s.c:</b>      | Subcutaneous  |
| <b>SB:</b>       | Storage buffer  |
| <b>SCGE:</b>     | Single cell gel electrophoresis                                     |
| <b>SDS-PAGE:</b> | Sodium dodecyl sulphate-polyacrylamide gel electrophoresis          |
| <b>SF:</b>       | <i>Sutherlandia frutescens</i>                                      |
| <b>Smac:</b>     | Second mitochondrial activator of caspases                          |
| <b>SOD:</b>      | Superoxide dismutase  |
| <b>SSC:</b>      | Side scattered light  |
| <b>STAT1:</b>    | Signal transducer and activator of transcription 1                  |
| <b>STZ:</b>      | Streptozotocin  |
| <b>TA:</b>       | Thymine-Adenine   |
| <b>TBA:</b>      | Thiobarbituric acid   |

|                 |  |
|-----------------|--|
| <b>TBARS:</b>   | Thiobarbituric acid reactive substances                                  |
| <b>tBid:</b>    | Truncated Bid  |
| <b>TBS:</b>     | Tris buffered saline   |
| <b>TCA:</b>     | Tricarboxylic acid   |
| <b>TCR:</b>     | Transcription-coupled repair   |
| <b>TEMED:</b>   | Tetramethylethylenediamine   |
| <b>TGase:</b>   | Tissue transglutaminase  |
| <b>TIGAR:</b>   | Tumour suppressor protein p53 induced glycolysis and apoptosis regulator |
| <b>TNF:</b>     | Tumour necrosis factor   |
| <b>TNFR:</b>    | TNF receptor   |
| <b>TRADD:</b>   | TNFR associated death domain   |
| <b>tRNA:</b>    | Transfer RNA   |
| <b>TUNEL:</b>   | Terminal deoxynucleotidyl transferase nick end labelling                 |
| <b>UDP:</b>     | Uridine diphosphate  |
| <b>UTP:</b>     | Uridine triphosphate   |
| <b>UV:</b>      | Ultraviolet  |
| <b>·OH:</b>     | Hydroxyl radical   |
| <b>3-D:</b>     | Three dimensional  |
| <b>4HNE:</b>    | 4-hydroxynonenal   |
| <b>8-HO-dG:</b> | 8-Hydroxy 20-deoxyguanosine  |

# Chapter 1

## INTRODUCTION

### 1.1 Toxicology

According to Paracelsus, a significant figure in the history of science and medicine during the late Middle Ages, “All substances are poisons; there is none which is not a poison. The right dose differentiates a poison from a remedy” (Langman and Kapur, 2006).

The traditional definition of toxicology is “the science of poisons” (Langman and Kapur, 2006), however toxicology, like medicine, is both a science and an art (Roberfroid, 1995). The science of toxicology involves studying the properties of chemicals and their effects on living organisms, whereas the art of toxicology is the predictive phase of the discipline aimed at assessing the potential adverse effects of chemicals in order to help preserve and protect human health (Roberfroid, 1995).

The history of toxicology has been interesting and varied, but never dull. The discipline dates to earliest man, who used animal venoms and plant extracts for hunting, waging war and assassinations, and has evolved rapidly during the past century. In addition, the modern era of toxicology continues to develop and expand by assimilating knowledge and techniques from most branches of the basic sciences, such as biology, chemistry, physics and mathematics. This complex mixture has resulted in an exciting, innovative and diversified field that is serving science and the community at large. Few disciplines can point to both basic sciences and direct application at the same time. Toxicology, the study of adverse effects of xenobiotics on living organisms, is unique in this regard (Amdur *et al.*, 1991).

A well established branch of the multidisciplinary field of toxicology is environmental toxicology, which is concerned primarily with the harmful effects of chemicals that are encountered incidentally because they are in the atmosphere, in the food chain, or present in occupational or recreational environments (Langman and Kapur, 2006).

Environmental toxicology encompasses the diverse and powerful biological effects of the mycotoxins (Steyn, 1995), a varied group of species-specific secondary metabolites produced

by toxigenic fungi (Amdur *et al.*, 1991). It has been well established that mycotoxins adversely affect human or animal health and are found mainly in post-harvest crops such as cereal grains or forages (Hussein and Brasel, 2001).

Among the various mycotoxins, the aflatoxins have been the subject of the most extensive research (Amdur *et al.*, 1991). Aflatoxin B<sub>1</sub>, synthesised by strains of *Aspergillus flavus* and *Aspergillus parasiticus*, is the most toxic member of the group and is usually present in the highest concentration under natural conditions (Meerdink, 2002). It is an extremely biologically reactive compound, altering a number of biochemical systems (Amdur *et al.*, 1991). Although the liver is clearly the principal target organ for AFB<sub>1</sub>, the lung, kidney and colon have also been implicated as potential targets following dietary and inhalational exposure (Wang and Groopman, 1999; Bedard and Massey, 2006). In addition, it is the most carcinogenic of the aflatoxins with the International Agency for Research on Cancer reporting that there is sufficient evidence to classify AFB<sub>1</sub> as a Group I carcinogen (Bedard and Massey, 2006). For these reasons, AFB<sub>1</sub> poses a major threat to human and animal health, and determination of its biological mechanism of action has understandably been the focus of much research (Coulombe, 1993).

Plants have played an important role in the treatment of various human ailments and, indeed, most new clinical applications of plant secondary metabolites and their derivatives over the last half century have been applied towards combating human disease (Balunas and Kinghorn, 2005). Herbal medicines represent a major component of this revolution (Fernandes *et al.*, 2004). Unfortunately, there is a great deal of confusion about their identification, effectivity, therapeutic doses, toxicity, standardisation and regulation (Chattopadhyay, 2003).

One of the best known multi-purpose medicinal plants in Southern Africa, SF, is used for a wide range of indications, including cancer, viral diseases and inflammatory conditions (Fernandes *et al.*, 2004).

With the interest that has been generated by the general public, university researchers and multinationals across the globe into ethnobotany, there is now more than ever a golden opportunity to continue making a worthwhile contribution to healthcare.

## **1.2 Objectives**

Based on the many controversial claims of SF, this study analysed the therapeutic potential of an SF aqueous extract against AFB<sub>1</sub>-induced cytotoxicity in cultured HepG<sub>2</sub> cells.

The objectives of this study were to investigate:

- The cytotoxicity of SF, when administered individually and in combination with AFB<sub>1</sub>, on HepG<sub>2</sub> cells
- The influence of SF, L-can and AFB<sub>1</sub>, when administered individually and in combination, on cellular redox state, genome integrity, protein integrity and apoptosis of HepG<sub>2</sub> cells.



## Chapter 2

# LITERATURE REVIEW

### 2.1 Introduction

#### 2.1.1 Mycotoxins

Fungi synthesise a wide range of secondary metabolites, many of which have been linked with the precipitation of adverse health effects in both animals and humans. These ubiquitous compounds have been allocated the term mycotoxins (D'Mello and MacDonald, 1997).

Mycotoxins encompass a large and structurally diverse group of toxins (Neal, 1995). It has been determined that approximately 25% of the world's food supply is contaminated by mycotoxins annually (Coulombe, 1993). Cereal plants may become contaminated by mycotoxins due to fungi growing either as pathogens on plants or saprophytically on stored plants (Handl and Richard, 2007). Temperature extremes, humidity, drought, excessive moisture in the field and in storage, variations in harvesting practices, and insect infestation are some of the major environmental factors that contribute to the severity of mycotoxin contamination (Coulombe, 1993).

The deleterious effects imposed by mycotoxins are referred to as mycotoxicoses (Handl and Richard, 2007). Even though evidence of mycotoxicoses can be traced back to ancient times, the momentum for mycotoxin research was not provided until 1960, when the so called 'Turkey-X' disease caused 100 000 turkey poults to die from an acute necrosis of the liver and hyperplasia of the bile duct following the consumption of groundnuts contaminated with *Aspergillus flavus*. As a result of this event subsequent research eventually led to the isolation and identification of the aflatoxins (D'Mello and MacDonald, 1997). Stimulated by the discovery of the aflatoxins, the search for mycotoxins in food has led to the identification of over 100 toxigenic fungi and more than 300 mycotoxins (Wang and Groopman, 1999).

#### 2.1.2 Aflatoxins and aflatoxicosis

The aflatoxins, of which there are five (B<sub>1</sub>, B<sub>2</sub>, G<sub>1</sub>, G<sub>2</sub> and M) of concern as natural contaminants in food, are mycotoxins produced by a closely related group of aspergilli; *A. flavus*, *A. parasiticus* and *A. nomius* (Moss, 2002).

Diseases caused due to aflatoxin consumption are collectively termed aflatoxicosis. It has been reported that acute aflatoxicosis results in direct liver damage and subsequent illness or death whereas chronic aflatoxicosis results in immunosuppression, cancer, and other slow pathological conditions (Ubagai *et al.*, 2008).

The foremost concern regarding the aflatoxins encompasses their carcinogenic properties (Kuilman *et al.*, 2000). Aflatoxin B<sub>1</sub> is the most prevalent and carcinogenic of the aflatoxins, and the International Agency for Research on Cancer has classified AFB<sub>1</sub> as a Group I carcinogen (an agent that is carcinogenic to humans) (Madhusudhanan *et al.*, 2004).

In all animal species examined to date, including man, the liver frequently demonstrates to be the primary target organ for AFB<sub>1</sub> (Neal, 1995), with low levels of chronic exposure resulting in neoplasia, primarily liver cancer (Wang and Groopman, 1999). Primary liver cancer ranks fifth in frequency among all malignancies in the world and is the third most common cause of cancer mortality. Hepatocellular carcinoma accounts for approximately 90% of primary liver cancers (El-Serag and Rudolph, 2007) with the great majority of liver cancer occurring in either eastern Asia or sub-Saharan Africa (McGlynn and London, 2005).

For these reasons, mycotoxins pose a major threat to public and animal health, and determination of the biological mechanism of action of mycotoxins has understandably been the focus of much research.

## **2.2 Cellular Metabolism**

### **2.2.1 Activation**

Aflatoxin B<sub>1</sub> is a low molecular weight, lipophilic molecule that is efficiently absorbed after ingestion of AFB<sub>1</sub>-contaminated food. The toxin itself is not carcinogenic, but is metabolised within the body to produce an ultimate carcinogenic metabolite (McLean and Dutton, 1995).

There is an abundance of evidence which reports that many mycotoxins require metabolic activation in order to induce a toxic response (Neal, 1995) and although early investigations were concerned with the possibility that AFB<sub>1</sub> is a direct-acting carcinogen, subsequent investigations clearly demonstrate that biotransformation mediates a key role in the disposition, toxicity and carcinogenicity of AFB<sub>1</sub> (Guengerich *et al.*, 1998).

The mechanism of AFB<sub>1</sub> hepatocarcinogenesis is specifically related to activation by the hepatic cytochrome P<sub>450</sub>-dependent polysubstrate monooxygenase enzyme superfamily (CYP<sub>450</sub>) after transport of the toxin across the plasma membrane (Awney *et al.*, 2002). The CYP<sub>450</sub> isoenzymes involved in both epoxidation and hydroxylation of AFB<sub>1</sub> are mainly CYP1A2 and CYP3A4 (Lee *et al.*, 2005). In humans, CYP3A4 appears to be the dominant CYP<sub>450</sub> involved in the biotransformation of AFB<sub>1</sub> (Guengerich *et al.*, 1998).

Aflatoxin B<sub>1</sub> is bioactivated by epoxidation of the terminal furan ring double bond, resulting in the generation of the AFB<sub>1</sub>-8,9-epoxide, a stereoisomer which can exist in both an *exo* (AFB<sub>1</sub>-*exo*-8,9-epoxide) and an *endo* (AFB<sub>1</sub>-*endo*-8,9-epoxide) conformation (Bedard and Massey, 2006; Figure 2.1).

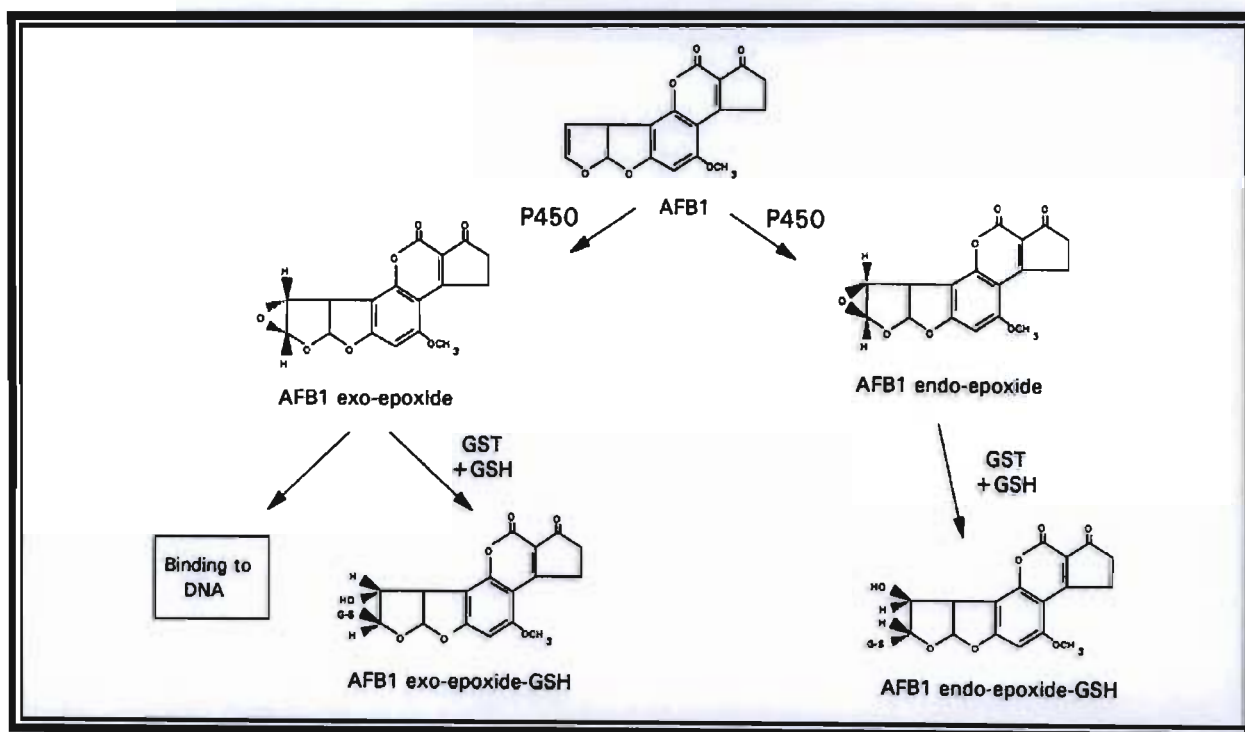


**Figure 2.1** Glutathione S-transferase-catalysed conjugation of aflatoxin B<sub>1</sub> *exo*- and *endo*-epoxide with glutathione (Stewart *et al.*, 1996).

The microsomal monooxygenase system is also responsible for converting AFB<sub>1</sub> into polar metabolites such as AFM<sub>1</sub>, AFP<sub>1</sub> and AFQ<sub>1</sub>, all three of which can be efficiently eliminated by hepatocytes. The toxin may alternatively be converted (reversibly) by an NADPH-reductase to aflatoxicol, which may thus serve as a reservoir for AFB<sub>1</sub> (McLean and Dutton, 1995).

### 2.2.2 Detoxification

The activating enzymes are not the only determinants of sensitivity to AFB<sub>1</sub>-induced toxicity (Stewart *et al.*, 1996). Activities of detoxifying enzymes are also decisive, and glutathione S-transferase (GST)-catalysed conjugation of GSH to the generated AFB<sub>1</sub>-8,9-epoxides is in fact presumed to play the most important role in preventing epoxide binding to target macromolecules (Lorico *et al.*, 2002; Figure 2.1). The GST's, which comprise a gene superfamily, are a group of microsomal and cytosolic enzymes that catalyse the conjugation of reduced GSH to a range of electrophilic compounds. This reaction constitutes the initial step of the mercapturic acid pathway, a process which facilitates the excretion of many xenobiotics. Because conjugation of the electrophilic AFB<sub>1</sub>-8,9-epoxide with GSH is an alternative fate to binding to nucleophilic centres in cellular macromolecules, GST's play a key role in the protection of tissues from AFB<sub>1</sub>-induced toxicity (Stewart *et al.*, 1996).

The AFB<sub>1</sub>-8,9-epoxides might also be detoxified by UDP-glucuronyl-transferase, sulphotransferases (Coulombe, 1993) and possibly by the epoxide hydrolase systems as well (McLean and Dutton, 1995).

The removal of AFB<sub>1</sub> metabolites (AFB<sub>1</sub>-GSH and glucuronide conjugates) from the liver is mediated via biliary excretion (Towner *et al.*, 2002). In fact, the elimination of GSH conjugates is a decisive step of the detoxification process, because their accumulation can lead to inhibition of GST's which may then have deleterious consequences with respect to cellular function and viability (Lorico *et al.*, 2002). Once released in the bile however, these conjugates may be hydrolysed by intestinal microflora which facilitates the release of AFB<sub>1</sub> for enterohepatic circulation and reabsorption. Most of the other aflatoxins form glucuronide or sulphate conjugates and are excreted in the urine (McLean and Dutton, 1995). Therefore, the ultimate toxicity of AFB<sub>1</sub> depends on the enzymes that bioactivate it to the AFB<sub>1</sub>-8,9-epoxides and on the enzymes that detoxify AFB<sub>1</sub> and/or the AFB<sub>1</sub>-8,9-epoxides (Stewart *et al.*, 1996).

The extent of GSH conjugation of AFB<sub>1</sub> is a major factor in variations in risk of different animal species to AFB<sub>1</sub>-induced toxicity (Coulombe, 1993). Esaki and Kumagai (2002) showed that GST activity is low in the rat, quail and turkey, all of which are susceptible species, but high in resistant species such as the hamster, mouse, guinea-pig and mastomys. Thus, GST-catalysed detoxification, rather than microsomal activation, is the critical

determinant of species susceptibility to the deleterious effects of AFB<sub>1</sub> (Stewart *et al.*, 1996). However, Hayes *et al.* (1991) suggests that the potential mechanisms associated with resistance to AFB<sub>1</sub> toxicity includes not only high detoxification activity but also low capacity to form AFB<sub>1</sub>-8,9-epoxides as well as increased AFB<sub>1</sub> efflux from cells and high DNA repair capacity.

### **2.2.3 Interaction with biomolecules**

#### **2.2.3.1 Nucleic acids**

Nucleophilic hetero-atoms (nitrogen and oxygen) in the organic bases of nucleic acids are susceptible to electrophilic attack by metabolites of mycotoxins subsequently resulting in the formation of covalent adducts. Any alterations in nucleic acid (DNA and RNA) structure mediated by these adducts may lead to impaired DNA and RNA template activity thus promoting the inhibition of DNA, RNA and protein synthesis (McLean and Dutton, 1995).

##### **2.2.3.1.1 Aflatoxin B<sub>1</sub>-DNA adduct formation**

For reasons that remain elusive, the AFB<sub>1</sub>-endo-8,9-epoxide is reported to be more stable than the exo-isomer. However, the reactivity of the exo-isomer with DNA is at least 1 000-fold greater than the endo-isomer. It is suggested that the most reasonable explanation for such differences in biological activity is because the intercalation of the furanocoumarin entity between DNA bases seems to favourably position the exo-isomer for SN<sub>2</sub> attack by the nitrogen number seven (N<sup>7</sup>) atom of guanine (Gua) residues (Guengerich, 2003). It has also been reported that nucleophilic attack by N<sup>7</sup> of Gua is possibly blocked by the oxirane ring of the endo-isomer upon its intercalation into DNA (Bedard and Massey, 2006).

During the intercalation of the exo-isomer into DNA, a peripheral proton field is created and imposes proximity effects (Guengerich *et al.*, 1998) which facilitate the generation of trans-8,9-dihydro-8-(N<sup>7</sup>-guanyl)-9-hydroxyaflatoxin B<sub>1</sub> (AFB<sub>1</sub>-N<sup>7</sup>-Gua, Figure 2.2), the primary AFB<sub>1</sub>-DNA adduct (Bedard and Massey, 2006). The imidazole ring of AFB<sub>1</sub>-N<sup>7</sup>-Gua bears a positive charge making the adduct fairly labile and allowing for it to undergo one of the following three reactions (Figure 2.2): (1) release of AFB<sub>1</sub>-8,9-dihydrodiol, restoring guanylic sites in DNA; (2) depurination, leading to the formation of an apurinic (AP) site in DNA; and (3) base-catalysed hydrolysis during which the imidazole ring opens, forming a stable AFB<sub>1</sub>-formamidopyrimidine adduct (AFB<sub>1</sub>-FAPY) (Smela *et al.*, 2001; Bedard and Massey, 2006).

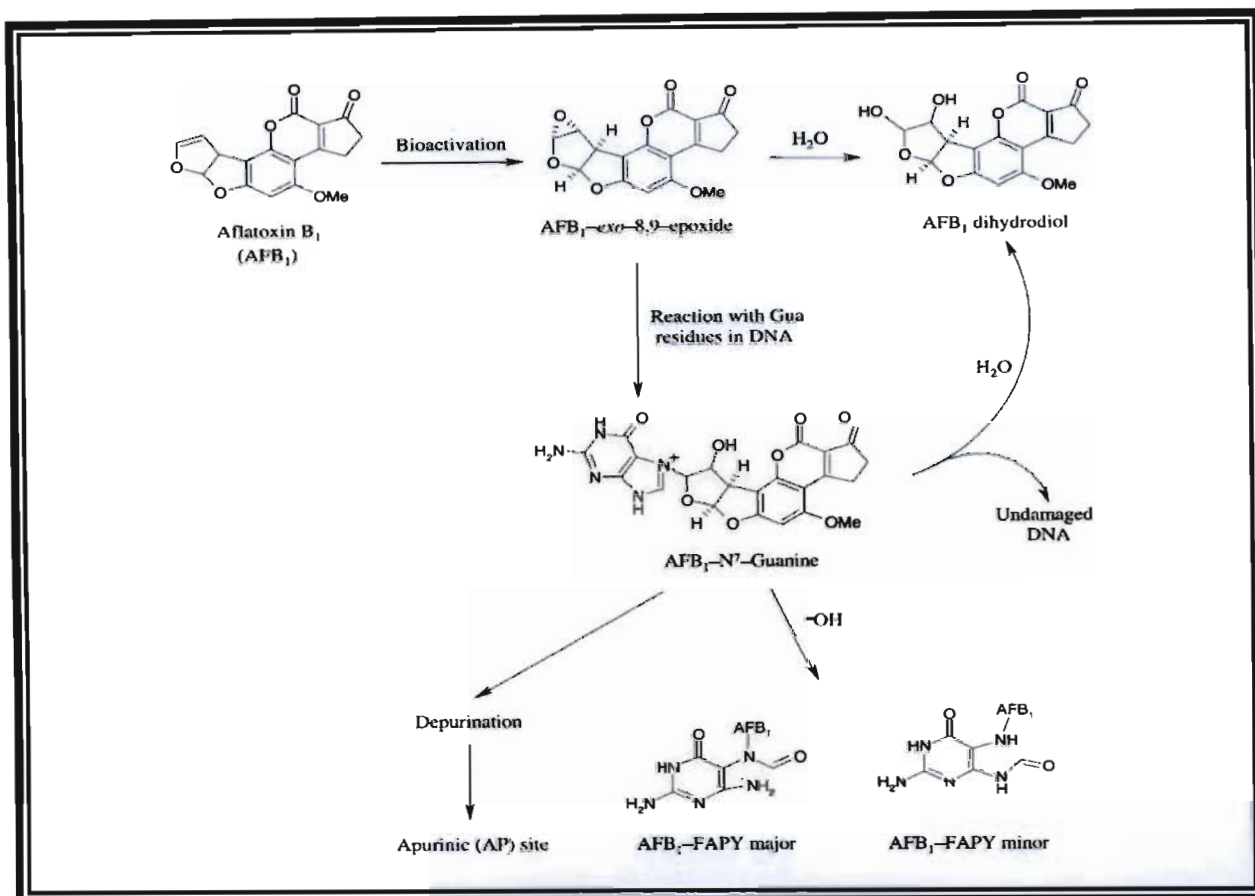


**Figure 2.2 Aflatoxin B<sub>1</sub>-DNA adduct formation (Bedard and Massey, 2006).**

The AFB<sub>1</sub>-8,9-dihydrodiol undergoes a base-catalysed, ringopening rearrangement to form a dialdehyde (Guengerich *et al.*, 1998). It is reported that the dihydrodiol and dialdehyde are not genotoxic (Guengerich, 2003). The other two lesions formed by AFB<sub>1</sub>, the AP site and AFB<sub>1</sub>-FAPY, have not been studied in sufficient detail to conclude definitively whether or not they contribute significantly to AFB<sub>1</sub>-induced toxicology (Smela *et al.*, 2001).

The mutational asymmetry observed for AFB<sub>1</sub>-N<sup>7</sup>-Gua is consistent with structural models indicating that the AFB<sub>1</sub> moiety of the AFB<sub>1</sub>-N<sup>7</sup>-Gua adduct is covalently intercalated on the 5' face of the Gua residue. It is thus suggested that this adduct specifically induces the genetic requirements for mutagenesis. Aflatoxin B<sub>1</sub>-DNA adducts possess the capacity of forming repair-resistant adducts or may induce error-prone DNA repair resulting in single-strand breaks, frame shift mutations or base pair substitutions. Mispairing of adducts could induce both transversion and transition mutations (Wang and Groopman, 1999).

The most commonly observed mutation induced by chemically reactive forms of AFB<sub>1</sub>, for example AFB<sub>1</sub>-8,9-exo-epoxide, is a GC to TA transversion which occurs in the third position of codon 249 of the p53 gene (Gerbes and Caselmann, 1993). The biochemical consequence of this mutation is an arginine to serine alteration in the p53 protein. This mutation appears to be unique to AFB<sub>1</sub>-induced liver tumours, as tumours presumably induced by other factors fail to consistently show this genetic change. The resulting mutation prevails in hepatocellular carcinomas of people that consume AFB<sub>1</sub>-contaminated food (Smela *et al.*, 2001).

### 2.2.3.2 Proteins

Aflatoxin B<sub>1</sub> reacts with various liver proteins particularly albumin, to form a stable adduct (Amaya-Farfan, 1999). In fact, the AFB<sub>1</sub>-albumin adduct is correlated with levels of the AFB<sub>1</sub>-DNA adduct in the liver and is used to examine exposure (Wild *et al.*, 1996). Proteins that bind AFB<sub>1</sub> reversibly may thus serve as reservoirs of the toxin, prolonging toxin exposure, or they may serve as carriers in the transport of reactive metabolites (McLean and Dutton, 1995).

It is proposed that AFB<sub>1</sub>, on entering the cell, is translocated in a non-covalently bound form (by cellular proteins) to microsomes for activation by microsomal enzymes (McLean and Dutton, 1995).

Chih *et al.* (1993) investigated the formation of AFB<sub>1</sub>-protein complexes. It was reported that several cellular proteins (pyruvate kinase>albumin>carbonic anhydrase>RNase>histones) bind to AFB<sub>1</sub>. It has also been reported that AFB<sub>1</sub> binds to nuclear proteins (free nuclear proteins>histones>chromatin-bound non-histone proteins) (Yu *et al.*, 1988).

The formation of AFB<sub>1</sub>-DNA adducts is implicated in AFB<sub>1</sub>-induced carcinogenesis; however the mechanism by which AFB<sub>1</sub> or its derivatives are translocated to the nucleus remains elusive. Evidence suggests that AFB<sub>1</sub> and/or its metabolites become cytoplasmically bound to molecules destined for the nucleus. In this regard, Chih *et al.* (1993) showed that a toxin-protein complex is translocated to the nucleus. It is thus possible that AFB<sub>1</sub> translocates the nuclear pore as a ligand-bound complex by binding non-covalently to proteins destined for the nucleus, for example histones, thus facilitating its uptake, activation and subsequent damage to DNA.

It is suggested that the structure and activity of proteins may be detrimentally altered by non-specific-irreversible covalent (conformational change resulting in denaturation or blocking of binding sites) and specific-reversible non-covalent (competitive binding) binding with the toxin (McLean and Dutton, 1995). Enzyme inactivation is a further consequence of toxin binding (Amaya-Farfan, 1999).

Besides AFB<sub>1</sub> itself or the generated exo-isomer interacting with proteins, the dialdehyde generated from the AFB<sub>1</sub>-8,9-dihydrodiol is capable of condensing with primary amino acid groups, such as lysine, and other cellular constituents, forming Schiff bases (Guengerich *et al.*, 1998) thus also contributing to alterations in protein/enzyme structure and function.

### **2.2.3.3 Effects on the mitochondrion**

Liver mitochondrial injury is indeed one of the dominant features of AFB<sub>1</sub> toxicity.

The cytochrome complexes represent the major redox components of the mitochondrial respiratory chain (Sajan *et al.*, 1995). Doherty and Campbell (1973) reported that the major site of electron transport inhibition by AFB<sub>1</sub> was between cytochromes *b* and *c*<sub>1</sub>. It was also determined that AFB<sub>1</sub> ( $2.5\text{-}4.8 \times 10^{-4}\text{M}$ ) mediated up to 44% inhibition of electron transport in an actively respiring rat liver mitochondrial preparation.

Pai *et al.* (1975) investigated the effects of AFB<sub>1</sub> ( $1 \times 10^{-4}\text{M}$ ) on rat liver mitochondrial function and also reported that AFB<sub>1</sub> inhibited electron transport between cytochromes *b* and *c*<sub>1</sub>. It was further demonstrated that AFB<sub>1</sub> ( $1 \times 10^{-6}\text{M}$ ) uncoupled oxidative phosphorylation.

In other studies, Obidoa and Obonna (1981) reported a concentration-dependent inhibition of rat liver mitochondrial succinate dehydrogenase and ATPase by AFB<sub>1</sub>, whereas Sajan *et al.* (1995) reported 31%, 36% and 41% decreases in cytochrome oxidase, succinoxidase and succinate dehydrogenase activity respectively, after analysing liver mitochondria of AFB<sub>1</sub>-treated (7mg/kg body weight, i.p) rats. Additionally, Obidoa (1986) further demonstrated the capacity of AFB<sub>1</sub> to inhibit cytochrome oxidase activity in isolated rat liver mitochondria.

Mitochondrial DNA encodes several major enzyme complexes involved in oxidative phosphorylation (Schatz and Manson, 1974). It is suggested that mitochondrial DNA, which is less protected by associated histones than nuclear DNA, is a major target for carcinogen



binding. It was shown that the extent of AFB<sub>1</sub> adduct formation with mitochondrial DNA was several-fold more than that with nuclear DNA (Niranjan *et al.*, 1981). Because mitochondria lack excision repair mechanisms and protective histones, the AFB<sub>1</sub>-DNA adducts formed contribute to defective synthesis of respiratory enzymes. Adduct formation of AFB<sub>1</sub> with mitochondrial proteins may also modify respiratory enzymes (Sajan *et al.*, 1995).

Mitochondrial membranes are rich in phospholipids. Thus, lipophilic carcinogens such as AFB<sub>1</sub> can readily interact with the phospholipid bilayer and cause changes in mitochondrial membrane fluidity (Sajan *et al.*, 1995). In addition, AFB<sub>1</sub> treatment generates ROS which are known to damage membranes by lipid peroxidation (Shen *et al.*, 1994). The mitochondrial membrane may therefore be affected by lipid peroxidation induced by AFB<sub>1</sub> and this too can impair associated functions.

### **2.3 Effects on Macromolecular Biosynthesis**

Inhibition of macromolecular biosynthesis is a major metabolic effect of AFB<sub>1</sub> (McLean and Dutton, 1995). This action has been equated with its ability to bind to DNA and thus affect RNA transcription and translation as well as polyribosome profiles and protein synthesis, a consequence of which is cell death (Scaife, 1971).

#### **2.3.1 DNA**

One of the initial measurable effects of AFB<sub>1</sub> on cells and tissues is the inhibition of DNA synthesis. This may occur after the covalent binding of AFB<sub>1</sub> to DNA and/or proteins, leading to modification of the DNA template and/or inactivation of certain enzymes in DNA synthesis. It has also been shown that covalent binding of AFB<sub>1</sub> to membrane proteins may reduce the uptake of thymidine and other precursor nucleotides which are necessary for DNA synthesis (McLean and Dutton, 1995).

Iwaki *et al.* (1990) reported a 30% inhibition of DNA synthesis in human hepatic cells exposed to AFB<sub>1</sub> (1 µg/ml). Further analysis revealed that AFB<sub>1</sub>-associated cellular components were mainly DNA, RNA, and proteins.

In a similar study, Meneghini and Schumacher (1977) demonstrated inhibition of DNA synthesis when African green monkey cells were incubated for 3 h with AFB<sub>1</sub> (0.1 µg/ml). On

the basis of pulse labelled DNA analysis, the authors concluded that AFB<sub>1</sub> blocked initiation of DNA replication rather than elongation.

### 2.3.2 RNA

It has been established that AFB<sub>1</sub>, when administered *in vivo* or activated *in vitro*, inhibits rat liver nuclear and nucleolar RNA synthesis (Yu *et al.*, 1988). According to Roy (1968), a metabolite of AFB<sub>1</sub> rather than the toxin itself inhibits DNA-dependent RNA synthesis.

Wagner and Drews (1965) investigated the effects of a single dose of AFB<sub>1</sub> (1.25mg/kg body weight, i.p) on the metabolism of rat liver nuclear RNA. The authors observed a 50% decrease in the incorporation of labelled RNA precursors into nuclear RNA. It was further shown that AFB<sub>1</sub> impaired the formation of the 35S ribosomal precursor RNA and the 28S RNA.

Floyd *et al.* (1968) demonstrated the inhibition of nucleolar RNA synthesis by AFB<sub>1</sub>, whereas studies by Wagner and Unterreiner (1982) revealed 91%, 77% and 75% inhibition of total RNA synthesis, tRNA synthesis and protein synthesis respectively, by AFB<sub>1</sub>.

Aflatoxin B<sub>1</sub> has also been shown to inhibit UTP incorporation into RNA (Clifford *et al.*, 1976) as well as to mediate the inhibition of nucleoplasmic RNA polymerase (Prasanna *et al.*, 1978).

The effects of AFB<sub>1</sub> on hepatocyte RNA synthesis was investigated by Ch'ih *et al.* (1983). It was reported that AFB<sub>1</sub> (50µM) inhibited macromolecular synthesis by greater than 70% after a 3 h incubation whereas at lower concentrations (0.05-10µM), dose-and time-dependent decreases in cell viability and, RNA and protein synthesis were observed.

### 2.3.3 Protein

The inhibition of protein synthesis by AFB<sub>1</sub> may arise directly via inactivation of biosynthetic enzymes or indirectly via an alteration of DNA template activity, inhibition of RNA synthesis or translation, and/or interference with amino acid transport (McLean and Dutton, 1995).

It is currently admitted that AFB<sub>1</sub> impairs protein synthesis in the liver, an effect that is expected to occur as a consequence of altered transcription (Sarasin and Moulr, 1973). Rao (1971) determined that liver protein synthesis of *Macaco irus* was inhibited by 50% when

these monkeys were administered single oral doses of AFB<sub>1</sub> (2mg/kg) for 3 h. Concomitant with this change was an extensive disaggregation of polyribosomes.

In another study, Sidransky *et al.* (1977) demonstrated the disaggregation of free and membrane-bound polyribosomes accompanied by inhibition of protein synthesis in rat liver after the administration of AFB<sub>1</sub> (6mg/kg body weight, i.p).

John and Miller (1969) utilised isolated perfused male Sprague-Dawley rat liver to study the influence of AFB<sub>1</sub> on the net synthesis of the plasma proteins albumin, fibrinogen,  $\alpha_1$ -acid glycoprotein and  $\alpha_2$ -(acute phase) globulin. A dose-dependant (125-1 000 $\mu$ g) inhibition of protein synthesis was observed 4 h after perfusion.

Sarasin and Moulr (1973) investigated the early effects of AFB<sub>1</sub> administration on protein synthesis in rat liver. After a single injection (1mg/kg body weight, i.p) inhibition of protein synthesis by AFB<sub>1</sub> progressively increased to a level of approximately 85%. In addition, disaggregation of polysomes began 4 h after AFB<sub>1</sub> administration then progressively increased, reaching a maximum of approximately 60%. The authors concluded that a direct action of the toxin on the translational process might account for the early inhibition of protein synthesis.

On the basis of [<sup>14</sup>C]-leucine incorporation with the postmitochondrial supernatant, Wagner and Unterreiner (1981) demonstrated an 80% inhibition of polypeptide synthesis when rats were treated with AFB<sub>1</sub> (3mg/kg body weight, i.p) for 24 h. In addition, overall protein synthesis was inhibited by 67%. The authors also observed a 20% inhibition in leucine-specific aminoacyl-tRNA synthesis accompanied by an inhibition of aminoacyl-tRNA synthetase activity. It was concluded that inhibition of protein synthesis by AFB<sub>1</sub> is in part due to decreased aminoacyl-tRNA levels caused by inhibited aminoacyl-tRNA synthetases.

## **2.4. Specific Effects**

### **2.4.1 Oxidative damage**

The intracellular generation of ROS and its impairment to cellular components such as enzymes, membrane lipids, proteins and nucleic acids have been implicated in the cytotoxicity and carcinogenicity of certain chemical carcinogens (Shen *et al.*, 1995). Oxidative damage caused by AFB<sub>1</sub> may be one of the underlining mechanisms for AFB<sub>1</sub>-induced cell injury and

DNA damage (Shen *et al.*, 1994). In fact, Souza *et al.* (1999) reported that oxidative stress is the principle manifestation of AFB<sub>1</sub>-induced toxicity.

Although the mechanism underlying AFB<sub>1</sub> hepatotoxicity has not been fully elucidated, it is suggested that toxicity may ensue through the generation of intracellular ROS during the metabolic processing of AFB<sub>1</sub> by CYP<sub>450</sub> in the liver (Preetha *et al.*, 2006). Lipid peroxidation is one of the main manifestations of oxidative stress and has been demonstrated to mediate a key role in the toxicity and carcinogenesis of many carcinogens (Shen *et al.*, 1994). Many studies have reported the induction of lipid peroxidation by AFB<sub>1</sub> both *in vivo* and *in vitro* (Shen *et al.*, 1994; Shen *et al.*, 1995, Madhusudhanan *et al.* 2004; Meki *et al.*, 2004; Lee *et al.*, 2005; Jodynis-Liebert *et al.*, 2006; Preetha *et al.*, 2006). Thus ROS induction is regarded to play a key role in the toxicity and carcinogenicity of AFB<sub>1</sub>.

#### **2.4.2 Repair of Aflatoxin B<sub>1</sub>-induced DNA damage**

Evolution has allowed for the generation of an intricate network of highly conserved DNA repair systems to maintain genetic integrity. One of these systems is nucleotide excision repair (NER), a DNA damage removal mechanism that affords protection to the genome. The NER is divided into two subpathways; global genome repair (GGR) and transcription coupled repair (TCR). In GGR, the entire genome is screened for DNA lesions and is suggested to be transcription-independent. With TCR however, lesions that arrest RNA polymerase on the transcribed strand of active genes are investigated in particular. It is suggested that AFB<sub>1</sub>-induced DNA damage is repaired by NER in mammalian systems and that NER is an important mechanism for enzymatic repair of AFB<sub>1</sub>-DNA adducts (Bedard and Massey, 2006).

Thus, susceptibility and resistance to the toxic and carcinogenic effects of AFB<sub>1</sub> may depend on several factors; bio-activating and detoxifying CYP<sub>450</sub>, GST activity, effective cellular removal of AFB<sub>1</sub> detoxification products, the ability for excision of AFB<sub>1</sub> adducts from DNA as well as repair of AFB<sub>1</sub>-induced DNA damage.

The perceived importance of the aflatoxins, in particular AFB<sub>1</sub>, is reflected in the pace of research leading to their identification, full chemical characterisation and elucidation of imposed adverse health effects.

## **2.5 *Sutherlandia frutescens***

Evidence suggests that approximately 80% of Africans depend upon ethnomedicine for their access to daily healthcare (Ojewole, 2008). Thus, it is not the case that traditional medicine offers an alternative for African people but rather that it is in fact their only source of treatment (Hartnett *et al.*, 2005).

Almost 50% of all current pharmaceuticals are derived from plants (Mills *et al.*, 2005a). Southern Africa has a rich diversity of medicinal plants with an estimated 3 000 that are regularly used (van Wyk, 2008). One of the best known multi-purpose medicinal plants that are used for various preparations is SF, a flowering shrub of the pea family (Fabaceae) (Sia, 2004). Decoctions of SF have been used for a variety of medicinal purposes for many years. It is widely believed that the Khoi and Nama people were the first to use it against fevers as well as for the cleansing of open wounds (Chadwick *et al.*, 2007). It is known to be used by cultural groups for a variety of other ailments which include indigestion, oesophagitis, peptic ulcers, dysentery, cancer, diabetes, colds, asthma, kidney and liver conditions, rheumatism, urinary tract infections and stress (van Wyk, 2008). The known side-effects of SF include mild diarrhoea, mild diuresis, and dizziness (Mills *et al.*, 2005a).

There exists a long history of seemingly safe usage of SF (Mills *et al.*, 2005a). Plants that are used in traditional medicine are assumed safe, due to their long-term use and are considered to have insignificant side effects because they are 'natural'. However, this may not necessarily be true and is somewhat circumstantial since it is important to determine the toxicology of plant extracts, especially those that are used frequently over long periods (Reid *et al.*, 2006).

### **2.5.1 Toxicity**

A toxicology screening in a primate model utilised dosages of SF up to 9 times greater than recommended with no noted clinical, haematological or physiological toxicity (Mills *et al.*, 2005a). Additionally, a recent clinical trial reported safety of SF leaf powder by concluding that consumption of a daily dose of 800mg for 3 months was tolerated by healthy human volunteers in the absence of significant adverse events (Ojewole, 2008). For these reasons it is possible that SF is now available in a tablet form with a recommended dosage of 600mg daily.

### 2.5.2 Chemistry

Chemical compounds which have been isolated from SF include pinitol, secondary plant metabolites such as saponins, flavonoids, free amino acids such as gamma-amino-butyric-acid (GABA) and L-can (van Wyk, 2008), arginine, asparagine, alanine, proline, leucine, phenylalanine and tryptophan (Tai *et al.*, 2004) as well as a series of other components including methyl parabens, propyl parabens, hexadecanoic acid, gamma sitosterol, stigmasterol, and several long-chain alcohols typically found in plants (Sia, 2004).

When SF leaves were analysed, high levels of the free amino acids asparagine (up to 35.0mg/g), proline (up to 7.5mg/g) and arginine (up to 6.7mg/g) were detected. In addition, it was determined that up to 14mg/g of pinitol was present in the leaves of SF (van Wyk and Albrecht, 2008).

Pinitol was described as being active against acute oedema in rat models as well as mediating a reduction of pro-inflammatory cytokines, such as tumour necrosis factor- $\alpha$  (TNF- $\alpha$ ) and interleukin-1 $\beta$  (IL-1 $\beta$ ) (Sia, 2004). More importantly, pinitol is a known anti-diabetic agent. It is thought to exert an insulin-like effect, thereby lowering blood sugar levels and increasing the bioavailability of glucose for cellular metabolism (van Wyk and Albrecht, 2008).

There is approximately 0.4mg/g of GABA in SF tablets (Tai *et al.*, 2004). This inhibitory neurotransmitter mediates its primary effects outside the central nervous system (van Wyk, 2008). In this regard, its potential activity against anxiety and stress has been reported (Sia, 2004). It was also shown to inhibit tumour cell migration (van Wyk and Albrecht, 2008).

The seeds of Fabaceae contain non-protein amino acids, the most prominent being L-can. However, L-can is also found within the leaves of SF which contain approximately 14.5mg/g of the compound (van Wyk and Albrecht, 2008). Other evidence demonstrated that there is 3mg/g of L-can present in SF tablets (Tai *et al.*, 2004). L-canavanine is a potent L-arginine (L-arg) analogue and possesses antimetabolic activities and properties as a result. It also displays antibacterial, antifungal, and antiviral capacity (Sia, 2004).

### **2.5.3 Pharmacology**

#### **2.5.3.1 Diabetes**

The incidence of type II diabetes is increasing worldwide. It has been demonstrated that SF is a potential hypoglycaemic mediator for the treatment of type II diabetes (Chadwick *et al.*, 2007). After crushed SF leaves in drinking water were administered to Wistar rats fed a high fat diet, Chadwick *et al.* (2007) determined that the plant extract normalised insulin levels and glucose uptake in peripheral tissues (muscle and fat), suppressed intestinal glucose uptake and mediated glucose clearance with no noted weight gain. The authors concluded that SF is an efficient hypoglycaemic mediator compared to metformin for example, which is a drug that is commonly utilised for the treatment of type II diabetes.

Ojewole (2004) investigated the hypoglycaemic effects of the plants shoot aqueous extract when administered to streptozotocin (STZ)-induced diabetic rats. It was shown that SF (50-800mg/kg, i.p) caused significant ( $p < 0.05-0.001$ ) hypoglycaemia in these animals. It was determined that the maximum reduction of blood glucose levels by SF in normoglycaemic rats was 25.43% and the hypoglycaemic effect was even higher in STZ-treated rats.

Other studies reported that pinitol, when administered to hypoinsulinaemic STZ-induced diabetic mice, was capable of reducing blood sugar levels in these animals (Sia *et al.*, 2004).

#### **2.5.3.2 HIV**

It has been reported by doctors and health care workers that HIV-infected people who consumed SF displayed improved appetite and weight gain, improved CD4<sup>+</sup> counts, decreased viral loads as well as general mood improvements (Harnett *et al.*, 2005).

With regard to HIV treatment in Africa specifically, patients often opt for traditional healing systems as a means of primary care. This is possibly associated with the difficulties in accessing antiretroviral treatment. What is known for sure is that the use of traditional medicines by Africans living with HIV is widespread (Mills *et al.*, 2005a).

### **2.5.3.3 Antioxidant properties**

Reactive oxygen species, such as hydrogen peroxide ( $\text{H}_2\text{O}_2$ ) and superoxide ( $\text{O}_2^-$ ) contribute to the pathogenesis of many inflammatory conditions. In this regard, anti-inflammatory properties of herbal medications are possibly due to their antioxidant activities (Fernandes *et al.*, 2004).

Fernandes *et al.* (2004) used luminol and lucigenin enhanced chemiluminescence to investigate the  $\text{H}_2\text{O}_2$  and  $\text{O}_2^-$  scavenging properties of an SF water extract in neutrophils. It was reported that SF possessed  $\text{H}_2\text{O}_2$  and  $\text{O}_2^-$  scavenging activities at concentrations as low as  $10\mu\text{g/ml}$ .

By utilising a 70% ethanolic extract Tai *et al.* (2004) demonstrated the hydroxyl radical ( $\cdot\text{OH}$ ) scavenging activity of SF. It was estimated by the authors that  $0.5\mu\text{l}$  of the SF ethanolic extract possessed  $\cdot\text{OH}$  scavenging activity equivalent to  $10\mu\text{M}$  of Trolox, a chemical with potent antioxidant activity.

### **2.5.3.4 Anticonvulsant properties**

Ojewole (2008) investigated the anticonvulsant properties of an SF aqueous extract against pentylenetetrazole, picrotoxin and bicuculline-induced seizures in *Balb/C* mice. It was determined that the extract (50-400mg/kg, i.p) significantly ( $p < 0.05-0.001$ ) delayed the onset of and antagonised only pentylenetetrazole-induced seizures.

### **2.5.3.5 Anti-inflammatory properties**

Upregulation of cyclooxygenase (COX)-2 frequently occurs in various malignancies. The enzyme is normally involved in prostaglandin (PG) biosynthesis and inflammation. Plant extracts have inhibited COX-2 induction both *in vitro* and *in vivo* (Kundu *et al.*, 2005). In this regard, Kundu *et al.* (2005) investigated the effect of an SF methanolic extract on the expression of COX-2 in mouse skin stimulated with the tumour promoter 12-O-tetradecanoylphorbol-13-acetate. It was determined that SF suppressed COX-2 expression by 26% and 48% at doses of 100mg and 200mg respectively.

### **2.5.3.6 Stress**

A study by Prevo *et al.* (2008) illustrated the attenuation of adrenal  $\text{CYP}_{450}$  enzymes, *CYP17* and *CYP21*, by an aqueous extract of SF. The authors suggested that SF was able to affect the catalytic activity of these enzymes, which are normally involved in the biosynthesis of steroid



hormones, due to observed reductions in glucocorticoid levels. These findings provide preliminary scientific appraisal for the stress relieving properties of SF.

#### **2.5.3.7 Antimutagenic, antimetabolic and pro-apoptotic properties**

It has been determined that most cancer chemotherapeutic agents severely affect the host's normal cells. As a consequence, the employment of natural products has now been considered as an alternative in the control of cancer (Steenkamp and Gouws, 2006).

Using the Ames test, Reid *et al.* (2006) demonstrated that SF possesses antimutagenic activity. Dichloromethane extracts comprising both leaf and stem material of SF were utilised and it was concluded that the extract has chemopreventative potential. In a more recent study, Ntuli *et al.* (2007) used the Salmonella mutagenicity assay and also demonstrated antimutagenic properties of SF by using ethylacetate and 50% aqueous methanolic extracts of the plant.

A study by Steenkamp and Gouws (2006) showed that an aqueous leaf extract of SF (50µg/ml) induced growth inhibition of both the human prostate cancer cell line, DU-145 as well as the human breast carcinoma cell line, MCF-7.

Stander *et al.* (2007) investigated the influence of a crude SF ethanolic extract on MCF-7 cells. Compared to the control, the SF-treated cells displayed morphological hallmarks of apoptosis including cytoplasmic shrinking, membrane blebbing and the presence of apoptotic bodies. In addition, cDNA microarray analysis revealed a total of 345 genes to be statistically significantly ( $p < 0.05$ ) differentially expressed. Amongst these genes were the TNF superfamily members (DR4 and DR5) as well as other genes which play important roles in apoptosis, growth inhibition and Nuclear Factor- $\kappa$ B (NF- $\kappa$ B) signalling.

Signal transducer and activator of transcription 1 (STAT1) regulates p53 stability by inhibiting the Mouse double minute 2 (Mdm2) gene, a major factor that controls p53 degradation. PIAS1 protein interacts with STAT1 to reduce its activity. PIAS1 gene expression was downregulated in SF-treated (50µg/ml) MCF-7 cells (Stander *et al.*, 2007). This effect of SF signifies a possible mechanism for its pro-apoptotic/anticancer properties.

By utilising ethanolic extracts of SF, Tai *et al.* (2004) showed differential *in vitro* anti-proliferative properties of this herbal medication by demonstrating a concentration-dependent

inhibition of growth of various human cell lines including the leukaemia Jurkat cell line, MCF-7 and the promyelocyte cell line, HL60.

Chinkwo (2005) examined the apoptotic properties of a crude aqueous SF whole plant extract on Caski cells (cervical carcinoma), CHO cells (Chinese Hamster Ovary) and the Jurkat T lymphoma cell line. Caski and CHO cells were treated with 3.5mg/ml SF for 8 and 24 h. Morphologically, cell death was evidenced in Caski and CHO cells by cell shrinkage and disintegration as well as a reduction in cell number. The author suggested that there were constituents in the extract that induced the observed morphological changes and cell death.

During apoptosis there results an externalisation of a phospholipid, phosphatidylserine (PS), in the plasma membrane of the associated cell. Chinkwo (2005) utilised the apoPercentage™ assay and efficiently demonstrated this process in SF-treated CHO cells. In addition, the author used the crossmon trichrome stain and showed that chromatin condensation, a morphological feature of apoptotic cells, was induced in CHO cells exposed to the plant extract.

When Jurkat T cells were incubated with SF (3.5mg/ml) for 6 h and analysed by flow cytometry (Annexin-V staining), the resulting histogram illustrated that more than 84% of the cells were apoptotic Chinkwo (2005).

Medicinal plants have become popular as an alternate healthcare source because of several claimed advantages such as fewer side-effects, better patient compliance, relatively low cost, high accessibility as well as high acceptability due to their long history of use (Brown *et al.*, 2008). *Sutherlandia frutescens* (known in isiZulu as 'unwele', in English as 'cancerbush' and in Afrikaans as 'kankerbos') is a popular medicinal plant and has a long history of ethnomedical usage by a variety of African cultures (Ojewole, 2008). Recent evidence has displayed a range of pharmacological properties that lends credence in providing convincing support for the array of traditional uses that have been claimed and documented for so long. Although the exact mechanisms of action mediated by the various extracts derived from SF are currently unknown, existing evidence documents that the medicinal plant is indeed effective in inhibiting inflammation as well as possesses anti-oxidant, hypoglycaemic and, antimutagenic and antiproliferative properties in both *in vitro* and *in vivo* experimental systems. However, the true benefits of this plant need to be scientifically evaluated in a clinical setting.

## 2.6 L-canavanine

### 2.6.1 Natural sources and functions of L-canavanine

L-Canavanine was first identified in 1929 when it was isolated from seeds of *Canavalia ensiformis* (jack bean) (Ding *et al.*, 1999). It is found in leguminous plants, particularly members of the Lotaideae family, a subdivision of Leguminosae (Bence and Crooks, 2003).

L-canavanine has two functions in the plant. It is well suited to store nitrogen in plant seeds due to its high nitrogen content (31.8%). It therefore serves as an efficient nitrogen storing compound and is thus fundamental to the plant's chemical defence system (Rosenthal, 1977).

Another very important function afforded by L-can in plants is its protective property against insects and other herbivores. It has been shown to deleteriously affect the growth and development of organisms that consume plants containing the compound. When the tobacco hornworm *Manduca sexta* ingested L-can, the resulting effects included stunted development and growth attenuation of this plant-eating insect (Rosenthal, 1988). This property of L-can provides a formidable chemical barrier against predation by nonadapted species and consequently presents a measure of defence for the plant against certain insects and herbivores.

### 2.6.2 Physicochemical properties of L-canavanine

L-Canavanine is a  $\delta$ -oxa-analogue of L-arg. The oxyguanidino group of L-can is structurally and electronically different from the guanidino group of L-arg (Figure 2.3). The electron density of the guanidino group is diminished due to the destabilising effect of the oxygen atom (Bence and Crooks, 2003). As a result, the guanidino group of L-arg has a pKa value of 12.48 compared to 7.05 for the oxyguanidino group of L-can (Swaffar *et al.*, 1994).

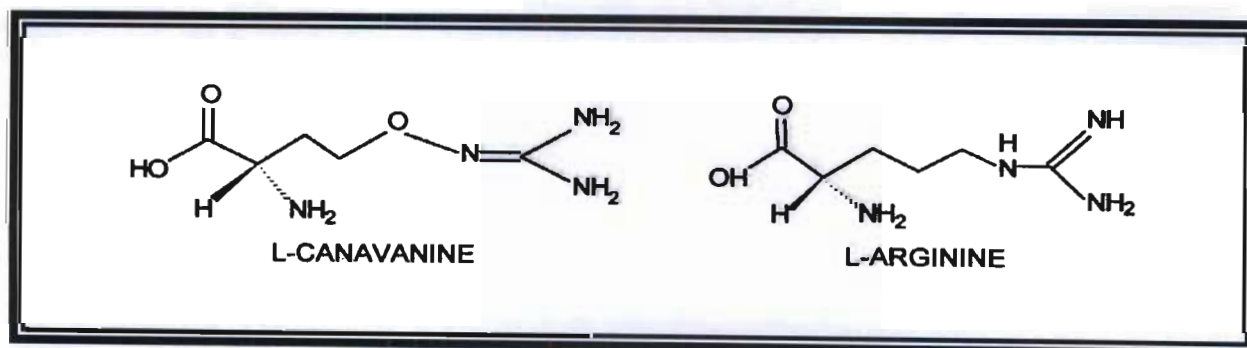


Figure 2.3 L-canavanine and L-arginine (Rosenthal, 1997).

When compared to L-arg, it has been established that L-can is less basic, slightly longer and exists mostly in the amino, rather than imino tautomeric form. These differences may be faint but they indeed have an evident effect on the differing physiological actions of L-can and L-arg. L-arginine for example, is a very important amino acid that is necessary for normal growth and development of cells (Bence and Crooks, 2003). L-canavanine on the other hand is cytotoxic and holds promise as a novel antimetabolite (Swaffar *et al.*, 1994).

### **2.6.3 Mechanism of action of L-canavanine**

Aminoacyl-tRNA synthetases are enzymes that are central to the maintenance of protein synthesis. These enzymes mediate the aminoacylation of their cognate tRNA to a specific amino acid. Aminoacyl-tRNA synthetases identify structural features of their associated tRNA and subsequently catalyse the esterification of their complementary amino acid to the associated tRNA thereby forming an aminoacyl-tRNA. The aminoacyl-tRNA activates the carboxylic acid of the amino acid in order to promote peptide bond formation and also provides a mechanism which allows for correct positioning as well as proper incorporation of the amino acid in a growing peptide chain (Bence and Crooks, 2003).

Arginyl-tRNA synthetase is a unique aminoacyl-tRNA synthetase in that it functions to load its complementary amino acid, L-arg, to arginyl-tRNA (Bence and Crooks, 2003). Some of the antimetabolic properties of L-can are presumed to be based on the inability of arginyl-tRNA synthetase to efficiently distinguish L-can from L-arg (Rosenthal and Dahlman, 1991b). During the synthesis of native proteins, the positively charged L-arg residues form ionic pairs with negatively charged amino acid residues. These interactions are critical in sustaining structural integrity and thus function of the associated protein. The substitution of an L-arg residue in a protein with L-can may considerably affect important interactions that function to institute the tertiary and quaternary structure of the protein (Rosenthal *et al.*, 1989). The resulting erroneous integration of L-can into proteins instead of L-arg leads to an induction of structural changes that ultimately alter protein function. At the same time, L-can further induces overall protein synthesis thereby accelerating the formation of aberrant proteins. This process forms the basis of L-can's antimetabolic activity (Rosenthal and Dahlman, 1991b).

L-canavanine may be a substrate or inhibitor of other L-arg utilising enzymes and/or pathways. Two such pathways are the polyamine and the nitric oxide synthase (NOS) pathways.

It is known that within mammalian cells the arginases mediate the divalent cation-dependent hydrolysis of L-arg to facilitate the synthesis of the nonprotein amino acid L-ornithine, which is the biosynthetic precursor of the polyamines (Ash, 2004).

Nitric oxide synthase however, utilises L-arg for the biosynthesis of nitric oxide (NO) and L-citrulline. The NOS reaction occurs in two steps, each requiring molecular oxygen (O<sub>2</sub>) and reduced NADPH as co-substrates (Luzzi and Marletta, 2005). Luzzi and Marletta (2005) have shown that L-can is an inhibitor of NOS. It was established that L-can functions as a substrate for the NOS reaction since it was shown to be converted to L-homoserine by the enzyme.

### **2.6.3.1 L-canavanine is loaded to arginyl-tRNA**

Using yeast, Allende and Allende (1964) were the first to demonstrate that L-can was loaded to arginyl-tRNA. Once L-can is loaded to arginyl-tRNA, its integration into the growing polypeptide chain is thereafter mandatory, the consequence of which is the formation of L-can-containing, structurally aberrant proteins (Rosenthal, 1977).

Other experiments demonstrated that L-can binds to arginyl-tRNA synthetase in a manner analogous to that of L-arg since both compounds bind to the active site of the enzyme in a virtually identical manner (Bence and Crooks, 2003).

### **2.6.3.2 L-canavanine is incorporated into proteins in place of L-arginine**

Studies have provided evidence that L-can can be loaded to arginyl-tRNA as well as be subsequently integrated into a growing peptide chain.

Evidence which established that L-can is incorporated into proteins was provided by Redman *et al.* (1983). Albumin was isolated after HepG<sub>2</sub> cells were incubated with L-can and it was determined that the albumin synthesised by L-can-treated cells displayed lower electrophoretic mobility compared to the albumin obtained from the control cells.

Other studies demonstrated the incorporation of L-can into proteins after *E. coli* K12 cells were exposed to L-[<sup>14</sup>C]-can. Antibodies specific to alkaline phosphatase were utilised and [<sup>14</sup>C]-labelled protein was isolated. The protein was thereafter analysed and compared to native protein, which contained 20-22 L-arg residues. Analysis of L-canavanyl proteins revealed that as many as 19 L-arg residues were replaced with L-can (Bence and Crooks, 2003).

Trypsin readily hydrolysed the native prohormones of glucagon, insulin, and somatostatin in anglerfish islets cells. In contrast, these prohormones resisted tryptic hydrolysis when cells were incubated with L-can. Trypsin normally cleaves the peptide chain at L-arg residues. The author suggested that the inability of the prohormones to be cleaved by trypsin was due to L-can incorporation in place of L-arg (Noe, 1981).

In addition, Rosenthal and Dahlman (1991a) determined that L-can replaced approximately one out of every three L-arg residues in the haemolymph of newly emerged *Manduca sexta* larvae following administration of L-guanidinoxy-<sup>14</sup>C]-can.

#### **2.6.3.3 Incorporation of L-canavanine results in altered protein conformation**

Vitellogenin, synthesised by the female locust (*Locusta migratoria migratoriodes*), is utilised in the synthesis of an essential protein called vitellin. L-canavanine was incorporated into vitellogenin in place of L-arg after exposure of the locust to L-can. It was established that 18 of the 200 L-arg residues in vitellogenin were substituted with L-can and that the incorporation of L-can into vitellogenin induced a three dimensional conformation of L-canavanyl-vitellogenin that was significantly different compared to that of native vitellogenin (Rosenthal *et al.*, 1989).

#### **2.6.3.4 Incorporation of L-canavanine alters protein function**

In response to a bacterial infection, lysozyme, a hydrolytic enzyme, is induced in insects and it functions to protect the organism by mediating lysis of the bacterial cell wall. Rosenthal and Dahlman (1991b) demonstrated that lysozyme function was adversely affected due to incorporation of L-can into its structure in place of L-arg. *Manduca sexta* were exposed to L-can and thereafter stimulated to produce lysozyme. It was established that L-can had substituted 21% of the L-arg in the induced lysozyme. Consequently, it was determined that L-can substitution resulted in a 49.5% loss of lysozyme activity.

Thomas and Rosenthal (1987) investigated the toxicity of L-can in Sprague-Dawley rats. The most significant changes noted after a single dose of L-can (2.0g/kg, s.c) were severe attenuations of serum aspartate (asp) and alanine aminotransferase activity.

Conformational and electronic changes are induced in proteins when L-can is incorporated into a nascent peptide chain in place of L-arg. A consequence of such substitution is the induction

of functional changes in the L-can-containing proteins. The above-mentioned effects represent the biochemical basis for the antimetabolic properties of L-can.

#### **2.6.4 Anticancer properties of L-canavanine**

Both *in vitro* and *in vivo* studies have displayed anticancer properties of L-can.

Berjjs and Green (1986) investigated the toxicity of L-can in the normal canine kidney epithelial cell line, Madin-Darby canine kidney (MDCK) as well as its chemically transformed derivative MDCK-T<sub>1</sub>. The normal cell line exhibited minimal cell death; however after 4 days of exposure to L-can more than 90% of the transformed cell line was killed.

Another study showed that L-can was cytotoxic to the human uterine sarcoma cell lines MES-SA (parental) and Dx-5 (MDR +), and to the human leukaemia cells lines K562 (parental) and K562-R7 (MDR +). Significant ( $p < 0.05$ ) cytotoxicity was observed in all cell lines after 72 h of exposure to concentrations greater than 1mM L-can (Worthen *et al.*, 1998).

In a more recent study, it was established that L-can mediated growth inhibition of the human lung adenocarcinoma cell line, A549, by arresting the cell cycle at the G<sub>1</sub> phase (Ding *et al.*, 1999).

L-canavanine was also cytotoxic to other human cancer cell lines including the bladder cancer cell line HTB9, and the cervical cancer cell line, HeLa. Exposure of each cell line to 3mM L-can for 48 h resulted in greater than 75% cell death (Bence and Crooks, 2003).

It has been established that L-can was cytotoxic not only to MIA PaCa-2 cells (Swaffar *et al.*, 1994), but also to other human pancreatic cancer cell lines such as PANC-1, CFPAC-1, Capan-1 and BxPC-3. After 72 h of exposure to 3mM L-can, cell cycle analysis revealed that the percentage of cells in the G<sub>2</sub>/M phase increased 4-fold in MIA PaCa-2 cells and 6-fold in PANC-1 cells (Bence *et al.*, 2003).

L-Canavanine does not only mediate cytotoxicity when evaluated *in vitro*, but also possesses the capacity to mediate shrinkage of tumour growth *in vivo*.

Thomas *et al.* (1980) instituted a study to assess the potential value of L-can as an anticancer agent. Tumours were induced in Fischer rats after a single injection (s.c) of a 10% tumour cell suspension (w/v). A 22% reduction in tumour volume was noted in animals receiving L-can (3.0g/kg) daily for 5 days. In addition, a 60% reduction in tumour volume was eminent in the 3.0g/kg-daily-for-9-day's treatment group. This study demonstrated the capacity of L-can to mediate significant growth inhibition of solid tumours in rats.

In a similar investigation, mice carrying an H5V tumour were used and a significant ( $p < 0.05$ ) reduction in tumour volume was noted when these animals were treated with L-can (30mg/kg, i.p) (Bence and Crooks, 2003).

In addition to the toxicity induced by L-can itself, L-canaline (L-2-amino-[4-aminooxy] butanoic acid), a metabolite of L-can metabolism (Rosenthal, 1981) may also contribute to L-can cytotoxicity.

### **2.6.5 Mechanisms of L-canaline toxicity**

L-canavanine is cleaved hydrolytically by arginase to yield L-canaline and urea. L-canavanine's structural analogy to L-arg corresponds exactly to the relationship of L-canaline to L-ornithine (Rosenthal, 1981). Rosenthal (1981) demonstrated that the possible basis of L-canaline's antimetabolic properties result from its ability to bind with pyridoxal phosphate, rendering the B<sub>6</sub> moiety of enzymes such as L-tyrosine decarboxylase employing this cofactor inactive. It was shown that L-canaline reacts with the aldehydic carbon atom of the pyridoxal phosphate moiety of B<sub>6</sub>-containing enzymes which leads to the blocking of the reactive  $\omega$ -NH<sub>2</sub> group. A Schiff's base linkage is thus formed and a concomitant loss in catalytic activity results.

In addition, a 27 % decrease in brain glutamic acid levels was noted when Rosenthal (1997) treated male Sprague-Dawley rats with 100 $\mu$ g of L-canaline.

It has also been reported that stable oximes are formed following the rapid reaction of L-canaline with glyoxylate and other 2-oxo acids, thereby indicating L-canaline's ability to scavenge 2-oxo-containing metabolites such as pyruvate and enabling it to mediate its anti-metabolic effects via depletion of tricarboxylic acid (TCA) cycle reserves (Rosenthal, 1981).



## 2.7 Apoptosis

Programmed cell death, also referred to as apoptosis, is an important physiological process that plays a crucial role in regulating the number of cells during the process of development and even throughout an organisms life, by mediating the removal of cells at the appropriate time (Zimmermann *et al.*, 2001). Cell death occurs in response to an array of stimuli and during the process of apoptosis it occurs in a strictly controlled, regulated manner (Dash, 2005).

During apoptosis, it is apparent that organelle integrity is maintained and that little external leakage of the contents of the apoptotic cell can be detected. As a consequence of such strict regulation, apoptotic cells do not mediate an inflammatory response (Slater *et al.*, 1995), making apoptosis distinct from another type of cell death called necrosis. During necrosis, the cell swells, its mitochondria dilate, organelles dissolve and the plasma membrane ruptures, releasing cytoplasmic material, often leading to an inflammatory response and potentially, to adverse health effects (Desagher and Martinou, 2000). In addition, necrosis appears to be an unregulated, passive process that is triggered by nonphysiological stimuli and unlike apoptosis it does not require energy or the synthesis of nucleic acids and proteins (Kim *et al.*, 2001).

It has been postulated that the dysregulation of the apoptotic process tends to play an integral role in the pathogenesis of a variety of human diseases and pathological conditions (Kaufmann and Hengartner, 2001). Cancer for example, is a disease characterised by little or no apoptosis due to mutations that are present which reduces the susceptibility of cells to apoptosis. Whereas cancer is a disease during which too little apoptosis occurs, there are other diseases where too much apoptosis is presumed to be the problem. In this regard, apoptosis is thought to account for most of the cell death as well as the progressive loss of neurons in neurodegenerative diseases such as Alzheimer's or Parkinson's disease (Dash, 2005). Other diseases associated with apoptosis include rheumatoid arthritis, acute neurological injuries, and cardiovascular diseases as well as AIDS. Therefore, the precise understanding and knowledge of the exact mechanisms involved in the process of apoptosis may prove important in the design of new therapeutic strategies (Zimmerman *et al.*, 2001).

During the early stages of apoptosis a family of proteins induces the cleavage of important cellular substrates required for normal function. These substrates include structural proteins in

the cytoskeleton as well as other degradative enzymes such as DNases, which cleave DNA in the nucleus (Dash, 2005).

Recently, rapid progress has been made in providing evidence for identifying the molecules that are responsible for the regulation and execution of apoptosis (Song and Steller, 1999). The proteolytic cleavages that occur during apoptosis are mediated by caspases – aspartate-directed cysteine proteases that selectively mediate the cleavage of more than 100 substrates when mammalian cells are subject to apoptosis (Kaufmann and Hengartner, 2001).

The biochemical features which have been documented to be associated with apoptosis include internucleosomal cleavage of DNA which leads to an oligonucleosomal ‘‘ladder’’ and PS translocation (Zimmermann *et al.*, 2001).

The consequence of such biochemical changes as well as the cleavage of susceptible substrates is the appearance of morphological changes in the cell (Dash, 2005). Morphological features that are used to define apoptotic cells include blebbing of the cell membrane, condensation of chromatin (due to breakdown of chromatin and nuclear structural proteins), nuclear fragmentation, loss of adhesion and rounding (in adherent cells), and cell shrinkage (due to cleavage of lamins and actin filaments) (Zimmermann *et al.*, 2001). Small membrane enclosed vesicles called apoptotic bodies may also be observed (Desagher and Martinou, 2000).

Apoptosis is thus a critical process that provides a safe and efficient way to continuously turnover cells in any tissue as well as provides an organism with the ability to remove specific or even surplus cells during developmental processes (Slater *et al.*, 1995).

### **2.7.1 Mechanisms of apoptosis**

There exist many mechanisms by which apoptosis can be induced and the sensitivity of cells to apoptotic stimuli may vary depending on various factors. In some cases apoptotic stimuli may comprise an extrinsic signal involving the ligation of cell surface receptors called death receptors (DRs) which generally occurs in damaged or virus infected cells (Dash, 2005). In other cases, apoptosis may be induced by intrinsic signals that arise following cellular stress, which include exposure to radiation or chemicals, growth factor deprivation, oxidative stress and physical damage especially to DNA and cell membranes (Fraser *et al.*, 1996; Dash, 2005).

### 2.7.1.1 Extrinsic cell death signalling

Death receptors are cell surface receptors that mediate the transmission of apoptotic signals initiated by specific ligands. They play a crucial role in apoptosis by functioning to activate an immediate caspase cascade following ligand binding. Induction of apoptosis via this mechanism is very rapid (Dash, 2005).

Cell surface DRs belong to the TNF receptor (TNFR) superfamily. The best-characterised family members include Fas (CD95) and TNFR1. Additional members of the TNFR superfamily include DR3 (Apo3), DR4, DR5 (Apo2) and DR6 (Ashe and Berry, 2003).

Death receptors are type I transmembrane proteins, a common feature of which is the presence of extracellular cysteine-rich domains which are involved in receptor-ligand interactions, and intracellular death domains (DDs), which function to bind to homologous domains on cytoplasmic adaptor molecules (Kaufmann and Hengartner, 2001; Figure 2.4).

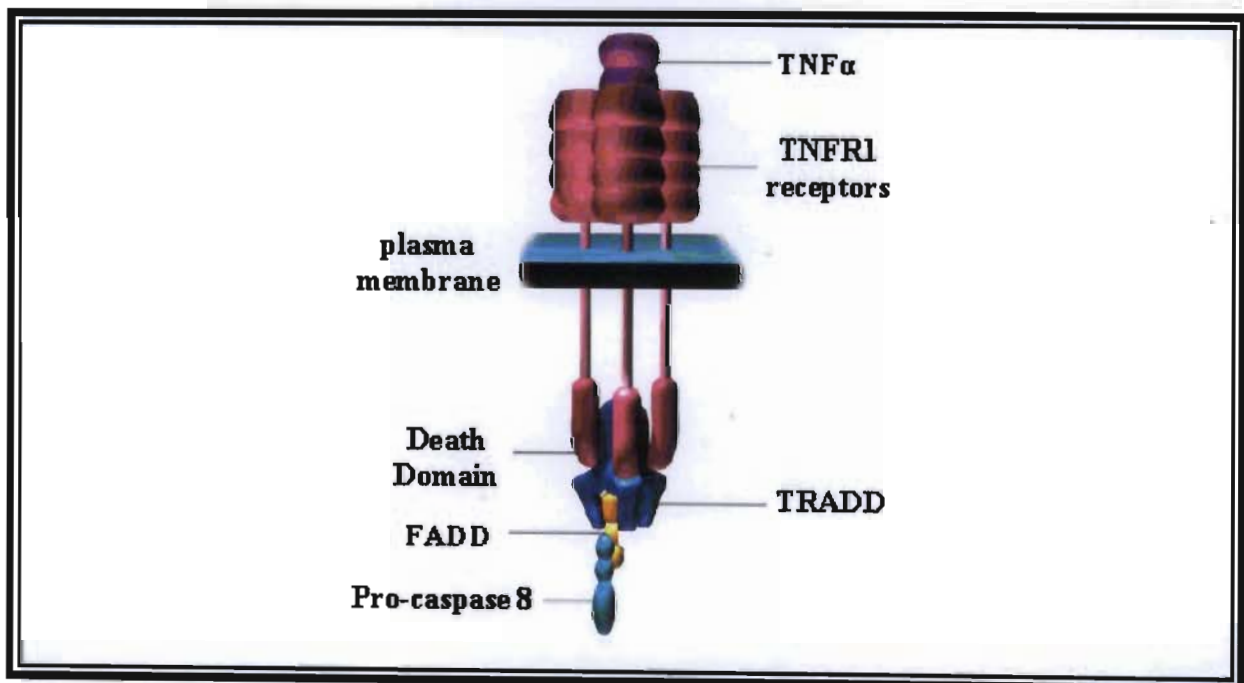


**Figure 2.4** Tumour necrosis factor- $\alpha$  signalling (Dash, 2005).

It has been documented that the ligand for these receptors is a trimer (Dash, 2005). Binding of extracellular ligands, such as Fas (a glycosylated cell surface molecule found abundantly in liver) to its cognate receptor is thus presumed to induce trimerisation of the receptor (Song and

Steller, 1999). After trimerisation and subsequent activation of DRs, other DD-containing proteins are recruited and serve as adaptor molecules in the signal transduction cascade (Ashe and Berry, 2003). An example is the association of the adaptor molecule FADD (Fas-associated death domain) to Fas (Kaufmann and Hengartner, 2001). FADD itself has a DD, and binds to Fas via DD-DD interactions (Zimmermann *et al.*, 2001). In addition to its DD, FADD also possesses a death effector domain (DED) which mediates its association with other DED containing proteins such as pro-caspases 8 (Ashe and Berry, 2003; Figure 2.4 and Figure 2.5).

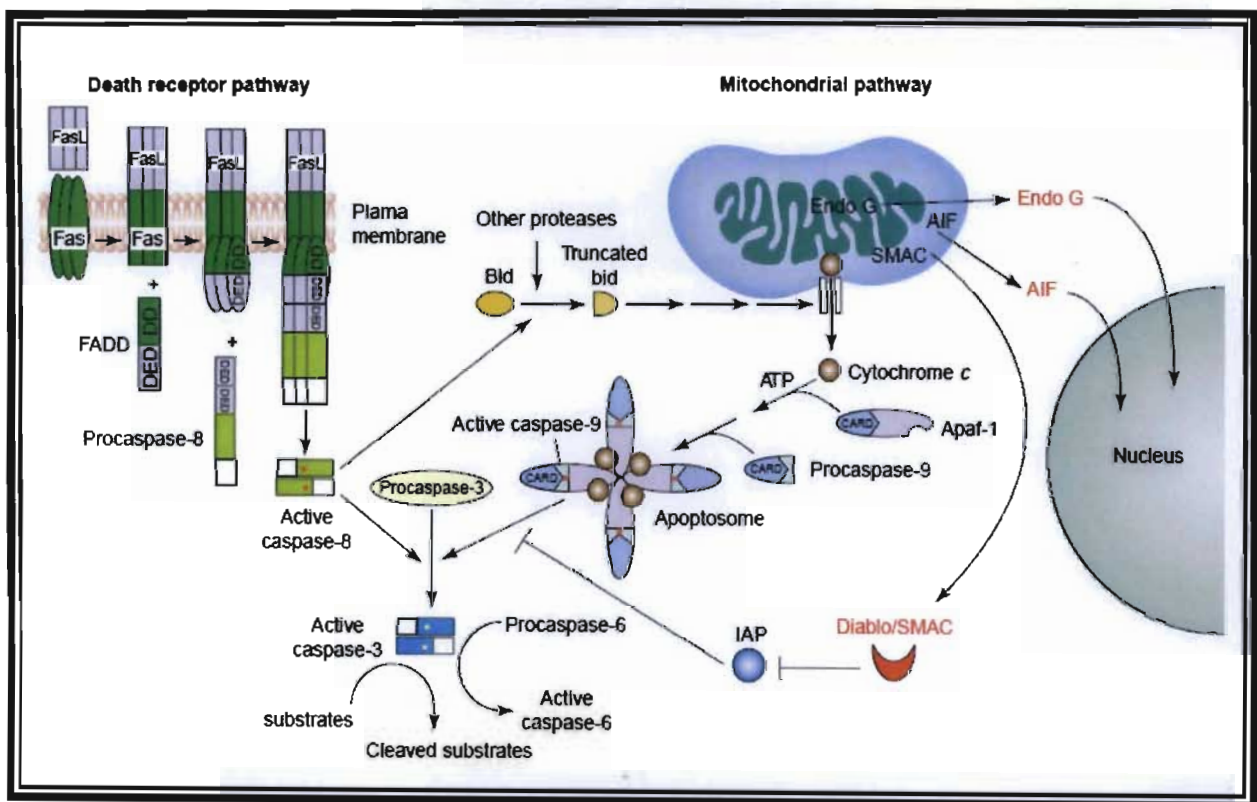


**Figure 2.5 Multiple pathways of caspase activation (Kaufmann and Hengartner, 2001).**

Pro-caspase 8 (FLICE – Fas activated protein like IL-1 $\beta$  converting enzyme) is thus able to associate with FADD via its own DED. The complex of proteins – Fas, FADD and pro-caspase 8 – is also known as the death inducing signalling complex (DISC) (Dash, 2005). The activation of procaspase-8 follows an “induced proximity” model (Chowdhury *et al.*, 2008). In this model, formation of the DISC after recruitment of procaspase-8 molecules to the Fas-FADD complex, juxtaposes multiple procaspase-8 zymogens, an event that mediates the autoproteolytic liberation of active caspase-8 into the cytosol (Kaufmann and Hengartner,

2001). Caspase-8 can then cleave downstream caspases such as caspase-3. Caspase-8 also cleaves a pro-apoptotic member of the Bcl-2 family, Bid, to truncated Bid (tBid) (Song and Steller, 1999). Truncated Bid is involved in the release of the mitochondrial proapoptotic factors: cytochrome c, Smac (second mitochondrial activator of caspases)/Diablo, AIF (apoptosis inducing factor) and endonuclease G (Ashe and Berry, 2003).

Despite the commonality of DISC association, DR-initiated signalling diverges in different cells. There are two types of cells using distinct Fas signalling pathways that have been identified (Ashe and Berry, 2003). In 'type I' cells, following DR ligation results the vigorous activation of caspase-8 and subsequently caspase-3. In all other cells ('type II'), caspase-8 activation is generally insufficient to mediate caspase-3 activation. Instead, caspase-8 cleaves the cytoplasmic protein Bid (Kaufmann and Hengartner, 2001). Thus, the extrinsic apoptotic pathway recruits an intrinsic apoptotic pathway (Ashe and Berry, 2003).

It is presumed that other DRs also activate caspase-8 through the same induced proximity mechanism (Kaufmann and Hengartner, 2001). It is likely that DR4 and DR5 signals similarly to Fas (Dash, 2005).

Signalling via TNFR1 however, is more complex than that occurring through the aforementioned receptors because of the requirement for another adapter protein known as TNFR-1-associated DD (TRADD). TRADD binds the ligated TNFR1 via DD-DD interactions (Zimmermann *et al.*, 2001; Figure 2.4). It is then able to recruit FADD to the complex, resulting in pro-caspase-8 recruitment and activation (Fraser *et al.*, 1996). Additionally, TNFR1 is able to mediate apoptosis by recruitment of another adapter molecule called RAIDD [RIP (receptor-interacting protein)-associated ICH-1 / CED-3 homologous protein with a death domain]. RAIDD associates with RIP via DD-DD interactions and contains a CARD (caspase recruitment domain) through which it can interact with and activate pro-caspase-2. Active caspase-2 functions similarly to caspase-8 and also cleaves Bid to tBid (Ashe and Berry, 2003).

In addition to the pathway mediated by Fas, an alternate, FADD-independent pathway exists. Daxx, an alternate Fas-binding protein, binds specifically to the Fas DD and mediates the activation of the Jun NH<sub>2</sub>-terminal kinase (JNK) pathway. Daxx may thus function as a link

between Fas and apoptosis signal-regulating kinase-1 (ASK1), a mitogen activated protein (MAP) kinase kinase kinase that is also able to activate apoptosis (Ashe and Berry, 2003).

#### **2.7.1.2 Intrinsic cell death signalling**

Mitochondria play an indispensable role in apoptosis (Zimmermann *et al.*, 2001). Various types of apoptotic stimuli, such as cytotoxic stress, oxidative stress, heat shock and DNA damage lead to the release of cytochrome c from the intermembrane space of the mitochondrion into the cytoplasm. A consequence of mitochondrial release of cytochrome c is the activation of the downstream execution phase of apoptosis (Chowdhury *et al.*, 2008). This phase of apoptosis is referred to as the intrinsic or mitochondrial pathway of apoptosis and is mediated by members of the Bcl-2 family of proteins (Aravind *et al.*, 1999), originally discovered as a proto-oncogene in follicular B-cell lymphoma (Zimmermann *et al.*, 2001). It has been demonstrated that many of these proteins are associated with the outer mitochondrial membrane (Aravind *et al.*, 1999).

The precise mechanism by which the Bcl-2 family regulates apoptosis remains controversial (Song and Steller, 1999). Some of these proteins are anti-apoptotic, while others are pro-apoptotic (Dash, 2005). They have been well characterised and their classification is based on the presence or absence of Bcl-2 homology (BH) domains of which there are four that exist (BH1-BH4) (Ashe and Berry, 2003). The anti-apoptotic members such as Bcl-2, Bcl-xL, Bcl-w, Mcl-1, A1, NR-13, and Boo, contain at least BH1 and BH2 (those most similar to Bcl-2 contain all four BH domains) (Zimmermann *et al.*, 2001). Two subfamilies of proapoptotic Bcl-2 family members have been identified; the bax family (Bax, Bok, and Bak), containing BH1, BH2, and BH3, and the BH3-only family [Bid, Bim, Bik, Bad, Bmf, Hrk, PUMA (p53-upregulated modulator of apoptosis) and Noxa] (Ashe and Berry, 2003).

Under normal cellular conditions, cytochrome c remains isolated in the inner mitochondrial membrane by being loosely (via ionic interactions) or tightly (via through hydrophobic interactions) bound to cardiolipin (Pretet, 2002). The precise mechanisms by which it is released from the mitochondrion are not clearly understood (Pretet, 2002), however, after its release, caspases are activated by a high molecular mass cytoplasmic complex referred to as the apoptosome and the cell is subsequently subject to undergo apoptosis (Zimmermann *et al.*, 2001; Chowdhury *et al.*, 2008).

It has been documented that after cellular damage or stress, Bax (generated due to activation of p53 during DNA damage-induced apoptosis) and Bak (generated by ionising radiation), which normally reside in the cytoplasm, translocate to the outer mitochondrial membrane. Here, they undergo a conformational change thereby allowing tBid to facilitate their insertion into the mitochondrial membrane (Kaufmann and Hengartner, 2001). It has been shown that Bax and other Bcl-2 proteins have structural similarities with pore-forming proteins. It was therefore suggested that Bax forms a transmembrane pore across the outer mitochondrial membrane, leading to the loss of membrane potential and efflux of pro-apoptotic factors (Dash, 2005) including cytochrome c, Smac, AIF and endonuclease G (Hofseth *et al.*, 2004).

On the contrary, anti-apoptotic Bcl-2 family members such as Bcl-2 itself, function at least in part, by selectively binding to the 'active' Bax, thereby preventing its insertion into the outer mitochondrial membrane (Kaufmann and Hengartner, 2001).

When cytochrome c is released from the mitochondrion into the cytosol, it interacts with apoptotic protease-activating factor-1 (Apaf-1) and ATP (Adrain and Martin, 2001; Figure 2.5). Apaf-1 has a CARD, which facilitates its interaction with pro-caspase-9. In the presence of cytochrome c and ATP, Apaf-1 undergoes a conformational change that exposes its CARD, thus inducing the recruitment of pro-caspase-9 (via CARD-CARD interactions). A consequence of such interactions is the generation of the cytochrome c–Apaf-1–procaspase-9 'apoptosome' and subsequent caspase-9 activation (Adams and Cory, 2002). Caspase-9 can then directly activate caspase-3 and 7, resulting in the orderly death of the cell via strictly regulated proteolytic processing of various downstream targets (Ashe and Berry, 2003).

It has recently been discovered that a protein with the dual name Smac/Diablo which is released from the mitochondria along with cytochrome c during apoptosis (Adrain and Martin, 2001), binds to domains within the inhibitor of apoptosis proteins (IAPs) to remove their inhibitory effect on caspase activity, thus promoting apoptosis (Ashe and Berry, 2003).

Another mitochondrial factor released together with cytochrome c and implicated in apoptosis is AIF, a flavoprotein that, once released from the mitochondrion, translocates to the nucleus (Ashe and Berry, 2003). In the nucleus, AIF induces DNA fragmentation and chromatin condensation, two key morphological features of apoptosis (Kaufmann and Hengartner, 2001).

Mitochondria also release endonuclease G, which is implicated in apoptotic DNA degradation (Kaufmann and Hengartner, 2001).

Thus, the sensitivity of cells to apoptotic stimuli depends on the balance of pro- and anti-apoptotic Bcl-2 proteins (Dash, 2005) and the exit from the mitochondrion indicates a new conflicting role for cytochrome c as a life-taker compared to its normal life-sustaining role in the electron transport chain (ETC) (Adrain and Martin, 2001).

### **2.7.2 Caspases**

The aspartate-specific cysteine protease (caspase) cascade is now envisaged to be the key pathway by which apoptotic cell death is orchestrated (Zimmermann *et al.*, 2001). An efficiently functional, well regulated apoptotic program requires multiple caspases and the contribution of the various caspases to the different phases of apoptosis is very critical (Algeciras-Schimmich *et al.*, 2002).

Caspases are similar in amino acid sequence, structure, and substrate specificity and are among the most specific proteases, having an unusual and absolute requirement for cleavage of their targets after asp residues. Consequently, due to the presence of asp in caspases themselves, these proteases are able to auto-activate or to be activated by other caspases as part of an amplification cascade (Zimmermann *et al.*, 2001).

Caspases are present within the cell as inactive latent pro-forms (zymogens) (Song and Steller, 1999) and contain three domains; an N-terminal prodomain, a large subunit containing the active site cysteine and a C-terminal small subunit (Zimmermann *et al.*, 2001).

Based on the structure of the prodomain and their functions, the caspases consist of 15 mammalian members, categorised into 3 subclasses. Those that contain large prodomains (caspase-1, 4, 5, 12, 13 and 14) play a role in cytokine maturation and inflammatory responses, and are referred to as inflammatory caspases (group-I). The second group of caspases have long prodomains containing either DED domains (caspase-8 and 10) or a CARD (caspase-2 and 9) and are called initiator of apoptosis caspases. Caspases that contain short prodomains (Group III) are called executioner caspases (caspase-3, 6, and 7) (Chowdhury *et al.*, 2008).



During caspase activation, which generally follows the induction of apoptosis through extrinsic or intrinsic death mechanisms, pro-caspases are cleaved at asp residues which facilitate the removal of the inhibitory pro-domain and consequently generate two distinct subunits (Song and Steller, 1999; Figure 2.5). These subunits are able to assemble into active proteases which then initiate apoptosis (Chowdhury *et al.*, 2008). Activation of the executioner caspases is often referred to as the apoptotic commitment point (Ashe and Berry, 2003).

Via adaptor molecules, DRs recruit initiator caspases-2, 8 or 10 whereas intrinsic death signals result in the activation of caspase-9 (Ashe and Berry, 2003; Figure 2.5). These caspases can then activate other caspases eventually promoting the activation of the executioner caspases, which are responsible for the cleavage of key cellular proteins that leads to the typical morphological changes observed in cells undergoing apoptosis (Dash, 2005).

Caspases bind to their substrates via interactions of the active site cleft with amino acids in the cleavage site. Substrates of caspases are categorised as nuclear proteins (lamin A and B, chromosome scaffold binding proteins, ribonucleoprotein-associated proteins), DNA metabolism and repair proteins (DNA-replication proteins, RNA-polymerase), protein kinases, signal transduction pathway proteins (phospholipases), cytoplasmic proteins (gelsolin, actin, adherens), cell cycle and cell proliferative proteins (p21, p27, pRB) and other apoptosis related proteins (Chowdhury *et al.*, 2008).

The caspase that is ultimately responsible for majority of the apoptotic effects is the most prevalent caspase, caspase-3. It is however supported by caspase-6 and 7. These three effector caspases initiate the apoptotic phenotype by facilitating cleavage and/or degradation of several critical cellular substrates. An example is DNA fragmentation mediated by the action of caspase-3 on a complex of caspase-activated deoxyribonuclease (CAD) and iCAD, its inhibitor. Under non-apoptotic circumstances CAD is present in an inactive complex with iCAD (Zimmermann *et al.*, 2001). During apoptosis however, active caspase-9 damages nuclear pores, allowing nuclear entry of caspase-3 which in turns cleaves iCAD, thus liberating CAD and allowing apoptotic DNA fragmentation and chromatin digestion (Kaufmann and Hengartner, 2001). In addition, it is believed that membrane blebbing observed during apoptosis occurs due to the cleavage of gelsolin and fodrin, a consequence of which is the dissociation of the plasma membrane from the cytoskeleton (Zimmermann *et al.*, 2001).

Caspase activity is inhibited by different groups of natural inhibitors (Aravind *et al.*, 1999). Many proteins that prevent cell death via caspase activation have been identified. The most well known are the IAPs, which bind to and inhibit active caspase-3, 7 and 9 (Chowdhury *et al.*, 2008) or stimulate proteasomal degradation of caspase-3 and 7 (LeBlanc, 2003).

The action of caspases may also be regulated at other levels including blockade of caspase activation at the DISC (Chowdhury *et al.*, 2008). A molecule referred to as cFLIP (FLICE inhibitory protein) is able to block Fas-mediated apoptosis (Zimmermann *et al.*, 2001). It is an inactive caspase homologue, whose catalytic site is damaged thus enabling it to serve as a dominant negative modulator of caspase activity. It inhibits the activation of procaspase-8 at the DISC by blocking and thus preventing its processing (Chowdhury *et al.*, 2008). It is recruited to the ligated Fas signalling complex, but cannot convey the death signal required to initiate apoptosis (Zimmermann *et al.*, 2001).

Apoptosis is thus a complex process involving many protein families, subcellular compartments, and signal transduction cascades and, cell type and mode of apoptotic induction are critical factors with respect to which apoptotic pathway is recruited.

### **2.7.3 The role of p53 in apoptosis**

The gene that encodes p53 is a well-defined tumour suppressor gene (Chen, 1999). Tumour suppressor protein p53 is frequently referred to as the 'guardian of the genome' or the 'cellular gatekeeper' (Brooks and Gu, 2003). At the biological level, p53 has been implicated as a key mediator of the cellular response to DNA damage (Haffner and Oren, 1995). One well defined role of p53 is to survey cellular stress and induce apoptosis, if necessary (Hofseth *et al.*, 2004). However, the mechanism of p53-mediated apoptosis in response to cellular stresses such as DNA damage remains poorly understood (Moll and Zaika, 2001).

Mouse double minute 2, an E3 ligase in an ubiquitinase pathway, which binds to p53 and promotes its polyubiquitination and degradation by proteasomes, normally maintains p53 at low levels within the cell (Brooks and Gu, 2003). p53 and Mdm2 are phosphoproteins, both of which contain several phosphorylation sites (Kubbutat and Vousden, 1998).

DNA damage results in the formation of DNA chain breaks and changes in chromatin structure that activate chromatin-bound protein kinases such as ATM (ataxia telangiectasia mutated protein) and ATR (ATM related) which then phosphorylate p53 (Hickman *et al.*, 2002). Another protein kinase, double-stranded DNA-dependent protein kinase (DNA-PK), is activated by double-stranded DNA breaks and also phosphorylates p53 (Kubbutat and Vousden, 1998). Phosphorylation of p53 results in a reduction of p53-Mdm2 binding (Lohrum and Vousden, 2000; Figure 2.6). Acetylation of p53 also contributes to preventing the binding of Mdm2 to p53 and enzymes such as CBP/p300, a protein possessing histone acetyl transferase (HAT) activity, mediates the acetylation of p53 (Brooks and Gu, 2003). Additionally, internal aberrations such as the deregulation of cellular oncogenes may lead to p53 stabilisation. Overexpression of some oncogenes induces expression of 14/19ARF which can bind directly to Mdm2 reducing its capacity to bind p53 (Hickman *et al.*, 2002).

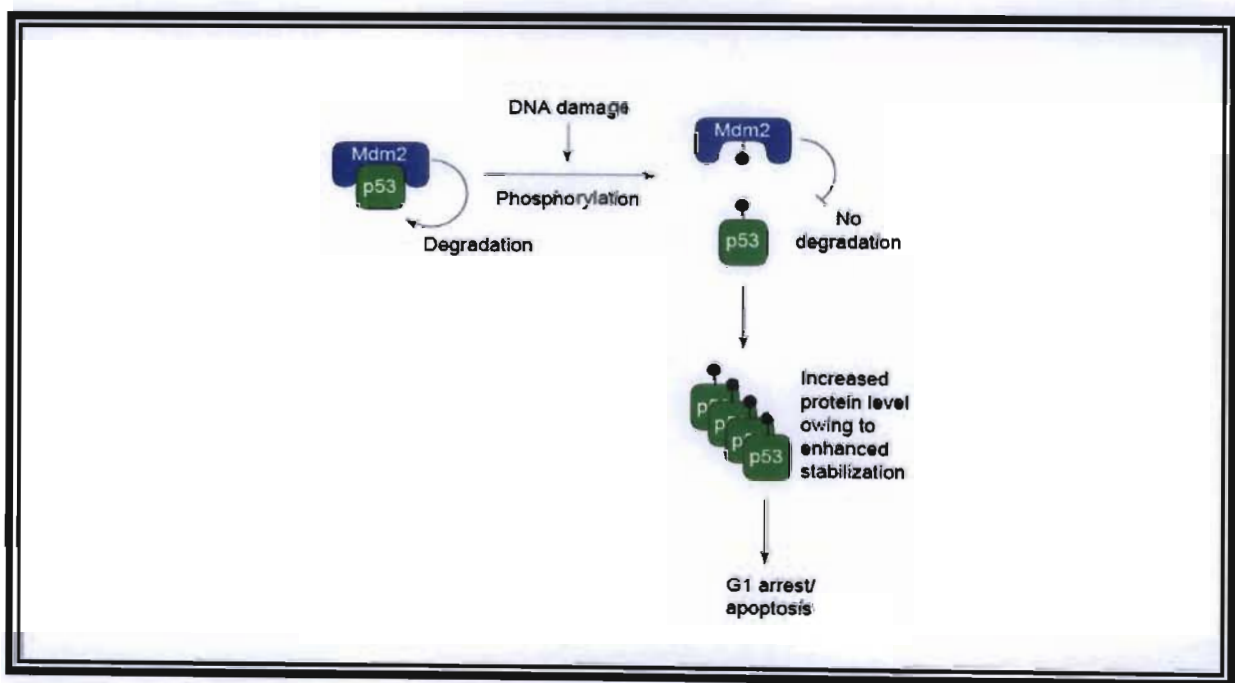


**Figure 2.6 Regulation of p53 stability and function in response to genotoxic stress (Kubbutat and Vousden, 1998).**

It is possible that phosphorylation, acetylation and binding of 14/19ARF to Mdm2, contribute to the resistance of p53 to Mdm2-mediated degradation and a subsequent increase in the levels and activity of p53 (Lohrum and Vousden, 2000).

After p53 activation, it accumulates in the nucleus where it binds to specific DNA sequences and induces transcription (Komarova and Gudkov, 1998). Transcriptional activation and transcriptional repression are the best described biochemical functions ascribed to p53 and are important for apoptosis induction (Yu and Zhang, 2005). Apoptosis-associated genes that are upregulated in response to p53 activation include Bax (Bensaad and Vousden, 2007), Fas, Apaf-1 (Ashe and Berry, 2003), DR4, DR5 (Yu and Zhang, 2005), Bid (Hofseth *et al.*, 2004), PUMA and Noxa (Hickman *et al.*, 2002). In contrast, apoptosis-associated genes postulated to be suppressed by p53 include Bcl-2, Bcl-xL (Yu and Zhang, 2005) and cFLIP (Ashe and Berry, 2003).

p53 also promotes apoptosis via transcription-independent mechanisms. It forms complexes with anti-apoptotic Bcl-2 proteins via its DNA-binding domain (Zeimet, 2003), promotes the activation of Bax and mediates the cell surface redistribution of Fas (Ashe and Berry, 2003).

p53 possesses the capacity of adjusting the biological response to the nature of the activating signal. In particular, it can stimulate apoptosis when cells are confronted with severe, irreparable damage, whilst mediating growth arrest when cellular damage is minimal, thus enabling the cell to repair the damage and resume normal life and function (Shmueli and Oren, 2007). The induction of the cyclin-dependent kinase inhibitor p21 (*waf1/cip1*) is an example of a principal effector of growth arrest (Kubbutat and Vousden, 1998).

#### **2.7.4 The modulation of apoptosis by different heat shock gene products**

As a consequence of being alive, cells of all organisms constantly endure a multitude of “damages” induced by internal as well as external factors. As a result, living systems have evolved many strategies to facilitate repair of the damage and/or eliminate the damaged components (Arya *et al.*, 2007).

Damage to cells can elicit two opposing responses; apoptosis, and the heat shock response (HSR), which prevents damage and/or mediates a recovery process to maintain cell survival. Interactions between these pathways are critical in determining the fate of a cell (Beere, 2004).

The HSR is a carefully coordinated series of biochemical and genetic events often involving rapid induction of heat shock protein (Hsp) gene expression in response to stress (Powers and

Workman, 2007). Heat shock proteins were first discovered in 1962 as a set of highly conserved proteins whose expression was induced by various stresses (Garrido *et al.*, 2001). These proteins can be induced by many stresses including those imposed by heat shock, chemotherapeutic agents, ultraviolet (UV) irradiation, TNF (Beere, 2004), amino acid analogues, infection, inhibitors of energy metabolism, heavy metals (Li *et al.*, 2000), ischemia (Sharp *et al.*, 1999) and oxidative stress (Kim *et al.*, 2005).

The Hsp's are highly conserved and are abundant in nearly all subcellular compartments (Santoro, 2000). They are classified into distinct families on the basis of their molecular weights, functions and amino acid sequences (Arya *et al.*, 2007). There are many members of the Hsp family, the most important of which are Hsp70 and Hsp90 (Sharp *et al.*, 1999).

In physiological conditions some of the Hsp's function as intracellular molecular chaperones (Pockley, 2003). The term chaperone is assigned to a protein that selectively recognises and binds to the exposed hydrophobic surfaces of a non-native protein in a noncovalent interaction in order to inhibit irreversible aggregation (Slavotinek and Biesecker, 2001).

Some of the important house-keeping functions of molecular chaperones include: (1) import of proteins into cellular compartments; (2) folding of proteins in the cytosol, mitochondria and endoplasmic reticulum (ER); (3) refolding of misfolded proteins; (4) prevention of protein aggregation; (5); degradation of unstable proteins (6) dissolution of protein complexes; and (7) control of regulatory proteins (Garrido *et al.*, 2001).

Besides their function in regulating cellular homeostasis as molecular chaperones, another interesting example of the integrative roles of Hsp's is their involvement in the apoptotic pathways and subsequent promotion of cell survival (Arya *et al.*, 2007).

The accumulation of denatured/abnormally folded proteins as a consequence of cellular stress results in the formation of aggregates that perturbs normal cellular function and prompts cell death (Parcellier *et al.*, 2003). Such denatured proteins initiate the HSR by binding to Hsp90, resulting in the dissociation of Hsp90 from certain heat-shock factor (Hsf) proteins (Figure 2.7). Under normal conditions, Hsp90 binds to and suppresses the Hsf's. The dissociation of Hsp90 from Hsf's results in the phosphorylation of Hsf's by protein kinase C (PKC) for

example, a consequence of which is Hsf activation. The activated Hsf's then form trimers which bind to the promoter region of the Hsp70 gene and stimulate transcription. This leads to a substantial increase in Hsp70 mRNA and protein levels within the stressed cells. Following its synthesis, Hsp70 binds to denatured proteins in an attempt to restore the tertiary structure and enzymatic activity of the affected proteins in a cycle that is driven by ATP hydrolysis. Denatured proteins are therefore able to serve as a stimulus for the induction of the expression of Hsp70, and Hsp70 can in turn restore protein structure and function (Sharp *et al.*, 1999).

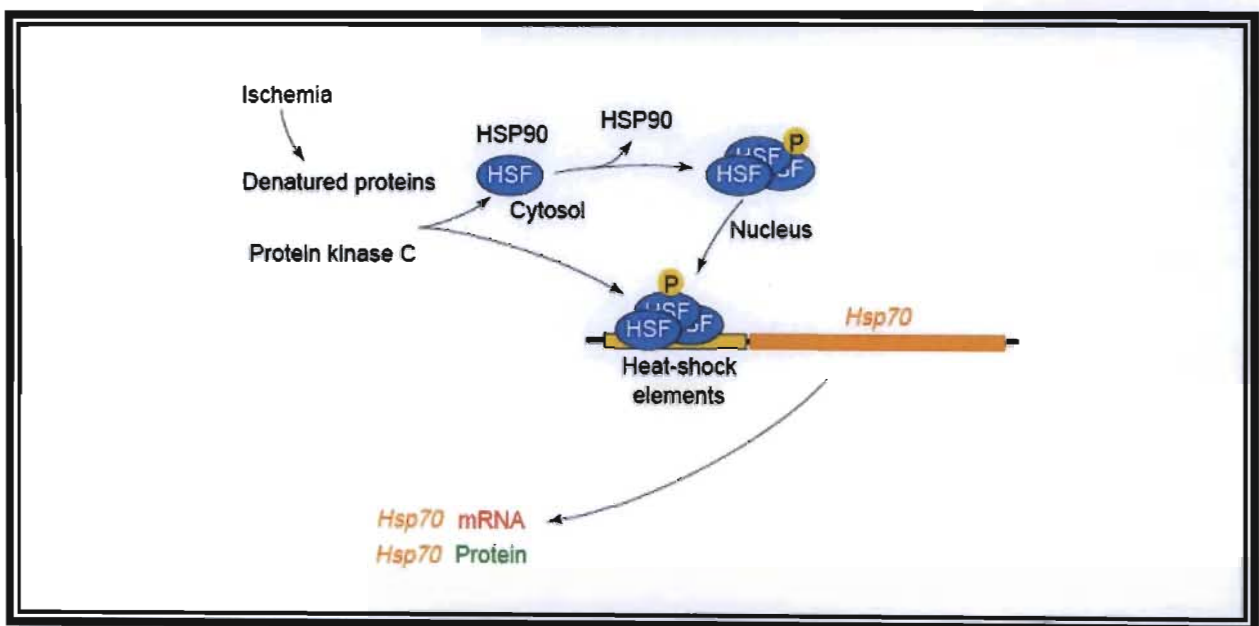


**Figure 2.7** The mechanism of heat shock protein 70 production (Sharp *et al.*, 1999).

### 2.7.4.1 Heat shock protein 70

Heat shock protein 70 is an ATP-dependant inducible Hsp (Sharp *et al.*, 1999) that interacts with almost all newly synthesised, unfolded proteins (Powers and Workman, 2007).

The following describes the role of Hsp70 in apoptosis:

- It interacts directly with the CARD of Apaf-1, either preventing its oligomerisation (LeBlanc, 2003) or maintaining the oligomer in a conformation incompatible with pro-caspase-9 recruitment thus preventing apoptosome formation (Beere, 2004).
- It associates with the N-terminal region of AIF via its peptide domain thereby preventing the nuclear import of AIF after its release from mitochondria (Beere, 2004).

- Hsp70 can inhibit JNK mediated cell death by suppressing JNK phosphorylation either directly and/or through direct inhibition of ASK1 (Arya *et al.*, 2007). JNK phosphorylates c-Myc and p53 both of which mediate mitochondrial release of cytochrome c. JNK is also implicated in the release of Smac from mitochondria. The ability of Hsp70 to disrupt JNK signalling could thus impact on many pathways in the apoptotic process and possibly represents the underlying mechanism of Hsp70-mediated suppression of cytochrome c release (Beere, 2004).
- It has also been shown to directly associate with p53 and c-myc (Parcellier *et al.*, 2003).
- Hsp70 prevents Bax from undergoing a conformational change and translocation to the mitochondria (Powers and Workman, 2007).
- It binds to and inhibits caspase-3 activity (Sreedhar and Csermely, 2004).
- The integrity of the lysosomal membrane is maintained by Hsp70, thereby preventing the release of hydrolases such as cathepsin into the cytosol and subsequently impeding a lysosome-mediated caspase independent cell death pathway (Arya *et al.*, 2007).
- It suppresses TNF-induced apoptosis in many cell types (Beere, 2004).
- It prevents the cleavage and activation of Bid (Beere, 2004).
- Bag-1 is a co-chaperone identified as an anti-apoptotic protein because of its ability to bind Bcl-2. It also binds to and sequesters FADD (Sreedhar and Csermely, 2004). Hsp70 binds to and modulates the function of Bag-1 (Sharp *et al.*, 1999).

#### **2.7.4.2 Heat shock protein 90**

Heat shock protein 90 is also an ATP-dependant chaperone which is quite abundant and constitutes approximately 1-2% of total cellular protein. Its chaperone functions involve ensuring the correct conformation, activity, intracellular localisation and proteolytic turnover of proteins involved in cell growth, differentiation and survival (Powers and Workman, 2007).

Like Hsp70, it inhibits apoptosis by directly binding to Apaf-1 and preventing the formation of the apoptosome (Sreedhar and Csermely, 2004).

Apoptotic-inducing signals are intimately coupled to cell-survival signals. One pathway that promotes cell survival utilises a serine/threonine kinase, Akt, which is activated via phosphoinositide 3 kinase, by an array of growth factors (Arya *et al.*, 2007). Phosphorylation

stabilises Akt, which activates NF- $\kappa$ B, but can also induce phosphorylation of Bad, resulting in the dissociation of Bad from Bcl-xL (Beere, 2004). Phosphorylated Bad can then be sequestered by the 14-3-3 protein in the cytosol. Consequently, translocation of Bad to mitochondria and subsequent downstream apoptotic events are not triggered (Sreedhar and Csermely, 2004).

Although TNF is a potent inducer of cell death, it can also contribute to cell survival via NF- $\kappa$ B. This serves as an important link in many biological processes including stress responses, cell growth or death (Arya *et al.*, 2007).

Under normal physiological conditions, NF- $\kappa$ B is bound and sequestered in the cytosol by its inhibitor I $\kappa$ B. Upon exposure to stimuli, such as TNF, I $\kappa$ B is subsequently degraded. This promotes the release of NF- $\kappa$ B, which can translocate to the nucleus and initiate the transcription of cell survival genes. Phosphorylation and subsequent inactivation of I $\kappa$ B is facilitated by a protein kinase complex termed I $\kappa$ B kinase (IKK). TNF mediates the activation of IKK via its association with signal transducing molecules like RIP (Arya *et al.*, 2007).

Hsp90 interacts with and is essential for the stability of RIP (Parcellier *et al.*, 2003). It also directly interacts with and maintains the activity of Akt by inhibiting its dephosphorylation (Beere, 2004). In addition, Hsp90 and its co-chaperone Cdc37 assist in the formation of active IKK or Akt complexes. All of these effects of Hsp90 mediate the disassociation of NF- $\kappa$ B from its inhibitor and promotes cell survival (Arya *et al.*, 2007).

Besides its direct role of promoting cell survival, the Hsp90-Akt complex can also indirectly promote cell survival by inhibition of JNK-mediated cell death through phosphorylation and subsequent inactivation of ASK1 (Arya *et al.*, 2007).

At any point in time, a living cell is a multi-tasking system in which a multitude of signals are processed; however the responses to any one or more of these activities have to be integrative. Due to the nature of their functions, Hsp's appear to be significant co-ordinators of cellular signals and responses (Arya *et al.*, 2007). Thus, their involvement in a multitude of intracellular actions places them as central coordinators in determining the fate of a cell.



## Chapter 3

# CELL CULTURE AND CYTOTOXICITY

### 3.1 Introduction

The culture of cells and tissues is now a frequently utilised technique in a variety of disciplines from the basic sciences of cell and molecular biology to the rapidly evolving field of biotechnology (Freshney, 1992).

The interest in cellular *in vitro* models is due to the fact that they represent the elementary living unit and, at least theoretically, cells from any species and tissue can be cultivated, including those of human origin. Moreover, this type of experimentation bypasses most of the ethical problems associated with human experimentation, involves a reduction of animal studies that are often in the public protest limelight, and also reduces the financial costs incurred by animal studies (Clynes, 1998).

The list of different cell types which can now be grown in culture is extensive (Freshney, 1992) presumably because *in vitro* culture facilitates a controlled and manipulated environment, in which the biochemical mechanisms of toxicity can be more specifically analysed.

### 3.2 The cell and its environment

It is presumed that the best environment for growing cells *in vitro* is one providing as closely as possible the conditions they experience *in vivo*. The essential requirements for an optimum cell culture environment are temperature and pH, gas phases, a suitable substrate and media containing the necessary nutrients (Freshney, 1992).

#### 3.2.1 Temperature and pH

The optimal temperature for cell culture depends on the body temperature of the organism from which the specific cell type was obtained. Thus, the temperature required for optimal growth of most human cell lines is 37°C which is accomplished *in vitro* by the use of a humidified carbon dioxide (CO<sub>2</sub>) incubator.

Ideally, pH should be near 7.4 at the initiation of a culture and not fall below a value of 7.0.

### **3.2.2 Gas phases**

The most important gases required *in vitro* are O<sub>2</sub> and CO<sub>2</sub>. It is necessary to supply O<sub>2</sub> to the medium throughout the life of the culture and this is accomplished by maintaining O<sub>2</sub> tension at atmospheric pressure. The rule is that the bicarbonate and CO<sub>2</sub> tension must be in equilibrium. Hepes is a satisfactory buffer able to perform this function by maintaining the correct pH without the requirement of an enriched atmosphere (Freshney, 1992).

### **3.2.3 Substrate**

Some cultures can be propagated in suspension, but most are propagated as a monolayer, anchored to a substrate. Polystyrene which has been treated to make it wettable and give it a net negative charge is now utilised almost universally as a substrate. Single use polystyrene flasks provide a simple and reproducible environment for cultured cells because they can be sealed, do not need a humid CO<sub>2</sub> incubator and provide better protection against contamination (Freshney, 1992).

### **3.2.4 Medium**

The culture medium is by far the most important single factor in culturing cells. The extracellular medium must meet the essential requirements (nutritional, hormonal and stromal factors) for survival and growth (Freshney, 1992).

A complete culture medium (CCM) contains Eagle's minimum essential medium (EMEM; Appendix 1), foetal calf serum (FCS), L-glutamine as well as antibiotics and antifungal agents.

Eagle's minimum essential medium is a commercially prepared growth medium that contains essential amino acids, vitamins and salts.

Foetal calf serum is a complex mixture of various small and large biomolecules with different, physiologically balanced growth promoting and growth inhibiting properties. Some of the major functions of FCS is to provide the following: basic nutrients, in solution and bound to proteins; hormones and growth factors for stimulating growth and specialised functions; attachment and spreading factors; binding proteins (albumin and transferrin) carrying hormones, vitamins, minerals and lipids; protection factors against mechanical damage; protease inhibitors as well as contribution to buffering (Freshney, 1992).

A given concentration of nutrients can only support a certain number of cells. One of the nutrients most likely to be exhausted first is L-glutamine, partly due to it spontaneously cyclising to pyrrolidine carboxylic acid and also because it can be enzymatically converted by serum and cellular enzymes to glutamic acid, leucine and isoleucine (Freshney, 1992). For these reasons, media is usually supplemented with a further 1% of L-glutamine.

In an attempt to counteract microbial and fungal contamination, media is also supplemented with Penstrep-Fungizone, a cocktail of antibiotics and antifungal agents. It contains Penstrep, a mixture of the antibiotics penicillin and streptomycin, and Fungizone, an antifungal agent.

### **3.3 The HepG<sub>2</sub> cell line**

The liver is the most important drug metabolising organ in mammals. Liver cell lines, which have retained the activities of drug metabolising enzymes involved in the activation and detoxification of carcinogens, reflect the cytotoxic effects of such substances better than stable mammalian cell lines, which are currently used in routine testing and require the addition of exogenous activation homogenates (Majer *et al.*, 2004).

One of the most promising lines is the human HepG<sub>2</sub> cell line which was originally isolated in 1979 from a primary hepatoblastoma of an 11-year-old Argentinean boy (Uhl *et al.*, 2000).

These cells have an epithelial like morphology which resembles liver parenchymal cells and they synthesise and secrete many of the plasma proteins characteristic for normal human liver cells (Knasmuller *et al.*, 1998). They have retained many of the functions of normal liver cells and express different inducible xenobiotic metabolising enzymes (phase I and phase II biotransformation enzymes) that play key roles in the activation and detoxification of DNA reactive carcinogens (Belloir *et al.*, 2006).

Isoenzymes of several CYP<sub>450</sub> families (including CYP3A4) which are responsible for the activation of diverse promutagens are present in HepG<sub>2</sub> cells. Apart from the CYP<sub>450</sub> isozymes, several other oxidoreductases involved in either electron transfer processes to CYP<sub>450</sub> isozymes or in the activation of ROS are also expressed by HepG<sub>2</sub> cells. In addition, they have no known point mutations in tumour suppressor genes, p53 and pRb (Knasmuller *et al.*, 1998).

In all animal species examined to date, including man, the liver frequently demonstrates to be the primary target organ for AFB<sub>1</sub> (Neal, 1995). It is for this and the abovementioned reasons that a liver cell line, specifically the HepG<sub>2</sub> cell line, was selected for this study.

### 3.4 Cytotoxicity testing

The broad aim of *in vitro* toxicity testing is to screen compounds in order to elucidate their general toxicity. Cell culture systems have different areas of application in toxicology according to the aim of the study, which can either be to investigate a particular mechanism or to screen chemicals (Clynes, 1998).

*In vitro* toxicity testing is based on a few assumptions which include: a) a variety of pathologies are related to a small number of crucial events at a cellular level, especially where acute toxicity is concerned; b) several elements of the organisms complexity may be mimicked *in vitro*; and c) the exposure conditions may be efficiently reproduced *in vitro* (Clynes, 1998).

The assay most commonly utilised to measure cytotoxicity *in vitro* involves the use of a tetrazolium salt, methyl thiazol tetrazolium or MTT [3,(4,5-dimethylthiazol-2-yl)-2,5-diphenyl tetrazolium bromide] (Freshney, 1992). This technique is particularly useful for cells which are metabolically active but not proliferating and is based on the capacity of mitochondrial dehydrogenase enzymes (succinate dehydrogenase) to reduce the yellow, water-soluble salt into a purple insoluble formazan product. The insoluble crystals may then be dissolved in dimethyl sulfoxide (DMSO) and the absorbance can be read with a spectrophotometer (560nm). The amount of formazan produced is directly proportional to cell number thus allowing for the determination of cell viability and proliferation by this assay (Clynes, 1998).

The aim of this chapter was to utilise the MTT assay to determine IC<sub>50</sub> values after exposure of HepG<sub>2</sub> cells to various dilutions of an SF water extract, when administered individually and in combination with AFB<sub>1</sub>.

## **3.5 Materials and Methods**

### **3.5.1 Ethical approval**

This study was given full ethical approval by the Biomedical Research Ethics Committee (Reference No: BE050/08).

### **3.5.2 Materials**

Aflatoxin B<sub>1</sub> and L-can were purchased from Sigma (SA). A bottle of SF tablets (60 x 300mg) was obtained from Phyto Nova Natural Medicines (SA). Penstrep-Fungizone, EMEM, FCS, culture flasks, 96-well plates and sterilin tubes were purchased pre-sterilised from Adcock Ingram (SA). Ethanol, phosphate buffered saline (PBS) tablets and DMSO was acquired from Merck (SA).

### **3.5.3 Methodology**

#### **3.5.3.1 Cell culture environment**

Prior to work being conducted in the tissue culture laboratory, hands were sanitised with 5% hibitane (chlorhexidine gluconate), an antiseptic which sterilises and provides moisture, reducing the risk of dry skin and loosely adherent micro-organisms serving as a source of contamination. Personal protective equipment including sterile gloves and a clean laboratory coat were also worn. All cell culture procedures were conducted under a microbiological safety cabinet equipped with a UV light and continuous laminar flow. The cabinet was always sterilised with 70% ethanol both before and after use. In addition, gloves as well as all materials and equipment used during the session were swabbed with 70% ethanol before any work commenced.

#### **3.5.3.2 Preparation of cell culture media and freezing medium**

Cells were maintained in EMEM containing 10% FCS supplemented with 1% L-glutamine and 1% Penstrep-Fungizone.

Dimethyl sulfoxide was added at a concentration of 10% to CCM. This served as a freezing medium for storing cells at -80°C. Dimethyl sulfoxide is a dipolar organic solvent and was utilised as a cryoprotective agent because it doesn't crystallise at -80°C, a property which enables it to form a protective layer around the cell during cryopreservation and minimise the formation of ice crystals.

### **3.5.3.3 Trypsinisation**

Trypsin is a proteolytic enzyme that aids in the digestion of connective tissue of cells and their cell membranes.

Trypsinisation was conducted by initially discarding the spent culture medium from the tissue culture flask. Cells were then rinsed with three changes of pre-warmed (37°C) PBS so that the residual culture medium and any cellular debris was effectively removed. This process was efficiently carried out by briefly shaking the flask containing PBS and thereafter discarding the PBS-wash solution. Pre-warmed (37°C) trypsin was thereafter added to the culture flask (just enough to submerge the attached cell monolayer). The flask was then sealed and placed in the incubator (37°C) for approximately 2 minutes. Following the incubation period, cells were visualised using an inverted light microscope (Olympus IXSI; 20x magnification) to observe morphological changes of the cells. Cells were considered to be trypsinised if they were rounded and if the intercellular processes were no longer visible.

The trypsin solution was then discarded followed by the addition of pre-warmed (37°C) CCM to the culture flask. The FCS in CCM serves as an inhibitor of trypsin thus neutralising the residual trypsin in the flask which may otherwise result in damage to cell surface receptors if the cells are exposed for too long. The flask was then energetically shaken until the cells were in suspension. Cells were then counted and subsequently subcultured or utilised for specific assays.

### **3.5.3.4 Cell counting by dye exclusion using a haemocytometer**

Trypan blue (0.4%) was utilised in a dye exclusion procedure for cell counting. The principle is that non-viable cells readily take up the dye and are visualised as being stained blue whereas viable cells are visualised as unstained cells because they are unable to take up the dye.

Cell numbers were determined using a Neubauer haemocytometer which comprised 2 chambers, each further consisting of nine 1mm squares (Figure 3.1, A-E). Prior to cell counting, the haemocytometer was sterilised with 70% ethanol and a coverslip was affixed to it.

Cells were thereafter brought into suspension by trypsinisation and a cell counting solution containing 150µl CCM, 50µl trypan blue and 50µl of the CCM-cell suspension was made up in an eppendorf, vortexed and allowed to stand for 5 minutes. The resulting solution provided a dilution factor of 1:5.

With the coverslip in place, 15µl of the cell counting solution was then pipetted into each chamber of the haemocytometer. The solution was allowed to be drawn out of the pipette and into each chamber by capillary action. The haemocytometer was then placed under the microscope and bright field settings accompanied by a magnification of 20x were employed for cell counting. A separate count of viable and non-viable cells was carried out. Starting with chamber 1 of the haemocytometer, all cells present in the 1mm corner squares (Figure 3.1, A-D) as well as the middle square (Figure 3.1, E) were counted. Cells present on the boundary lines of these squares were ignored.

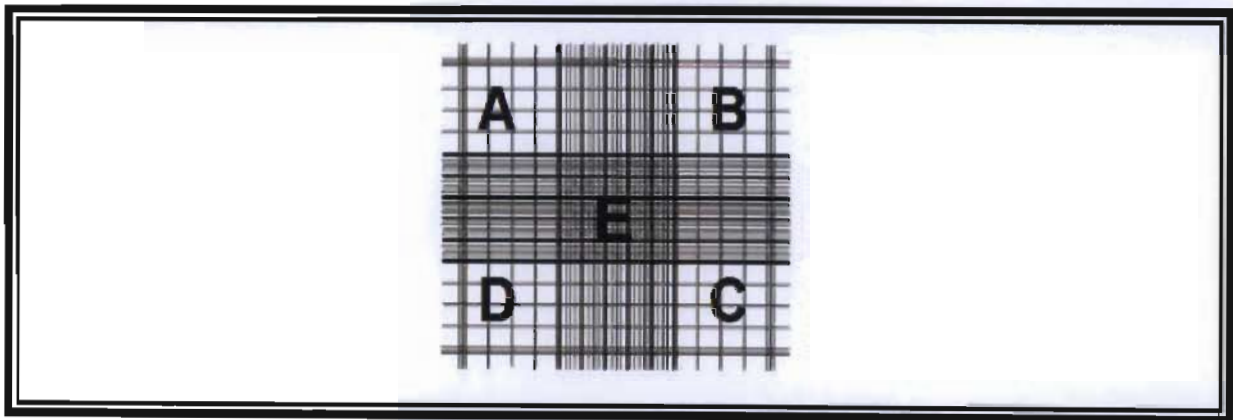


**Figure 3.1** Diagram of a haemocytometer (Thomson, 2008).

The live cells were then averaged by dividing the total count by five. Dead cells were similarly averaged. Both averages were then added to obtain a total cell count for the first chamber. This counting procedure was repeated for the second chamber and a final cell count was obtained by averaging the total cell count of both chambers.

The number of cells present within a millilitre (ml) of a particular sample (cells/ml) was then calculated by multiplying the final cell count by 10 000 and then by 5 (dilution factor). The number of cells present within the entire sample was then calculated by multiplying the cells/ml by the total volume (ml) of sample.

### **3.5.3.5 Preparation of the *Sutherlandia frutescens* aqueous extract**

*Sutherlandia* tablets were crushed to a fine powder using a pestle and mortar, and subsequently weighed. An SF aqueous extract was thereafter prepared by initially boiling (in a sealed beaker) a mixture (1.2g/10ml) of the SF powdered tablets and deionised water (dH<sub>2</sub>O). After 30 minutes, the resulting mixture was allowed to cool to room temperature, transferred to 50ml sterilin tubes and centrifuged at 1 000 rpm for 5 minutes at 24°C. Thereafter, the supernatants were removed, passed through 0.45µm filters into a 250ml bottle and autoclaved at 115°C for 30 minutes. The resulting solution served as the crude SF aqueous extract.

### **3.5.3.6 Preparation of stock solutions**

It was necessary to determine IC<sub>50</sub> values for each compound under investigation prior to conducting any assays. Selection of an IC<sub>50</sub> for AFB<sub>1</sub> (1µM) and L-can (2mM) was based on previous studies (Uhl *et al.*, 2000; Majer *et al.*, 2004; McKean *et al.*, 2006) and (Swaffar *et al.*, 1994; Ding *et al.*, 1999; Jang *et al.*, 2002) respectively.

Aflatoxin B<sub>1</sub> (1mg) was initially dissolved in ethanol (300µl) and made up to a final volume of 10ml in CCM to yield a stock solution with a concentration of 321µM. For purposes of the MTT assay, a 25µM AFB<sub>1</sub> solution was prepared utilising the 321µM AFB<sub>1</sub> stock solution.

Essentially, cells treated with AFB<sub>1</sub> were exposed to 0.0092% ethanol. In order to obtain consistency of measurement, the control and L-can stock solutions as well as the SF dilutions were prepared such that the cells incubated with these samples would also be exposed to the same percentage of ethanol.

A 4mM stock solution (10ml) of L-can was prepared by dissolving 7.05mg L-can in CCM.

Dilutions (1:1.5, 1:3, 1:4.5 and 1:6) of SF in CCM were made utilising the SF aqueous extract.

The MTT stock solution (5mg/ml) was prepared by adding 1ml of PBS to 5mg MTT and vortexing until the salt was completely dissolved. The dye solution was utilised immediately after preparation.



### 3.5.3.7 Treatment, isolation and harvesting of HepG<sub>2</sub> cells

HepG<sub>2</sub> cells were grown to approximately 80% confluency in a 75cm<sup>3</sup> culture flask. Cells were rinsed with three changes of pre-warmed (37°C) PBS and thereafter harvested by trypsinisation and counted.

### 3.5.3.8 The methyl thiazol tetrazolium bioassay on cultured HepG<sub>2</sub> cells

The assay was conducted in triplicate for each sample under investigation.

For the control, SF only and AFB<sub>1</sub> only treatments (Figure 3.2), aliquots comprising 125µl of the CCM-cell suspension was dispensed into each of the relevant wells of a 96 well microtitre plate to give a final cell count of approximately 10 000 cells/well.

Subsequent to vortexing, 125µl aliquots of the control solution and SF dilutions (1:1.5, 1:3, 1:4.5, and 1:6) were dispensed into each of the relevant wells resulting in a final volume of 250µl/well. The final dilutions of the SF extract to which the cells were exposed were 1:3, 1:6, 1:9 and 1:12 respectively (Figure 3.2).

For the AFB<sub>1</sub> only treatment, 115µl of CCM was dispensed into the appropriate wells followed by the addition of 10µl of AFB<sub>1</sub> (25µM) to give a final volume of 250µl/well. The final concentration of AFB<sub>1</sub> to which cells were exposed was 1µM (Figure 3.2).

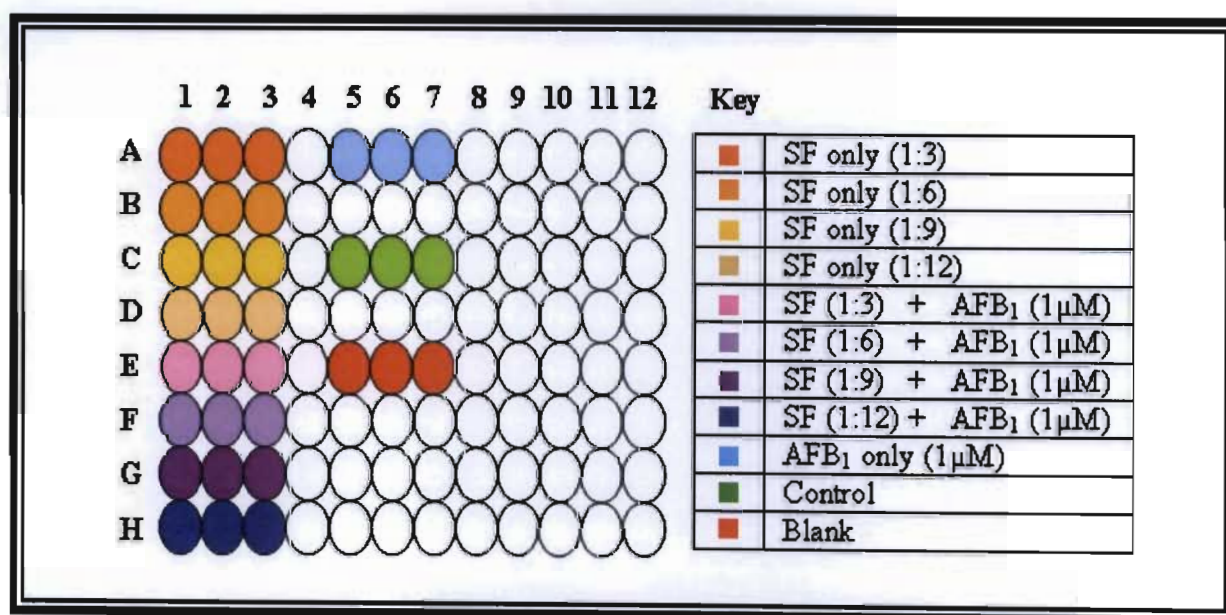


Figure 3.2 Schematic diagram of the treatment of cells for the MTT assay.

For the SF-AFB<sub>1</sub> combination treatment (Figure 3.2), the CCM-cell suspension was adjusted such that 115µl aliquots were added to each of the relevant wells yielding a final cell count of approximately 10 000 cells/well. Aliquots comprising 125µl of the SF samples and 10µl of AFB<sub>1</sub> (25µM) were then dispensed into each of the appropriate wells resulting in a final volume of 250µl/well. The final dilutions of SF and the final concentration of AFB<sub>1</sub> to which cells were exposed were 1:3, 1:6, 1:9, 1:12 and 1µM respectively.

The 96 well plate was then sealed with parafilm, swabbed with 70% ethanol and incubated (37°C) for 24 h. Following the incubation period, the supernatant of each well was discarded and the cells in each well were resuspended with 100µl of CCM. A blank control (Figure 3.2) containing only CCM (100µl) was also included in order to correct background absorbance. A 10µl aliquot of the MTT stock solution (5mg/ml) was then added to each well. The plate was subsequently covered with foil and returned to the incubator (37°C). After 4 h of incubation, the plate was centrifuged at 1 000 rpm for 5 minutes at 24°C and the supernatant of each well was discarded followed by the addition of DMSO (100µl) into each well. The plate was incubated (37°C) once more for an hour, removed from the incubator and allowed to cool to room temperature before measuring the optical densities of the samples at 560nm with a reference wavelength of 620nm using a Bio-Tek µQuant microplate spectrophotometer.

### 3.5.3.9 Data analysis and statistics

The net MTT-dependant absorbance of each sample was calculated by subtracting the average absorbance of the blank from the average absorbance of each sample. Samples were compared for differences using one-way ANOVA and the Tukey-Kramer multiple comparisons test (GraphPad InStat Software, version 3.06). A probability value (p) of less than 0.05 (p<0.05) was considered as statistically significant (\* indicates significant (p<0.05) differences between treated and control groups; # indicates significant (p<0.05) differences between SF and SF-AFB<sub>1</sub>; ° indicates significant (p<0.05) differences between AFB<sub>1</sub> and SF-AFB<sub>1</sub>). Data are represented as % cell viability plus or minus the standard deviations.

% Cell viability was calculated by utilising the following equation:

$$\% \text{ Cell viability} = \frac{\text{mean absorbance of treated cells}}{\text{mean absorbance of control cells}} \times 100$$

### 3.6 Results and Discussion

The MTT assay is a convenient tool for rapidly assessing metabolism, functional capacity and cell viability. It is based on the ability of mitochondria within viable cells to reduce the yellow MTT salt to a purple formazan product which can subsequently be quantified spectrophotometrically. Due to such reduction, the assay facilitates a quantitative, convenient method for evaluating a cell population's response to external factors, whether it is an increase in cell viability, no effect, or a decrease in cell viability.

Aflatoxin B<sub>1</sub> is the most prevalent and carcinogenic of the aflatoxins, and the toxic effects of AFB<sub>1</sub> have been studied extensively *in vitro*. In all animal species examined to date, including man, the liver is the primary target organ for AFB<sub>1</sub> toxicity (Neal, 1995).

*Sutherlandia frutescens* is a plant that has broad therapeutic potential and more specifically, it is perceived by some to have the ability to treat cancer.

Based on the many controversial claims of the effects of AFB<sub>1</sub> and SF, the MTT assay was utilised in order to investigate the cytotoxic potential of SF when administered individually and in combination with AFB<sub>1</sub>.

A typical dose-dependent viability response was observed when cultured HepG<sub>2</sub> cells were incubated with increasing dilutions of SF (1:3, 1:6, 1:9, and 1:12) either individually or in combination with AFB<sub>1</sub> (1 $\mu$ M) for 24 h (Figure 3.3).

Statistical analysis to examine the effects on cellular reduction of MTT, using one-way ANOVA, revealed that cytotoxicity was significant ( $p < 0.001$ ) following all treatments, when compared to the control.

The exposure of cells to SF only for 24 h resulted in cell viability increasing by 17%, 67%, 80% and 90% with dilutions of 1:3, 1:6, 1:9 and 1:12 respectively (Table 3.1).

These findings demonstrate that SF inhibits proliferation of the HepG<sub>2</sub> carcinoma cell line in a dose-dependant manner and correlates with other studies (Tai *et al.*, 2004; Chinkwo, 2005; Steenkamp and Gouws, 2006; Stander *et al.*, 2007). Steenkamp and Gouws (2006) demonstrated that a hot water leaf extract of SF inhibited growth of both the prostate cancer

cell line, DU-145 as well as the breast carcinoma cell line, MCF-7. In addition, Chinkwo (2005) found a crude aqueous whole plant extract of SF to induce cytotoxicity in Caski cells, CHO cells and the Jurkat T lymphoma cell line. Further to utilising aqueous extracts of the plant, other authors (Tai *et al.*, 2004; Stander *et al.*, 2007) used ethanolic extracts and have showed dose-dependent induction of cell death of several cancer cell lines (MCF7, Jurkat T cell line, MDA-MB-468 and HL60).

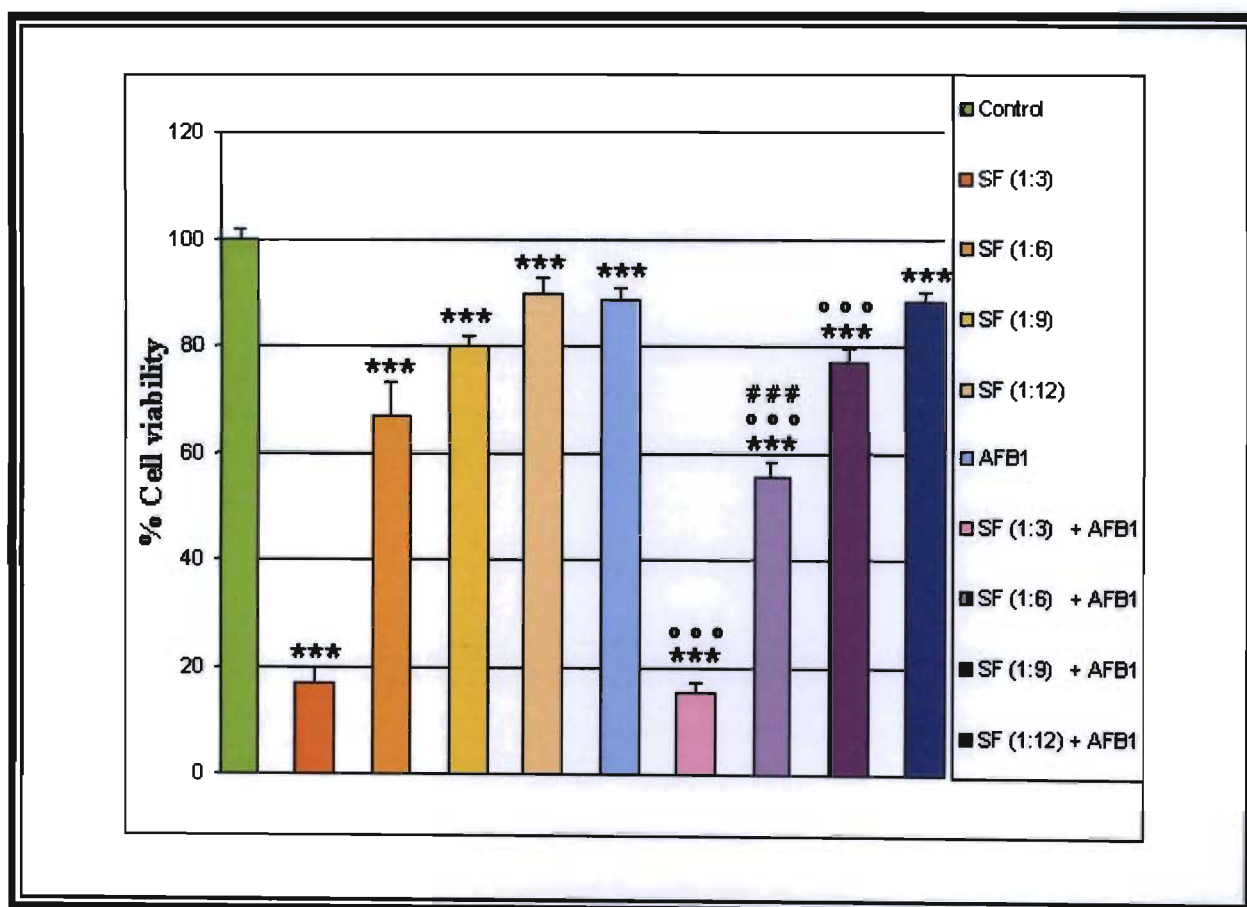


**Figure 3.3** The effect of SF, AFB<sub>1</sub> and SF-AFB<sub>1</sub> combination treatments on cell viability of the HepG<sub>2</sub> cell line. \*\*\*p<0.001, °°°p<0.001, ###p<0.001.

It is unclear how SF might influence mitochondrial activity and metabolism resulting in the observed dose-dependant decreases in cellular ability to reduce MTT. Many investigations utilising SF have been studied from a chemical point of view. L-canavanine, one of the active substances of SF, is known to exhibit tumouricidal and/or cytotoxic activity (Green *et al.*, 1980; Thomas *et al.*, 1980; Swaffar *et al.*, 1994; Ding *et al.*, 1999).

It has been demonstrated that L-can induces the synthesis and subsequent accumulation of aberrant proteins due to its erroneous integration into proteins instead of L-arg. It is suggested that this process forms the basis of L-can's antimetabolic activity (Schachtele *et al.*, 1968; Hare, 1969).

**Table 3.1: Mean cell viability as a percentage of the control  $\pm$  SD following exposure of HepG<sub>2</sub> cells to SF only and SF-AFB<sub>1</sub> combination treatments.**

| SF dilution | Cell viability (%) – SF only | Cell viability (%) – SF-AFB <sub>1</sub> (1 $\mu$ M) |
|-------------|------------------------------|--|
|             |                              |  |
| <b>1:3</b>  | 17 $\pm$ 3.2                 | 15 $\pm$ 1.6   |
| <b>1:6</b>  | 67 $\pm$ 6.2                 | 55 $\pm$ 2.8 <sup>###</sup>                          |
| <b>1:9</b>  | 80 $\pm$ 1.9                 | 77 $\pm$ 2.6   |
| <b>1:12</b> | 90 $\pm$ 3.0                 | 88 $\pm$ 1.7   |

Wilkie (1970) demonstrated the inhibitory effects of L-can on mitochondrial function in *Saccharomyces cerevisiae*, which was detected as inhibition of growth, greatly reduced respiratory activity and considerable decreases in the synthesis of cytochromes *a* and *b*. Moreover, Winston and Bosmann (1971) reported inhibition of both rat liver and brain mitochondrial systems by L-can.

In addition to its inhibitory effects on the mitochondrion, studies have demonstrated that L-can induces oxidative stress (Riganti *et al.*, 2003) and genotoxicity (Schachtele *et al.*, 1968; Hare, 1969; Cervera *et al.*, 1983).

Cell viability may also be influenced by L-canaline due to its ability to form oximes that scavenge essential metabolites such as pyruvate and oxaloacetate, thereby depleting TCA cycle reserves and interfering with ATP production (Rosenthal, 1997). Significant energy depletion will inevitably lead to a loss of cell function and cell death (Amdur *et al.*, 1991).

Therefore, cytotoxicity by SF may be ascribed to the ability of L-can to influence protein structure and function, mitochondrial activity, genomic integrity as well as the redox state of cells, the consequence of which may be cell death. However, the bioactivity of SF is possibly due to the synergistic effects of the many compounds present in the extract and may not be

solely dependent on a single compound, but rather a host of phytochemicals thereby resulting in a relatively complex mechanism of action (Stander *et al.*, 2007).

After 24 h of incubation, AFB<sub>1</sub> (1 $\mu$ M) was shown to be significantly ( $p < 0.001$ ) cytotoxic to HepG<sub>2</sub> cells (Figure 3.3). Liver mitochondrial injury is one of the dominant features of AFB<sub>1</sub> toxicity. The ability of AFB<sub>1</sub> to influence mitochondrial function can be attributed to its inhibitory effects on the ETC and oxidative phosphorylation (Doherty and Campbell, 1973; Pai *et al.*, 1975). It has been reported that AFB<sub>1</sub> specifically inhibits succinate dehydrogenase (Obidoo and Obonna, 1981; Sajan *et al.*, 1995), the same enzyme that reduces MTT.

In addition to its negative effects on the mitochondrion studies have demonstrated the capacity of AFB<sub>1</sub> to mediate oxidative stress (Shen *et al.*, 1995; Shen *et al.*, 1996; Awey *et al.*, 2002; Towner *et al.*, 2002; Lee *et al.*, 2005) and genotoxicity (Amstad *et al.*, 1984; El-Khatib *et al.*, 1998; O'Brien *et al.*, 2000; Uhl *et al.*, 2000; Raj *et al.*, 2001; Ehrlich *et al.*, 2002; Majer *et al.*, 2004), the consequences of which may be cellular lethality.

Other findings showed that co-administration of SF along with AFB<sub>1</sub> resulted in cell viability increasing by 15%, 55%, 77% and 88% with 1:3, 1:6, 1:9, 1:12 SF and AFB<sub>1</sub> (1 $\mu$ M) respectively (Table 3.1).

When SF-AFB<sub>1</sub> and SF only data were compared, it was revealed that cell viability for all the combination (SF-AFB<sub>1</sub>) treatments were lower than the corresponding individual (SF only) treatments (Table 3.1). A statistically significant ( $p < 0.001$ ) difference between SF (1:6) and the corresponding SF (1:6)-AFB<sub>1</sub> treatment was noted (Figure 3.3).

Data also demonstrated statistically significant ( $p < 0.001$ ) differences between AFB<sub>1</sub> only and SF-AFB<sub>1</sub>, except for when SF (1:12) and AFB<sub>1</sub> were combined (Figure 3.3).

Based on these findings, both compounds appear to be working simultaneously when administered in combination, however the precise mechanisms by which they act in concert to influence cell viability are not fully understood.

Despite the substantial progress in the development of anticancer therapies, the incidence of cancer is still increasing worldwide. One of the most reasonable approaches to reduce the risk

of cancer is chemoprevention, a relatively new and promising strategy of cancer prevention. Since the majority of cancer chemotherapeutic agents severely affect the host's normal cells, utilisation of natural products has now been contemplated of exceptional value in the control of cancer. Recently, attention has been focused on the identification of plants such as SF as potential sources of chemotherapeutic agents.

However, little is known regarding the pharmacology of compounds contained in SF extracts, thus complicating the correlation between *in vitro* and *in vivo* results. To facilitate SF effectiveness *in vivo*, the active substances must be absorbed and presented to the targets at concentrations that can exert an effect. The manufacturer of SF recommends a daily dose of two tablets (600mg), three times a day for HIV/AIDS patients. However, the dosage for cancer treatment remains elusive. Assuming a patient of 60kg has a 36L fluid compartment, each tablet contains 3mg of L-can as the active component and SF is consumed with 100% absorption, then the plasma concentration of L-can will be approximately 0.5 $\mu$ g/ml (Tai *et al.*, 2004). This concentration is much lower than the concentration of L-can found to have antiproliferative effects *in vitro* (2mM = 352 $\mu$ g/ml).

Thus, future research pertaining to the pharmacokinetics of bioactive principles, following the ingestion of SF, is crucial to facilitate accurate interpretation of *in vitro* data and for the development of suitable *in vivo* experiments. Furthermore, it is anticipated that some of the compounds in SF, if structurally identified and characterised, may be effective candidates for anticancer drug development.

### **3.7 Conclusion**

Based on the findings of this assay, it was concluded that the 1:6 dilution for both the individual (SF only) and combined (SF-AFB<sub>1</sub>) treatments would be utilised for all further experiments.

The claim by traditional healers that SF has anticancer properties has been partially validated in this study by the MTT assay which revealed an aqueous extract of the plant to possess significant cytotoxic activities *in vitro* on the human hepatocellular carcinoma cell line, HepG<sub>2</sub>. Overall, the MTT assay proved to be an efficient colorimetric technique for assessing the cytotoxicity of SF when administered alone and in combination with AFB<sub>1</sub>.

## Chapter 4

# CELLULAR REDOX STATE

### 4.1 Introduction

Aerobic organisms are continually subjected to ROS, derivatives of O<sub>2</sub> that are generated as products or by-products by a range of enzymatic reactions during various cellular processes (Liu *et al.*, 2008). Within a normal cell, there always exists an exquisite balance between pro- and antioxidant pathways (Sreedhar and Csermely, 2004). When this balance tips toward the oxidant side, or when a disruption of redox signalling and control occurs, oxidative stress ensues (Liu *et al.*, 2008).

### 4.2 Reactive oxygen species and oxidative stress

Reactive oxygen species such as O<sub>2</sub><sup>-</sup>, H<sub>2</sub>O<sub>2</sub> and ·OH can be generated by a variety of mechanisms which include the mitochondrial and microsomal ETC, xanthine oxidase and other flavoprotein oxidases, auto-oxidation of hydroquinones, catecholamines, thiols, intracellular xenobiotic mechanisms (CYP<sub>450</sub>), NADP (H)-oxidase, peroxisome metabolism as well as by the auto-oxidation of haemoglobin (Sreedhar and Csermely, 2004).

A wide array of enzymatic and nonenzymatic antioxidant defences exists in order to avoid redox imbalance and oxidative stress. The primary defence system includes superoxide dismutase (SOD), glutathione peroxidase (GPX) and catalase (CAT) (Mateas and Sanchez-Jimeanez, 2000). For example O<sub>2</sub><sup>-</sup> is dismutated by SOD to H<sub>2</sub>O<sub>2</sub>, and H<sub>2</sub>O<sub>2</sub> could either be converted to water by CAT or GPX (utilises GSH) (Awney *et al.*, 2002). On the other hand, H<sub>2</sub>O<sub>2</sub>, contrary to O<sub>2</sub><sup>-</sup>, is able to cross cell membranes and once inside cells it can participate with transition metal ions such as iron (Fe) and copper (Cu) via Fenton chemistry (equation 1).



Hydrogen peroxide may subsequently be reduced by electron donors such as NADPH, hydroquinone, ascorbic acid or GSH to ·OH, which is widely regarded as the most reactive form of ROS as it readily reacts with cellular components to cause oxidative damage such as lipid peroxidation and oxidative DNA damage (Shen *et al.*, 1996; Goetz and Luch, 2008).



Secondary defence's mainly combat processes elicited by free radicals and the compounds comprising this defence system include ascorbic acid (vitamin C),  $\alpha$ -tocopherol (vitamin E), GSH,  $\beta$ -carotene, vitamin A, NADPH and urate (Mateas and Sanchez-Jimeanez, 2000).

The term 'oxidative stress' describes the adverse interactions of molecular O<sub>2</sub> or of its reactive derivatives (ROS) with biomolecules such as DNA, proteins, and lipids, as well as the damage initiated via oxidative modification of these cellular molecules which subsequently contributes to the pathogenesis of various human diseases (Goetz and Luch, 2008).

Subsequent to its production intracellularly, ROS may damage DNA. Reactivity of ROS towards DNA induces point mutations, DNA-DNA and DNA-protein crosslinks, sister chromatid exchanges (Goetz and Luch, 2008), base damage, both single- and double-strand breaks and often the subsequent production of clastogenic factors (Blount *et al.*, 1989). Site-specific DNA damage is predominantly induced by  $\cdot$ OH. 8-Hydroxy 20-deoxyguanosine (8-HO-dG) represents the most extensively studied oxidative DNA modification (Goetz and Luch, 2008).

As much as 1% of the O<sub>2</sub> consumed by the average human cell may be diverted to the oxidative modification of proteins. Enzyme inhibition by ROS occurs following oxidation of proteinaceous amino acids such as cysteine, methionine, histidine, and tryptophan (Gracy *et al.*, 1999). In addition, oxidation of proteins can result in major physical changes in protein structure (fragmentation of the backbone or oxidation of the side-chains) leading to unfolding and conformational changes which can have consequential effects on biological function. Moreover, reactive species including hydroperoxides or peroxides can also be induced following the oxidation of proteins thus potentiating oxidative stress (Davies, 2005).

Indeed, DNA and proteins are often more significant targets of injury than are lipids, and lipid peroxidation often occurs late in the injury process (Halliwell and Chirico, 1993). Lipid peroxidation is commonly regarded as a deleterious process, induced by free radicals, leading to structural modification of complex lipid-protein assemblies such as biomembranes and lipoproteins (Kuhn and Borchert, 2002).

A free radical is defined as any species capable of independent existence and possesses one or more unpaired electrons. If two radicals coincide, they can combine their unpaired electrons to form a shared electron pair (covalent bond). Most biological molecules are nonradicals. When a radical gives one electron to, takes one electron from, or simply adds on to a nonradical, that nonradical becomes a radical. Thus, a feature of the reaction of free radicals with nonradicals is that they usually proceed as chain reactions and lipid peroxidation is the most studied biologically relevant free radical chain reaction (Halliwell and Chirico, 1993).

Polyunsaturated fatty acids (PUFAs) are particularly susceptible to lipid peroxidation. Hydrogen atoms in PUFAs contain a single electron and its removal by a free radical leaves behind an unpaired electron on the carbon atom to which it was originally attached. The resulting carbon-centred lipid radical thereafter undergoes molecular rearrangement, followed by reaction with O<sub>2</sub> to generate a peroxy radical. Peroxy radicals may then attack membrane proteins but are also capable of abstracting hydrogen from adjacent fatty acid side chains thus propagating the chain reaction of lipid peroxidation. Hence, a single initiation event can result in the conversion of hundreds of fatty acid side chains into lipid hydroperoxides (Halliwell and Chirico, 1993).

### **4.3 The role of glutathione**

The GSH redox cycle is an important component of the antioxidant machinery in cells (Meki *et al.*, 2004). Glutathione,  $\gamma$ -glutamylcysteinylglycine, is the most abundant non-protein thiol, being found in the millimolar range in most cells (Dickinson and Forman, 2002). It is synthesised from L-glutamate, L-cysteine and glycine in two consecutive steps, catalysed by  $\gamma$ -glutamyl-cysteine synthase (GCS) and glutathione synthase (Sies, 1999).

Glutathione is a molecule with many important cellular properties including a) its cysteinyl residue provides a nucleophilic thiol important for the detoxification of electrophilic metabolites and metabolically produced oxidising agents; b) its net negative charge and overall hydrophilicity greatly increases the aqueous solubility of the lipophilic moieties with which it becomes conjugated; c) its molecular weight ensures that its adducts are preferentially secreted via the biliary system and d) its unique tripeptide structure, including the N-terminal glutamyl

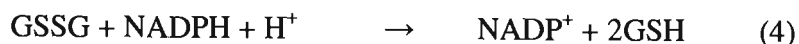
residue linked via a  $\gamma$ -glutamyl peptide bond, provides for specificity in GSH-enzyme interactions (Ketterer *et al.*, 1983).

It is able to form conjugates (GSH *S*-conjugates) with a variety of electrophilic compounds nonenzymatically, when the electrophile is very reactive, or more often via the action of GST. Conjugation with GSH is an essential aspect of both xenobiotic and normal physiological metabolism (Dickinson and Forman, 2002). Within mammals, GSH *S*-conjugates are preferentially secreted by the biliary system but may be further metabolised by hydrolysis and *N*-acetylation, resulting in *N*-acetylcysteinyl conjugates known as mercapturic acids, which may subsequently be excreted in urine (Dickinson and Forman, 2002).

Glutathione does not react directly with lipid hydroperoxides but its use as a substrate for GPX is recognised for the reduction of  $\text{H}_2\text{O}_2$  (equation 2) and lipid hydroperoxides (equation 3). During these reactions GSH is converted to glutathione disulfide (GSSG) and  $\text{H}_2\text{O}_2$  is reduced to water or the hydroperoxide is converted to its corresponding alcohol (Dickinson and Forman, 2002).



Glutathione disulfide can then be reduced to GSH by NADPH via the glutathione reductase reaction (equation 4) (Dickinson and Forman, 2002).



The critical role of GSH in protecting cells should be apparent based on the multitude of reactions through which it removes potentially harmful molecules from cells (Dickinson and Forman, 2002).

## 4.4 The GSH-Glo™ Glutathione assay

### 4.4.1 Principle and applications

The GSH-Glo™ Glutathione assay is a luminescence-based assay for the detection and quantification of GSH. Detection of GSH using this assay is based on the result of the combination of two chemical reactions (Figure 4.1).

The first reaction (GSH-Glo™ reaction) involves the generation of luciferin from a luminogenic substrate (Luciferin-NT), catalysed by GST in the presence of GSH. The second step (Luciferin Detection reaction) is initiated by adding an equal volume of Luciferin Detection Reagent which comprises firefly luciferase; an enzyme that is able to interact with the luciferin produced in the first reaction and subsequently mediate the generation of a stable “glow-type” luminescent signal. This signal is directly proportional to the amount of luciferin formed during the GSH-Glo™ reaction and is thus proportional to the amount of GSH present in the sample (Promega, 2007). The assay is ideal for many applications, including the measurement of GSH levels in various cell or tissue extracts as an indicator of cell viability or oxidative stress. It can also be used for screening drugs and new chemical entities for their capacity to modulate GSH levels in cells, tissues or blood (Promega, 2007).

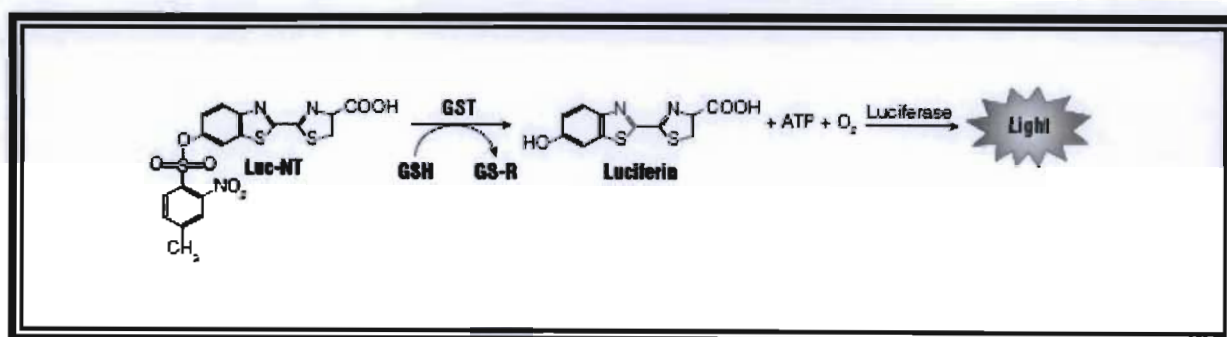


**Figure 4.1** The GSH-Glo™ and Luciferin Detection reactions of the GSH-Glo™ Glutathione assay (Promega, 2007).

## 4.5 The thiobarbituric acid reactive substances assay

### 4.5.1 Principle of the assay

Many assays are available to measure lipid peroxidation. One of the most commonly applied assays is the thiobarbituric acid (TBA) test or TBARS assay, which measures malondialdehyde (MDA) formed in peroxidising lipid systems (Halliwell and Chirico, 1993). This method is based on the condensation of two molecules of TBA with one molecule of MDA to form a pink chromogen (TBA pigment; Figure 4.2), the intensity of which is a measure of MDA concentration (lipid peroxidation) and can be measured by spectrophotometry at 532nm (Fernandez *et al.*, 1997).

The aim of this chapter was to utilise the GSH-Glo™ Glutathione assay and the TBARS assay to determine the influence of SF, L-can and AFB<sub>1</sub>, when administered individually and in combination, on cellular redox state.

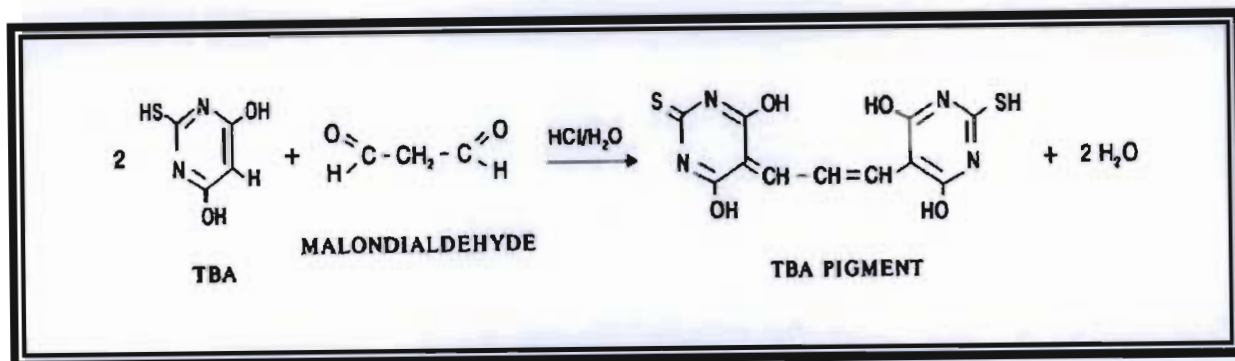


**Figure 4.2** Reaction between thiobarbituric acid and malondialdehyde to form the thiobarbituric acid pigment (Fernandez *et al.*, 1997).

## 4.6 Materials and methods

### 4.6.1 Materials

The GSH-Glo™ Glutathione Assay kit was purchased from Promega. The product components include Luciferin-NT, Glutathione *S*-Transferase, GSH-Glo™ Reaction Buffer, Luciferin Detection Buffer and the Luciferin Detection Reagent. Phosphoric acid (H<sub>3</sub>PO<sub>4</sub>), hydrochloric acid (HCl), TBA and butanol were acquired from Merck (SA). Butylated hydroxytoluene (BHT) was obtained from Sigma (SA). All other reagents and consumables utilised were obtained from the sources mentioned previously.

### 4.6.2 Methodology

#### 4.6.2.1 Treatment, isolation and harvesting of HepG<sub>2</sub> cells

HepG<sub>2</sub> cells were grown to approximately 80% confluency in 75cm<sup>3</sup> culture flasks. Cells were rinsed with three changes of pre-warmed (37°C) PBS following the removal of the spent culture medium from each flask. An aliquot of 6ml of each sample (Table 4.1) was thereafter dispensed into each appropriate flask and all six flasks were sealed and incubated at 37°C. After a 24 h incubation period, the supernatants from each flask were dispensed into appropriately labelled 15ml sterilin tubes and stored at -80°C. Cells were rinsed with three changes of pre-warmed (37°C) PBS and thereafter harvested by trypsinisation and counted.

#### 4.6.2.2 Preparation of the GSH-Glo™ Reagent 2X and Luciferin Detection Reagent

The GSH-Glo™ Reagent 2X was prepared by diluting the Luciferin-NT substrate and Glutathione S-Transferase 1:50 in GSH-Glo™ Reaction Buffer, whereas the Luciferin Detection Reagent was prepared by mixing the Luciferin Detection Buffer with the Luciferin Detection Reagent.

**Table 4.1: Preparation of samples**

| Sample                   | Volume of sample (µl)   | Final volume with CCM (ml) | Final dilution/ concentration of sample |
|--------------------------|-------------------------|----------------------------|---|
| Control                  | -                       | 12                         | -                                       |
| SF                       | 2000                    | 12                         | 1:6                                     |
| L-can                    | 6000 (4mM)              | 12                         | 2mM                                     |
| AFB <sub>1</sub>         | 37 (321µM)              | 12                         | 1µM                                     |
| SF + AFB <sub>1</sub>    | 2000 + 37 (321µM)       | 12                         | 1:6 + 1µM                               |
| L-can + AFB <sub>1</sub> | 6000 (4mM) + 37 (321µM) | 12                         | 2mM + 1µM                               |

#### 4.6.2.3 The GSH-Glo™ Glutathione assay on cultured HepG<sub>2</sub> cells

This assay was performed in duplicate and conducted under the laminar flow hood. Cell culture media contains serum and phenol red which interferes with the GSH-Glo™ assay chemistry; therefore the cells were assayed in PBS. An aliquot of 50µl containing approximately 10 000 cells from each treated sample was dispensed into individual wells of a white, opaque polystyrene flat-bottomed 96-well luminometer plate. In an attempt to achieve linear assay performance, a blank sample (negative control) containing only PBS (50µl) was also included in order to correct background luminescence. An aliquot of 50µl of the GSH-Glo Reagent 2X was then dispensed into each well. The plate was then covered with foil in order to prevent direct exposure of the samples to light because the luminescent signal obtained during the assay is rapidly degraded in the presence of light. The plate was then placed on an orbital shaker at 200 rpm for 3 minutes to facilitate efficient mixing of the contents of each well. After a 30 minute incubation period (room temperature), the foil was removed and 100µl of the Luciferin Detection Reagent was added to each well. The plate was then covered, briefly mixed once again on the orbital shaker and incubated at room temperature for 15 minutes. The foil cover was then removed and the plate was placed into the GloMax Multi Detection System (Promega), a luminometer which was utilised for the measurement of signals generated during

the assay. The instrument had preinstalled software for various luminometry-based assays and the GSH-Glo assay software was selected.

#### **4.6.2.4 The thiobarbituric acid reactive substances assay on cultured HepG<sub>2</sub> cells**

Approximately  $2 \times 10^6$  cells per treatment were transferred to appropriately labelled 15ml sterilin tubes and pelleted by centrifugation at 1 000 rpm for 5 minutes at 24°C. Thereafter, the supernatant from each tube was carefully removed, so as to prevent any disruption of the pellet. The pellets of cells were then resuspended in 500µl of 0.2% H<sub>3</sub>PO<sub>4</sub>. The cell suspensions were then passed through a 25 gauge needle approximately twenty five times. This process provided efficient homogenisation, allowing for rupturing of the cells and subsequent release of intracellular constituents. An equal amount (500µl) of 2% H<sub>3</sub>PO<sub>4</sub> was thereafter added to each homogenate and the resulting solution was briefly vortexed. A 400µl aliquot of the homogenate from each sample was then dispensed into appropriately labelled glass test tubes. A blank sample (negative control) containing homogenate from the control was also included in order to correct background absorbance. A 200µl aliquot of 7% H<sub>3</sub>PO<sub>4</sub> was then dispensed into each test tube followed by the addition of 400µL TBA/BHT solution (BHT is added to the TBA solution to prevent oxidation in the reaction during heating) to each sample, and 400µL of 3mM HCl to the blank. All test tubes were briefly vortexed and the pH of each solution was subsequently adjusted to 1.5 using 1M HCl. The test tubes were thereafter placed in a water bath (100°C). After 15 minutes, the tubes were removed and allowed to cool to room temperature before pipetting 1.5ml of butanol into each tube. All test tubes were subsequently vortexed for approximately 1 minute each and the samples were allowed to settle. Approximately 500µl of the butanol (which comprised the upper phase of the solutions present in the test tubes) was then transferred to appropriately labelled eppendorfs and centrifuged at 13 200 rpm for 6 minutes at 24°C. A 100µl aliquot of each sample was then pipetted into individual wells of a 96-well microtiter plate. This part of the assay was performed in triplicate. The absorbance of the butanol phase was measured at 532nm (maximum absorbance for TBARS) with a reference wavelength of 600nm using a Bio-Tek µQuant microplate spectrophotometer.

#### 4.6.2.5 Data analysis and statistics

Data acquired from the GSH assay are represented as relative light units (RLU) plus or minus the standard deviations and TBARS data are represented as mean absorbance (nm) values plus or minus the standard deviations. The net GSH-dependant luminescence or net TBARS-dependant absorbance of each sample was calculated by subtracting the average luminescence/absorbance of the blank control from the average luminescence/absorbance of each sample. Samples were compared for differences using one-way ANOVA and the Tukey-Kramer multiple comparisons test (GraphPad InStat Software, version 3.06). A probability value (p) of less than 0.05 ( $p < 0.05$ ) was considered as statistically significant (\* indicates significant ( $p < 0.05$ ) differences between treated and control groups; # indicates significant ( $p < 0.05$ ) differences between treated groups).

#### 4.7 Results and Discussion

Within a normal cell, there is always a balance between pro- and antioxidant pathways. However, upon stress stimuli, an imbalance of the redox milieu develops and leads to the accumulation of ROS (Sreedhar and Csermely, 2004).

Reactive oxygen species such as  $O_2^-$ ,  $H_2O_2$  and  $\cdot OH$ , can be generated by a variety of mechanisms (Sreedhar and Csermely, 2004) and their capacity to readily react with cellular components and cause oxidative damage has been well documented.

Within normal cells, a primary defence against oxidative damage is provided by antioxidants such as GSH (Meki *et al.*, 2004).

To evaluate the effects of SF, L-can and AFB<sub>1</sub> on the cellular redox state, the GSH-Glo™ Glutathione assay the TBARS assay were employed.

The results of the GSH-Glo™ Glutathione assay illustrates that all samples evoked an increase in cellular GSH content when compared to the control (Figure 4.3). Intracellular GSH content is a function of the balance between its use and synthesis. Although its utilisation is beneficial to the cell, GSH must be regenerated. One way of doing so is via the reduction of GSSG by glutathione reductase to regenerate GSH at the expense of NADPH, but the replacement of GSH is principally due to *de novo* synthesis following increased transcription of GCS



(Dickinson and Forman, 2002). Because GCS is feedback inhibited by GSH, depletion of GSH (by conjugation reactions via GST or by GSSG formation) can result in a short term increase in GSH synthesis. To some extent, a decrease in GSH will cause a transient increase in the activity of pre-existing GCS by decreasing the feedback inhibition by GSH, resulting in a short term increase in GSH synthesis (Dickinson and Forman, 2002). Thus, the observed increases in GSH content after administration of all samples (Figure 4.3) can be due to such a mechanism.

In addition, a remarkably large number of compounds, including oxidants and GSH-conjugating agents have been shown to increase GSH synthesis through increased transcription of GCS. One particularly well studied inducer of GSH biosynthesis is the lipid peroxidation end product 4-hydroxynonenal (4HNE) (Dickinson and Forman, 2002). Therefore, the increases in GSH levels (Figure 4.3) may also be ascribed to increased oxidative stress.

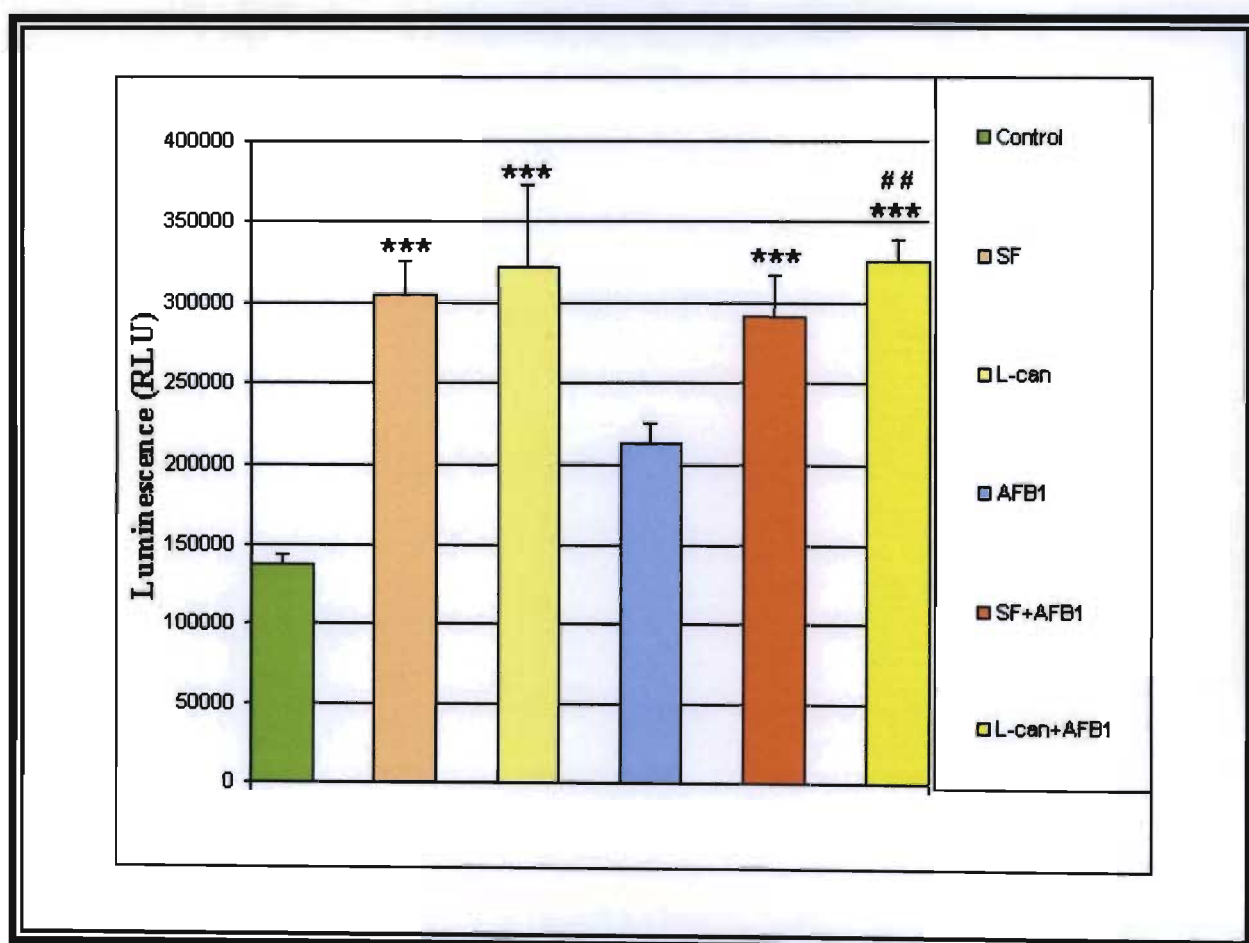


**Figure 4.3** The effect of SF, L-can, AFB<sub>1</sub>, SF-AFB<sub>1</sub> and L-can-AFB<sub>1</sub> treatments on intracellular levels of GSH in HepG<sub>2</sub> cells. \*\*\*p<0.001, ## p<0.01.

Furthermore, DNA damage induced by ROS results in the formation of DNA chain breaks and changes in chromatin structure, a consequence of which is p53 activation and stabilisation (Hickman *et al.*, 2002). The tumour suppressor protein p53 (TP53), can then activate the expression of several genes, one of which is a gene named TIGAR (TP53-induced glycolysis and apoptosis regulator) which has been shown to function by lowering the intracellular levels of fructose-2,6-bisphosphate (F-2,6-BP), a substrate that promotes glycolysis by activation of phosphofruktokinase-1. Enhanced TIGAR expression lowers F-2,6-BP levels, thereby slowing glycolysis and redirecting glucose to the pentose phosphate pathway (PPP). The PPP is a major source of NADPH which is utilised by glutathione reductase to regenerate GSH from GSSG (Bensaad and Vousden, 2007). Increased TIGAR activity is therefore a certain possibility following genomic insult and may represent a mechanism by which GSH levels are restored and subsequently maintained within cells. It is thus presumed that the increased GSH levels (Figure 4.3) are due, to a certain extent, to increased TIGAR activity which occurs as a result of ROS-induced DNA damage.

In this study, the lowest level of lipid peroxidation occurred after the administration of SF. When compared to the control sample, the 1.28-fold ( $p < 0.001$ ) decrease in TBARS levels (Figure 4.4) was accompanied by a 2.22-fold ( $p < 0.001$ ) increase in cellular GSH levels (Figure 4.3) when HepG<sub>2</sub> cells were incubated with SF for 24 h.

The observed protective effects of SF may be ascribed to its free radical scavenging properties as reported by Fernandes *et al.* (2004), who, on the basis of luminol and lucigenin enhanced chemiluminescence, showed that an SF hot water extract possessed O<sub>2</sub><sup>-</sup> as well as H<sub>2</sub>O<sub>2</sub> scavenging activities, and Tai *et al.* (2004), who demonstrated the ·OH scavenging activity of SF by utilising a 70% ethanolic extract of the plant.

Although the exact mechanism by which SF mediates this protective effect remains elusive, it may be due to the role of flavonoids, one of the various bioactive compounds isolated from SF (van Wyk, 2008). Flavonoids are low molecular weight, secondary plant phenolics characterised by the flavan nucleus. Most of the beneficial health effects of flavonoids can be ascribed to their antioxidant and chelating abilities. The protective effects of flavonoids in biological systems are due to their capacity to transfer electrons to free radicals, chelate metal catalysts, activate antioxidant enzymes, reduce  $\alpha$ -tocopherol radicals and inhibit oxidases

(Heim *et al.*, 2002). Thus, the inhibitory effects on lipid peroxidation by SF can be attributed to the presence of various bioactive components such as flavonoids present in the plant extract.

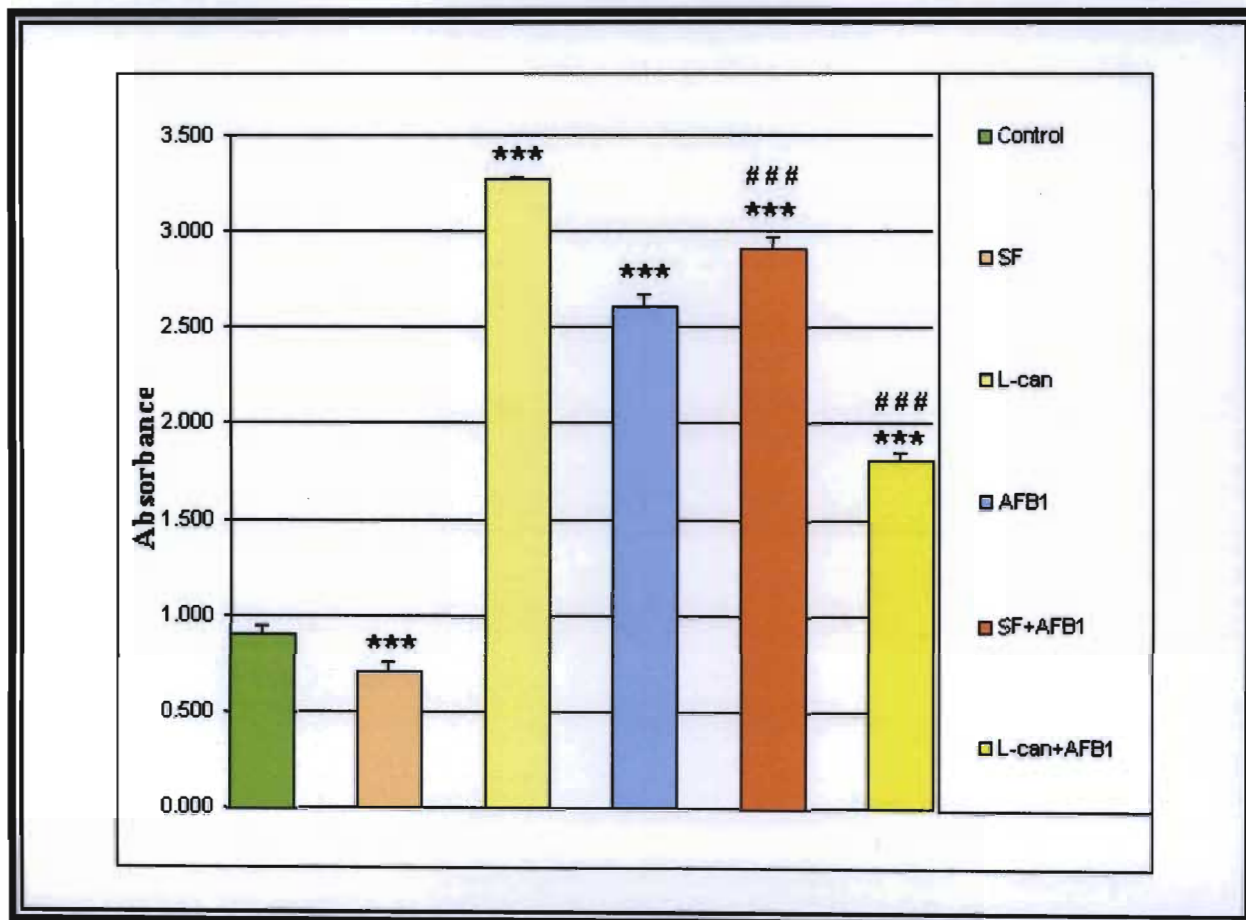


**Figure 4.4** The effect of SF, L-can, AFB<sub>1</sub>, SF-AFB<sub>1</sub> and L-can-AFB<sub>1</sub> treatments on intracellular levels of MDA in HepG<sub>2</sub> cells. \*\*\*p<0.001, ###p<0.001.

A study by Ojewole (2004) showed that SF was able to induce significant ( $p<0.001$ ) hypoglycaemia in STZ-induced diabetic rats. In addition, Chadwick *et al.* (2007) demonstrated a significant ( $p<0.001$ ) increase in glucose uptake by muscle and adipose tissue of male Wistar rats receiving the plant extract. In this regard, it has been reported that pinitol, a constituent of SF, is capable of inducing an insulin-like effect by affecting cellular glucose uptake (Bates *et al.*, 2000).

It is therefore suggested that pinitol present in SF mediates an increase in cellular glucose uptake, the consequence of which is increased glycolysis and subsequently increased PPP flux.

As a result, more NADPH would be available for the regeneration of GSH. This may be a further mechanism by which GSH levels are increased by SF.

It has been reported that L-can is present in relatively high concentrations within SF (van Wyk and Albrecht, 2008). Thus, the observed increase in GSH levels after exposure of HepG<sub>2</sub> cells to SF can also be due to the role that L-can has in influencing the PPP (discussed below).

The highest level of lipid peroxidation was observed following the administration of L-can (2mM), which evoked a 3.61-fold ( $p < 0.001$ ) increase in TBARS levels when compared to the control (Figure 4.4).

To date, no experimental evidence exists to show the exact source of ROS which initiates lipid peroxidation in cells exposed to L-can; however the capacity of L-can to induce ROS and subsequent lipid peroxidation was demonstrated in a study by Riganti *et al.* (2003) who investigated the oxidative effects of L-can in a mouse glial cell line, N11. Using a luminol-amplified chemiluminescence experiment, Riganti *et al.* (2003) showed that L-can (1mM) significantly ( $p < 0.05$ ) increased ROS production in N11 cells. In addition, the authors observed a significant ( $p < 0.05$ ) increase in lipid peroxidation. It was concluded that L-can was able to induce oxidative stress in exposed cells which in turn favoured an increase of lipid peroxidation.

Nitric oxide synthases function to mediate the biosynthesis of NO and L-citrulline from the amino acid L-arg (Luzzi and Marletta, 2005). One critical function of NO is to act as a scavenger of reactive radical species thus preventing cellular damage. It is able to exert this protective action through reaction with alkoxyl and peroxy radicals, thus inhibiting lipid peroxidation. Moreover, it suppresses superoxide-hydrogen peroxide mediated cytotoxic effects by acting as a scavenger of ROS (Li and Wogan, 2005). It facilitates this effect by specifically scavenging the O<sub>2</sub><sup>-</sup> radical, leading to the synthesis of nitrate (Riganti *et al.*, 2003).

Luzzi and Marletta (2005) demonstrated that L-can is a selective inhibitor of NOS. It was established that L-can functioned as an alternate substrate for the NOS reaction since it was converted to L-homoserine by the enzyme. The consequence is decreased NO synthesis.

Hence, the significant ( $p < 0.001$ ) increase in lipid peroxidation by L-can (Figure 4.4) is possibly due to its ability to influence the role that NO has in cellular oxidant-buffering. However, this may not be the only mechanism by which L-can can induce oxidative effects. Riganti *et al.* (2003) reported that the increases in ROS and lipid peroxidation by L-can were independent of NOS inhibition, suggesting that L-can is able to influence an alternate pathway leading to ROS generation.

The substitution of an L-arg residue in a protein with L-can may considerably affect important interactions that function to institute the tertiary and quaternary structure of the protein (Rosenthal *et al.*, 1989). The resulting erroneous integration of L-can into proteins instead of L-arg leads to an induction of structural changes that ultimately alter protein function and at the same time accelerates the formation of aberrant proteins (Rosenthal and Dahlman, 1991b).

Protein folding and post-translational modification are mediated by the ER (Hsieh *et al.*, 2007). The accumulation of aberrantly folded proteins within the cell and in the ER specifically, may result in a proposed overload of the ER (Remy *et al.*, 1998). A consequence of such effects is ER stress which is processed via certain signalling pathways one of which is the ER overload response (EOR). The EOR mediates calcium ( $\text{Ca}^{2+}$ ) efflux from the lumen of the ER as well as the release of reactive oxygen from the mitochondrion (Hsieh *et al.*, 2007). The released  $\text{Ca}^{2+}$  can then activate ROS producing enzymes such as cyclooxygenase and/or lipoxygenase (Remy *et al.*, 1998). This is another possible mechanism by which L-can induces ROS formation.

It is known that in L-can the methylene group close to the guanidine moiety is replaced by an  $\text{O}_2$  atom which has an electron withdrawing centre thus making L-can less basic than L-arg. In addition, the chemical substitution of L-can adds further lone electron pairs to the L-arg molecule (Riganti *et al.*, 2003). Therefore it is also possible that one of these features might also account for the ability of L-can to trigger the generation of ROS.

Together with a significant increase in TBARS levels induced by L-can (Figure 4.4), was a 2.35-fold ( $p < 0.001$ ) increase in cellular GSH levels when evaluated against the control (Figure 4.3). This effect may be due to the increased transcription of GCS by lipid peroxidation end products such as 4HNE (Dickinson and Forman, 2002).

The activity of the GCS holoenzyme can be negatively regulated by S-nitrosylation (Dickinson and Forman, 2002), the biochemical process which involves reversible coupling of NO to various target proteins (Iyer *et al.*, 2008). Due to its structural similarity to L-arg, it is suggested that L-can contributed to relieving the negative regulation of GCS by S-nitrosylation because its inhibition of NOS decreases the bioavailability of NO for S-nitrosylation. A consequence of this is increased GCS activity accompanied by increased GSH synthesis. This process is postulated to be a further contributor to the observed increase in GSH levels after L-can administration (Figure 4.3).

Furthermore, Riganti *et al.* (2003) demonstrated a significant ( $p < 0.05$ ) increase in the flux of the PPP when N11 cells were exposed to 1mM L-can for 3 h. As a result, the increased levels of GSH by L-can (Figure 4.3) may be due to increased NADPH production via the PPP.

Previous studies (Shen *et al.*, 1994; Madhusudhanan *et al.* 2004; Meki *et al.*, 2004; Lee *et al.*, 2005; Jodynis-Liebert *et al.*, 2006; Preetha *et al.*, 2006) demonstrated that oxidative damage might play a role in the cytotoxic and genotoxic effects of AFB<sub>1</sub>.

Shen *et al.* (1996) investigated the formation of ROS in rat hepatocytes treated with AFB<sub>1</sub>. In this study, a fluorescent probe, 2',7'-dichlorofluorescein diacetate (DCFH-DA) was used for the measurement of intracellular ROS formation in cultured rat hepatocytes. The principle of this assay is that DCFH-DA diffuses through the cell membrane and is enzymatically hydrolysed by intracellular esterases to the non-fluorescent dichlorofluorescein (DCFH). In the presence of ROS, DCFH is rapidly oxidised to the highly fluorescent dichlorofluorescein (DCF). When hepatocytes were treated with 1 $\mu$ M AFB<sub>1</sub>, a significant ( $p < 0.05$ ) increase in fluorescence intensity was observed as early as 0.5 h. After 4 h incubation, the fluorescence intensity was about three times higher than that in the control group. These findings clearly demonstrated that AFB<sub>1</sub> enhanced intracellular ROS formation in cultured rat hepatocytes.

In another study, Shen *et al.* (1995) showed significant increases of MDA as early as 12 h in rat hepatocytes exposed to AFB<sub>1</sub> (1 $\mu$ M). Malondialdehyde concentration reached a peak at 48 h and remained at a significantly high level up to 72 h. In this study the effects of SOD and CAT on AFB<sub>1</sub>-induced MDA generation was also investigated. It was observed that MDA concentration in these two groups were significantly ( $p < 0.05$ ) lower than in the AFB<sub>1</sub> group.

There was also a significant ( $p < 0.05$ ) protective effect afforded by desferal (DFO) on AFB<sub>1</sub>-induced MDA generation. Desferal readily chelates Fe<sup>3+</sup> to form a redox-inert Fe (III) complex, which removes Fe<sup>3+</sup> from the redox cycle, and prevents ·OH formation via the Fenton reaction. The liver is particularly vulnerable to free radical-induced damage involving Fe, because it is stored in large amounts as ferritin and haemosiderin (Towner *et al.*, 2003). Overall, it was demonstrated that AFB<sub>1</sub> was capable of inducing lipid peroxidation in cultured rat hepatocytes and the protective effects of SOD, CAT and DFO against lipid peroxidation indicated that O<sub>2</sub><sup>-</sup>, H<sub>2</sub>O<sub>2</sub> and ·OH are intermediates in oxidative damage induced by AFB<sub>1</sub> exposure.

The present data is in agreement with other studies (Shen *et al.*, 1995; Shen *et al.*, 1996) and showed that AFB<sub>1</sub> increases oxidative stress. Incubation of HepG<sub>2</sub> cells with 1 μM AFB<sub>1</sub> for 24 h had a significant ( $p < 0.001$ ) influence on TBARS levels (Figure 4.4), clearly evidenced by the 2.87-fold increase in lipid peroxidation when compared to the control. These findings indicate that the oxidation of lipids is mediated by free radicals induced subsequent to AFB<sub>1</sub> exposure.

It is well known that AFB<sub>1</sub> requires metabolic activation by CYP<sub>450</sub> to form the highly reactive metabolite AFB<sub>1</sub>-exo-8,9-epoxide in order to exert its cytotoxic and carcinogenic effects. On the other hand, it is also well documented that CYP<sub>450</sub> is an important source of intracellular ROS generation. Towner *et al.* (2002) utilised electron paramagnetic resonance (EPR) spin-trapping to search for free radicals produced *in vivo* by AFB<sub>1</sub>. It was demonstrated that preadministration of SKF525A, a CYP<sub>450</sub> inhibitor, prior to AFB<sub>1</sub> exposure resulted in a substantial decrease in the level of AFB<sub>1</sub>-induced radicals. These findings suggested that the free radicals induced by AFB<sub>1</sub> occurred as a result of CYP<sub>450</sub> activity.

Another possible origin of AFB<sub>1</sub>-induced free radicals could be the dialdehyde formed from the AFB<sub>1</sub>-8,9-dihydrodiol, which may be further metabolised to free radical intermediates (Towner *et al.*, 2002).

Thus the possible reason for AFB<sub>1</sub>-induced lipid peroxidation (Figure 4.4) is that AFB<sub>1</sub> was able to mediate the generation of oxygen-centred radicals that in particular attack cellular membranes rich in PUFAs initiating a chain reaction leading to peroxidation of the fatty acids.

In contrast to the significant ( $p < 0.001$ ) increase in TBARS levels after exposure of HepG<sub>2</sub> cells to AFB<sub>1</sub> (Figure 4.4), a marginal 1.56-fold increase in cellular GSH levels was noted (Figure 4.3). When compared to the control, the observed increase in GSH levels by AFB<sub>1</sub> was found to be insignificant ( $p > 0.05$ ). This finding is in agreement with studies conducted by Gyamfi and Aniya (1998) who reported an insignificant increase in hepatic GSH levels in Fischer 344 rats after 48 h following a single dose (1mg/kg, i.p) of AFB<sub>1</sub>. Similarly, in rats fed an AFB<sub>1</sub> contaminated diet (3mg/kg feed) for 15 days, no significant changes in hepatic GSH level were found (Abdel-Wahhab and Aly, 2003). Nevertheless, the observed increase in GSH levels due to AFB<sub>1</sub> exposure may be ascribed to the increased transcription of GCS by end-products of lipid peroxidation (Dickinson and Forman, 2002).

Mitochondria are the powerhouses of cells (Pieczenik and Neustadt, 2007). They operate by electron transport, the machinery of which is prone to leakage of a small percentage of electrons which become trapped by O<sub>2</sub>, forming O<sub>2</sub><sup>-</sup>. Manganese-SOD normally scavenges the O<sub>2</sub><sup>-</sup> produced by the ETC; however impairment of the electron transport machinery may cause more electrons to leak and form more O<sub>2</sub><sup>-</sup>. It has been suggested that O<sub>2</sub><sup>-</sup> is generated by the ETC (mainly complex I and III but also from complex II) when electron flow is interrupted by biochemical inhibitors. Therefore it is possible that mitochondria are the major source of intracellular free radicals, and that impairment of the ETC could increase mitochondrial ROS generation (Indo *et al.*, 2007).

Winston and Bosmann (1971) showed that L-can inhibited both rat liver and brain mitochondrial systems at a concentration of 0.1mg/ml, whereas Wilkie (1970) demonstrated the inhibitory effects of L-can on mitochondrial function in *Saccharomyces cerevisiae*. These particular effects were detectable as inhibition of growth, greatly reduced respiratory activity and decreases in the synthesis of the amounts of the mitochondrial enzymes cytochromes *a* (complex IV) and *b* (complex III).

Doherty and Campbell (1973) and Pai *et al.* (1975) reported the major site of inhibition of electron transport in rat liver by AFB<sub>1</sub> to be between cytochromes *b* and *c*<sub>1</sub> (complex III). Other studies (Obidoa and Obonna, 1981; Obidoa, 1986; Sajan *et al.*, 1995) demonstrated the inhibitory effect of AFB<sub>1</sub> on succinate dehydrogenase, cytochrome oxidase and ATPase activity, which could also contribute to an alteration in ETC function.



Therefore L-can and AFB<sub>1</sub> can independently impair the ETC. The consequence is increased ROS production and subsequent damage to various cellular components.

When considering the combined effects of the aforementioned compounds, TBARS results revealed that L-can co-administration along with AFB<sub>1</sub> evoked a 2-fold ( $p < 0.001$ ) increase in lipid peroxidation compared to the control (Figure 4.4). However, the same combination induced a 1.81-fold ( $p < 0.001$ ) and a 1.44-fold ( $p < 0.001$ ) decrease in TBARS levels when compared to lipid peroxidation induced after the individual administration of L-can and AFB<sub>1</sub> respectively.

The type of chemical interaction which describes the effect seen following the L-can-AFB<sub>1</sub> combination is antagonism, defined in terms of toxicology as 'exposure to a combination (L-can-AFB<sub>1</sub>) of chemicals, in which each chemical generally induces a defined toxic effect when given alone, but in combination produces a reduced toxic effect'.

The precise mechanisms by which these compounds act in concert to influence TBARS levels are not fully understood. It is clearly evident from the results that when combined, these compounds exhibit significant differences in bioactivity, which is assumed based on the differences in the observed effects when they are administered together compared to when each is given alone. The effects induced by such combination are probably due to the ability of each compound to influence the bioactivity of the other when administered in combination.

Within mammalian cells the arginases mediate the divalent cation-dependent hydrolysis of L-arg to the nonprotein amino acid L-ornithine (Ash, 2004). L-canavanine, being an analogue of L-arg, is also an inhibitor of the arginases. It is cleaved hydrolytically by arginase to yield L-canaline and urea (Rosenthal, 1981).

Modified tetrapyrroles are the most abundant pigments found in nature, their most famous representative being haem. Many enzymes such as the large group of CYP<sub>450</sub> enzymes rely on haem as a prosthetic group. The biosynthesis of haem requires the coordinated activity of up to 10 different enzymes one of which is aminolevulinic acid (ALA) synthase, a pyridoxal phosphate-dependent enzyme which mediates the condensation of glycine and succinyl-CoA

with the elimination of CO<sub>2</sub> to form ALA during the first step of haem biosynthesis (Heinemann *et al.*, 2008).

Rosenthal (1981) demonstrated the ability of L-canaline to bind with pyridoxal phosphate subsequently forming a Schiff's base linkage. It is therefore possible that L-canaline possesses the capacity to inhibit haem synthesis by binding to and sequestering pyridoxal phosphate thus rendering the molecule inactive and unavailable as a coenzyme for ALA synthase. As a result, this would be detrimental to haem synthesis and subsequently to CYP<sub>450</sub> (haem-containing enzymes).

The antagonistic effect of L-can on AFB<sub>1</sub>-induced ROS and lipid peroxidation may therefore be due to the role that L-canaline possibly has in mediating an inhibition of haem synthesis and a subsequent alteration in *CYP3A4* function. The consequence may well be reduced bioactivation of AFB<sub>1</sub> accompanied by decreased AFB<sub>1</sub>-induced ROS.

Other results in this study demonstrated that L-can-AFB<sub>1</sub> co-administration induced a 2.38-fold ( $p < 0.001$ ) increase in GSH levels compared to the control (Figure 4.3). In contrast, a marginal 1.01-fold ( $p > 0.05$ ) increase was noted when cellular GSH levels induced by L-can-AFB<sub>1</sub> were compared to that mediated by L-can.

More importantly, in addition to L-can significantly reducing the levels of TBARS when combined with AFB<sub>1</sub> (Figure 4.4), it also significantly ( $p < 0.01$ ) increased GSH content (Figure 4.3) which may further explain its ameliorative effect on AFB<sub>1</sub>-induced ROS and lipid peroxidation.

The increase in GSH levels by L-can-AFB<sub>1</sub> may be due to the effects of each compound. Aflatoxin B<sub>1</sub>-induced ROS and lipid peroxidation may have influenced GCS transcription. L-canavanine may have contributed to the increase in GSH levels in a similar way or by its effect on the PPP, and its ability to influence S-nitrosylation and subsequent activity of GCS.

The results indicate an inhibition of AFB<sub>1</sub>-induced ROS by L-can, and the high levels of GSH observed after L-can-AFB<sub>1</sub> co-administration (Figure 4.3) suggests that AFB<sub>1</sub>-induced ROS may have been conjugated to GSH, thus accounting for the reduced levels of TBARS (Figure 4.4).

Contrary to the L-can-AFB<sub>1</sub> combination, which induced a lower level of lipid peroxidation than each compound given alone, SF-AFB<sub>1</sub> induced a higher level of lipid peroxidation than each compound given alone (Figure 4.4). According to the results, SF co-administration along with AFB<sub>1</sub> evoked a 3.20-fold ( $p < 0.001$ ) increase in the oxidative damage to lipids compared to the control (Figure 4.4). In addition, a 4.12-fold ( $p < 0.001$ ) and a 1.12-fold ( $p < 0.001$ ) increase in TBARS levels by SF-AFB<sub>1</sub> was noted when compared to lipid peroxidation induced by the individual administration of SF and AFB<sub>1</sub> respectively (Figure 4.4).

The type of chemical interaction which describes the effect of the SF-AFB<sub>1</sub> combination is potentiation, defined in terms of toxicology as ‘exposure to a combination (SF-AFB<sub>1</sub>) of chemicals, in which one chemical generally induces no toxic effect when given alone (SF), but in combination with the other chemical (AFB<sub>1</sub>), which generally induces a defined toxic effect when given alone, produces a toxic effect greater than that which is induced by the toxic chemical itself’. Thus SF potentiates the lipid peroxidation induced by AFB<sub>1</sub>.

This effect may be attributed to the oxidative properties and effects of each compound. Aflatoxin B<sub>1</sub>-induced oxidative stress may have influenced TBARS levels and similarly L-can, which is known to exist in relatively high concentrations within SF.

Accompanied with the significant increase in TBARS levels following the co-administration of SF with AFB<sub>1</sub> (Figure 4.4) was a 2.13-fold ( $p < 0.001$ ) increase in cellular GSH content when evaluated against the control (Figure 4.3). In addition, SF-AFB<sub>1</sub> induced a 1.04-fold ( $p > 0.05$ ) decrease and a 1.37-fold ( $p > 0.05$ ) increase in GSH content when compared to GSH levels induced by the individual administration of SF and AFB<sub>1</sub> respectively.

The increase in GSH levels by this combination may be due to the effects of either compound. Aflatoxin B<sub>1</sub> and the L-can in SF may have influenced GCS transcription. In addition, the ability of L-can to influence S-nitrosylation and GCS activity as well as its effects on the PPP may have contributed to increase GSH. The observed elevation in cellular GSH content may also be due to the presence and activity of flavonoids, which might have substituted and consequently spared GSH due to their potent antioxidant capacity, and pinitol in SF.

The means by which SF-AFB<sub>1</sub> acts in concert to influence cellular redox state are not fully understood. As previously mentioned, when in combination, compounds may exhibit differences in bioactivity, which may be due to the capacity of each compound to influence the bioactivity of the other.

#### **4.8 Conclusion**

In conclusion, the results provide *in vitro* evidence that a single dose of AFB<sub>1</sub> led to a significant increase in lipid peroxidation at the end of the experimental period. As reported in the literature, such an effect is possible due to the capacity of AFB<sub>1</sub> to induce various ROS.

In addition, the data presented strongly suggests that SF and L-can are able to exert their effects via an alteration of the intracellular redox metabolism since their supplementation enhanced the antioxidant status of HepG<sub>2</sub> cells. The increase of intracellular GSH content to above normal levels by SF and L-can indicates that they play a vital role in mitigating AFB<sub>1</sub>-induced oxidative stress. The stronger effect of L-can compared to SF as depicted by the GSH and TBARS results is probably due to it being applied in a higher concentration than that which is present in the plant extract, thus indicating a concentration dependent effect.

Overall, the GSH and TBARS assays both served as efficient techniques in assessing the intracellular redox state following the exposure of HepG<sub>2</sub> cells to the various compounds under investigation in this study.

## **Chapter 5**

# **GENOMIC INTEGRITY**

### **5.1 Introduction**

Genomic DNA is under constant attack from both endogenous and exogenous sources of DNA damaging agents (Gasser and Raulet, 2006). Chemicals that interact with DNA can cause direct damage by covalent modifications, such as adducts or strand breaks, or can perturb DNA and chromatin function by non-covalent binding. Both types of interactions lead to genetic changes such as stalled replication, cell cycle delays, mutations and even cytotoxicity (Li *et al.*, 2007). DNA damage is thus directly deleterious to cells and accumulated damage may cause genomic instability, which in organisms with renewable tissues may result in cancer (Gasser and Raulet, 2006). Nucleic acid stains can be useful tools for investigating the integrity of DNA by fluorescence microscopy.

### **5.2 Fluorescence Microscopy**

A fluorescent compound absorbs light energy over a range of wavelengths that is characteristic for that compound. This absorption of light influences an electron in the compound to be raised to a higher energy level. The excited electron rapidly decays to its ground state, emitting the excess energy as a photon of light. This transition of energy is called fluorescence (BD Biosciences, 2000).

Absorption spectrum is the term given to the range over which a fluorescent compound can be excited. As more energy is consumed during absorption than is emitted in fluorescence, emitted wavelengths will be longer than those absorbed. The range of emitted wavelengths for a particular compound is termed its emission spectrum (BD Biosciences, 2000). The difference between the exciting and emitting wavelengths, known as the Stokes shift, is the critical property that makes fluorescence so powerful (Lichtman and Conchello, 2005).

Due to its intrinsic selectivity, fluorescence imaging has become the mainstay of microscopy in the service of biology. Many of the technical improvements in microscopes over the years have centred on increasing the contrast between what is interesting (signal) and what is not (background). Fluorescence microscopy is the prototypical example, as its primary aim is to

reveal only the objects of interest in an otherwise black background (Lichtman and Conchello, 2005).

Although many organic substances have intrinsic fluorescence (autofluorescence), and a few are useful for labelling of components in biological systems, the typical approach to fluorescence microscopy is to take advantage of synthesised compounds. Over the past several decades, organic chemists have devised a variety of fluorescent probes that provide a means of labelling virtually any imaginable aspect of a biological system. Molecules that are used by virtue of their fluorescent properties are called fluorophores (Lichtman and Conchello, 2005). Examples of fluorophores are ethidium bromide (EtBr) and Hoechst 33342.

The light source in fluorescence microscopy is usually a xenon or high pressure mercury vapour lamp, which emits from the UV into the red wavelengths (Figure 5.1). A specific wavelength of light is used to excite the fluorophore present in the specimen. Such interactions initiate the release of longer wavelengths of light which can subsequently be imaged (White and Errington, 2005). This imaging is accomplished in the fluorescent microscope by utilising a combination of filters that are specific for the excitation and emission characteristics of the fluorophore concerned. There are usually three main filters: an excitation filter, a dichroic mirror and an emission filter (Wilson and Walker, 2005; Figure 5.1).

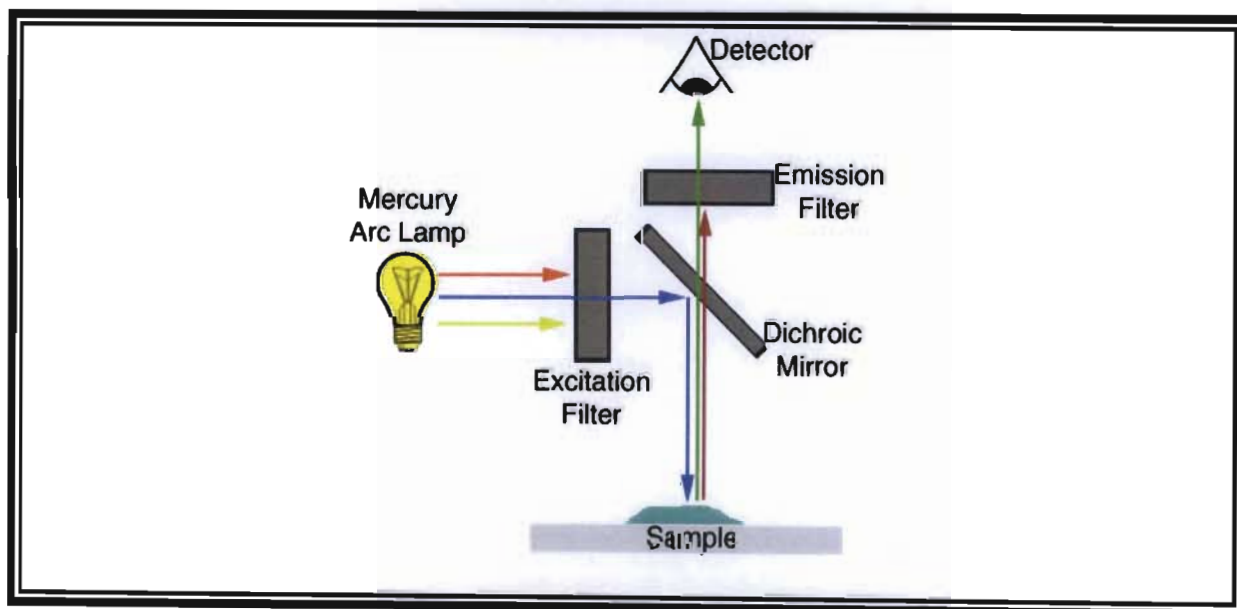


**Figure 5.1** Typical filter setup of a fluorescence microscope (Innes, 2008).

For example, the commonly used fluorophore EtBr is optimally excited at a wavelength of 510nm and emits maximally at 595nm. A set of glass filters for viewing EtBr requires that all wavelengths of light from the lamp be blocked except the 510nm light. The excitation filter allows a maximum amount of 510nm light to pass through it, which is then directed to the specimen via the dichroic mirror (Figure 5.1). Any EtBr in the specimen is subsequently excited by the 510nm light and the resulting light that returns from the specimen passes back through the dichroic mirror and, the emission filter, which only allows light of 595nm to pass through to the detector, ensures that only the signal emitted from the fluorophore of interest reaches the detector. A sensitive digital camera is able to detect such signals efficiently (Wilson and Walker, 2005).

### 5.2.1 Fluorescent nucleic acid stains utilised for the analysis of genomic integrity

An example of a commonly utilised nucleic acid stain is the bisbenzimidazole, Hoechst 33342 (Figure 5.2). It is a cell membrane permeable supravital DNA stain that fluoresces bright blue upon stoichiometrically binding to the AT-rich regions of the minor groove of DNA (Freshney, 1992). Binding of Hoechst to DNA is stabilised by hydrogen bonding, van der Waals interactions and electrostatic interactions between the dye and DNA (Garner, 2008). Its fluorescence intensity is an index of DNA content, chromatin structure and conformation, and may be utilised to discriminate between cells in different phases of the cell cycle (Hawley and Hawley, 2004). Hoechst 33342 excitation is in the UV range of 350-363nm, while emission is recovered above 460nm (Freshney, 1992).

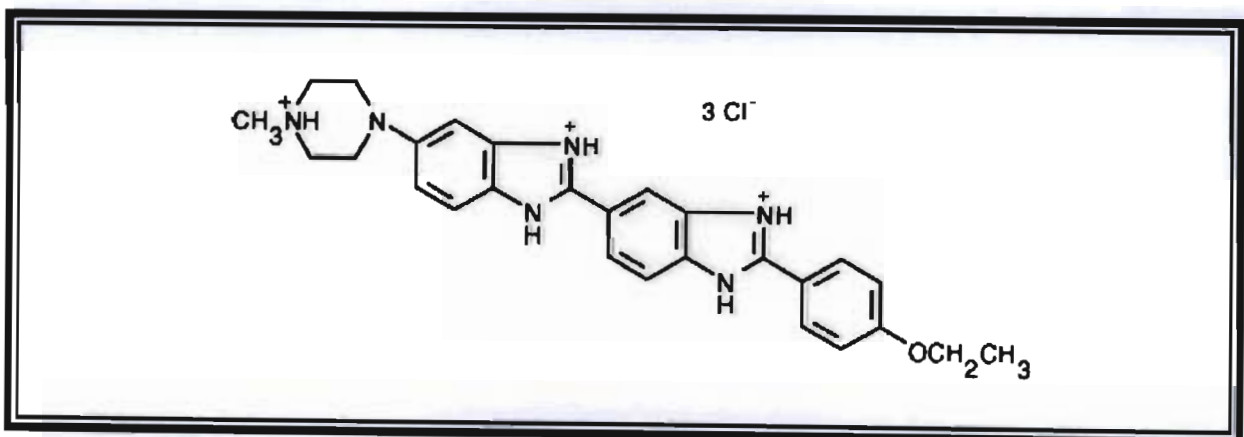
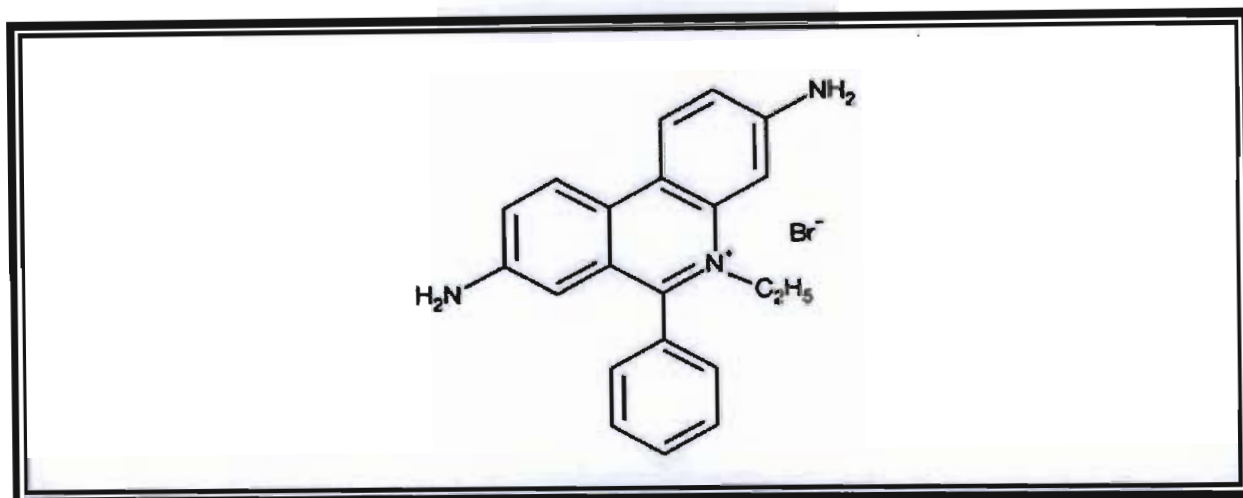


Figure 5.2 Chemical structure of Hoechst 33342 (Garner, 2008).

In addition, the most widely utilised DNA stain is the highly fluorescent dye, EtBr (Figure 5.3). It is a cyclic planar molecule about the size of one base pair, and is able to efficiently intercalate the stacked base pairs of DNA (Wilson and Walker, 2005). The partial positive charge on its exocyclic amines is important for mediating electrostatic attraction and hydrogen bonding interactions with DNA phosphate groups (Nafisi *et al.*, 2007).



**Figure 5.3** Chemical structure of ethidium bromide (Nafisi *et al.*, 2007).

It accumulates at the site of DNA and upon exposure to UV light it fluoresces orange-red. Ethidium bromide excitation occurs at 510nm, while emission is recovered at 595nm (Wilson and Walker, 2005). It is commonly utilised to stain DNA molecules resolved by agarose gel electrophoresis, however it may be employed for use in alternate DNA analysis assays, one of which is the comet assay.

### 5.3 The comet assay

#### 5.3.1 Principle and applications

The comet assay, also called the single cell gel electrophoresis (SCGE) and microgel electrophoresis (MGE) assay was first introduced by Ostling and Johanson (1984) as a microelectrophoretic technique for the direct visualisation of DNA damage in individual cells (Fairbairn *et al.*, 1995). Since then, the assay has been modified several times in order to improve its sensitivity for detecting DNA damage in isolated cells with the most widely utilised version being one described by Singh *et al.* (1988). In this version of the assay, a single cell suspension of the cell culture under investigation is embedded in low-melting-point-



agarose (LMPA) in a gel sandwich on a microscope slide, lysed by detergents at high salt concentrations and then electrophoresed for a short time under alkaline conditions. Under the influence of an electrical current, cells exhibiting DNA damage display increased migration of the DNA from the nucleus toward the anode, giving the appearance of a 'comet tail' (Rojas *et al.*, 1999). With increasing numbers of breaks, DNA 'strands' migrate freely into the tail of the comet, and at the extreme, the head and tail are well separated. Comet tail length increases with DNA damage and the distance of DNA migration from the body of the nuclear core is used to evaluate the extent of DNA damage (Fairbairn *et al.*, 1995).

The DNA damage detected by the assay can arise through various mechanisms, including DNA single- and double-strand breaks, DNA interstrand cross-linking, alkali labile sites and incompletely repaired excision sites (Rojas *et al.*, 1999). Virtually any eukaryotic cell can be processed for analysis of DNA damage using this assay (Fairbairn *et al.*, 1995).

A useful application of the comet assay is in the area of genetic toxicology and a number of investigators have used the assay to evaluate *in vitro* and/or *in vivo* genotoxicity of several chemicals (Rojas *et al.*, 1999).

The aim of this chapter was to utilise the comet assay and Hoechst 33342 staining to determine the influence of SF, L-can and AFB<sub>1</sub>, when administered individually and in combination, on genome integrity.

## **5.4 Materials and Methods**

### **5.4.1 Materials**

Low-melting-point-agarose and NaCl were purchased from Saarchem (SA), whereas slides and coverslips were acquired from Shalom (SA). Triton X-100, NaOH, EDTA, Tris, Na<sub>2</sub>EDTA and paraformaldehyde (PFA) were all obtained from Merck (SA). Hoechst 33342 (10mg/ml) was purchased from Invitrogen. All other reagents and consumables utilised were obtained from the sources mentioned previously.

### **5.4.2 Methodology**

#### **5.4.2.1 Treatment, isolation and harvesting of HepG<sub>2</sub> cells for the comet assay**

HepG<sub>2</sub> cells were treated and harvested as described in chapter 4, section 4.6.2.1.

#### 5.4.2.2 The comet assay on cultured HepG<sub>2</sub> cells

The procedure described for SCGE by Singh *et al.* (1988) was utilised with minor modifications. Initially, 1% LMPA (0.5g dissolved in 50ml PBS) was prepared by heating the mixture in a microwave until a clear solution was obtained. When the agarose had cooled to approximately 37°C, an initial layer (400µl) was pipetted toward the frosted end of a microscope slide (Lasec, 76 x 26mm) and covered with a coverslip (60 x 20mm). Slides were thereafter kept at 4°C for 10 minutes to allow for the agarose to solidify. 1% LMPA was used as the first layer in order to promote a solid foundation of support for the subsequent layers.

For the second and third layers, 0.5% LMPA (0.5g dissolved in 100ml PBS) was utilised. Briefly, after the removal of the coverslips from the first layer, a cell suspension (25µl containing approximately 20 000 cells) from the relevant treatment was mixed with 175µl of 0.5% LMPA (37°C) and pipetted onto the microscope slides already comprising the initial solidified layer. Slides were then covered with coverslips and maintained at 4°C for 10 minutes. The coverslips were thereafter removed and a third layer (200µl) of 0.5% LMPA (37°C) was pipetted onto the previous two solidified layers. Coverslips were then placed on each of the slides and the final layer of LMPA was allowed to solidify at 4°C for 10 minutes.

Coverslips were subsequently removed and all slides were immersed in freshly prepared cold lysing solution [500ml; 2.5M NaCl, 100mM EDTA, 1% Triton X-100, 10mM Tris (pH 10) and 10% DMSO] for 1 h at 4°C and protected from light.

After the 1 h incubation in lysing solution, all slides were removed, the excess lysing solution was drained off and the slides were placed side-by-side into the electrophoresis tank with the frosted ends closest to the cathode. The tank was thereafter filled with freshly prepared electrophoresis buffer (300mM NaOH, 1mM Na<sub>2</sub>EDTA; pH 13) to a level approximately 20mm above the slides. Prior to electrophoresis, the slides were equilibrated for 20 minutes in the alkaline electrophoretic solution, which contains low salt and no detergents. This period of incubation was to facilitate the unwinding of DNA. Following the 20 minute incubation, the tank was sealed and a current of 300mA (25V) was applied for 35 minutes (room temperature) using a Bio-Rad compact power supplier. After electrophoresis, all slides were removed, drained, placed on a tray and carefully washed with three changes of 5 minutes each of neutralisation buffer (0.4M Tris; pH 7.4) in order to remove detergents and alkali. Slides were

thereafter stained with 50 $\mu$ l EtBr (20 $\mu$ g/ml), covered with a coverslip and stored overnight at 4°C to facilitate efficient intercalation of the dye between the base pairs of DNA.

#### 5.4.2.3 Treatment of HepG<sub>2</sub> cells for Hoechst staining

HepG<sub>2</sub> cells were grown to approximately 80% confluency in a 25cm<sup>3</sup> culture flask. Cells were rinsed with three changes of pre-warmed (37°C) PBS and thereafter harvested by trypsinisation and counted. A CCM-cell suspension (2ml containing approximately 200 000 cells) was added onto a coverslip present in each well of a 6 well microtiter plate (1 well was utilised for each treatment). The plate was then sealed with parafilm, swabbed with 70% ethanol and incubated (37°C) overnight to facilitate the efficient attachment of the cells onto the coverslips. After the overnight incubation, the spent culture medium from each well was removed and cells were rinsed with three changes of pre-warmed (37°C) PBS. An aliquot of 3ml of the appropriate sample (Table 5.1) was subsequently added into the relevant wells. The plate was then sealed with parafilm, sterilised using 70% ethanol and incubated (37°C) for 24 h.

**Table 5.1: Preparation of samples**

| Sample                   | Volume of sample ( $\mu$ l)   | Final volume with CCM (ml) | Final dilution/ concentration of sample |
|--------------------------|-------------------------------|----------------------------|---|
| Control                  | -                             | 12                         | -                                       |
| SF                       | 2000                          | 12                         | 1:6                                     |
| L-can                    | 6000 (4mM)                    | 12                         | 2mM                                     |
| AFB <sub>1</sub>         | 37 (321 $\mu$ M)              | 12                         | 1 $\mu$ M                               |
| SF + AFB <sub>1</sub>    | 2000 + 37 (321 $\mu$ M)       | 12                         | 1:6 + 1 $\mu$ M                         |
| L-can + AFB <sub>1</sub> | 6000 (4mM) + 37 (321 $\mu$ M) | 12                         | 2mM + 1 $\mu$ M                         |

#### 5.4.2.4 Preparation of 10% paraformaldehyde and Hoechst 33342 stock solutions

A 10% PFA solution was prepared by initially dissolving 2g of PFA in 18ml of PBS. This mixture was then vortexed and heated (60°C) in a water bath until a clear solution was obtained. The pH of this solution was adjusted to 7.4 and made up to 20mls with PBS.

An aliquot of 5 $\mu$ l of a Hoechst 33342 stock solution (10mg/ml) was topped to 10ml with PBS in order to obtain a Hoechst 33342 working solution with a concentration of 5 $\mu$ g/ml.

#### **5.4.2.5 Hoechst 33342 staining**

Cells were washed with three changes of pre-warmed PBS (37°C) subsequent to the overnight incubation and then fixed to the coverslips by adding 2ml of a 10% PFA solution into each well. After 5 minutes, the used fixative was decanted and each coverslip subsequently washed with PBS. A 100 $\mu$ L aliquot of the Hoechst 33342 working solution was then pipetted onto each coverslip and the plate was covered and incubated at 37°C. After a 15 minute incubation period, PBS was utilised to wash the stained cells and remove any residual Hoechst working solution. A 2ml aliquot of PBS was then added to each well and the plate was sealed.

#### **5.4.2.6 Instrumentation and analysis of samples**

All images were analysed using an Olympus IXSI inverted microscope equipped with 510-560nm excitation and 590nm emission filters (SCGE), and 350nm excitation and 450nm emission filters (Hoechst). The microscope was connected to a personal computer-based analysis system (Analysis LS Research Software) and a charge-coupled device (CCD) digital camera (CC-12) which was utilised to capture images.

With regards to SCGE, the degree of DNA damage for each cell was quantified as comet tail length ( $\mu$ m), the distance from the end of the head to the end of the tail. A total of 60 individual cells were randomly selected and screened (200x magnification) per treatment (30 cells from each of two replicate slides).

#### **5.4.2.7 Data analysis and statistics**

Data acquired from the comet assay are represented as the mean comet tail length ( $\mu$ m) plus or minus the standard deviations. Samples were compared for differences using one-way ANOVA and the Kruskal-Wallis test (GraphPad InStat Software, version 3.06). A probability value (p) of less than 0.05 ( $p < 0.05$ ) was considered as statistically significant (\* indicates significant ( $p < 0.05$ ) differences between treated and control groups; # indicates significant ( $p < 0.05$ ) differences between treated groups).

## 5.5 Results and Discussion

HepG<sub>2</sub> cells have retained many of the functions of normal liver cells and express different inducible xenobiotic metabolising enzymes. These cells have been extensively used in metabolism studies and are recommended for the detection/screening of mutagens (Belloir *et al.*, 2006).

Xenobiotics can induce chromosomal damage by direct and indirect action. By the first mechanism, covalent adducts are formed between the xenobiotic and/or possible metabolites thereof, and DNA; by the second mechanism, the xenobiotic and/or its metabolites may induce the formation of reactive secondary agents upon interaction with non-DNA targets. The secondary agents which can then facilitate DNA damage are mostly ROS, lipid-hydroperoxides and their degradation products (Amstad *et al.*, 1984). Besides oxidative damage directly inflicted on DNA by free radicals, there are other indirect mechanisms by which radicals can cause DNA damage. Lipid peroxides enter the nucleus where they react with Fe<sup>2+</sup> to generate the alkoxyl radical which attacks DNA. Also, intracellular Ca<sup>2+</sup> levels increase as a result of oxidative damage to cell membranes and Ca<sup>2+</sup> then enters the nucleus where it can activate nucleases which cause DNA strand breaks (Meki *et al.*, 2004).

DNA damage results in the formation of DNA chain breaks that activate chromatin-bound protein kinases which function to phosphorylate p53 (Hickman *et al.*, 2002) leading to its activation and accumulation (Komarova and Gudkov, 1998). Tumour suppressor protein p53 may stimulate apoptosis when cells are confronted with severe, irreparable damage (Shmueli and Oren, 2007). A characteristic alteration in nuclear morphology occurring as a consequence of apoptosis is chromatin condensation (Wang *et al.*, 2008).

To evaluate the effects of SF, L-can and AFB<sub>1</sub> on genomic integrity, the comet assay and Hoechst 33342 staining were employed. These assays are rapid and sensitive techniques which can be utilised to analyse DNA integrity at the individual cell level.

Based on results of the comet assay, the nuclear material of cells exposed to the control can be clearly visualised as a large, compact, intact core of DNA with very little visible DNA migration or damage (Figure 5.4a). The average comet tail length for the nuclei of these cells was statistically determined to be  $8.6 \pm 1.9\mu\text{m}$  (Figure 5.5). This result was consistent with that

shown by Hoechst 33342 staining which revealed the nuclei of the control cells to appear small and dull with no observable chromatin condensation (Figure 5.6a).

In contrast, the strongest effect was seen with AFB<sub>1</sub> (Figure 5.4d), where incubation of HepG<sub>2</sub> cells with 1 $\mu$ M AFB<sub>1</sub> for 24 h induced a significant ( $p < 0.001$ ) influence on comet tail length ( $156.8 \pm 18.7\mu\text{m}$ ) (Figure 5.5), evidenced by the 18-fold increase in DNA migration when compared to the control ( $8.6 \pm 1.9\mu\text{m}$ ).

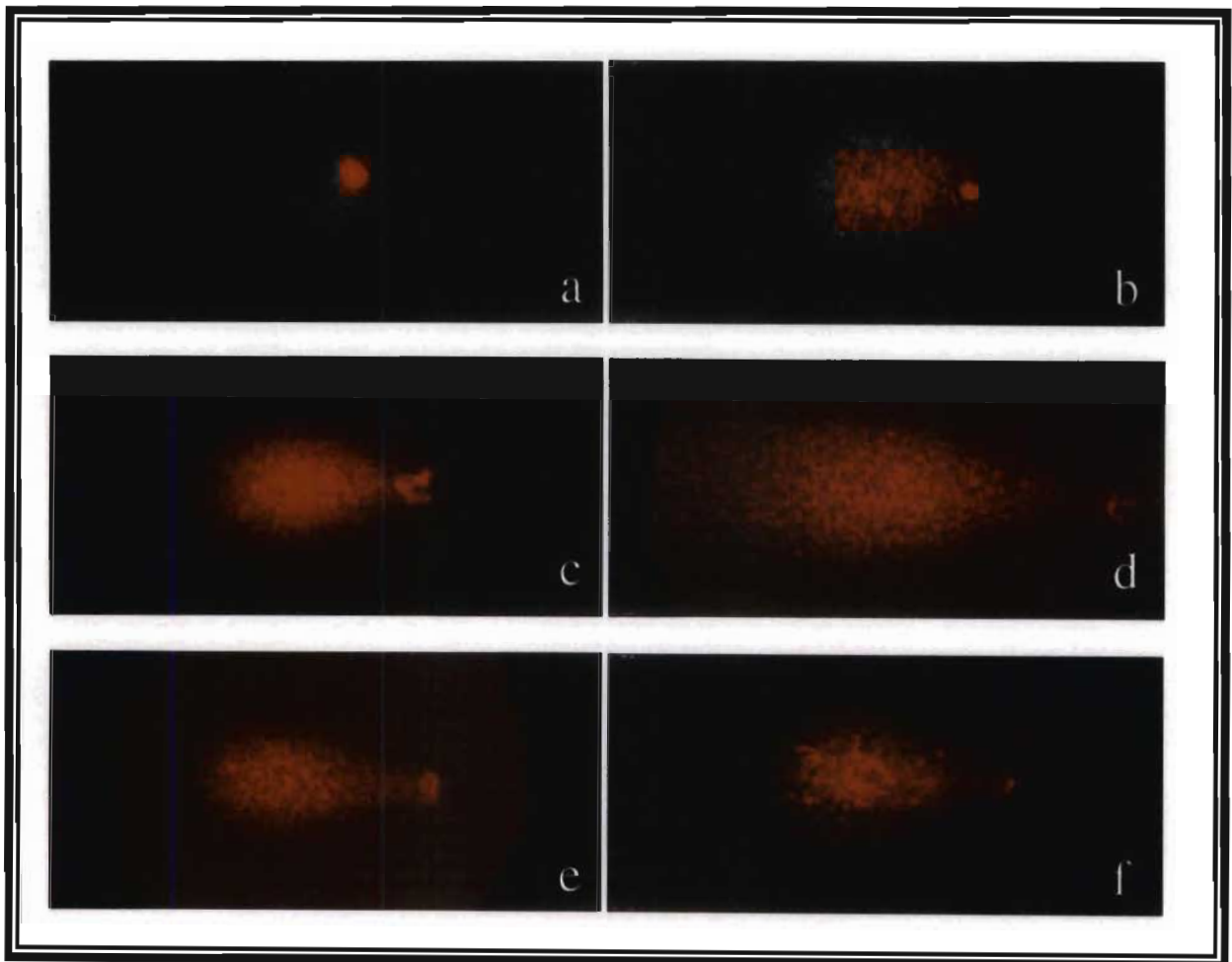


**Figure 5.4** Ethidium bromide staining of HepG<sub>2</sub> cells (400x magnification).

The data obtained is in agreement with other studies (Amstad *et al.*, 1984; El-Khatib *et al.*, 1998; O'Brien *et al.*, 2000; Raj *et al.*, 2001; Ehrlich *et al.*, 2002) which have established that AFB<sub>1</sub> damages DNA. A study by Uhl *et al.* (2000) demonstrated the ability of AFB<sub>1</sub> to induce a dose-dependent (0, 0.008, 0.01, 0.03, 0.1, 0.3 and 1.0 $\mu$ M) increase in DNA migration of

HepG<sub>2</sub> cells after 24 h. The lowest concentration of AFB<sub>1</sub> that caused a significant positive result was 0.008μM. Additionally, Majer *et al.* (2004) investigated the induction of micronuclei in HepG<sub>2</sub> cells exposed to AFB<sub>1</sub> (0.0, 0.1, 0.5, 1.0μM) for 24 h. It was shown that AFB<sub>1</sub> induced micronuclei in a dose-dependant manner with the strongest response that caused a significant effect being observed at concentrations greater than or equal to 0.5μM.

It has been suggested by Amstad *et al.* (1984) and Shen *et al.* (1994) that oxidative stress mediated by AFB<sub>1</sub> may be one of the underlining mechanisms for AFB<sub>1</sub>-induced DNA damage. Results from the TBARS assay (Chapter 4) showed that AFB<sub>1</sub> induced a significant (p<0.001) increase in lipid peroxidation. This finding facilitates the presumption that one of the major contributors to the DNA damage observed after AFB<sub>1</sub> administration is oxidative stress.

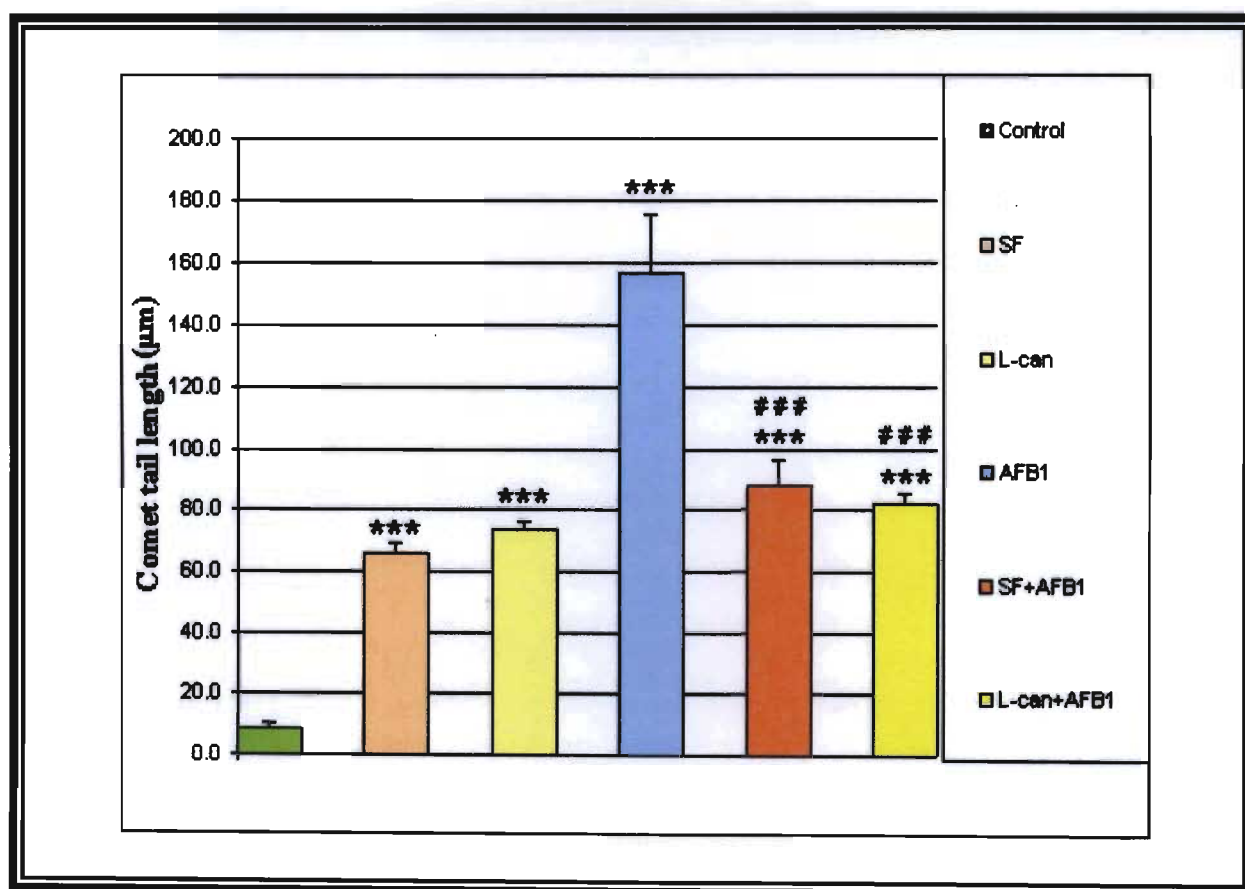


Figure 5.5 Induction of DNA migration by SF, L-can, AFB<sub>1</sub>, SF-AFB<sub>1</sub> and L-can-AFB<sub>1</sub> in HepG<sub>2</sub> cells. \*\*\*p<0.001, ###p<0.001.

An early important defence mechanism that can be activated in response to DNA damage comprises transient inhibition of cell cycle progression by inducing antiproliferating genes. During growth arrest, DNA is coiled and protected by histone proteins. Transient growth arrest allows the cell to repair and/or to replace damaged DNA and to mount an adaptive response against further DNA damage (Weber *et al.*, 2007).

Histones are small basic proteins within which lysine and arginine residues are abundant. Within the nuclei of all eukaryotic cells, genomic DNA is highly folded, constrained, and compacted by both histone and non-histone proteins in a dynamic polymer called chromatin (Jenuwein and Allis, 2001). Chromatin structure plays an important role in most processes pertaining to DNA metabolism (Escargueil *et al.*, 2008) and a well-known function of chromatin is its involvement in DNA packaging. Another function related to chromatin structure includes its ability to regulate processes such as DNA repair by controlling the accessibility of the different macromolecular machineries to their cognate substrates (Escargueil *et al.*, 2008).

Aflatoxin B<sub>1</sub> has been reported to bind many nuclear proteins one of which is histones (Yu *et al.*, 1988; Chih *et al.*, 1993). Besides AFB<sub>1</sub> itself or the generated *exo*-isomer interacting with proteins and histones specifically, the dialdehyde generated from the AFB<sub>1</sub>-8,9-dihydrodiol is capable of condensing with primary amino acid groups, such as lysine forming a Schiff's base (Guengerich *et al.*, 1998) and possibly contributing to alterations in histone structure and function. Thus, an additional mechanism by which AFB<sub>1</sub> influences DNA integrity is by its capacity to mediate alterations in histone structure, accompanied by subsequent perturbation of chromatin function.

The significant DNA damage induced by AFB<sub>1</sub> (Figure 5.4d) is accompanied by nuclei that exhibit stronger fluorescence (Figure 5.6d) compared to the control (Figure 5.6a) as illustrated by Hoechst staining. In addition, the nuclei of the AFB<sub>1</sub> treated cells display a slight reduction in size and exhibit a circular shape when compared to the nuclei of the control cells. Subsequent to Hoechst staining, apoptotic cells exhibit brighter fluorescence, a consequence of chromatin condensation (Lee and Shukla, 2005), which has previously been reported by Yoneyama *et al.* (1987) to occur in MDBK cells and primary foetal bovine kidney cells following exposure to AFB<sub>1</sub> for 24 h. In addition, studies conducted by O'Brien *et al.* (2000)



demonstrated extensive cell shrinkage and chromatin condensation when HepG<sub>2</sub> cells were incubated with AFB<sub>1</sub>. The difference in Hoechst 33342 fluorescence intensity between normal and apoptotic cells may also be attributed to a more rapid membrane uptake of the dye by cells undergoing apoptosis (Omar and Hu, 2003).

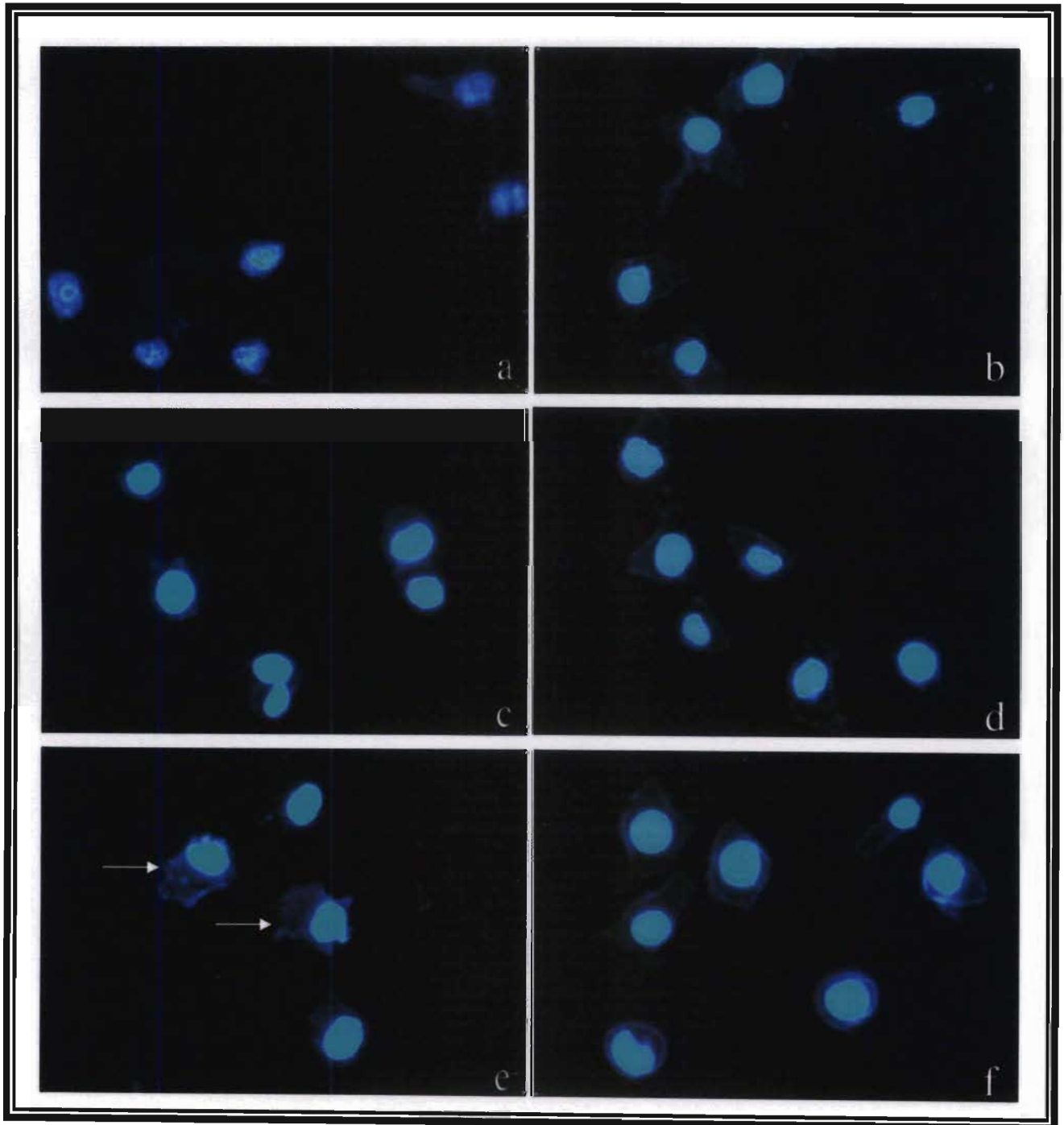


**Figure 5.6** Hoechst 33342 staining of HepG<sub>2</sub> cells (400x magnification).

Thus, the stronger fluorescence that these cells exhibit, due to chromatin condensation, is an indication of apoptosis, a consequence of which is presumed to occur following the deleterious effects of the toxin.

Other results demonstrated lower levels of activity after the individual administration of SF (Figure 5.4b) and L-can (Figure 5.4c), for which the average comet tail for the nuclei of these cells were  $66.3 \pm 2.7\mu\text{m}$  and  $73.5 \pm 2.7\mu\text{m}$  respectively (Figure 5.5). However, both samples did mediate a significant ( $p < 0.001$ ) increase in DNA migration when compared to the control ( $8.6 \pm 1.9\mu\text{m}$ ). These samples induced a similar intensity of DNA damage.

Results from the TBARS assay (Chapter 4) revealed SF to induce significantly ( $p < 0.001$ ) lower levels of lipid peroxidation. As a result, it is unlikely for SF-induced DNA damage to be a consequence of oxidative stress. It is therefore presumed that SF mediates DNA damage via an indirect mechanism which possibly involves the inhibition of DNA repair processes.

In contrast, it is suggested that one of the mechanisms by which L-can is able to mediate DNA damage is via its capacity to induce ROS and subsequent oxidative stress. This postulation is based on the high level ( $p < 0.001$ ) of lipid peroxidation induced by L-can as evidenced by data obtained from the TBARS assay (Chapter 4).

Studies conducted by Schachtele *et al.* (1968) and Hare (1969) demonstrate a possible mechanism by which L-can is able to influence DNA integrity. After exposing *Escherichia coli* to L-can, Schachtele *et al.* (1968) carried out electron microscopy studies which showed a profound change in nuclear organisation, characterised by extensive physical disruption of the nuclear region. The authors suggested that the lethal action of L-can was related to its integration into membrane bound proteins which resulted in the disruption of the *E. coli* genome. A similar study conducted by Hare (1969) illustrated the capacity of L-can to induce alterations in the nuclear architecture of mammalian cells. The observed alterations were characterised by the formation of irregular aggregates of nucleoplasmic contents frequently attached to the nuclear membrane. The author postulated that L-can was able to induce such an effect as a result of the formation of canavanyl protein-DNA aggregates.

Arginases facilitate the hydrolysis of L-arg to L-ornithine, which is the biosynthetic precursor of the polyamines (Ash, 2004). The polyamines (putrescine, spermidine and spermine) are organic cations of low molecular weight. As a consequence of their polybasic character, they adhere strongly to nucleic acids, stabilising DNA by neutralising the negative charges of the phosphate groups and decreasing the repulsion between the strands of DNA (Yerlikaya, 2004). Spermidine and spermine influence DNA to condense, aggregate and bend or contort the normal  $\alpha$ -helical structure (Criss, 2003). Studies have also shown that spermidine and spermine are able to stabilise chromatin and that polyamine-depleted cells undergo changes in chromatin and DNA structure (Berger *et al.*, 2007). In addition, many histone acetylases and deacetylases, which either add or remove acetyl groups from the lysine residues of all histones and subsequently influence histone function, are regulated by gene promoters and inhibitors, which, in turn, are controlled by polyamines (Criss, 2003). The polyamines therefore perform crucial functions related to the integrity of the genome and any perturbation of polyamine homeostasis may lead to alterations in polyamine pool sizes and as a result, may have critical consequences on DNA structure and integrity. Because it is an analogue of L-arg, L-can may therefore alter DNA integrity as a result of its inhibitory effect on the arginases and subsequent L-ornithine and polyamine synthesis.

When compared to control cells (Figure 5.6a), characterisation of cellular morphology after incubation with L-can (Figure 5.6c) revealed cytoplasmic shrinkage and chromatin condensation, both of which are morphological hallmarks of apoptosis (Stander *et al.*, 2007). This finding demonstrates the apoptotic inducing properties of L-can and is in agreement with Cervera *et al.* (1983) who used pulse and chase autoradiography and showed that the nuclei of HeLa S3 cells became round and compact with an accumulation of perichromatin granules and fibrils after exposure to L-can.

In addition, HepG<sub>2</sub> cells stained with Hoechst 33342 after exposure to SF displayed nuclei that were brightly fluoresced (figure 5.6b) compared to the control (figure 5.6a). As observed in the other treatments, these cells also exhibit chromatin condensation. Apoptosis is apparent based on the observed chromatin condensation as well as findings by Chinkwo (2005) who demonstrated chromatin condensation in CHO cells by SF.

Comet assay analysis subsequent to co-administration of L-can with AFB<sub>1</sub> ( $82.1 \pm 3.4\mu\text{m}$ ) revealed significant ( $p < 0.001$ ) increases in DNA migration compared to the control ( $8.6 \pm 1.9\mu\text{m}$ ) and L-can ( $73.5 \pm 2.7\mu\text{m}$ ) (Figure 5.5). However, when compared to the nuclei of AFB<sub>1</sub>-treated cells ( $156.8 \pm 18.7\mu\text{m}$ ), treatment with the same combination evoked a significant ( $p < 0.001$ ) decrease in DNA migration and comet tail length (Figure 5.4f).

The ability of L-canaline to mediate alterations in *CYP3A4* function was previously described (Chapter 4). The antagonistic effect of L-can on AFB<sub>1</sub>-induced DNA damage may be due to the role that L-canaline possibly has in mediating an inhibition of haem synthesis with a subsequent alteration in *CYP3A4* function. The consequence is presumably reduced bioactivation of AFB<sub>1</sub> accompanied by decreased AFB<sub>1</sub>-induced ROS and DNA damage.

In addition to the abovementioned, a further protective mechanism by which L-can possibly antagonises AFB<sub>1</sub>-induced DNA damage may result from enhanced conjugation of AFB<sub>1</sub>-induced ROS as well as the AFB<sub>1</sub>-epoxide with GSH. This is presumed based on results of the GSH assay (Chapter 4) which revealed the capacity of L-can to enhance the antioxidant status by mediating a significant ( $p < 0.01$ ) increase in intracellular GSH content and therefore playing a vital role in mitigating AFB<sub>1</sub>-induced oxidative stress and subsequent DNA damage.

Riganti *et al.* (2003) demonstrated a significant ( $p < 0.05$ ) increase in the flux of the PPP when N11 mouse glial cells were incubated with L-can. In addition to increased NADPH synthesis for the regeneration of GSH, the upregulation of the PPP can have other consequences of interest including an increase in other intermediate metabolites, such as ribose-5-phosphate, which could contribute to DNA synthesis and repair (Bensaad and Vousden, 2007). It has been demonstrated that L-can is an inhibitor of NOS, the consequence of which is decreased NO synthesis (Luzzi and Marletta, 2005). Nuclear enzymes associated with the repair of alkylated DNA are inhibited by NO. In the presence of NO the zinc finger motifs of DNA repair enzymes lose their integrity, resulting in inhibition of DNA repair (Kim *et al.*, 2001). It is therefore suggested that the antagonistic effect of L-can on AFB<sub>1</sub>-induced DNA damage may also be attributed to its capacity to indirectly promote DNA repair due to its ability to influence the PPP and as a consequence of NOS inhibition.

Incubation with L-can-AFB<sub>1</sub> (figure 5.6f) mediated cytoplasmic shrinkage with nuclei that were abnormally larger and rounder in shape when compared to the control cells (figure 5.6a). Once again, the intense chromatin condensation is an indication of apoptosis.

Regarding SF co-administration along with AFB<sub>1</sub>, the results illustrated significant ( $p < 0.001$ ) increases ( $88.2 \pm 8.2 \mu\text{m}$ ) in DNA migration compared to the control ( $8.6 \pm 1.9 \mu\text{m}$ ) and SF ( $66.3 \pm 2.7 \mu\text{m}$ ) (Figure 5.5). However, when compared to the nuclei of AFB<sub>1</sub>-treated cells ( $156.8 \pm 18.7 \mu\text{m}$ ), the same combination evoked a significant ( $p < 0.001$ ) antagonistic effect on DNA migration and comet tail length (Figure 5.4e).

In order to exert its cytotoxic and carcinogenic effects, AFB<sub>1</sub> requires metabolic activation by *CYP3A4*. Utilising microsome-based *in vitro* fluorometry, Mills *et al.* (2005b) reported significant decreases in *CYP3A4* activity by both a water extract (68.5% inhibition) as well as an ethanolic extract (95.7% inhibition) of SF. Thus, the protection afforded by SF against AFB<sub>1</sub>-induced DNA damage may be due to its inhibitory effect on *CYP3A4* activity and subsequent AFB<sub>1</sub> bioactivation.

The decrease in DNA damage after SF-AFB<sub>1</sub> exposure is also possibly due to the role of flavonoids present in SF. It is suggested that flavonoids present in SF may provide strong nucleophilic centres enabling them to react with electrophilic agents, thereby inactivating or scavenging them, but ultimately intercepting mutagens and consequently reducing DNA damage.

Protection by SF against AFB<sub>1</sub>-induced DNA damage may alternatively result from enhanced conjugation of AFB<sub>1</sub>-induced ROS as well as AFB<sub>1</sub>-epoxides with GSH for AFB<sub>1</sub> detoxification. This is based on results of the GSH assay (Chapter 4) which demonstrated that SF enhanced the antioxidant status, by increasing intracellular GSH content, when administered in combination with AFB<sub>1</sub>.

The protective effect that SF affords against AFB<sub>1</sub>-induced genotoxicity may also be due to L-can, present within the plant extract, to promote DNA repair due to its ability to influence the PPP and inhibit NOS.

Although Hoechst 33342 is a nucleic acid specific stain, the intense fluorescence imparted by this dye when it intercalates DNA also allows for visualisation of other cellular components such as the cell membrane. Based on this and when compared to the control sample (Figure 5.6a), not only do the nuclei of cells treated with SF-AFB<sub>1</sub> (Figure 5.6e) display strong Hoechst staining but the cells themselves exhibit membrane blebbing (Figure 5.6e; arrows) as well as cytoplasmic shrinkage. All three morphological features described are key hallmarks of apoptosis (Omar and Hu, 2003; Stander *et al.*, 2007).

## 5.6 Conclusion

In this study, the strongest effect was seen with AFB<sub>1</sub>. Such an effect was anticipated since this mycotoxin is postulated to be one of the most potent human carcinogens.

DNA damage including inefficient repair is expected to initiate the process of genotoxicity by AFB<sub>1</sub>. Modulation of these parameters by SF and L-can suggests that these compounds may afford protection against genotoxicity induced by AFB<sub>1</sub>. Protection by SF and L-can may be explained by both inhibition of CYP<sub>450</sub> enzymes and induction of phase II biotransformation enzymes. To obtain insight into this aspect, further investigation on the modulation of drug metabolising enzyme activities by SF and L-can in HepG<sub>2</sub> cells is necessary.

Overall, the comet assay was shown to be a useful technique for assessing the level of DNA damage induced by the samples under investigation in the current study. In addition, the outcomes of the comet assay and Hoechst staining demonstrated to be comparable.

## Chapter 6

# PROTEIN INTEGRITY

### 6.1 Introduction

Cells respond to the presence of toxic chemicals by numerous biochemical mechanisms. One of the key cellular responses to toxicant exposure, which could potentially be used as an early marker of toxicity, is the HSR (Golli *et al.*, 2006).

In mammalian cells, the 70kDa Hsp is the most abundant sub-group of the Hsp family and the most closely linked to cytoprotection following a variety of noxious events. The molecular mechanisms which induce Hsp70 expression following exposure of cells to xenobiotics, are not well understood, however it is generally admitted that the initial step is related to denaturation of cellular proteins (Golli *et al.*, 2006).

Denaturation is the conformational alteration of a biological macromolecule which entails a reversible or irreversible loss of its ability to perform a certain biological function (Meredith and Lepock, 1999). Heat shock / thermal stress (temperatures ranging between 40°C to 45°C) causes thermolabile proteins to destabilise and unfold thereby undergoing denaturation. Such unfolding facilitates the formation of molten globule intermediates (structures that exhibit a hydrophobic core and residual secondary features) that accumulate and form aggregates (Meredith and Lepock, 1999) which perturb normal cellular function and prompt cell death (Parcellier *et al.*, 2003).

In addition to thermal stress, oxidative stress has also been implicated in mediating protein denaturation (Meredith and Lepock, 1999). It has been demonstrated that  $\cdot\text{OH}$  and singlet oxygen produce covalently crosslinked protein aggregates with glyceraldehyde-3-phosphate dehydrogenase, alcohol dehydrogenase and myoglobin (Prinsze *et al.*, 1990). In this regard, studies involving gamma-rays have revealed that the  $\cdot\text{OH}$  mediates the oxidation of side chains of amino acid residues (cysteine, methionine, histidine, lysine, arginine, proline) in proteins and subsequently inhibits enzyme/protein function (Meredith and Lepock, 1999).

Essentially, oxidative stress that results in non-native modification of proteins causes thermolabile proteins to destabilise and undergo thermal denaturation at physiological temperatures (37°C). These modified proteins unfold and form a similar structure as produced by thermal stress, a molten globule intermediate, which is prone to aggregate (Meredith and Lepock, 1999).

Negative regulation of monomeric Hsf-1 is relieved by the accumulation of stress generated denatured protein that is prone to form aggregates. Heat shock factor-1 then undergoes trimerisation, gaining DNA binding activity with subsequent activation of Hsp transcription and synthesis (Meredith and Lepock, 1999). Increased intracellular levels of Hsp help the cell survive stresses (Verma *et al.*, 2007).

In general, the protective mechanism of Hsp's is believed to involve their capacity as molecular chaperones, by binding to partially denatured proteins and assisting to refold these proteins into more stable native structures (Verma *et al.*, 2007). In addition, it has been suggested that the cytoprotective effect of Hsp's might arise from their ability to assist in the transfer of newly synthesised proteins into mitochondria, helping to maintain mitochondrial integrity, or by preventing apoptosis by inhibiting caspase activity. On the other hand, Hsp's may exert their anti-apoptotic effect downstream of caspases (Robertson *et al.*, 1999).

Heat shock protein 70 was shown to acquire both enhanced peptide binding ability and peptide complex stability under oxidative conditions (Sreedhar and Csermely, 2004). Park *et al.* 2007 reported that unregulated oxidative stress could induce differential expression of Hsp's, which in turn may play distinct roles in cellular defence. The redox state of the cell has also been reported to influence Hsp synthesis via a direct activation of Hsf-1 (Sreedhar and Csermely, 2004). According to the literature, the potential mechanisms involved in Hsp protection against ROS include maintenance of ATP levels as well as prevention of protein degradation, lipid peroxidation and increases in intracellular Ca<sup>2+</sup> levels (Golli *et al.*, 2006). Another mechanism by which Hsp expression may afford cytoprotection against induced oxidative injury is thought to be due to their ability to decrease ROS by raising the intracellular concentration of GSH as well as preventing the malfolding of endogenous antioxidant enzymes (CAT, SOD and GPX) and enhancing their levels and activities (Hassen *et al.*, 2007).



In addition to Hsp's, p53 is a central factor in cellular stress responses. It governs the adaptive and protective responses following several types of exo- and endogenous damage, such as DNA damage, hypoxia, oxidative stress, and spindle damage (Latonen and Laiho, 2005).

Upon activation, p53 is considered to determine the fate of the cell (Latonen and Laiho, 2005). The biological end-points of p53 induction are growth arrest, which can be transient or permanent (senescence or differentiation), or apoptosis (Meek, 2004).

Tumour suppressor protein p53 arrests the cell cycle in the G<sub>1</sub> and G<sub>2</sub> phases. In the DNA damage response, it participates in DNA repair and recombination by regulating transcription and by direct interaction with components of the repair and recombination machineries (Latonen and Laiho, 2005).

The ability of p53 to induce apoptosis may be its most important tumour-suppressive function. It induces several genes that contribute to both death receptor (Fas, DR5) and mitochondrial (Apaf-1, Bax, Noxa, p53AIP1 and PUMA) apoptotic pathways (Latonen and Laiho, 2005).

## **6.2 Sodium dodecyl sulphate-polyacrylamide gel electrophoresis**

### **6.2.1 Principle of the technique**

Sodium dodecyl sulphate-polyacrylamide gel electrophoresis (SDS-PAGE) is a method commonly used for analysing protein mixtures qualitatively and is based on the separation of proteins according to size. Samples to be resolved by SDS-PAGE are initially briefly boiled in a sample buffer containing  $\beta$ -mercaptoethanol and SDS. The  $\beta$ -mercaptoethanol reduces any disulphide bridges holding together the protein tertiary structure, whereas SDS, an anionic detergent, binds strongly to and denatures the protein. Each protein present within the sample is thereafter fully denatured and opens up into a rod-shaped structure with a series of negatively charged SDS molecules along the polypeptide chain. This treatment results in all proteins becoming linear and possessing a uniform charge (Wilson and Walker, 2005).

The sample buffer also contains an ionisable tracking dye, bromophenol blue, which allows for the electrophoretic run to be monitored, and sucrose or glycerol, which gives the sample solution density thus allowing for the sample to settle easily through the electrophoresis buffer to the bottom when pipetted into the loading well (Wilson and Walker, 2005). The samples to

be separated are in fact not directly loaded into the main separating gel but rather into a stacking gel, the purpose of which is to concentrate the protein sample into a sharp band before it enters the main separating gel.

After the samples are loaded and the electrophoresis buffer added, the current is switched on and the negatively charged protein-SDS complexes move toward the anode and because they have the same charge per unit length, they travel into the separating gel under the applied electrical field with the same mobility. However, as they pass through the separating gel, the proteins separate due to the molecular sieving properties of the gel (Wilson and Walker, 2005).

The gel consists of a three dimensional network which is formed by the cross-linking of long polyacrylamide chains comprising polymerised acrylamide monomers. The pore size of the gel depends on the concentration of acrylamide, which determines the average polymer chain length, and bis, which determines the extent of cross-linking (Andrews, 1986). In essence, the smaller the protein, the more easily it will move through the pores of the gel, whereas large proteins are retarded by frictional resistance due to the sieving properties of the gel (Wilson and Walker, 2005).

When the dye reaches the bottom of the gel, the current is switched off, and the gel is removed and stained using an appropriate staining solution. The gel is then destained in a solution that removes the unbound background stain from the gel, leaving stained proteins visible on a clear background. Using the stained gel, the molecular weights of specific proteins in the sample can be determined by comparing its mobility with those of a number of standard proteins of known molecular weight that are simultaneously run on the same gel (Wilson and Walker, 2005). The gel can alternatively be placed into transfer buffer and utilised for western blotting.

## **6.3 Western Blotting**

### **6.3.1 Principle of the technique**

Western blotting, also known as protein blotting or immunoblotting, evolved from DNA (Southern) blotting and RNA (Northern) blotting (Kurien and Scofield, 2006). It is a technique that allows for equal amounts of protein extracted from cells or tissues, to be separated by SDS-PAGE, electrophoretically transferred from the gel to an adsorbent support membrane such as nitrocellulose and to subsequently be probed with antibodies. Primary polyclonal or

monoclonal antibodies react specifically with antigenic epitopes presented by target proteins attached to the membrane (Figure 6.1). A secondary antibody, conjugated with horseradish peroxidase (HRP) is then applied and binds to the primary antibody-antigen complex (Otsuki *et al.*, 2003).

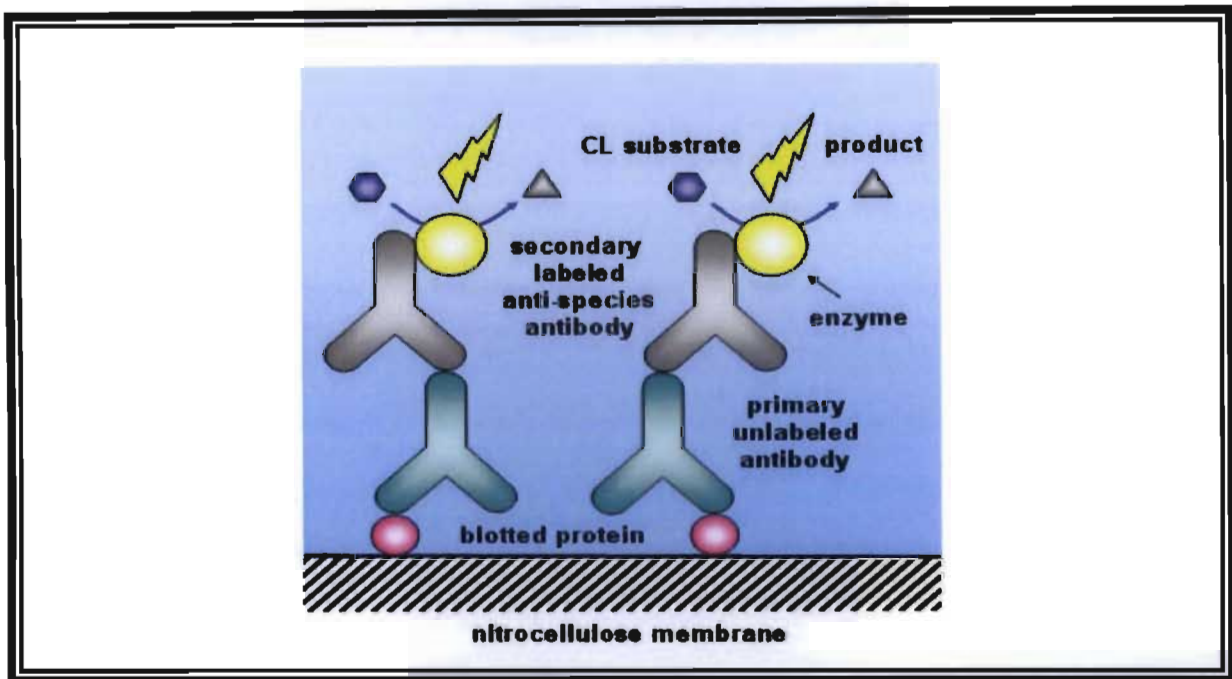


**Figure 6.1 Chemiluminescent detection in western blotting (Roda *et al.*, 2003).**

Chromogenic or radioisotope labelling methods may be used to visualise the bound components, however, the most sensitive nonradioactive method currently available for HRP-conjugated secondary antibodies is enhanced chemiluminescence (Clynes, 1998). In the presence of  $H_2O_2$  and the chemiluminescent (CL) substrate luminol, HRP oxidises the luminol which becomes excited and immediately decays via a light-emitting pathway. The intensity of the light signal generated by this reaction is increased 1 000-fold by the presence of a chemical enhancer thus allowing easy visualisation of the antigens present on the membrane. Less than 1pg of protein can be detected using this method and exposure time is typically less than 1 minute (Kurien and Scofield, 2006).

A number of important characteristics of protein antigens can be determined using the technique of western blotting, namely, the presence and quantity of the antigen, its relative

molecular weight and the efficiency with which it can be extracted from crude protein preparations (Clynes, 1998).

The aim of this chapter was to utilise SDS-PAGE and western blotting to determine the influence of SF, L-can and AFB<sub>1</sub>, when administered individually and in combination, on Hsp70, Hsp90 and p53 expression.

## **6.4 Materials and methods**

### **6.4.1 Materials**

CytoBuster™ protein extraction reagent was purchased from Merck (SA). Bicinchoninic acid (BCA), copper (II) sulphate (CuSO<sub>4</sub>), β-mercaptoethanol and all antibodies were acquired from Sigma (SA). Acrylamide/bis, ammonium persulphate (APS), the molecular weight marker, the Silver Stain Plus kit, nitrocellulose membranes, non-fat dry milk, Tween20 and the Immune-Star HRP substrate kit were all purchased from Bio-Rad. Glycerol, KH<sub>2</sub>PO<sub>4</sub>, acetic acid and methanol were obtained from Saarchem (SA). Glycine, SDS, TEMED, K<sub>2</sub>EDTA and DTT were purchased from Merck (SA). All other reagents and consumables utilised were obtained from the sources mentioned previously.

### **6.4.2 Methodology**

#### **6.4.2.1 Treatment, isolation and harvesting of HepG<sub>2</sub> cells**

HepG<sub>2</sub> cells were treated and harvested as described in chapter 4, section 4.6.2.1.

#### **6.4.2.2 Protein isolation**

Approximately  $3 \times 10^6$  cells per treatment were transferred to appropriately labelled 15ml sterilin tubes and pelleted by centrifugation. The supernatant from each tube was thereafter carefully removed, so as to prevent any disruption of the pellet. The pellet of cells was then resuspended in PBS to facilitate a wash step and this was followed by further centrifugation. Each of the aforementioned centrifugation steps was carried out at 1 000 rpm for 5 minutes at 24°C. The washed pellet was then resuspended in 500µl of the CytoBuster™ protein extraction reagent (a formulation of detergents optimised for efficient extraction of soluble proteins from mammalian cells) followed by incubation on ice for 5 minutes. Thereafter, a final centrifugation step at 5 000 rpm for 10 minutes at 24°C was utilised and the resulting

supernatants (450 $\mu$ l) which served as the crude protein extract were transferred to appropriately labelled 1ml eppendorfs and kept on ice until utilised.

#### **6.4.2.3 Protein quantification and standardisation**

Protein concentrations were quantified spectrophotometrically using the BCA assay by which total protein concentration was determined by a colour change of the sample solution from green to purple in proportion to protein concentration. The BCA assay relies on two reactions. First, the peptide bonds in protein reduce  $\text{Cu}^{2+}$  ions to  $\text{Cu}^{1+}$ . The amount of  $\text{Cu}^{2+}$  reduced is proportional to the amount of protein present in the solution and second, two molecules of BCA chelate with each  $\text{Cu}^{1+}$  ion, forming a purple-coloured product that strongly absorbs light at a wavelength of 562nm. The concentration of protein in each sample was determined by comparison to a protein of known concentration, bovine serum albumin (BSA), which was serially diluted (0, 0.2, 0.4, 0.6, 0.8 and 1.0mg/ml) in order to construct a standard curve (Appendix 2). The assay was performed in duplicate using a 96-well microtitre plate. An aliquot of 25 $\mu$ L of each sample (supernatant) and the relevant standards (BSA) were added to appropriately labelled wells. The BCA working solution (202 $\mu$ l, 4 $\mu$ l  $\text{CuSO}_4$  and 198 $\mu$ l BCA) was thereafter dispensed into each of these wells and the microtitre plate was incubated (37 $^\circ\text{C}$ ) for 30 minutes. After incubation, the absorbance of the various samples were read at 562nm using a spectrophotometer. The absorbance's of the standards (BSA) obtained were used to construct a standard curve, from which the protein concentration of each sample was determined. All samples were thereafter diluted using storage buffer [0.1M  $\text{KH}_2\text{PO}_4$  (pH 7.4), 0.5mM  $\text{K}_2\text{EDTA}$ , 0.1mM DTT and 0.25M sucrose] and standardised to a final protein concentration of 1mg/ml (Appendix 2).

#### **6.4.2.4 Sodium dodecyl sulphate-polyacrylamide gel electrophoresis**

The Mini-PROTEAN 3 SDS-PAGE apparatus (Bio-Rad) was assembled according to manufacturer's instructions. A 12% resolving gel [ $\text{dH}_2\text{O}$ , 1.5M Tris-HCl (pH 8.8), 10% (w/v) SDS, 30% Acrylamide/bis, 10% APS (fresh daily), TEMED] was prepared and added in-between the cleaned glass plates by using a pasteur pipette (this was done very carefully so as to prevent the formation of air bubbles). A layer of  $\text{dH}_2\text{O}$  was added on top of the resolving gel so that a smooth interface was created for efficient addition of the stacking gel. Once the gel had set, the  $\text{dH}_2\text{O}$  was removed by being absorbed to filter paper that was carefully placed in-

between the two glass plates containing the gel. A 4% stacking gel [dH<sub>2</sub>O, 0.5M Tris-HCl (pH 6.8), 10% (w/v) SDS, 30% Acrylamide/bis, 10% APS, TEMED] was then added in-between the glass plates. A Bio-Rad plastic comb was placed into the stacking gel between the glass plates in order to create sample loading wells. Once the gels had set, the gel cassette sandwich was removed from the casting stands and clamped into the electrode assembly.

Sample buffer [dH<sub>2</sub>O, 0.5M Tris-HCl (pH 6.8), glycerol, 10% SDS, β-mercaptoethanol, 1% bromophenol blue] was thereafter added (1:1) to the protein samples, which were then boiled for 5 minutes in order to activate the β-mercaptoethanol and SDS to allow for reduction and unfolding of proteins. Wells were subsequently loaded with 20μg of total protein from the relevant sample. A molecular weight marker (Mwt) was loaded into a separate well in order to facilitate identification of the relative weights of the resolved proteins.

The inner chamber assembly was then placed in the electrophoresis mini tank and a 2x electrode buffer (dH<sub>2</sub>O, Tris, glycine, SDS; pH 8.3) subsequently added. The apparatus was sealed and the tank was then placed in a container approximately half-filled with ice. Samples were then allowed to resolve by electrophoresis (150V, using a Bio-Rad compact power supplier) until the tracker dye reached the bottom of the gel. After electrophoresis, gels were removed and either stained by silver staining (Figure 6.2) or the resolved proteins were electroblotted to nitrocellulose membranes.

#### **6.4.2.5 Silver staining**

All reagents utilised for silver staining were from the Bio-Rad Silver Stain Plus kit. Following electrophoresis, the gels were placed in the fixative enhancer solution [200ml methanol (50% v/v), 40ml acetic acid (10% v/v), 40ml fixative enhancer concentrate (10% v/v), 120ml dH<sub>2</sub>O] and fixed for 20 minutes with gentle agitation. The fixative enhancer solution was thereafter decanted and the gels were rinsed with two changes of 10 minutes each of 400ml dH<sub>2</sub>O. Gels were then placed into the staining solution (35ml dH<sub>2</sub>O, 5ml silver complex solution, 5ml reduction moderator solution, 5ml image development reagent, 50ml development accelerator solution) and after the desired staining was achieved they were transferred to 5% acetic acid for 15 minutes to stop the staining reaction. The acetic acid was thereafter decanted and gels were rinsed for 5 minutes in dH<sub>2</sub>O.

#### **6.4.2.6 Western blotting**

The electrophoresed gels were removed from the SDS-PAGE apparatus and placed in transfer buffer (25mM Tris, 192mM glycine, 20% v/v methanol; pH 8.3), for 10 minutes (to allow the gel and proteins to equilibrate). The blotting membrane, nitrocellulose, as well as the fibre pads and filter paper were appropriately cut according to the dimensions of the gel and prepared by submerging in dH<sub>2</sub>O and thereafter soaking in transfer buffer until they were ready to be used. The gel sandwich was assembled by first placing a fibre pad on the area of the gel holder cassette that would be placed near to the cathode. A piece of filter paper was then placed onto the first fibre pad. The equilibrated gel with the migrated protein samples was then placed on the filter paper, followed by the nitrocellulose membrane. The membrane was cut at a corner which corresponded to the upper area of the gel into which the molecular weight marker was loaded. This facilitates efficient identification at a later stage of the procedure. An additional piece of filter paper and a final fibre pad was then placed on the nitrocellulose membrane. Any trapped air bubbles which might reduce the efficiency of the transfer or distort band patterns were removed by rolling a glass rod over the final fibre pad. The gel holder cassette was then firmly closed, tightly clamped (to prevent skewing of the bands or band spreading during transfer) and placed into the transfer module and subsequently into the mini tank. The tank was then filled with transfer buffer (incorporation of methanol in the transfer buffer allows for the stabilisation of the gel during transfer as well as to increase the binding capacity of nitrocellulose for protein). A teflon coated magnetic stirrer was added into the tank to help maintain even buffer temperature and ion distribution during the transfer process. The apparatus was sealed and the tank was then placed in a container approximately half-filled with ice. Resolved proteins were then electroblotted to the nitrocellulose membranes at a constant current of 400mA for 1 h.

After the transfer, the nitrocellulose membranes were removed and unoccupied sites were blocked overnight (4°C) with 5% (5g) non-fat dry milk in TTBS [100ml; Tris-buffered saline (TBS) containing 0.5% Tween20] in order to reduce background noise and prevent nonspecific binding by antibodies. The spent non-fat dry milk was discarded after the overnight blocking and each membrane was then incubated (room temperature) for 1 h with the relevant primary antibody (anti-mouse Hsp70, 90 or p53). Primary antibodies were diluted 1:1 500 in 1% BSA in TTBS. After incubation, the primary antibody was removed and the membranes were

thoroughly washed with three changes of 10 minutes each of TTBS. The membranes were subsequently incubated (room temperature) with an HRP-conjugated anti-mouse IgG secondary antibody (diluted 1:2 000 in 1% BSA in TTBS) for 1 h. The secondary antibody was thereafter removed and the membrane was subject to a further three 10-minute washes with TTBS. During each wash step and antibody-incubation periods, the blot was subject to mild agitation by placing the container within which it was present, on an orbital shaker.

#### **6.4.2.7 Instrumentation and analysis of samples**

The GelDoc XRS apparatus (Bio-Rad), an instrument equipped with a digital camera, enabled capturing of images of both the silver-stained gels (white epiluminescence) as well as the nitrocellulose membranes (chemiluminescence). The instrument was connected to a personal computer equipped with the Bio-Rad Quantity One 4.4.1 software which enabled further analysis of the gels and blots.

Development of each membrane was facilitated by utilising chemiluminescence. Briefly, the two chemiluminescence reagents (luminol/enhancer and peroxide buffer) comprising the Bio-Rad Immune-Star HRP substrate kit were mixed in a 1:1 ratio. Approximately 4ml of this mixture was subsequently poured onto the nitrocellulose membrane which was allowed to incubate (room temperature) in the dark for 3 minutes. Thereafter, the membrane was placed into the GelDoc XRS chamber and the images of the protein bands on the membrane became visible following development using Chemi Hi Sensitivity exposure.

#### **6.4.2.8 Data analysis and statistics**

Data was analysed using ImageJ 1.41 image processing and analysis software and are represented as relative band density plus or minus the standard deviations. Groups were compared for differences using one-way ANOVA and the Kruskal-Wallis test (GraphPad InStat Software, version 3.06). A probability value (p) of less than 0.05 ( $p < 0.05$ ) was considered as statistically significant (\* indicates significant ( $p < 0.05$ ) differences between treated and control groups; # indicates significant ( $p < 0.05$ ) differences between treated groups).



## 6.5. Results and Discussion

Studies have indicated that Hsp synthesis increases together with elevated levels of ROS (Becker *et al.*, 1990; Schoeniger *et al.*, 1994; Flanagan *et al.*, 1998). In addition, several published data have reported that many sources of oxidative stress can lead to the upregulation of Hsp's (Ma *et al.*, 1998; Kim *et al.*, 2005; Yu *et al.*, 2006; Weber *et al.*, 2007; Gaultieri *et al.*, 2008). Reactive oxygen species are therefore regarded to play a key role in the expression of Hsp's.

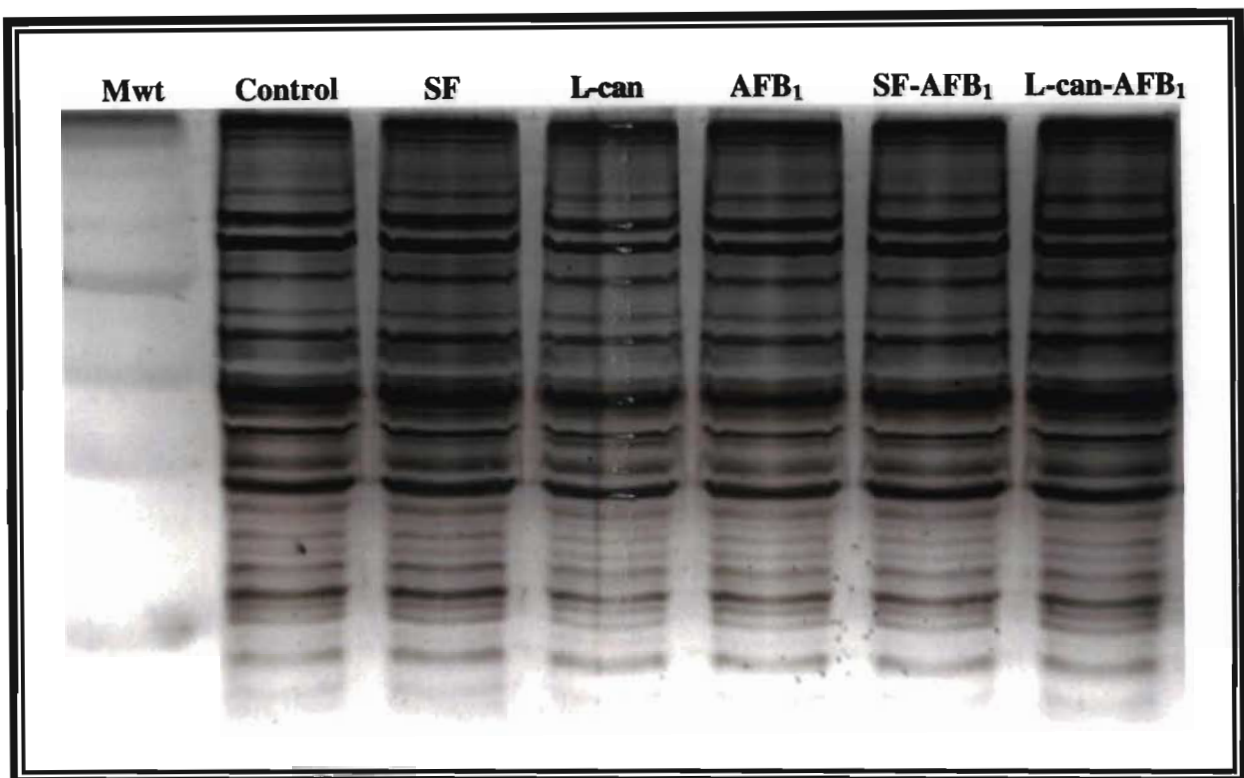


**Figure 6.2** Silver staining of crude HepG<sub>2</sub> cellular proteins resolved by SDS-PAGE.

Mycotoxins have been shown to induce Hsp70 expression (Hassen *et al.*, 2005; Golli *et al.*, 2006; Zourgui *et al.*, 2008). In this regard, Meki *et al.* (2004) reported a 2.5-fold elevation of Hsp70 expression in rat liver when male Sprague-Dawley rats were treated with AFB<sub>1</sub> (50µg/kg body weight) via gastric intubation. In addition, a statistically significant ( $p < 0.001$ ) increase in lipid peroxidation was induced by AFB<sub>1</sub>. The authors concluded that the increasing levels of Hsp expression may be ascribed to the oxidative effect of AFB<sub>1</sub>.

This study is in agreement with Meki *et al.* (2004) as it is apparent from the present data that incubation of HepG<sub>2</sub> cells with 1μM AFB<sub>1</sub> for 24 h induced a significant ( $p < 0.001$ ) increase in Hsp70 (Figure 6.3) as well as Hsp90 (Figure 6.4) expression as evidenced by the 1.30-fold and 1.51-fold increases respectively, when compared to the control.

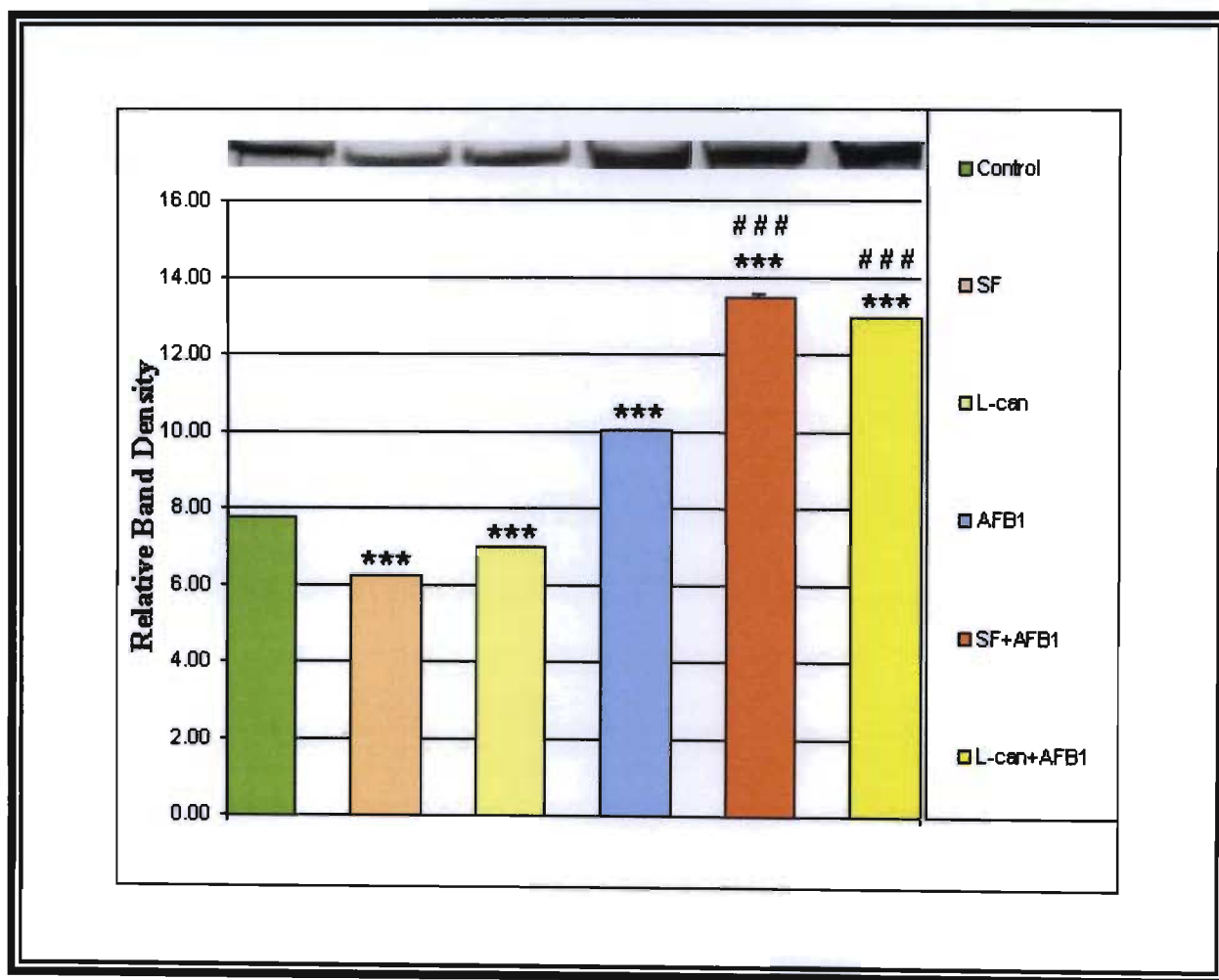


**Figure 6.3** Western blot analysis of Hsp70 protein levels in HepG<sub>2</sub> cells treated with SF, L-can, AFB<sub>1</sub>, SF-AFB<sub>1</sub> and L-can-AFB<sub>1</sub>. \*\*\* $p < 0.001$ , ### $p < 0.001$ .

The increases in Hsp expression by AFB<sub>1</sub> may be attributed to its oxidative effect, which has been demonstrated as one of the underlining mechanisms for AFB<sub>1</sub>-induced cytotoxicity. Results from the TBARS assay (Chapter 4) showed that AFB<sub>1</sub> significantly ( $p < 0.001$ ) increased lipid peroxidation in HepG<sub>2</sub> cells. It may therefore be reasonable to assume that ROS generated by AFB<sub>1</sub> may have oxidised amino acid side chains of proteins, yielding carbonyl

derivatives. In addition, MDA, a product of lipid peroxidation, has also been shown to form reactive carbonyl derivatives of proteins. Carbonyl groups can also be introduced into proteins by reactions with alkenes (conjugated dienes) produced during lipid peroxidation (Madhusudhanan *et al.*, 2004). Protein carbonylation is a sign of irreversible oxidative damage, often leading to a loss of protein function (Zourgui *et al.*, 2008). Therefore, as a consequence of AFB<sub>1</sub>-induced ROS and associated lipid peroxidation, the affected proteins may aggregate and initiate the HSR.

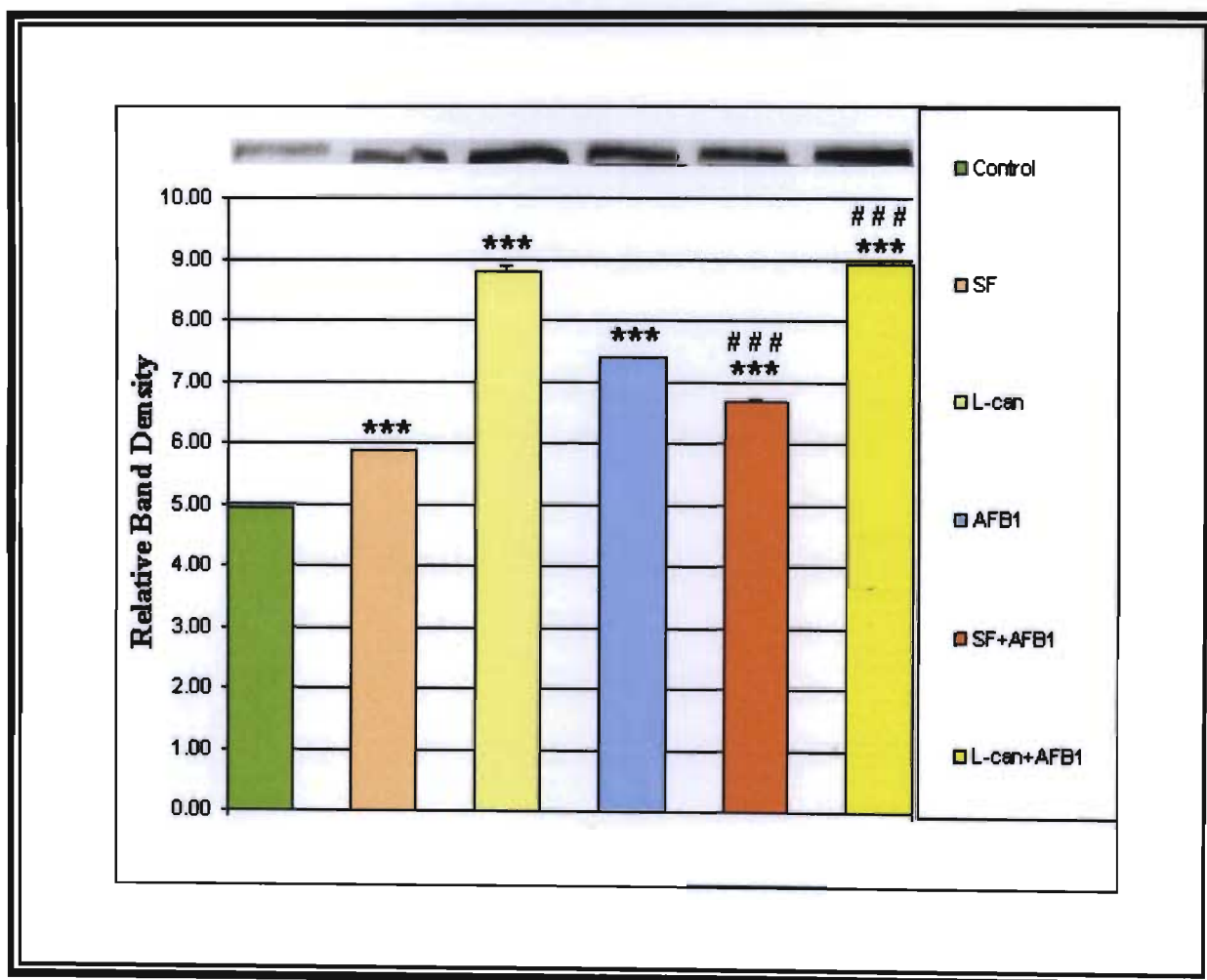


**Figure 6.4** Western blot analysis of Hsp90 protein levels in HepG<sub>2</sub> cells treated with SF, L-can, AFB<sub>1</sub>, SF+AFB<sub>1</sub> and L-can+AFB<sub>1</sub>. \*\*\*p<0.001, ###p<0.001.

In addition to its oxidative effect, AFB<sub>1</sub> is known to react and interact with various liver proteins to form a stable adduct (Amaya-Farfan, 1999). It is suggested that the structure and

activity of proteins may be detrimentally altered following non-specific-irreversible covalent and specific-reversible non-covalent binding with the toxin (McLean and Dutton, 1995). Enzyme inactivation is a further consequence of toxin binding (Amaya-Farfan, 1999). In addition to AFB<sub>1</sub> itself or the generated exo-isomer interacting with proteins, the dialdehyde generated from the AFB<sub>1</sub>-8,9-dihydrodiol is capable of condensing with primary amino acid groups, such as lysine, and other cellular constituents, forming a Schiff's base (Guengerich *et al.*, 1998) thus also contributing to alterations in protein/enzyme structure and function. It is therefore presumed that AFB<sub>1</sub> possibly interacted with and mediated alterations in protein structure and function, thereby inducing the observed increases in Hsp70 (Figure 6.3) and Hsp90 (Figure 6.4) expression.

The ability of AFB<sub>1</sub> to influence p53 expression in HepG<sub>2</sub> cells was previously investigated by Reddy *et al.* (2006). On the basis of a pan-tropic p53 protein ELISA, a decrease in p53 levels was noted after exposure to AFB<sub>1</sub> (11µg/ml).

Using western blotting, Van Vleet *et al.* (2006) reported a concentration-dependent (0.015-15µM) decline in p53 expression when human bronchial epithelial cells, B-CMV1A2 and B3A4, were incubated with AFB<sub>1</sub>.

The present data is in agreement with Reddy *et al.* (2006) and Van Vleet *et al.* (2006) as it also illustrates a decrease ( $p > 0.05$ ) in p53 expression after exposure of HepG<sub>2</sub> cells to AFB<sub>1</sub> (1µM) (Figure 6.5).

The tumour suppressor gene p53 is the most commonly mutated gene (approximately 50%) in all human cancers. Using restriction fragment length polymorphism, Aguilar *et al.* (1993) reported that AFB<sub>1</sub> preferentially induced the transversion of GC to TA in the third position of codon 249 of the p53 gene in HepG<sub>2</sub> cells. It is therefore suggested that the observed decrease in p53 expression by AFB<sub>1</sub> (Figure 6.5) could be due to a mutation and thus the carcinogenic potential of AFB<sub>1</sub> is owed to its ability, at least in part, to interfere with the molecular mechanism of cell cycle regulation.

In addition to oxidative stress, there are other agents which may interfere with protein folding. These are usually stress protein inducers which include amino acid analogues. The latter agents

are structural analogues of natural amino acids. They become rapidly incorporated into newly synthesised proteins thereby inducing irreversible aberrant protein formation and accumulation which ultimately leads to the induction of stress proteins, such as Hsp70 (Remy *et al.*, 1998).

Li and Laszlo (1984) studied the effect of amino acid analogues on the induction of Hsp's in the Chinese hamster fibroblasts cell line (HA-1). It was determined that exposure of HA-1 cells to L-can in particular, mediated enhanced synthesis of three major mammalian Hsp's with molecular weights 70, 87 and 110kDa.

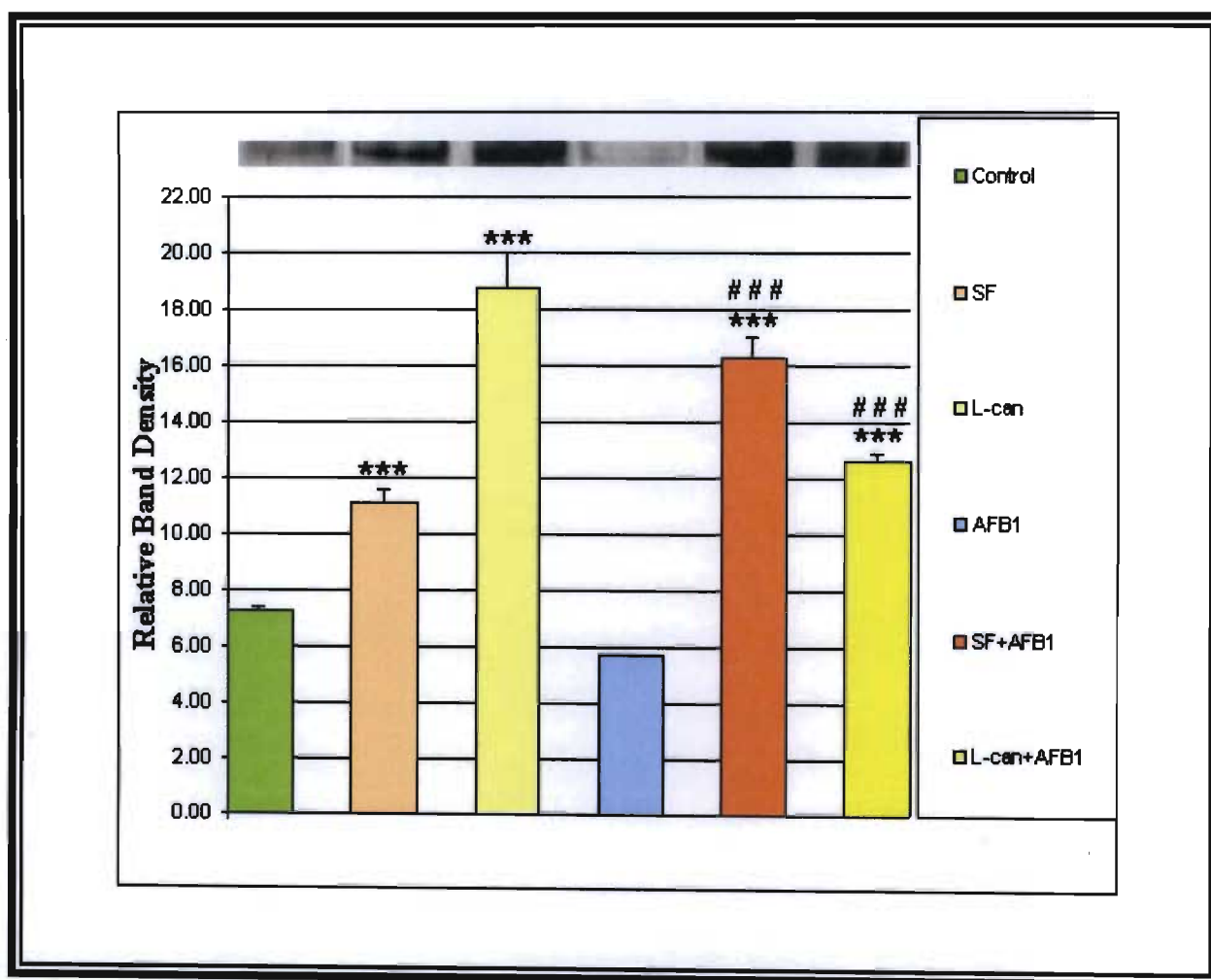


**Figure 6.5** Western blot analysis of p53 protein levels in HepG<sub>2</sub> cells treated with SF, L-can, AFB<sub>1</sub>, SF-AFB<sub>1</sub> and L-can-AFB<sub>1</sub>. \*\*\*p<0.001, ###p<0.001.

The product of the Ion gene in *Escherichia coli*, a protease known as La, mediates the degradation of aberrant proteins. Goff and Goldberg (1985) investigated whether the presence

of abnormal proteins stimulated the expression of this gene. Cells were induced to synthesise aberrant polypeptides following treatment with L-can. Treated cells displayed a 3-fold increase in Ion gene expression. Importantly, the induction of Ion by abnormal proteins required the heat shock regulatory gene *htpR*. Thus, the presence of aberrant proteins after exposure to L-can may be a common signal required for the induction of heat shock proteins (Goff and Goldberg, 1985).

In addition, Robertson *et al.* (1999) investigated the effect of L-can on the induction of Hsp70 expression in FL5.12 cells. These authors reported a 2-fold increase in Hsp70 expression after cells were incubated for 4 h with 10mM L-can.

Based on the findings of the above-mentioned studies (Li and Laszlo, 1984; Goff and Goldberg, 1985; Robertson *et al.*, 1999), it is suggested that one mechanism by which L-can is able to influence Hsp expression involves its ability to induce aberrant protein formation and accumulation. A further mechanism involves its capacity to induce ROS and subsequent oxidative stress (Riganti *et al.*, 2003). This postulation is based on the high level ( $p < 0.001$ ) of lipid peroxidation induced by L-can as evidenced by results of the TBARS assay (Chapter 4).

Thus, when compared to the control, both mechanisms can be employed to explain the significant ( $p < 0.001$ ) 1.79-fold increase in Hsp90 expression by L-can (Figure 6.4).

In contrast, L-can induced a significant ( $p < 0.001$ ) 1.11-fold decrease in Hsp70 expression when compared to the control (Figure 6.3). A possible mechanism can be envisioned to explain such a result. While L-can leads to the accumulation of analogue-substituted proteins that are believed to be responsible for the accumulation of Hsp70, it could be that newly synthesised Hsp70 itself is aberrant or dysfunctional (Robertson *et al.*, 1999).

When compared to the control, a 2.59-fold ( $p < 0.001$ ) increase in p53 expression was noted after incubation of HepG<sub>2</sub> cells with L-can (Figure 6.5). This finding correlates with Ding *et al.* (1999) who also established the ability of L-can (0-2mM) to cause p53 protein induction *in vitro*.

Tumour suppressor protein p53 plays an essential role in maintaining genomic integrity (Liu *et al.*, 2008). Following DNA damage, p53 levels and activity are subsequently increased and

lead to transcriptional activation of its target genes (p21) responsible for cell cycle arrest (Latonen and Laiho, 2005), so as to extend the time available for DNA repair. Conversely, replication of damaged cells is avoided through activation of apoptosis (Ricordy *et al.*, 2002). In this regard, it is suggested that one of the mechanisms by which L-can is able to mediate an increase in p53 expression is via its capacity to induce ROS and subsequent DNA damage. This postulation is based on the high level ( $p < 0.001$ ) of lipid peroxidation induced by L-can as evidenced by results from the TBARS assay (Chapter 4) as well as the significant ( $p < 0.001$ ) increase in DNA migration as revealed by the comet assay (Chapter 5).

Other results in this study (Figure 6.3) demonstrated lower levels of Hsp expression following the administration of SF, which induced a significant ( $p < 0.001$ ) 1.25-fold decrease in Hsp70 expression when evaluated against the control.

The lower levels of Hsp70 expression can be attributed to the free radical scavenging and antioxidant properties of the plant which contribute to the maintenance of low levels of intracellular ROS. This is supported by results of the TBARS and GSH assays (Chapter 4) which illustrated that SF induced significantly ( $p < 0.001$ ) lower levels of lipid peroxidation and significantly ( $p < 0.001$ ) higher levels of GSH respectively, compared to the control. As a result, it is unlikely for SF-induced Hsp70 expression to be a consequence of oxidative stress.

In contrast, SF induced a significant ( $p < 0.001$ ) 1.20-fold increase in Hsp90 expression compared to the control (Figure 6.4). This result may be due to the effects of L-can which is present in relatively high concentrations within SF (van Wyk and Albrecht, 2008).

Exposure of HepG<sub>2</sub> cells to SF caused a 1.53-fold ( $p < 0.001$ ) increase in p53 expression when compared to the control (Figure 6.5). Comet assay analysis revealed SF to mediate a significant ( $p < 0.001$ ) increase in DNA migration (Chapter 5). It is therefore presumed that increased p53 expression by SF occurred as a result of the genotoxic effect of the plant extract on the HepG<sub>2</sub> cell line.

When compared to the control, western blot analysis revealed that L-can-AFB<sub>1</sub> evoked 1.68-fold ( $p < 0.001$ ) and 1.82-fold ( $p < 0.001$ ) increases in Hsp70 (Figure 6.3) and Hsp90 (Figure 6.4) expression respectively. The same combination mediated significant ( $p < 0.001$ ) increases in

Hsp70 expression (Figure 6.3) when compared to Hsp protein levels induced by the individual administration of L-can and AFB<sub>1</sub>. In addition, L-can-AFB<sub>1</sub> induced 1.01-fold ( $p>0.05$ ) and 1.20-fold ( $p<0.001$ ) increases in Hsp90 expression (Figure 6.4) compared to that induced by L-can and AFB<sub>1</sub> respectively.

The observed increases in Hsp expression may be due to the oxidative properties of the combination as evidenced by the significant increase ( $p<0.001$ ) in TBARS levels (Chapter 4) after exposure of HepG<sub>2</sub> cells to L-can-AFB<sub>1</sub>.

When assessed against the control, p53 was upregulated 1.74-fold ( $p<0.001$ ) by L-can-AFB<sub>1</sub> (Figure 6.5). The same combination evoked a 1.49-fold ( $p<0.001$ ) decrease and a 2.19-fold ( $p<0.001$ ) increase in p53 levels when compared to expression induced after individual administration of L-can and AFB<sub>1</sub> respectively.

Results from the comet assay (Chapter 5) showed that L-can-AFB<sub>1</sub> caused a significant ( $p<0.001$ ) antagonistic effect on DNA migration and comet tail length when compared to AFB<sub>1</sub>-treated cells. In this regard, it is reasonable to assume that L-can mediated an upregulation of p53 thereby promoting cell cycle arrest to facilitate the repair of AFB<sub>1</sub>-induced DNA damage.

Regarding SF-AFB<sub>1</sub>, immunoblotting illustrated the combination to induce 1.75-fold ( $p<0.001$ ) and 1.36-fold ( $p<0.001$ ) increases in Hsp70 (Figure 6.3) and Hsp90 (Figure 6.4) expression respectively, compared to the control. When combined, these compounds also mediated significant ( $p<0.001$ ) increases in Hsp70 (Figure 6.3) expression compared to that induced after individual exposure to SF and AFB<sub>1</sub>. Furthermore, SF-AFB<sub>1</sub> evoked a 1.14-fold ( $p<0.001$ ) increase and a 1.11-fold ( $p<0.001$ ) decrease in Hsp90 expression when assessed against expression induced after individual administration of SF and AFB<sub>1</sub> respectively (Figure 6.4).

Based on the results of the TBARS assay (Chapter 4), which revealed SF-AFB<sub>1</sub> to mediate a significant ( $p<0.001$ ) increase in lipid peroxidation, it is suggested that the oxidative stress induced after co-administration of these compounds contributed to the observed increases in Hsp expression.



The p53 protein measurements showed that SF-AFB<sub>1</sub> caused a 2.25-fold (p<0.001) upregulation in the p53 gene product when evaluated against the control (Figure 6.5). Further analysis demonstrated that this combination induced significant (p<0.001) increases in p53 levels when compared to p53 expression induced by individual exposure to SF and AFB<sub>1</sub>.

Similarly to L-can-AFB<sub>1</sub>, SF-AFB<sub>1</sub> mediated a significant (p<0.001) decrease in DNA damage when compared to AFB<sub>1</sub>-treated cells (Chapter 5). Therefore, the increased levels of p53 may be regarded as a protective mechanism, eliciting cell cycle arrest in order to facilitate the repair of AFB<sub>1</sub>-induced DNA damage.

It is apparent that when combined these compounds act simultaneously to increase Hsp70 expression. However, the precise mechanisms by which the combination treatments influence cellular Hsp and p53 expression levels remain elusive. As previously mentioned (Chapter 4), when in combination, these compounds may exhibit differences in bioactivity, which can be attributed to the ability of each compound to influence the bioactivity of the other.

## **6.6 Conclusion**

The findings of the current study approves the strong correlation between oxidative stress and Hsp induction thus supporting the oxidative character of AFB<sub>1</sub> as assessed in this study by the increase of TBARS, Hsp70 and Hsp90 levels. In addition, the p53-mediated response to AFB<sub>1</sub> treatment may indicate that these cells are at an increased risk of developing mutations.

The capacity of SF and L-can to influence Hsp and p53 protein expression, when administered individually and in combination with AFB<sub>1</sub>, is unclear and requires further investigation.

Among the stressors that have been demonstrated to result in Hsp and p53 induction is a rather extensive list of biotic and abiotic compounds and toxicants which have led some to suggest that the induction of these molecules may be a universal response to cytotoxicity. Based on the results of this study, it can be concluded that Hsp and p53 induction is undoubtedly more complex than originally envisioned.

## Chapter 7

# CELLULAR DEATH

### 7.1 Introduction

The one certainty of life is death. This may be the reason for the tremendous interest in understanding the mechanisms of death. At the cellular level, it is clearly evident that death is not always a stochastic event (Burgering and Kops, 2002). Cell death may be divided into two classes, apoptosis and necrosis (Edinger and Thompson, 2004).

Apoptosis is a form of cell death during which an individual cell undergoes an internally controlled transition from an intact metabolically active state into a number of shrunken remnants retaining their membrane bound integrity (Slater *et al.*, 1995). For cell death to be identified as apoptosis, nuclear condensation and fragmentation, cleavage of chromosomal DNA into internucleosomal fragments and packaging of the deceased cell into apoptotic bodies without plasma membrane breakdown must be observed (Edinger and Thompson, 2004). It is apparent that lysis of internal organelles does not occur during this process, and little external leakage of the contents of the dying cell can be detected. Consequently, apoptotic cells do not induce an inflammatory response. Instead, the shrunken apoptotic bodies are phagocytosed by macrophages and their contents recycled. Apoptosis is therefore able to provide an organism both with a safe and efficient way to continuously turnover cells in any tissue, and the capacity to remove specific cells during development (Slater *et al.*, 1995). The morphologic features of apoptosis occur after the activation of caspases by either death receptor ligation or the release of apoptotic mediators from the mitochondrion. In addition, cell death by apoptosis requires energy in the form of ATP (Edinger and Thompson, 2004).

In contrast to apoptosis, necrosis has been traditionally regarded to be a passive form of cell death. It is the consequence of a bioenergetic catastrophe resulting from ATP depletion to a level incompatible with cell survival and is thought to be initiated mainly by cellular 'accidents' such as physical damage or toxic insults (Edinger and Thompson, 2004). Biochemical hallmarks of apoptosis such as activation of specific caspases and oligonucleosomal DNA fragmentation are usually absent in necrotic cells. Morphologically, necrosis is considerably different from 'classical' apoptosis (Proskuryakov *et al.*, 2003). This

form of cell death is typified by osmotic swelling of the cell and organelles (commonly mitochondria) (Lockshin and Zakeri, 2002). Swelling during necrosis is emphasised in the term “oncosis” (derived from “oncos” meaning swelling), a term for cell death in opposition to apoptosis (Proskuryakov *et al.*, 2003). In addition, necrosis is also characterised morphologically by the breakdown of the plasma membrane and an induction of inflammation around the dying cell, attributable to the rapid efflux of cell constituents and proinflammatory molecules into the extracellular space (Edinger and Thompson, 2004).

The importance of properly balanced cell survival and cell death within an organism is undeniable (LeBlanc, 2003). A better understanding of the mechanisms that regulate cell death pathways is necessary in order to improve the current therapeutic strategies as well as to define new strategies in various diseases (Solary *et al.*, 1996).

## **7.2 Flow cytometry**

Flow cytometry is a technology that simultaneously measures and then analyses several physical characteristics of single particles as they flow in a fluid stream through a beam of light (BD Biosciences, 2000). The particles analysed by flow cytometry are often cells. More recently however, flow techniques have also been used to analyse bacteria, sperm, plankton and individual particles that are not cells at all, for example viruses (Hawley and Hawley, 2004). A flow cytometer comprises three functional systems namely fluidics, optics and electronics, and the properties measured include a particles relative size, relative granularity or internal complexity and relative fluorescence intensity (BD Biosciences, 2000).

### **7.2.1 Fluidics**

The most important essential feature of any flow cytometer is the fluidics system, the purpose of which is to transport particles in a fluid stream to a laser beam for interrogation (Freshney, 1992). To obtain consistency of measurement, the stream transporting the particles should ideally be positioned in the centre of the laser beam and only one cell or particle should move through the laser beam at a given moment (BD Biosciences, 2000). This is accomplished by the design of the flow chamber in the fluidics system which causes the fluid to accelerate the particles in a manner that restricts them to the centre of the fluid stream, a process referred to as hydrodynamic focussing (Hawley and Hawley, 2004).

### **7.2.2 Optics**

The optical system consists of excitation optics and collection optics (BD Biosciences, 2000).

The excitation optics comprises a laser and, spherical and cylindrical lenses that are used to shape and focus the laser beam (BD Biosciences, 2000). The use of a laser beam is undoubtedly the best illumination source because firstly, the light is very bright and secondly, the beam emitted by a laser is coherent. Light is thus polarised and the beam is essentially parallel. In flow cytometry, the argon ion laser is commonly utilised (Freshney, 1992).

Once a cell or particle passes through the laser light, light scattering (forward or side) occurs (BD Biosciences, 2000). Light scattering depends on a number of optical processes including diffraction, reflection and refraction. Forward scattered light (FSC) is proportional to size or cell-surface area and is a measurement of diffracted light (Freshney, 1992) whereas side scattered light (SSC) is proportional to cell granularity or internal complexity and is a measurement of refracted or reflected light (BD Biosciences, 2000).

In addition to scattered light, the cell may also impart fluorescent light (Hawley and Hawley, 2004). There are many fluorescent dyes that are useful in flow cytometry due to their ability to bind various cytochemical components and their subsequent detection aids in the investigation and analysis of various cellular processes. A key property of a fluorescent dye which determines its potential use in flow cytometry is its excitation wavelength, which must match the 488nm light emitted by the laser beam (BD Biosciences, 2000).

Once a cell passes through the laser beam, the emitted light signals are directed to appropriate photodetectors via dichroic mirrors (optical mirrors) and optical filters (bandpass and shortpass filters). These components comprise the collection optics (BD Biosciences, 2000).

Fluorescence and SSC light signals are diverted to photomultiplier tubes (PMTs) whereas a photodiode collects the FSC signals (BD Biosciences, 2000).

### **7.2.3 Electronics**

The detected light signals are converted into proportional electronic signals (voltage pulses) by the photodetectors (BD Biosciences, 2000) and each voltage pulse is then assigned a digital value by an Analog-to-Digital Converter (ADC) (Hawley and Hawley, 2004).

#### **7.2.4 Data collection and display**

Flow cytometric data is stored according to a standard format, the flow cytometry standard. Once a data file had been saved, cell populations can be displayed in several different formats (BD Biosciences, 2000). A single parameter can be displayed using a monodimensional histogram, whereas bivariate data can be displayed on dot plots or contour maps. Three dimensional (3-D) data can also be viewed by utilising x, y and z axes of a 3-D plot (Freshney, 1992).

#### **7.3 Flow cytometric detection of apoptosis/necrosis**

The importance of apoptosis in the regulation of cellular homeostasis has mandated the development of several proficient assays capable of measuring different aspects of the process. Apoptosis assays based on flow cytometry have proven particularly useful because they are rapid, quantitative and provide an individual cell-based mode of analysis. Furthermore, the multiparametric nature of flow cytometry facilitates the detection of more than one cell death characteristic in a single assay (Hawley and Hawley, 2004).

Within viable cells, PS is located on the cytoplasmic surface of the cell membrane. Following the induction of apoptosis, rapid alterations occur at the cell surface. One of these are plasma membrane alterations involving the translocation of PS from the inner part of the plasma membrane to the outer layer, by which it becomes exposed at the external surface of the cell (Zimmermann *et al.*, 2001).

*In vitro* detection of PS can be achieved through its interaction with Annexin-V, a protein which binds in a  $\text{Ca}^{2+}$ -dependent manner to negatively charged phospholipid surfaces and shows high specificity for and binds with high affinity to PS (Figure 7.1). This protein can thus be utilised as a sensitive probe for PS exposure and is therefore suitable for the efficient detection of apoptotic cells in cell populations. In flow cytometric applications, Annexin-V is conjugated to fluorescein isothiocyanate (FITC), a fluorochrome (Roche, 2005). As previously mentioned (Chapter 5), a key property of a fluorescent dye which determines its potential use in flow cytometry is its excitation wavelength. Fluorescein isothiocyanate is suitable for flow cytometric applications as it possesses an excitation wavelength of 488nm and emits light signals possessing a wavelength of 518nm (Roche, 2005).

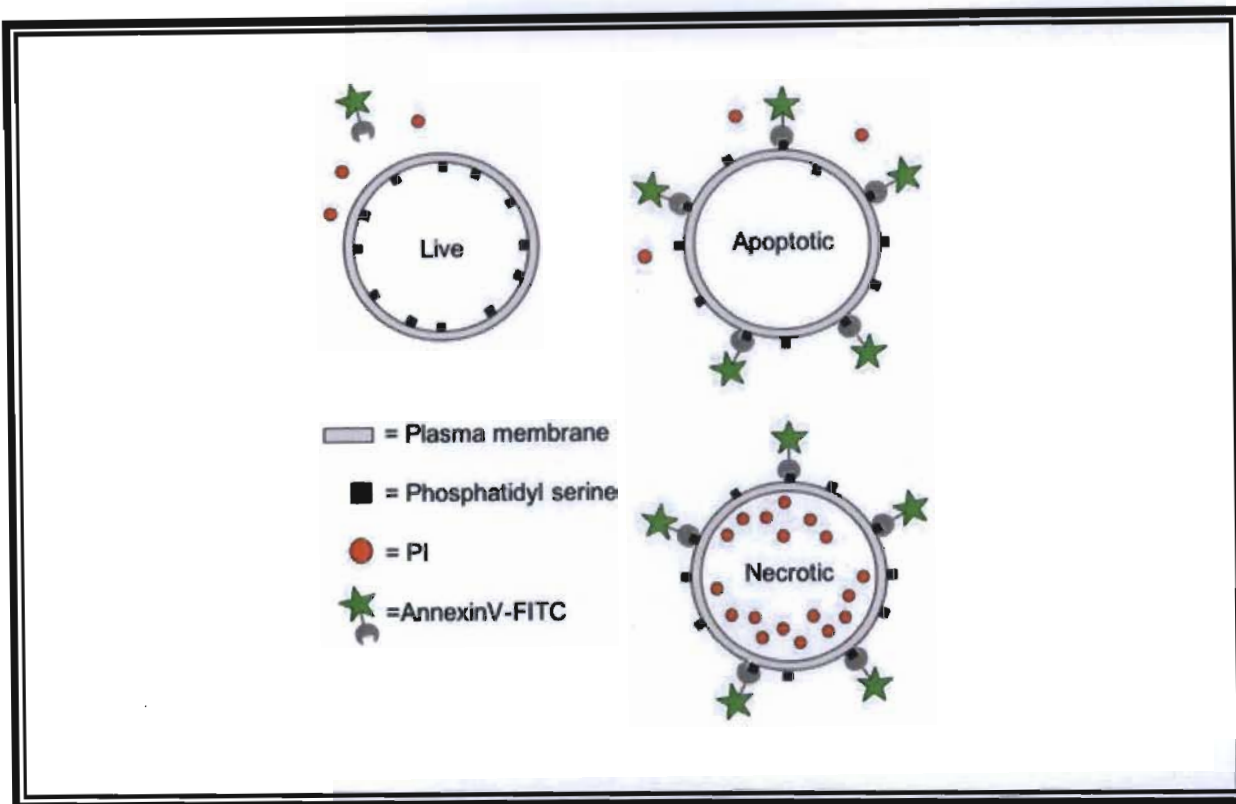


**Figure 7.1 Principle of Annexin-V-FITC and PI staining (Nicoll, 2004).**

Since necrotic cells also expose PS as a result of loss of membrane integrity, apoptotic cells have to be differentiated from necrotic cells during analysis. The simultaneous application of a DNA stain, propidium iodide (PI), allows the discrimination of necrotic cells from Annexin-V stained cells, as PI stains DNA of leaky necrotic cells only (Figure 7.1). Propidium iodide functions to intercalate the DNA helix with a resultant increase in fluorescence of about 20-fold. It is suitable for usage in flow cytometry as it possesses an excitation wavelength of 488nm and emits light signals possessing a wavelength of 617nm (Roche, 2005). Therefore, cells which are positive for only Annexin-V are regarded as apoptotic whereas cells positive for both Annexin-V and PI are regarded as necrotic (Figure 7.1).

The aim of this chapter was to utilise the Annexin-V-Fluos staining kit via flow cytometry to determine whether SF, L-can and AFB<sub>1</sub>, when administered individually and in combination, induces apoptosis and/or necrosis of HepG<sub>2</sub> cells.

## **7.4 Materials and methods**

### **7.4.1 Materials**

The Annexin-V-Fluos kit was purchased from Roche Diagnostics. All other reagents and consumables utilised were obtained from the sources mentioned previously.

### **7.4.2 Methodology**

#### **7.4.2.1 Treatment, isolation and harvesting of HepG<sub>2</sub> cells**

HepG<sub>2</sub> cells were treated and harvested as described in chapter 4, section 4.6.2.1.

#### **7.4.2.2 Preparation of Annexin-V-Fluos labelling solution**

The Annexin-V-Fluos labelling solution was prepared by diluting 20µl each of the Annexin-V-Fluos labelling reagent and the PI solution in 1ml incubation buffer.

#### **7.4.2.3 Staining procedure of cultured HepG<sub>2</sub> cells**

Approximately  $1 \times 10^6$  cells per treatment were transferred to appropriately labelled 15ml sterilin tubes and pelleted by centrifugation. The supernatant from each tube was thereafter carefully removed, so as to prevent any disruption of the pellet. The pellet of cells was then resuspended in PBS to facilitate a wash step and this was followed by further centrifugation. Each of the aforementioned centrifugation steps was carried out at 1 000 rpm for 5 minutes at 24°C. The washed pellet was then resuspended in 100µl of the Annexin-V-Fluos labelling solution and incubated (room temperature) in the dark for 15 minutes.

#### **7.4.2.4 Instrumentation and analysis of samples**

A FACS calibur benchtop flow cytometer (BD Biosciences) was utilised for analysis of all samples. Subsequent to the incubation period, a 500µl aliquot of incubation buffer was added to each sample of stained cells in suspension. The tubes containing the samples were then gently shaken and placed into the flow cytometer. Analysis of all samples was conducted utilising an excitation wavelength of 488nm with subsequent FL1 (Annexin-V-FITC-PS) and FL3 (propidium iodide-DNA) signals being detected via 515nm and 600nm bandpass filters respectively. Electronic compensation of the instrument was performed prior to analysis in order to exclude overlapping of the two emission spectra.

#### **7.4.2.5 Data analysis and statistics**

The instrument was connected to a personal computer and data was acquired and analysed using FlowJo 8.7.1 software. Dot plots (Figure 7.2 – Figure 7.5) were used to display the two parameter data obtained. A quadrant marker was used to divide the two parameter plots into four quadrants to distinguish populations that are considered negative, single positive, or double positive. The lower-left quadrant (population 1 - viable cells) contains cells that are negative for both parameters (Annexin-V-FITC negative, PI negative), the lower-right quadrant (population 2 - apoptotic cells) contains cells that are positive for the x-axis parameter (Annexin-V-FITC positive) but negative for the y-axis parameter (PI negative), the upper-right quadrant (population 3 - necrotic cells) contains cells that are positive for both parameters (Annexin-V-FITC positive, PI positive) and the upper left quadrant (population 4) contains cells that are positive for the y-axis parameter (PI positive).

### **7.5 Results and Discussion**

Apoptosis is described as an active, programmed process of autonomous cellular dismantling that avoids eliciting inflammation, whereas necrosis has been characterised as cell death resulting from environmental perturbations with uncontrolled release of inflammatory cellular contents (Nasri *et al.*, 2006).

In the present study, Annexin-V-FITC binding and PI staining by flow cytometry were used as criteria for distinguishing viable, apoptotic and necrotic cells. Apoptotic cells were identified on the basis of their PS externalisation, whereas necrotic cells were identified by DNA intercalation of PI. The potential for induction of apoptosis and necrosis differed remarkably between the compounds under investigation.

Fluorescence activated cell sorting analysis demonstrated that L-can was the most potent ingredient to cause apoptosis (33.6%) in HepG<sub>2</sub> cells (Table 7.1). In addition, the double staining of red fluorescence with PI showed that the compound also induced a 1.87-fold increase in the amount (6.17%) of necrotic cells when compared to the control.

L-canavanine has been shown to possess cytotoxic effects on many human cancer cell lines such as the colon cancer cell line HT-29 (Green and Ward, 1983), the uterine sarcoma cell lines MES-SA and Dx-5, the leukaemia cells lines K562 and K562-R7 (Worthen *et al.*, 1998),



the lung adenocarcinoma cell line A549 (Ding *et al.*, 1999), the bladder cancer cell line HTB9, the cervical cancer cell line HeLa (Bence and Crooks, 2003) as well as the pancreatic cell lines MIA PaCa-2 (Swaffar *et al.*, 1994), PANC-1, CFPAC-1, Capan-1 and BxPC-3 (Bence *et al.*, 2003). In addition, L-can does not only mediate cytotoxicity when evaluated *in vitro*, but also possesses the capacity to mediate shrinkage of tumour growth in both mice (Green *et al.*, 1980) and rats (Thomas *et al.*, 1980).

**Table 7.1: The percentage of viable, apoptotic and necrotic cells determined using flow cytometry.**

| Sample                 | % Viable cells | % Apoptotic cells | % Necrotic cells |
|------------------------|----------------|-------------------|------------------|
| Control                | 94.3           | 2.16              | 3.3              |
| SF                     | 95.4           | 2.73              | 1.48             |
| L-can                  | 59.8           | 33.6              | 6.17             |
| AFB <sub>1</sub>       | 93.7           | 4.49              | 1.65             |
| SF-AFB <sub>1</sub>    | 95.8           | 2.58              | 1.02             |
| L-can-AFB <sub>1</sub> | 97.8           | 0.79              | 1.1              |

The induction of apoptosis is an efficient strategy for cancer therapy. Using human acute leukaemia Jurkat T cells, Jang *et al.* (2002) investigated whether apoptosis is associated with the anticancer activity of L-can. It was reported that cell viability was 35% after a 36 h treatment period with 2.5mM L-can. DNA fragmentation was also easily detectable at 2.5mM L-can. In addition, flow cytometric analysis revealed that the sub-G<sub>1</sub> phase, which represents apoptotic cells, increased in a dose-dependent manner (1.25, 2.5, 5.0mM). Western blotting conducted by these authors showed that the level of active caspase-3 also increased concentration-dependently. The authors concluded that L-can-induced apoptotic DNA fragmentation accompanied the activation of caspase-3.

L-canavanine may influence apoptosis via a number of mechanisms. One of the proposed apoptotic-inducing mechanisms of L-can involves its influence on NO synthesis. Nitric oxide synthases synthesise NO from L-arg. It has been established that L-can is an analogue of L-arg and further demonstrated that L-can functions as an alternate substrate for the NOS reaction (Luzzi and Marletta, 2005) thus preventing the synthesis of NO.

One of the key mechanisms by which NO regulates the function of various target proteins is through S-nitrosylation, a biochemical process which involves the reversible coupling of NO to a reactive cysteine thiol leading to the formation of molecules referred to as S-nitrosothiols (Iyer *et al.*, 2008). Formation of nitrosylated proteins is an important, post-translational modification of protein structure which modulates protein function (Kim *et al.*, 2001).

Nitric oxide is known to inhibit apoptosis through S-nitrosylation of various proteins that are involved in the apoptotic cascade. An example is the nitrosylation of pro-apoptotic caspases such as caspase-8, 9 and 3 at their active site cysteine which subsequently inhibits their enzymatic activity (Iyer *et al.*, 2008).

Fas ligand is able to induce the down-regulation of cFLIP via ubiquitin-mediated proteasomal degradation (Iyer *et al.*, 2008). It has been demonstrated that cFLIP can be nitrosylated, thereby preventing its ubiquitination and subsequent degradation. Since cFLIP is a key regulator of death receptor signalling that inhibits the recruitment of procaspase 8 to the DISC, its nitrosylation is therefore an important mechanism via which NO inhibits apoptosis (Dash *et al.*, 2007). Similarly, nitrosylation of Bcl-2 prevents its ubiquitination and subsequent degradation. Bcl-2 and cFLIP are anti-apoptotic proteins. Therefore, prevention of their degradation by nitrosylation will promote their anti-apoptotic activity and thus the anti-apoptotic properties of NO (Iyer *et al.*, 2008).

Protein kinase C plays an important role in apoptosis. Phosphorylation of cFLIP by PKC has been shown to prevent its recruitment to the DISC and to thus sensitise cells to apoptosis. It has been demonstrated that in normal cells, NO inhibits the activity of PKC via nitrosylation. This process leads to prevention of the phosphorylation of cFLIP by PKC thus allowing cFLIP to be recruited to the DISC, essentially blocking the activation of caspase-8 and preventing apoptosis (Dash *et al.*, 2007).

Nitric oxide is present in high concentrations in blood, extracellular fluid and also at even higher concentrations within cells. Due to its lipophilic nature, it can rapidly cross cell membranes and enter intracellular compartments where it interacts with and activates its target protein, a haem-containing protein, guanylyl cyclase. Activation of guanylyl cyclase by NO, leads to the formation of cyclic GMP (cGMP) from the nucleotide GTP (Bruckdorfer, 2005).

Cyclic GMP-dependent mechanisms can be mimicked by an analogue of cGMP, 8-bromo-cGMP. In PC12 cells, 8-Bromo-cGMP blocked caspase-3 activity and activation as well as cytochrome c release. Apoptosis was also affected in hepatocytes after exposure to 8-Bromo-cGMP which mediated a reduction in TNF $\alpha$ -induced apoptosis and caspase-3 activity (Kim *et al.*, 2001).

Another mechanism of cGMP-dependent inhibition of apoptosis by NO involves ceramide. In human U937 monocytes, ceramide was shown to potentiate, whereas NO inhibited TNF $\alpha$ -induced TRADD recruitment and caspase activity (Kim *et al.*, 2001).

Tissue transglutaminase (TGase) is a member of the TGase family catalysing protein cross-linking by transamidation. There are several classes of enzymatically active TGases identified as having an important role in packing the cell at the late phase of apoptosis to prevent a massive inflammatory process (Sreedhar and Csermely, 2004). Another target of NO which serves as an apoptotic effector molecule is the TGases. S-nitrosylation of the tissue TGase active site by NO prevents apoptosis due to inhibition of the enzyme (Kim *et al.*, 2001).

Experiments in Jurkat cells have demonstrated that NO attenuates apoptosis by inhibiting Apaf-1/caspase-9 and subsequently promotes the formation of an inactive apoptosome complex (Li and Wogan, 2005).

Since L-can is an inhibitor of NO synthesis, it would therefore prevent the anti-apoptotic properties of NO. This may be a possible mechanism by which L-can induces apoptosis.

It is well established that L-can induces the synthesis and subsequent accumulation of misfolded proteins due to its structural similarity to L-arg. The accumulation of aberrantly folded proteins within the cell and in the ER specifically, may result in a proposed overload of the ER (Remy *et al.*, 1998), a consequence of which is ER stress, and leads to Ca<sup>2+</sup> efflux from the lumen of the ER as well as the release of reactive oxygen from the mitochondrion (Hsieh *et al.*, 2007). The released ROS may contribute to oxidative stress but the Ca<sup>2+</sup> may contribute to cellular lethality in a variety of ways. For example, normal cytoskeletal organisation is perturbed when intracellular Ca<sup>2+</sup> increases, apparently as a result of Ca<sup>2+</sup>-mediated dissociation of actin microfilaments and an activation of phospholipases and proteases. In

addition, the released  $\text{Ca}^{2+}$  can also activate certain endonucleases, which results in DNA fragmentation and chromatin condensation (Amdur *et al.*, 1991), two morphological hallmarks of apoptosis (Edinger and Thompson, 2004; Stander *et al.*, 2007). Lastly, the released  $\text{Ca}^{2+}$  can activate ROS producing enzymes such as cyclooxygenase and/or lipoxygenase (Remy *et al.*, 1998) further contributing to oxidative stress and cellular damage.

The ability of L-can to elicit a marked oxidative effect in HepG<sub>2</sub> cells was revealed in the present study as indicated by the high level of lipid peroxidation induced by the compound (Chapter 4). Therefore, L-can-induced ROS may be a further mechanism which contributed to the observed cellular lethality, since excess oxidative stress kills cells either by apoptosis or necrosis (Kannan and Jain, 2000).

It has been suggested that ROS, and related secondary oxidant species such as lipid hydroperoxides, might be triggers or mediators of apoptosis (Raffray and Cohen, 1997). Apoptosis may serve as a fail-safe device to prevent cells from proliferating uncontrollably in the face of persistent oxidative stress (Kannan and Jain, 2000).

Candidate mechanisms underlying ROS-stimulated apoptosis may differ but probably include either p53-mediated effects due to DNA strand breaks or cellular sensors detecting non-specific changes, for example  $\text{Ca}^{2+}$  accumulation, ATP depletion, and thiol group disturbance (Raffray and Cohen, 1997). In addition, it has been suggested that the global shutdown of mitochondrial function under conditions of oxidative stress could contribute to apoptosis because of the dramatic depletion in cellular energy supply (Kannan and Jain, 2000). In contrast, ROS-mediated lipid peroxidation end products such as 4HNE have been shown to induce necrotic cell death (Proskuryakov *et al.*, 2003).

Thus, it seems that oxidative stress induces an apoptotic response when cells can maintain their reducing capacity against ROS, whereas necrosis is triggered when this reducing homeostasis is disturbed, for example by excess of ROS or damage of natural antioxidative systems (Proskuryakov *et al.*, 2003).

The inhibitory effects of L-can on mitochondrial function as demonstrated by Wilkie (1970) and Winston and Bosmann (1971) may also contribute to mitochondrial ROS generation as well as depletion in cellular energy, both of which can prompt cell death.

On the basis of western blotting, the highest level of p53 expression was observed after L-can administration (Chapter 6). Tumour suppressor protein p53 triggers a variety of cell cycle regulatory events to limit the proliferation of damaged cells. The ability of this 'gate keeper' gene to inhibit cell growth is due, at least in part, to its ability to bind to specific DNA sequences, and activate the transcription of target genes which encode proteins involved in cell cycle control (p21, Mdm2) and apoptosis (PIG3, Bax, DR5, PUMA, p53AIP1) (Zhang *et al.*, 2008). The findings of this study therefore suggest that induction of p53 by L-can (Chapter 6) could act as a transcriptional activator for the high level of apoptosis induced by the compound.

Western blotting also demonstrated that exposure to L-can impaired Hsp70 induction in HepG<sub>2</sub> cells (Chapter 6). This absence of an important protective mechanism could be relevant for the cumulative destructive effects of L-can thus leading to the observed levels of apoptosis and necrosis.

Cellular lethality may also be mediated by L-canaline. It has been reported that stable oximes are formed following the rapid reaction of L-canaline with glyoxylate and other 2-oxo acids. The ability of L-canaline to form oximes indicates its capacity to scavenge essential 2-oxo-containing metabolites such as pyruvate and oxaloacetate, thus depleting TCA cycle reserves and interfering with ATP production (Rosenthal, 1997). Significant energy depletion will inevitably lead to loss of cell function and cell death (Amdur *et al.*, 1991).

Other results revealed that treatment with SF for 24 h resulted in a 1.26-fold increase of the cell population that was positive for Annexin-V staining (Table 7.1). The data exhibited that SF induced the exposure of PS on the surface of approximately 2.73% of HepG<sub>2</sub> cells. In contrast, a 2.23-fold decrease in the amount (1.48%) of necrotic cells was noted after exposure to SF.

Different types of cancer chemopreventive agents, including natural products have been studied for efficacy both *in vitro* and *in vivo* (Chou *et al.*, 2003). *Sutherlandia* has been shown

to possess cytotoxic effects on many human cancer cell lines such as the prostate cancer cell line DU-145 (Steenkamp and Gouws, 2006), MCF-7 (Steenkamp and Gouws, 2006; Stander *et al.*, 2007), the leukaemia Jurkat cell line, the mammary adenocarcinoma cell line MDA-MB-468, as well as the promyelocyte cell line HL60 (Tai *et al.*, 2004).

Recently, extracts prepared from a variety of plants were demonstrated to possess the ability in triggering the apoptotic pathway (Chou *et al.*, 2003). In this regard, Chinkwo (2005) investigated the apoptotic properties of a crude aqueous SF whole plant extract. Results showed that CHO cells exposed to SF exhibited several morphological features (PS externalisation, chromatin condensation, and DNA fragmentation) associated with apoptosis. In addition, other results from the same study revealed that 84% of Jurkat T cells were apoptotic following Annexin-V staining and analysis by flow cytometry. The author suggested that there were active constituents in the plant extract that induced the observed morphological changes and cell death.

Incidentally, one of the bioactive compounds isolated from SF is flavonoids (van Wyk, 2008). Flavonoids have been shown to possess apoptotic effects on some cancer cells such as colon cancer cells, cervical cancer cells, prostate cancer cells, lung cancer cells and oesophageal cancer cells (Zhang *et al.*, 2008). Therefore, apoptosis induced by SF may be attributed to the presence and activity of flavonoids present within the plant extract.

The observed levels of apoptosis and necrosis induced by SF (Table 7.1) may also be ascribed to the cytotoxic potential of L-can present within the plant extract.

Other results in this study revealed SF to induce significantly low levels of lipid peroxidation accompanied by a marked increase in cellular GSH levels (Chapter 4). As a result, it is unlikely for SF-induced apoptosis to be a consequence of oxidative stress.

From apoptosis and necrosis profiles using flow cytometry, it was determined that AFB<sub>1</sub> exerted a distinct apoptotic effect. When evaluated against the control (Figure 7.2), HepG<sub>2</sub> cells treated with AFB<sub>1</sub> exhibited a 2.08-fold increase apoptosis (Figure 7.3). In contrast, a 2-fold decrease in the amount (1.65%) of necrotic cells was observed after AFB<sub>1</sub> exposure (Table 7.1).

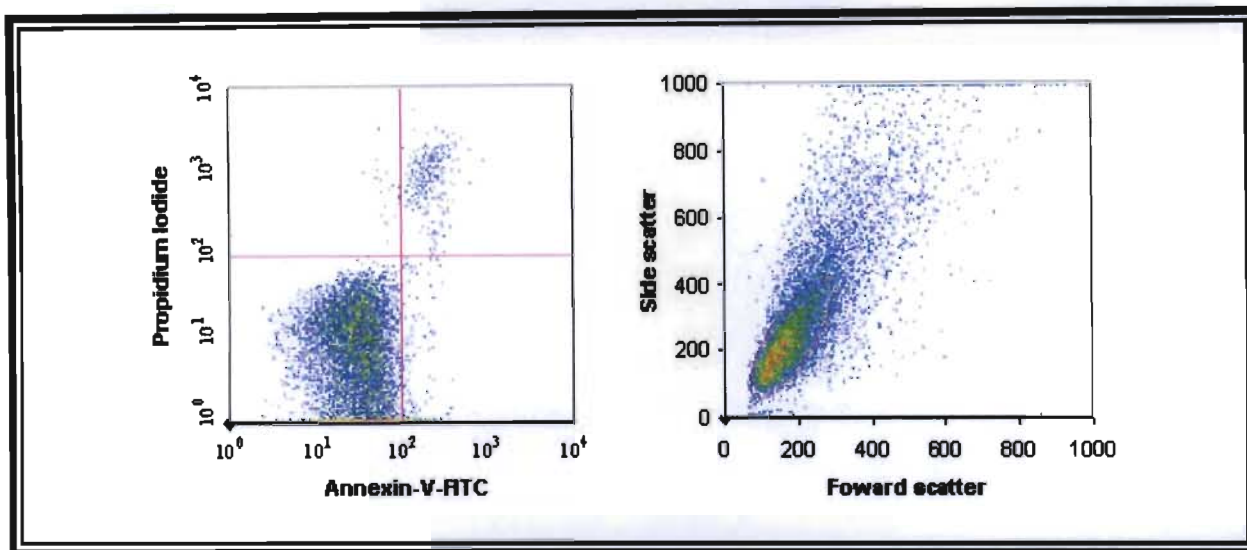


**Figure 7.2** Dot-plots showing Annexin-V-FITC versus propidium iodide fluorescence of HepG<sub>2</sub> cells (control).

The ability of AFB<sub>1</sub> to mediate apoptosis in HepG<sub>2</sub> cells was previously investigated by O' Brien *et al.* (2000). These authors demonstrated that AFB<sub>1</sub> produced DNA fragmentation in a dose-dependant (1-80 $\mu$ M) manner. Additional analysis by flow cytometry revealed a dose-dependent increase in apoptotic cells by AFB<sub>1</sub>. To further confirm that cell death was mediated via apoptosis, these authors employed the TUNEL assay and observed a dose-dependent increase in TUNEL-positive cells.

In addition, Reddy *et al.* (2006) reported the development of several morphological features associated with apoptosis when HepG<sub>2</sub> cells were incubated with AFB<sub>1</sub> (11 $\mu$ g/ml). These were chromatin condensation, DNA fragmentation, nuclear breakdown, membrane blebbing and cell fragmentation with the formation of apoptotic bodies.

The results of the present study correspond to the findings of O' Brien *et al.* (2000) and Reddy *et al.* (2006) by demonstrating that AFB<sub>1</sub> induces apoptosis of HepG<sub>2</sub> cells.

Caspase-3 plays a major role in the execution of apoptotic cell death (Meki *et al.*, 2004). In this regard, a number of studies, both *in vivo* (Meki *et al.*, 2001; El-Gibaly *et al.*, 2003; Meki *et al.*, 2004; Abbès *et al.*, 2008) and *in vitro* (Guerra *et al.*, 2005; Van Vleet *et al.*, 2006) have

demonstrated increases in caspase-3 activity by AFB<sub>1</sub> and suggested that caspase-3 activation is essential for the occurrence of the apoptotic phenotype of cell death induced by AFB<sub>1</sub>.

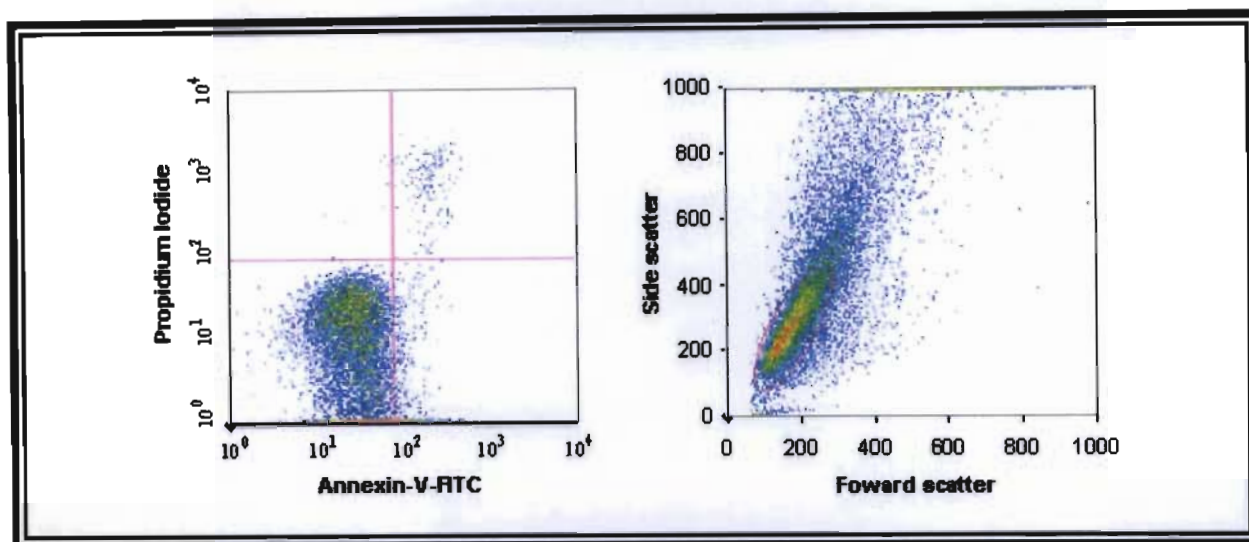


**Figure 7.3** Dot-plots showing Annexin-V-FITC versus propidium iodide fluorescence of HepG<sub>2</sub> cells (AFB<sub>1</sub>).

In addition, caspase-3 substrate cleavage has been observed under oxidative stress. Incidentally, one of the manifestations of AFB<sub>1</sub>-induced toxicity is oxidative stress, and it is accepted that oxidative stress is an apoptotic inducer (Meki *et al.*, 2004).

Therefore, on the basis of previous studies (Shen *et al.*, 1994; Shen *et al.*, 1995, Shen *et al.*, 1996; Madhusudhanan *et al.* 2004; Meki *et al.*, 2004; Lee *et al.*, 2005; Jodynis-Liebert *et al.*, 2006; Preetha *et al.*, 2006) which have outlined the capacity of AFB<sub>1</sub> to mediate oxidative stress as well as the results of the TBARS assay from the present study (Chapter 4), it is suggested that AFB<sub>1</sub>-induced ROS may be a potential mechanism which contributed to the observed levels of apoptosis and necrosis (Figure 7.3). Furthermore, the capacity of AFB<sub>1</sub> to influence mitochondrial function, specifically the ETC (Doherty and Campbell, 1973; Pai *et al.*, 1975; Obidoa and Obonna, 1981; Obidoa, 1986) is also suggested to contribute to mitochondrial ROS generation as well as ATP depletion, the consequence of which may be cellular lethality via apoptosis or necrosis.

Studies have shown that AFB<sub>1</sub> possesses DNA damaging potential due to its ability to mediate a marked genotoxic effect (Amstad *et al.*, 1984; El-Khatib *et al.*, 1998; O'Brien *et al.*, 2000;



Raj *et al.*, 2001; Ehrlich *et al.*, 2002). It has been demonstrated that AFB<sub>1</sub> is metabolised to an epoxide which produces DNA adducts causing DNA strand breaks and point mutations (Meki *et al.*, 2004). Accordingly, the results of the comet assay (Chapter 5) revealed AFB<sub>1</sub> to mediate a marked increase in DNA migration when compared to the control. One of the responses of normal cells to severe DNA damage is the induction of cell death by apoptosis (Raj *et al.*, 2001). Therefore, the significant DNA damage induced by AFB<sub>1</sub> may also serve as a trigger for the 2.08-fold increase in apoptosis (Figure 7.3).

After 24 h of incubation in the presence of SF-AFB<sub>1</sub>, approximately 2.58% of cells were positively stained with Annexin-V (Table 7.1). When evaluated against the control (Figure 7.2), it was revealed that this combination (Figure 7.4) evoked a marginal 1.19-fold increase in the number of apoptotic cells. In contrast, a minimal 1.06-fold decrease was noted when apoptosis levels induced by SF-AFB<sub>1</sub> were compared to that mediated following individual administration of SF. However, when compared to AFB<sub>1</sub>-exposed cells, treatment with the same combination mediated a marked (1.74-fold) antagonistic effect on apoptosis levels. In addition, PI staining revealed only 1.02% of HepG<sub>2</sub> cells to exhibit necrosis when incubated with SF-AFB<sub>1</sub>.

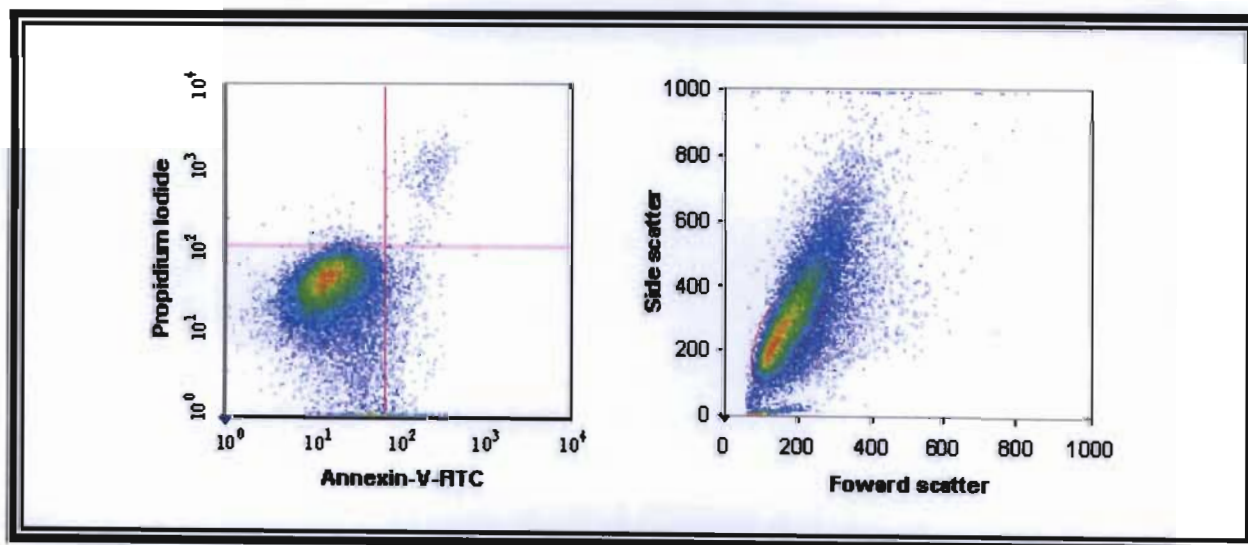


**Figure 7.4** Dot-plots showing Annexin-V-FITC versus propidium iodide fluorescence of HepG<sub>2</sub> cells (SF-AFB<sub>1</sub>).

It has been well documented that AFB<sub>1</sub> requires metabolic activation by *CYP3A4* to form the highly reactive AFB<sub>1</sub>-exo-8,9-epoxide in order to exert its cytotoxic effects. As previously mentioned (Chapter 5), Mills *et al.* (2005b) reported significant decreases in *CYP3A4* activity by SF. Thus, the protective effect of SF towards AFB<sub>1</sub>-induced apoptosis can be ascribed to its inhibition of *CYP3A4* activity and subsequent AFB<sub>1</sub> bioactivation.

The observed protective effects of SF may also be due to its antioxidant and free radical scavenging properties as reported by Fernandes *et al.* (2004) and Tai *et al.* (2004). In addition, the high levels of GSH observed following the co-administration of SF-AFB<sub>1</sub> (Chapter 4) suggests enhanced anti-oxidant status of the cells, a condition which would effectively ameliorate AFB<sub>1</sub>-induced ROS as well as facilitate enhanced conjugation of AFB<sub>1</sub>-epoxides with GSH for AFB<sub>1</sub> detoxification.

Heat shock proteins are important regulators of lethal programs. The most studied of them is Hsp70, which can inhibit apoptosis caused by various stimuli. In addition, the overexpression of Hsp's has been shown to protect cells from necrosis as well (Proskuryakov *et al.*, 2003). Based on the results of western blotting (Chapter 6), the protective effect of SF against AFB<sub>1</sub>-induced apoptosis and necrosis can also be attributed to the significant ( $p < 0.001$ ) increases in Hsp70 and Hsp90 expression induced by SF-AFB<sub>1</sub>.

Another protective mechanism which can be envisioned is related to the upregulation of p53. It is presumed that the increased levels of p53 induced by SF-AFB<sub>1</sub> (Chapter 6) is able to mediate cell cycle arrest in order to facilitate efficient repair of AFB<sub>1</sub>-induced DNA damage thus protecting cells against apoptosis and necrosis.

A minimal amount of cells were detected in an apoptotic (0.79%) or necrotic (1.1%) state by FACS analysis of HepG<sub>2</sub> cells treated with L-can-AFB<sub>1</sub> for 24 h (Table 7.1). Further analysis revealed that this combination (Figure 7.5) mediated evident decreases in the levels of apoptosis (2.73-fold) and necrosis (3-fold) when compared to the control (Figure 7.2). When compared to AFB<sub>1</sub>-exposed cells, further antagonism by L-can-AFB<sub>1</sub> on apoptosis (5.68-fold) and necrosis (1.5-fold) was noted. In addition, when evaluated against L-can treated cells, L-can-AFB<sub>1</sub> evoked an astounding 32.81% decrease in apoptosis levels accompanied by a 5.6-fold decrease in necrosis levels.

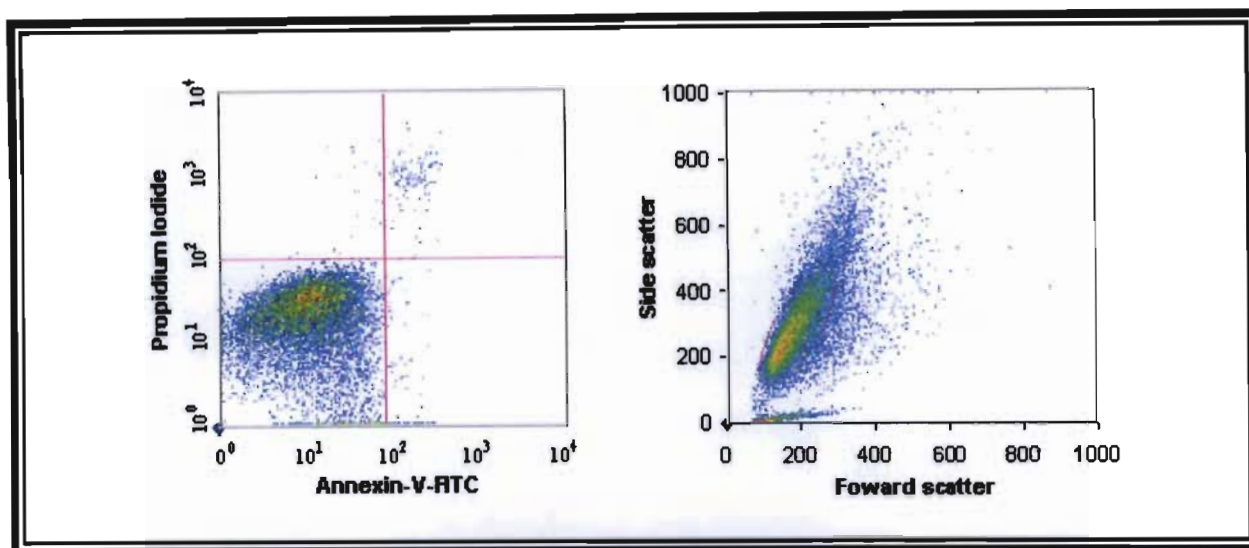


**Figure 7.5** Dot-plots showing Annexin-V-FITC versus propidium iodide fluorescence of HepG<sub>2</sub> cells (L-can-AFB<sub>1</sub>).

Van Ness *et al.* (1998) found that lysine residues are important for conferring high AFB<sub>1</sub>-epoxide conjugation activity. In addition, studies have shown that the AFB<sub>1</sub> dialdehyde condenses with the epsilon amino group of lysine to form a Schiff's base (Sabbioni *et al.*, 1987; Amaya-Farfan, 1999; Guengerich *et al.*, 2002). It is proposed that these are the mechanisms by which AFB<sub>1</sub> forms adducts with proteins such as albumin (Sabbioni *et al.*, 1987; Chih *et al.*, 1993; Amaya-Farfan, 1999; Guengerich *et al.*, 2002) and histones (Yu *et al.*, 1988; Chih *et al.*, 1993), both of which are rich in lysine.

It is also known that albumin contains a high concentration of L-arg in its peptide chain (Aoki and Takeuchi, 1997; Bosshart and Heinzelmann, 2002) and that L-arg is abundant in histones as well (Jenuwein and Allis, 2001). Therefore, in addition to binding to the side-chain amino group of lysine, it is proposed that AFB<sub>1</sub> and/or its metabolites are also able to condense with L-arg possibly via the strongly basic nitrogen atoms in its guanidine moiety (Törnqvist *et al.*, 2002). This postulation is substantiated by many studies which have documented that AFB<sub>1</sub> inhibits NO synthesis by possibly binding to L-arg (Moon, 1998; Moon and Pyo, 1999; Moon *et al.*, 1999a; Moon *et al.*, 1999b; Moon *et al.*, 1999c).

Because L-can is an analogue of L-arg, it is possible for AFB<sub>1</sub> and/or its metabolites to also bind to L-can, most probably via its oxyguanidino group. It is therefore suggested that when

combined, AFB<sub>1</sub> becomes sequestered by L-can thereby forming an adduct and reducing the cytotoxicity of each compound resulting in the observed lower levels of apoptosis and necrosis (Figure 7.5).

The decreases in the levels of apoptosis and necrosis may also be due to the protective effect afforded by the overexpression of Hsp's induced by L-can-AFB<sub>1</sub> co-administration (Chapter 6). In addition, results of the GSH assay (Chapter 4) reveal the highest level of GSH to be present after exposure of cells to L-can-AFB<sub>1</sub>. Thus, the enhanced anti-oxidant status of the cells may have provided efficient protection against ROS-mediated cellular lethality. This is further evidenced by the significant decreases in lipid peroxidation following administration of L-can-AFB<sub>1</sub>, when compared to that induced by individual administration of each compound (Chapter 4). It is also possible that the highly electrophilic AFB<sub>1</sub>-epoxides may have been diverted to detoxification rather than interaction with cellular biomolecules owing to the increased GSH levels.

The low levels of apoptosis and necrosis by this combination (L-can-AFB<sub>1</sub>) can additionally be attributed to the increased p53 levels (Chapter 6), which play an important role in arresting the cell cycle and mediating DNA repair thus preventing cell death.

The ability of these compounds to act in combination and influence cell viability is not fully understood. However, it is presumed that the effects induced by such combination may be due to the capacity of each compound to influence the bioactivity of the other when combined.

## **7.6 Conclusion**

Apoptosis is among the number of pathways that can be exploited for cancer prevention and treatment (Zhang *et al.*, 2008). In this regard, the results of the present study not only corroborate the findings of many published studies but it also confirms the potential of L-can as an anti-cancer agent due its potent apoptotic-inducing properties.

Other findings of this study provide scientific evidence demonstrating the ability of SF and L-can to attenuate the apoptosis-inducing activity of AFB<sub>1</sub>.

The stronger effect of L-can compared to the SF extract is probably because it was applied in a higher concentration than that which is present in the extract, indicating a concentration dependent effect.

Overall, flow cytometry was shown to be a valuable procedure as it offered the opportunity to evaluate a number of parameters. It can be efficiently utilised to analyse mechanisms of toxic insult by measuring aspects of the cell cycle, disruption of the mitochondrial membrane potential or induction of apoptosis or necrosis. The ease of the application and the high throughput make this technology well suited for screening tests.

## Chapter 8

### CONCLUSION

Aflatoxin B<sub>1</sub>, a food contaminant, has been implicated as a causative agent in human hepatic and extrahepatic carcinogenesis (Awney *et al.*, 2002).

It is suggested that oxidative damage caused by AFB<sub>1</sub> may be one of the underlying mechanisms of AFB<sub>1</sub>-induced cell injury and DNA damage, which eventually leads to carcinogenesis. In this study, it was shown that AFB<sub>1</sub> exposure caused a significant increase in the level of TBARS, an index of cellular lipid peroxidation, thereby confirming that ROS is involved in AFB<sub>1</sub>-induced cellular injury of HepG<sub>2</sub> cells. To date, little or no experimental evidence exists showing the exact source of ROS which initiates lipid peroxidation in AFB<sub>1</sub>-exposed HepG<sub>2</sub> cells. Therefore, further research is required for the direct detection of ROS formed inside hepatocytes following AFB<sub>1</sub> exposure. It was also noted that supplementation with L-can significantly reduced AFB<sub>1</sub>-induced lipid peroxidation which can be attributed to the enhanced antioxidant status of cells as evidenced by the increase of intracellular GSH content.

The hepatotoxicity induced in HepG<sub>2</sub> cells by AFB<sub>1</sub> was further confirmed by results of the comet assay which revealed the strongest effect to be observed after exposure to the toxin and it is notable in this context that AFB<sub>1</sub> has been ranked as one of the most potent human carcinogens (Uhl *et al.*, 2000). More importantly, the results also indicate the efficacy of SF and L-can to significantly reduce AFB<sub>1</sub>-induced DNA damage.

Flow cytometry was found to be a suitable tool for cell viability determination and showed that AFB<sub>1</sub> exerted a distinct apoptotic effect. In contrast, Annexin-V-PI staining demonstrated that SF and L-can ameliorated AFB<sub>1</sub>-induced increases in apoptosis and necrosis.

A wide variety of compounds have been shown to provide protection against AFB<sub>1</sub>-induced hepatotoxicity. Many of these compounds are able to modulate AFB<sub>1</sub>-induced hepatotoxicity by mediating alterations in biotransformation pathways (Klein *et al.*, 2002). In this regard, a possible mechanism of protective action exerted by SF in AFB<sub>1</sub>-treated HepG<sub>2</sub> cells is related to a study conducted by Mills *et al.* (2005b), who demonstrated the ability of SF to decrease

*CYP3A4* activity. Incidentally, *CYP3A4* is the key enzyme involved in the bioactivation of AFB<sub>1</sub> to the highly reactive AFB<sub>1</sub>-exo-8,9-epoxide. Therefore, a proposed mechanism by which SF reduces AFB<sub>1</sub>-induced toxicity is via a decrease in the activity of *CYP3A4*, leading to a decrease in AFB<sub>1</sub>-exo-8,9-epoxide formation and consequently reduced toxicity.

According to its chemical composition and biological properties, further mechanisms of cytoprotection afforded by SF possibly include: a) a blockade of initial DNA damage, related to the presence of flavonoids (van Wyk, 2008) and their ability to act as scavengers of free radicals (Fernandes *et al.*, 2004; Tai *et al.*, 2004) as well as b) an inactivation/detoxification of carcinogenic AFB<sub>1</sub> metabolites, which is related to its antimutagenic activity (Reid *et al.*, 2006; Ntuli *et al.*, 2007).

The most important detoxification mechanism of the AFB<sub>1</sub>-exo-8,9-epoxide is via GST mediated conjugation with GSH (Lee *et al.*, 2005). In this regard, protection against AFB<sub>1</sub>-induced cytotoxicity may result from enhanced conjugation of AFB<sub>1</sub> metabolites with GSH to facilitate AFB<sub>1</sub> detoxification. This is presumed based on the elevated levels of intracellular reduced GSH after co-administration of SF and L-can with AFB<sub>1</sub>.

Cytoprotection by SF and L-can against AFB<sub>1</sub>-induced toxicity is further substantiated by the significant increases in the expression of Hsp70, a protein, which when overproduced enhances cell survival (Gabai *et al.*, 1997).

In conclusion, the results documented in the present study support the potential of an aqueous extract of SF as an effective cytoprotective agent. The bioactivity of SF is possibly related to the combined effects of the many phytochemicals found within the extract, thereby resulting in a relatively complex mechanism of action. In this regard, further investigation is warranted for the isolation and characterisation of individual compounds to elucidate their structure and functional capacity, which may be helpful in understanding the regulatory system of the bioactivity of AFB<sub>1</sub> by such natural compounds. Overall, the above-mentioned properties of SF, together with its low toxicity, suggest that this plant may hold future promise as a protective feed additive, which can be utilised as part of an overall management strategy to improve human health.

## REFERENCES

- Abbès, S., Salah-Abbès, J. B., Hetta, M. M., Ibrahim, M., Abdel-Wahhab, M. A., Bacha, H., Oueslati, R. (2008). Efficacy of Tunisian montmorillonite for *in vitro* aflatoxin binding and *in vivo* amelioration of physiological alterations. *Applied Clay Science*, **42** (1-2), 151-157.
- Abdel-Wahhab, M.A., Aly, S.E. (2003). Antioxidants and radical scavenging properties of vegetable extracts in rats fed aflatoxin-contaminated diet. *Agricultural and Food Chemistry*, **51** (8), 2409-2414.
- Adams, J. M. Cory, S. (2002). Apoptosomes: engines for caspase activation. *Current Opinion in Cell Biology*, **14** (6), 715-720.
- Adrain, C., Martin, S. J. (2001). The mitochondrial apoptosome: a killer unleashed by the cytochrome seas. *Trends in Biochemical Sciences*, **26** (6), 390-397.
- Aguilar, F., Hussain, S. P., Cerutti, P. (1993). Aflatoxin B<sub>1</sub> induces the transversion of G-T in codon 249 of the p53 tumor suppressor gene in human hepatocytes. *Genetics*, **90**, 8586-8590.
- Algeciras-Schimnich, A., Barnhart, B. C., Peter, M. E. (2002). Apoptosis-independent functions of killer caspases. *Current Opinion in Cell Biology* **14** (6), 721-726.
- Allende, C., Allende, J.E. (1964). Purification and substrate specificity of arginyl-ribonucleic acid synthetase from rat liver. *Biological Chemistry*, **239**, 1102-1106.
- Amaya-Farfan, J. (1999). Aflatoxin B<sub>1</sub>-induced hepatic steatosis: role of carbonyl compounds and active diols on steatogenesis. *Lancet*, **353** (9154), 747-748.
- Amdur, M. O., Doull, J., Klaassen, C. D. (eds.) (1991). *Casarett and Doull's Toxicology: The Basic Science of Poisons*. 4<sup>th</sup> edition. New York: Pergamon Press. 1, 5, 6, 11, 12, 28-29, 846.
- Amstad, P., Levy, A., Emerit, I., Cerutti, P. (1984). Evidence for membrane-mediated chromosomal damage by aflatoxin B<sub>1</sub> in human lymphocytes. *Carcinogenesis*, **5** (6), 719-723.



Andrews, A. T. (1986). *Electrophoresis: Theory, Techniques, and Biochemical and Clinical Applications*. 2<sup>nd</sup> edition. Oxford: Oxford University Press. 5-6.

Aoki, E., Takeuchi, I. K. (1997). Immunohistochemical localization of arginine and citrulline in rat renal tissue. *The Journal of Histochemistry & Cytochemistry*, **45** (6), 875-881.

Aravind, L., Dixit, V. M., Koonin, E. V. (1999). The domains of death: evolution of the apoptosis machinery. *TIBS*, **24** (2), 47-53.

Arya, R., Mallik, M., Lakhota, S. C. (2007). Heat shock genes - integrating cell survival and death. *Biosciences*, **32** (3), 595-610.

Ash, D. E. (2004). Structure and function of arginases. *The Journal of Nutrition*, **134** (10), 2760-2764.

Ashe, P. C., Berry, M. D. (2003). Apoptotic signaling cascades. *Progress in Neuro-Psychopharmacology & Biological Psychiatry*, **27** (2), 199-214.

Awney, H. A., Attih, A. M., Habib, S. L., Mostafa, M. H. (2002). Effect of melatonin on the production of microsomal hydrogen peroxide and cytochrome P-450 content in rats treated with aflatoxin B<sub>1</sub>. *Toxicology*, **172** (2), 143-148.

Balunas, M. J., Kinghorn, A. D. (2005). Drug discovery from medicinal plants. *Life Sciences*, **78** (5), 431-441.

Bates, S. H., Jones, R. B., Bailey, C. J. (2000). Insulin-like effect of pinitol. *British Journal of Pharmacology*, **130** (8), 1944-1948.

BD Biosciences. (2000). Introduction to flow cytometry: a learning guide. Manual, 11-11032-01, 1-52.

Becker, J., Mezger, V., Courgeon, A. M., Best-Belpomme, M. (1990). Hydrogen peroxide activates immediate binding of a *Drosophila* factor to DNA heat-shock regulatory element *in vivo* and *in vitro*. *European Journal of Biochemistry*, **189** (3), 553-558.

Bedard, L. L., Massey, T. E. (2006). Aflatoxin B<sub>1</sub>-induced DNA damage and its repair. *Cancer Letters*, **241** (2), 174-183.

Beere, M. (2004). 'The stress of dying': the role of heat shock proteins in the regulation of apoptosis. *Journal of Cell Science*, **117** (Part 13), 2641-2651.

Belloir, C., Singh, V., Daurat, C., Siess, M. H., Le Bon, A. M. (2006). Protective effects of garlic sulfur compounds against DNA damage induced by direct- and indirect-acting genotoxic agents in HepG2 cells. *Food and Chemical Toxicology*, **44** (6), 827-834.

Bence, A. K., Adams, V. R., Crooks, P. A. (2003). L-Canavanine as a radiosensitization agent for human pancreatic cancer cells. *Molecular and Cellular Biochemistry*, **244** (1-2), 37-43.

Bence, A. K., Crooks, P. A. (2003). The Mechanism of L-canavanine cytotoxicity: arginyl tRNA synthetase as a novel target for anticancer drug discovery. *Enzyme Inhibition and Medicinal Chemistry*, **18** (5), 383-394.

Bensaad, K., Vousden, K. H. (2007). p53: new roles in metabolism. *Trends in Cell Biology*, **17** (6), 286-291.

Berger, F. G., Kramer, D. L., Porter, C. W. (2007). Polyamine metabolism and tumorigenesis in the Apc<sup>Min/+</sup> mouse. *Biochemical Society Transactions*, **35** (Part 2), 336-339.

Berjts, M., Green, M. H. (1986). Selective cytotoxicity of L-canavanine in tumorigenic Madin-Darby canine kidney T<sub>1</sub> cells. *Chemico-Biological Interactions*, **60** (3), 305-315.

Blount, S., Griffiths, H. R., Lunec, J. (1989). Reactive oxygen species induce antigenic changes in DNA. *FEBS*, **245** (1), 100-104.

Bosshart, H., Heinzemann, M. (2002). Arginine-rich cationic polypeptides amplify lipopolysaccharide-induced monocyte activation. *Infection and Immunity*, **70** (12), 6904-6910.

Brooks, C. L., Gu, W. (2003). Ubiquitination, phosphorylation and acetylation: the molecular basis for p53 regulation. *Current Opinion in Cell Biology*, **15** (2), 164-171.

Brown, L., Heyneke, O., Brown, D., van Wyk, J. P. H., Hamman, J. H. (2008). Impact of traditional medicinal plant extracts on antiretroviral drug absorption. *Ethnopharmacology*, **119** (3), 588-592.

Bruckdorfer, R. (2005). The basics about nitric oxide. *Molecular Aspects of Medicine*, **26** (1-2), 3-31.

Burgering, B. M. T., Kops, G. J. P. L. (2002). Cell cycle and death control: long live forkheads. *TRENDS in Biochemical Sciences*, **27** (7), 352-360.

Cervera, J., Alamar, M., Martinez, A., Renau-Piqueras, J. (1983). Nuclear alterations induced by cadmium chloride and l-canavanine in HeLa S3 cells: accumulation of perichromatin granules. *Ultrastructure Research*, **82** (3), 241-263.

Ch'ih, J. J., Lin, T., Devlin, T. M. (1983). Effect of inhibitors of microsomal enzymes on aflatoxin B<sub>1</sub>-induced cytotoxicity and inhibition of RNA synthesis in the isolated rat hepatocytes. *Biochemical and Biophysical Research Communications*, **115** (1), 15-21.

Chadwick, W.A., Roux, S., Van de Venter, M., Louw, J., Oelofsen, W. (2007). Anti-diabetic effects of *Sutherlandia frutescens* in Wistar rats fed a diabetogenic diet. *Ethnopharmacology* **109** (1), 121-127.

Chattopadhyay, D. (2003). Advances in phytomedicine: ethnomedicine and drug discovery. *DDT*, **8** (12), 535.

Chen, X. (1999). The p53 family: same response, different signals? *Molecular Medicine*, **5** (9), 387-392.

Chih, J. J., Ewaskiewicz J. I., Taggart P., Devlin T. M. (1993). Nuclear translocation of aflatoxin B<sub>1</sub>-protein complex. *Biochemical and Biophysical Research Communications*, **190** (1), 186-191.

Chinkwo, K.A. (2005). *Sutherlandia frutescens* extracts can induce apoptosis in cultured carcinoma cells. *Ethnopharmacology*, **98** (1-2), 163-170.

Chou, C. C., Pan, S. L., Teng, C. M., Guh, J. H. (2003). Pharmacological evaluation of several major ingredients of Chinese herbal medicines in hepatoma Hep3B cells. *European Journal of Pharmaceutical Sciences*, **19** (5), 403-412.

Chowdhury, I., Tharakan, B., Bhat, G. K. (2008). Caspases - an update. *Comparative Biochemistry and Physiology*, **151** (1), 10-27.

Clifford, J. I., Garvican, L., Rees, K. R. (1976). The relationship between the turnover of UTP and RNA synthesis in cultured cells treated with aflatoxin B<sub>1</sub>. *Chemico-Biological Interactions*, **13** (2), 165-171.

Clynes, M. (ed.) (1998). *Animal Cell Culture Techniques*. Berlin: Springer. 98, 100, 395, 397, 414, 430.

Coulombe, R. A. (1993). Biological action of mycotoxins. *Dairy Science*, **76** (3), 880-891.

Criss, W. E. (2003). A review of polyamines and cancer. *Turkish Journal of Medical Science*, **33**, 195-205.

D'Mello, J. P. F., MacDonald, A. M. C. (1997). Mycotoxins. *Animal Feed Science Technology*, **69** (1-3), 155-166.

Dash, P. (2005). *Apoptosis*. Reproductive and Cardiovascular Disease Research Group [Website]. Available from: <<http://www.sgul.ac.uk/depts/immunology/%7Edash/apoptosis/index.htm>> 1-9.

Dash, P. R., McCormick, J., Thomson, M. J. C. B., Cartwright, J. J. E., Whitley, G. S. (2007). Fas ligand-induced apoptosis is regulated by nitric oxide through the inhibition of fas receptor clustering and the nitrosylation of protein kinase C. *Experimental Cell Research*, **313** (16), 3421-3431.

Davies, M J. (2005). The oxidative environment and protein damage. *Biochimica et Biophysica Acta*, **1703** (2), 93-109.

Desagher, S., Martinou, J. (2000). Mitochondria as the central control point of apoptosis. *Trends in Cell Biology*, **10** (9), 369-377.

Dickinson, D. A., Forman, H. J. (2002). Cellular glutathione and thiols metabolism. *Biochemical Pharmacology*, **64** (5-6), 1019-1026.

Ding, Y., Matsukawa, Y., Ohtani-Fujita, N., Kato, D., Dao, S., Fujii, T., Naito, Y., Yoshikawa, T., Sakai, T., Rosenthal, G. A. (1999). Growth inhibition of A549 human lung adenocarcinoma cells by L-canavanine is associated with p21/WAF1 induction. *Cancer Research*, **90** (1), 69-74.

Doherty, W. P., Campbell, T. C. (1973). Aflatoxin inhibition of rat liver mitochondria. *Chemico-Biological Interactions*, **7** (2), 63-77.

Edinger, A. L., Thompson, C. B. (2004). Death by design: apoptosis, necrosis and autophagy. *Current Opinion in Cell Biology*, **16** (6), 663-669.

Ehrlich, V., Darroudi, F., Uhla, M., Steinkellner, H., Gann, M., Majera, B. J., Eisenbauer, M., Knasmüller, S. (2002). Genotoxic effects of ochratoxin A in human-derived hepatoma (HepG2) cells. *Food and Chemical Toxicology*, **40** (8), 1085-1090.

El-Gibaly, I., Meki, A. M. A., Abdel-Ghaffar, S. K. (2003). Novel B melatonin-loaded chitosan microcapsules: *in vitro* characterization and antiapoptosis efficacy for aflatoxin B<sub>1</sub>-induced apoptosis in rat liver. *International Journal of Pharmaceutics*, **260** (1), 5-22.

El-Khatib, H. N., Akeila, M. A., El-magd, M. K. A. (1998). The mutagenic activity of aflatoxin B<sub>1</sub> in rat bone marrow. *Toxicology Letters*, **95** (1), 176.

El-Serag, H. B., Rudolph, K. L. (2007). Hepatocellular carcinoma: epidemiology and molecular carcinogenesis. *Gastroenterology*, **132** (7), 2557-2576.

Esaki, H., Kumagai, S. (2002). Glutathione-S-transferase activity toward aflatoxin epoxide in livers of mastomys and other rodents. *Toxicol*, **40** (7), 941-945.

Escargueil, A. E., Soares, D. G., Salvador, M., Larsen, A. K., Henriques, J. A. P. (2008). What histone code for DNA repair? *Mutation Research*, **658** (3), 259-270.

Fairbairn, D. W., Olive, P L., O'Neill, K. L. (1995). The comet assay: a comprehensive review. *Mutation Research*, **339** (1), 37-59.

Fernandes, A.C., Cromarty, A.D., Albrecht, C., Jansen Van Rensburg, C.E. (2004). The antioxidant potential of *Sutherlandia frutescens*. *Ethnopharmacology*, **95** (1), 1-5.

Fernandez, J., Perez-Alvarez, J. A., Fernandez-Lopez, J. A. (1997). Thiobarbituric acid test for monitoring lipid oxidation in meat. *Food Chemistry*, **59** (3), 345-353.

Flanagan, S. W., Moseley, P. L., Buettner, G. R. (1998). Increased flux of free radicals in cells subjected to hyperthermia: detection by electron paramagnetic resonance spin trapping. *FEBS Letters*, **431** (2), 285-286.

Floyd, L. R., Unuma, T., Busch, H. (1968). Effects of aflatoxin B<sub>1</sub> and other carcinogens upon nucleolar RNA of various tissues in the rat. *Experimental Cell Research*, **51** (2-3), 423-438.

Fraser, A., McCarthy, N., Evan, G. (1996). Biochemistry of cell death. *Current Opinion in Neurobiology*, **6** (1), 71-80.

Freshney, R. I. (ed.) (1992). *Animal Cell Culture: A Practical Approach*. 2<sup>nd</sup> edition. Oxford: IRL Press. 1, 7-9, 11, 15, 17, 52, 54-55, 166, 169, 181-183, 205, 279.

Gabai, V. L., Meriin, A. B., Mosseri, D. D., Caroni, A. W., Ritsi, S., Shifrin, V. I., Sherman, M. Y. (1997). Hsp70 prevents activation of stress kinases: a novel pathway of cellular thermotolerance. *The Journal of Biological Chemistry*, **272** (29), 18033-18037.

Garner, D. L. (2008). Hoechst 33342: The dye that enabled differentiation of living X- and Y-chromosome bearing mammalian sperm. *Theriogenology*, **71** (1), 11-21.

Garrido, C., Gurbaxani, S., Ravagnan, L., Kroemer, G. (2001). Heat shock proteins: endogenous modulators of apoptotic cell death. *Biochemical and Biophysical Research Communications*, **286** (3), 433-442.

Gasser, S., Raullet, D. (2006). The DNA damage response, immunity and cancer. *Seminars in Cancer Biology*, **16** (15), 344-347.

Gerbes, A. L., Caselmann, W. H. (1993). Point mutations of the P53 gene, human hepatocellular carcinoma and aflatoxins. *Hepatology*, **19** (2), 312-315.

Goetz, M. E., Luch, A. (2008). Reactive species: A cell damaging route assisting to chemical carcinogens. *Cancer Letters*, **266** (1), 73-83.

Goff, S. A., Goldberg, A. L. (1985). Production of abnormal proteins in *E. coli* stimulates transcription of ion and other heat shock genes. *Ultrastructure Research*, **41** (2), 587-595.

Golli, E. E., Hassen, W., Bouslimi, A., Bouaziz, C., Ladjimi, M. M., Bacha, H. (2006). Induction of Hsp70 in Vero cells in response to mycotoxins: Cytoprotection by sub-lethal heat shock and by Vitamin E. *Toxicology Letters*, **166** (2), 122-130.

Gracy, R. W., Talent, J. M., Kong, Y., Conrad, C. C. (1999). Reactive oxygen species: the unavoidable environmental insult? *Mutation Research*, **428** (1-2), 17-22.

Green, M. H., Brooks, T. L., Mendelsohn, J., Howell, S. B. (1980). Antitumor activity of L-canavanine against L1210 murine leukemia. *Cancer Research*, **40** (3), 535-537.

Green, M.H., Ward, J.F. (1983). Enhancement of human tumor cell killing by L-canavanine in combination with  $\gamma$ -radiation. *Cancer Research*, **40** (9), 4180-4182.

Gualtieri, M., Mantecca, P., Cetta, F., Camatini, M. (2008). Organic compounds in tire particle induce reactive oxygen species and heat-shock proteins in the human alveolar cell line A549. *Environment International*, **34** (4), 437-442.

Guengerich, F. P. (2003). Cytochrome P450 oxidations in the generation of reactive Electrophiles: Epoxidation and related reactions. *Archives of Biochemistry and Biophysics*, **409** (1), 59-71.

Guengerich, F. P., Arneson, K. O., Williams, K. M., Deng, Z., Harris, T.M. (2002). Reaction of aflatoxin B<sub>1</sub> oxidation products with lysine. *Chemical Research in Toxicology*, **15** (6), 780-792.

Guengerich, F. P., Johnson, W. W., Shaimada, T., Ueng, Y., Yamakazi, H., Langouet, S. (1998). Activation and detoxication of aflatoxin B<sub>1</sub>. *Mutation Research*, **402 (1-2)**, 121-128.

Guerra, M. C., Galvano, F., Bonsi, L., Speroni, E., Costa, S., Renzulli, C., Cervellati, R. (2005). Cyanidin-3-O-[beta]-glucopyranoside, a natural free-radical scavenger against aflatoxin B<sub>1</sub>- and ochratoxin A-induced cell damage in a human hepatoma cell line (HepG2) and a human colonic adenocarcinoma cell line (CaCo-2). *British Journal of Nutrition*, **94 (2)**, 211-220.

Gyamfi, M.A., Aniya, Y. (1998). Medicinal herb *Thonningia sanguinea* protects against aflatoxin B<sub>1</sub> acute hepatotoxicity in Fischer 344 rats. *Experimental Toxicology*, **17 (8)**, 418-423.

Haffner, R., Oren, M. (1995). Biochemical properties and biological effects of p53. *Current Opinion in Genetics and Development*, **5 (1)**, 84-90.

Halliwell, B., Chirico, S. (1993). Lipid peroxidation: its mechanism, measurement, and significance. *American Journal of Clinical Nutrition*, **57 (5)**, 715-725.

Handl, J., Richard, J. (2007). Worldwide occurrence of mycotoxins in commodities, feeds and feed ingredients. *Animal Feed Science and Technology*, **137**, 265-282.

Hare, J. D. (1969). Nuclear alterations in mammalian cells induced by L-canavanine. *Cellular Physiology*, **75 (1)**, 129-131.

Hartnett, S. M. Oosthuizen, M., van de Venter, M. (2005). Anti-HIV activities of organic and aqueous extracts of *Sutherlandia frutescens* and *Lobostemon trigonus*. *Ethnopharmacology*, **96 (1-2)**, 113-119.

Hassen, W., Ayed-Boussema, I., Oscoz, A. A., Lopez, A. D. C., Bacha, H. (2007). The role of oxidative stress in zearalenone-mediated toxicity in HepG2 cells: oxidative DNA damage, glutathione depletion and stress proteins induction. *Toxicology*, **232 (3)**, 294-302.



- Hassen, W., Golli, E. E., BAudrimont, I., Mobio, A. T., Ladjimi, M. M., Creppy, E. E., Bacha, H. (2005). Cytotoxicity and Hsp70 induction in HepG2 cells in response to zearalenone and cytoprotection by sub-lethal heat shock. *Toxicology*, **207** (2), 293-301.
- Hawley, T. S., Hawley, R. G. (eds.) (2004). *Flow Cytometry Protocols*. 2<sup>nd</sup> edition. New Jersey: Humana Press. 2-3, 8, 12, 16, 181, 141-142pp.
- Hayes, J. D., Judah, D. J., McLellan, L. I., Neal, G. E. (1991). Contribution of the glutathione S-transferases to the mechanisms of resistance to aflatoxin B<sub>1</sub>. *Pharmacology & Therapeutics*, **50** (3), 443-472.
- Heim, K. E., Tagliaferro, A. R., Bobilya, D. J. (2002). Flavonoid antioxidants: chemistry, metabolism and structure-activity relationships. *Journal of Nutritional Biochemistry*, **13** (10), 572-584.
- Heinemann, I. U., Jahn, M., Jahn, D. (2008). The biochemistry of heme biosynthesis. *Archives of Biochemistry and Biophysics*, **474**, 238-251.
- Hickman, E. S., Moroni, M. C., Helin, K. (2002). The role of p53 and pRB in apoptosis and cancer. *Current Opinion in Genetics & Development*, **12** (1), 60-66.
- Hofseth, L. J., Hussain, S. P., Harris, C. C. (2004). p53: 25 years after its discovery. *Trends in Pharmacological Sciences*, **25** (4), 177-181.
- Hsieh, Y., Su, I., Lei, H., Lai, M., Chang, W., Huang, W. (2007). Differential endoplasmic reticulum stress signaling pathways mediated by iNOS. *Biochemical and Biophysical Research Communications*, **359** (3), 643-648.
- Hussein, H. S., Brasel, J. M. (2001). Toxicity, metabolism, and impact of mycotoxins on humans and animals. *Toxicology*, **167** (2), 101-134.
- Indo, H. P., Davidson, M., Yen, H. C., Suenaga, S., Tomita, K., Nishii, T., Higuchi, M., Koga, Y., Ozawa, T., Majima, H. (2007). Evidence of ROS generation by mitochondria in cells with impaired electron transport chain and mitochondrial DNA damage. *Mitochondrion*, **7** (1-2), 106-118.

Innes, J. (2008). The John Innes Centre [Website]. Available from: <[http://www.jic.ac.uk/microscopy/more/T5\\_6.htm](http://www.jic.ac.uk/microscopy/more/T5_6.htm)> [Accessed: 25 October 2008, 11.45am].

Iwaki, M., Kitagawa, T., Akamatsu, Y., Aibara, K. (1990). Cytotoxic effects of aflatoxin B<sub>1</sub> and its association with cellular components in chicken embryo primary cultured cells. *Biochimica et Biophysica Acta (BBA) - General Subjects*, **1035** (2), 146-153.

Iyer, A. K. V., Azad, N., Wang, L., Rojanasakul, Y. (2008). Role of S-nitrosylation in apoptosis resistance and carcinogenesis. *Nitric Oxide*, **19** (2), 146-151.

Jang, M. H., Jun, D. Y., Rue, S. W., Han, K. H., Park, W., Kim, Y. H. (2002). Arginine antimetabolite L-canavanine induces apoptotic cell death in human Jurkat T cells via caspase-3 activation regulated by Bcl-2 or Bcl-xL. *Biochemical and Biophysical Research Communications*, **295** (2), 283-288.

Jenuwein, T., Allis, C. D. (2001). Translating the histone code. *Epigenetics*, **293** (5532), 1074-1080.

Jodynis-Liebert, J., Matławska, I., Bylka, W., Murias, M. (2006). Protective effect of *Aquilegia vulgaris* on aflatoxin B<sub>1</sub>-induced hepatic damage in rats. *Environmental Toxicology and Pharmacology*, **22** (1), 58-63.

John, D. W., Miller, L. L. (1969). Effect of aflatoxin B<sub>1</sub> on net synthesis of albumin, fibrinogen and  $\alpha_1$ -acid glycoprotein by the isolated perfused rat liver. *Biochemical Pharmacology*, **18**, 1135-1146.

Kannan, K., Jain, S. K. (2000). Oxidative stress and apoptosis. *Pathophysiology*, **7** (27), 153-163.

Kaufmann, S. H., Hengartner, M. O. (2001). Programmed cell death: alive and well in the new millennium. *Trends in Cell Biology*, **11** (12), 526-534.

Ketterer, B., Coles, B., Meyer, D. J. (1983). The role of glutathione in detoxication. *Environmental Health Perspectives*, **49**, 59-69.

Kim, P. K. M., Zamora, R., Petrosko, P., Billiar, T. R. (2001). The regulatory role of nitric oxide in apoptosis. *International Immunopharmacology*, **1** (8), 1421-1441.

Kim, Y. H., Park, E. J., Han, S. T., Park, J. W., Kwon, T. K. (2005). Arsenic trioxide induces Hsp70 expression via reactive oxygen species and JNK pathway in MDA231 cells. *Life Sciences*, **77** (22), 2783-2793.

Klein, P. J., van Vleet, T. R., Hall, J. O., Coulombe, R. A. (2002). Dietary butylated hydroxytoluene protects against aflatoxicosis in turkeys. *Toxicology and Applied Pharmacology*, **182** (1), 11-19.

Knasmuller, S., Parzefall, W., Sanyal, R., Ecker, S., Schwab, C., Uhl, M., Mersch-Sundermann, V., Williamson, G., Hietsch, G., Langer, T., Darroudi, F., Natarajan, A. T. (1998). Use of metabolically competent human hepatoma cells for the detection of mutagens and antimutagens. *Mutation Research*, **402** (1-2), 185-202.

Komarova, E. A., Gudkov, A. V. (1998). Could p53 be a target for therapeutic suppression? *Cancer Biology*, **8** (5), 389-400.

Kubbutat, M. H. G., Vousden, K. H. (1998). Keeping an old friend under control: regulation of p53 stability. *Molecular medicine*, **4** (6), 250-256.

Kuhn, H., Borchert, A. (2002). Regulation of enzymatic lipid peroxidation: the interplay of peroxidizing and peroxide reducing enzymes. *Free Radical Biology & Medicine*, **33** (2), 154-172.

Kuilman, M. E. M., Maas, R. F. M., Fink-Gremmels, J. (2000). Cytochrome P450-mediated metabolism and cytotoxicity of aflatoxin B<sub>1</sub> in bovine hepatocytes. *Toxicology in Vitro*, **14** (4), 321-327.

Kundu, J.K., Mossanda, K.S., Na, H-K., Surh, Y-J. (2005). Inhibitory effects of the extracts of *Sutherlandia frutescens* (L.) R.Br. and *Harpagophytum procumbens* DC. on phorbol ester-induced COX-2 expression in mouse skin: AP-1 and CREB as potential upstream targets. *Cancer Letters*, **218** (1), 21-31.

- Kurien, B. T., Scofield, R. H. (2006). Western blotting. *Methods*, **38** (4), 283-293.
- Langman, L. J., Kapur, B. M. (2006). Toxicology: then and now. *Clinical Biochemistry*, **39** (5), 498-510.
- Latonen, L., Laiho, M. (2005). Cellular UV damage responses - functions of tumor suppressor p53. *Biochimica et Biophysica Acta*, **1755** (2), 71- 89.
- LeBlanc, A. C. (2003). Natural cellular inhibitors of caspases. *Progress in Neuro-Psychopharmacology & Biological Psychiatry*, **27** (2), 215-229.
- Lee, J. K., Choi, E. H., Lee, K. G., Chun, H. S. (2005). Alleviation of aflatoxin B<sub>1</sub>-induced oxidative stress in HepG2 cells by volatile extract from *Allii Fistulosi Bulbus*. *Life Sciences*, **77** (23), 2896-2910.
- Lee, Y. J., Shukla, S. D. (2005). Pro- and anti-apoptotic roles of c-Jun N-terminal kinase (JNK) in ethanol and acetaldehyde exposed rat hepatocytes. *European Journal of Pharmacology*, **508** (1-3), 31-45.
- Li, C. Q., Wogan, G. N. (2005). Nitric oxide as a modulator of apoptosis. *Cancer Letters*, **226** (1), 1-15.
- Li, C., Lee, J., Ko, Y., Kim, J., Seo, J. (2000). Heat shock protein 70 inhibits apoptosis downstream of cytochrome c release and upstream of caspase-3 activation. *Biological Chemistry*, **275** (33), 25665-25671.
- Li, G. C., Laszlo, A. (1984). Amino acid analogs while inducing heat shock proteins sensitize CHO cells to thermal damage. *Cellular Physiology*, **122** (1), 91-97.
- Li, H. H., Aubrecht, J., Fornace, A. J. (2007). Toxicogenomics: overview and potential applications for the study of non-covalent DNA interacting chemicals. *Mutation Research*, **623** (1-2), 98-108.
- Lichtman, J. W., Conchello, J. A. (2005). Fluorescence microscopy. *Nature Methods*, **2** (12), 910-919.

- Liu, B., Chen, Y., Clair, D. K. S. (2008). ROS and p53: A versatile partnership. *Free Radical Biology & Medicine*, **44** (8), 1529-1535.
- Lockshin, R. A., Zakeri, Z. (2002). Caspase-independent cell deaths. *Current Opinion in Cell Biology*, **14** (6), 727-733.
- Lohrum, M. A. E., Vousden, K. H. (2000). Regulation and function of the p53-related proteins: same family, different rules. *Trends in Cell Biology*, **10** (5), 197-202.
- Lorico, A., Nesland, J., Emilson, E., Fodstad, O., Rappa, G. (2002). Role of the multidrug resistance protein 1 gene in the carcinogenicity of aflatoxin B<sub>1</sub>: investigations using mrp1-null mice. *Toxicology*, **171** (2-3), 201-205.
- Luzzi, S. D., Marletta, M. A. (2005). L-Arginine analogs as alternate substrates for nitric oxide synthase. *Bioorganic & Medicinal Chemistry Letters*, **15** (17), 3934-3941.
- Ma, Y., Cao, L., Kawabata, T., Yoshino, T., Yang, B. B., Okada, S. (1998). Cupric nitrilotriacetate induces oxidative damage and apoptosis in human leukemia HL-60 cells. *Free Radical Biology & Medicine*, **25** (4-5), 568-575.
- Madhusudhanan, N., KavithaLakshmi, S. N., Shanmugasundaram, K. R., Shanmugasundaram. E. R. B. (2004). Oxidative damage to lipids and proteins induced by aflatoxin B<sub>1</sub> in fish (*Labeo rohita*)-protective role of *Amrita Bindu*. *Environmental Toxicology and Pharmacology*, **17** (2), 73-77.
- Majer, B. J., Mersch-Sundermann, V., Darroudi, F., Laky, B., de Wit, K., Knasmüller, S. (2004). Genotoxic effects of dietary and lifestyle related carcinogens in human derived hepatoma (HepG2, Hep3B) cells. *Mutation Research*, **551** (1-2), 153-166.
- Mateas, J. M., Sanchez-Jimeanez, F. M. (2000). Role of reactive oxygen species in apoptosis: implications for cancer therapy. *The International Journal of Biochemistry & Cell Biology*, **32** (2), 157-170.
- McGlynn, K. A., London, W. T. (2005). Epidemiology and natural history of hepatocellular carcinoma. *Best Practice & Research Clinical Gastroenterology*, **19** (1), 3-23.

McKean, C., Tang, L., Tang, M., Billam, M., Wang, Z., Theodorakis, C. W., Kendell, R. J., Wang, J. S. (2006). Comparative acute and combinative toxicity of aflatoxin B<sub>1</sub> and fumonisin B<sub>1</sub> in animals and human cells. *Food and Chemical Toxicology*, **44** (6), 868-876.

McLean, M., Dutton, M. F. (1995). Cellular interactions and metabolism of aflatoxin: an update. *Pharmacology & Therapeutics*, **65** (2), 163-192.

Meek, D. W. (2004). The p53 response to DNA damage. *DNA Repair*, **3** (8-9), 1049-1056.

Meerdink, G. L. (2002). Mycotoxins. *Clinical Techniques in Equine Practice*, **1** (2), 89-93.

Meki, A. R. M. A., Esmail, E. E. D. F., Hussein, A. A., Hassanein, H. M. (2004). Caspase-3 and heat shock protein-70 in rat liver treated with aflatoxin B<sub>1</sub>: effect of melatonin. *Toxicon*, **43** (1), 93-100.

Meki, A. R., Abdel-Ghaffar, S. K., El-Gibaly, I. (2001). Aflatoxin B<sub>1</sub> induces apoptosis in rat liver: protective effect of melatonin. *Neuro Endocrinology Letters*, **22** (6), 417-426.

Meneghini, R., Schumacher, R. I. (1977). Aflatoxin B<sub>1</sub>, a selective inhibitor of DNA synthesis in mammalian cells. *Chemico-Biological Interactions*, **18** (3), 267-276.

Meredith, M. J., Lepock, J. R. (1999). On the path to the heat shock response: destabilization and formation of partially folded protein intermediates, a consequence of protein thiol modification. *Free Radical Biology & Medicine*, **26** (5-6), 737-745.

Mills, E., Cooper, C., Seely, D. Kanfer, I. (2005) a. African herbal medicines in the treatment of HIV: *Hypoxis* and *Sutherlandia*. An overview of evidence and pharmacology. *Nutrition Journal*, **4** (19), 1-6.

Mills, E., Foster, B. C., van Heeswijk, R., Phillips, E., Wilson, K., Leonard, B., Kosuge, K., Kanfer, I. (2005) b. Impact of African herbal medicines on antiretroviral metabolism. *AIDS*, **19** (1), 93-99.

Moll, U. M., Zaika, A. (2001). Nuclear and mitochondrial apoptotic pathways of p53. *FEBS Letters*, **493** (2-3), 65-69.

- Moon, E. Y. (1998). Aflatoxin B<sub>1</sub>-induced suppression of nitric oxide production in murine peritoneal macrophages. *Journal of Toxicology and Environmental Health*, **55** (7), 517-530.
- Moon, E. Y., Pyo, S. (2000). Aflatoxin B<sub>1</sub> inhibits CD14-mediated nitric oxide production in murine peritoneal macrophages. *International Journal of Immunopharmacology*, **22** (3), 237-246.
- Moon, E. Y., Rhee, D. K., Pyo, S. (1999) a. *In vitro* suppressive effect of aflatoxin B<sub>1</sub> on murine peritoneal macrophage functions. *Toxicology*, **133** (2-3), 171-179.
- Moon, E. Y., Rhee, D. K., Pyo, S. (1999) b. Inhibition of various functions in murine peritoneal macrophages by aflatoxin B<sub>1</sub> exposure *in vivo*. *International Journal of Immunopharmacology*, **21** (1), 47-58.
- Moon, E. Y., Rhee, D. K., Pyo, S. (1999) c. Involvement of NO, H<sub>2</sub>O<sub>2</sub> and TNF- $\alpha$  in the reduced antitumor activity of murine peritoneal macrophages by aflatoxin B<sub>1</sub>. *Cancer Letters*, **136** (2), 167-176.
- Moss, M. O. (2002). Risk assessment for aflatoxins in foodstuffs. *International Biodeterioration & Biodegradation*, **50** (3-4), 137-142.
- Nafisi, S., Saboury, A. A., Keramat., N., Neault, J. F., Tajmir-Riahi, H. A. (2007). Stability and structural features of DNA intercalation with ethidium bromide, acridine orange and methylene blue. *Journal of Molecular Structure*, **827** (1-3), 35-43.
- Nasri, T., Bosch, R. R., Voorde, S. T., Fink-Gremmels, J. (2006). Differential induction of apoptosis by type A and B trichothecenes in Jurkat T-lymphocytes. *Toxicology in Vitro*, **20** (6), 832-840.
- Neal, G. E. (1995). Genetic implications in the metabolism and toxicity of mycotoxins. *Toxicology Letters*, **82**, 861-867.
- Nicoll, A. K. (2004). Cell death and Apoptosis. SLS Flow Cytometry Core Facility [Website]. Available from: <[http://www.dundee.ac.uk/lifesciences/FACS/cell\\_death.htm](http://www.dundee.ac.uk/lifesciences/FACS/cell_death.htm)> [Accessed: 26 November 2008, 00:08am].

Niranjan, B. C., Bhat, N. K., Avadhani, N. C. (1981). Preferential attack of mitochondrial DNA by aflatoxin B<sub>1</sub> during hepatocarcinogenesis. *Science*, **215** (4528), 73-75.

Noe, B. D. (1981). Inhibition of islet prohormone to hormone conversion by incorporation of arginine and lysine analogs. *Biological Chemistry*, **256** (10), 4940-4946.

Ntuli, S. S. B. N., Gelderblom, W. C. A., Katerere, D. R., Ndodo, B. I. (2007). Mutagenic and antimutagenic effects of *Sutherlandia frutescens*. *South African Journal of Botany*, **73** (2), 332-333.

O'Brien, T., Babcock, G., Cornelius, J., Dingeldein, M., Talaska, G., Warshawsky, D., Mitchell, K. (2000). A comparison of apoptosis and necrosis induced by hepatotoxins in HepG2 Cells. *Toxicology and Applied Pharmacology*, **164** (3), 280-290.

Obidoa, O. (1986). Aflatoxin inhibition of rat liver mitochondrial cytochrome oxidase activity. *Biochemical medicine and Metabolic Biology*, **35** (3), 302-307.

Obidoa, O., Obonna, E. E. (1981). Aflatoxin inhibition of reversed electron transfer in rat liver mitochondria *in vitro*. *Biochemical Medicine*, **26** (1), 1-7.

Ojewole, J.A.O. (2004). Analgesic, anti-inflammatory and hypoglycemic effects of *Sutherlandia frutescens* R.Br. (variety incana E.MEY.) [Fabaceae] shoot aqueous extract. *Methods and Findings in Experimental and Clinical Pharmacology*, **26** (6), 409-416.

Ojewole, J.A.O. (2008). Anticonvulsant property of *Sutherlandia frutescens* R.Br. (variety incana E.Mey.) [Fabaceae] shoot aqueous extract. *Brain Research Bulletin*, **75** (1), 126-132.

Omar, A. I., Hu, B. (2003). Detection of early tissue injury *in vivo* using fluorescent cell death markers in rat dentate gyrus. *Neuroscience Letters*, **348** (3), 143-146.

Ostling, O., Johanson, K. J. (1984). Microelectrophoretic study of radiation-induced DNA damages in individual mammalian cells. *Biochemical and Biophysical Research Communications*, **123** (1), 291-298.



- Otsuki, Y., Li, Z., Shibata, M. A. (2003). Apoptotic detection methods - from morphology to gene. *Journal of Histochemistry and Cytochemistry*, **38** (3), 275-340.
- Pai, M. R., Bai, N. J., Venkitasubramanian, T. A. (1975). Effect of aflatoxins on oxidative phosphorylation by rat liver mitochondria. *Chemico-Biological Interactions*, **10** (2), 123-131.
- Parcellier, A., Gurbuxani, S., Schmitt, E., Solary, E., Garrido, C. (2003). Heat shock proteins, cellular chaperones that modulate mitochondrial cell death pathways. *Biochemical and Biophysical Research Communications*, **304** (3), 505-512.
- Park, J. W., Moon, C., Yun, S., Kim, S. Y., Bae, Y. C., Chun, M. H., Moon, C. I. (2007). Differential expression of heat shock protein mRNAs under *in vivo* glutathione depletion in the mouse retina. *Neuroscience Letters*, **413** (3), 260-264.
- Pieczenik, S. R., Neustadt, J. (2007). Mitochondrial dysfunction and molecular pathways of disease. *Experimental and Molecular Pathology*, **83** (1), 84-92.
- Pockley, A. G. (2003). Heat shock proteins as regulators of the immune response. *Lancet*, **362** (9382), 469-476.
- Powers, M. V., Workman, P. (2007). Inhibitors of the heat shock response: biology and pharmacology. *FEBS Letters*, **581** (19), 3758-3769.
- Prasanna, H. R., Gupta, S. R., Viswanathan, L., Venkitasubramanian, T. A. (1978). Comparative study of the effects of aflatoxin B<sub>1</sub> metabolites and  $\alpha$ -amanitin on rat liver RNA polymerase activities and chromatin template activities. *Toxicon*, **16** (3), 289-294.
- Preetha, S. P., Kanniappan, M., Selvakumar, E., Nagaraj, M., Varalakshmi, P. (2006). Lupeol ameliorates aflatoxin B<sub>1</sub>-induced peroxidative hepatic damage in rats. *Comparative Biochemistry and Physiology*, **143** (3), 333-339.
- Pretet, J. (2002). Step-by-step release of cytochrome c. *TRENDS in Cell Biology*, **12** (6), 251.
- Prevoo, D., Swart, P., Swart, A.C. (2008). The influence of *Sutherlandia frutescens* on adrenal steroidogenic cytochrome P450 enzymes. *Ethnopharmacology*, **118** (1), 118-126.

Prinsze, C., Dubbelman, T. M. A. R., Steveninck, J. V. (1990). Protein damage induced by small amounts of photodynamically generated singlet oxygen or hydroxyl radicals. *Protein Structure and Molecular Enzymology*, **1038** (2), 152-157.

Promega Corporation (2007). GSH-Glo™ Glutathione Assay. *Technical Bulletin*, **369**, 1-20.

Proskuryakov, S. Y., Konoplyannikov, A. G., Gabaib, V. L. (2003). Necrosis: a specific form of programmed cell death? *Experimental Cell Research*, **283** (1), 1-16.

Raffray, M., Cohen, G. M. (1997). Apoptosis and necrosis in toxicology: a continuum or distinct modes of cell death? *Pharmacology & Therapeutics*, **75** (3), 153-177.

Raj, H. G., Kohil, E., Rohil, V., Dwarakanath, B. S., Parmer, V. S., Malik, S., Adhikari, J. S., Tyagi, Y. K., Goel, S., Gupta, K., Bose, M., Olsen, C. E. (2001). Acetoxy-4-methylcoumarins confer differential protection from aflatoxin B<sub>1</sub>-induced micronuclei and apoptosis in lung and bone marrow cells. *Mutation Research*, **494** (1-2), 31-40.

Rao, K. S. (1971). Aflatoxin B<sub>1</sub> induced inhibition of liver protein synthesis *in vivo* and its role in fatty liver. *Biochemical Pharmacology*, **20** (10), 2825-2831.

Reddy, L., Bharti, O., Kanti, B. (2006). Aflatoxin B<sub>1</sub>-induced toxicity in HepG2 cells inhibited by carotenoids: morphology, apoptosis and DNA damage. *Biological chemistry*, **387** (1), 87-93.

Redman, C.M., Avellino, G., Yu, S. (1983). Secretion of proalbumin by Canavanine-treated HepG<sub>2</sub> Cells. *Biological Chemistry*, **258** (6), 3446-3452.

Reid, K.A., Maes, J., Maes, A., Van Staden, J., De Kimpe, N., Mulholland, D.A., Verschaeve, L. (2006). Evaluation of the mutagenic and antimutagenic effects of South African plants. *Ethnopharmacology*, **106** (1), 44-50.

Remy, C. K., Bates, E. E., Arrigo, A. (1998). Amino acid analogs activate NF- $\kappa$ B through redox-dependent I $\kappa$ B- $\alpha$  degradation by the proteasome without apparent I $\kappa$ B- $\alpha$  phosphorylation. *Biological Chemistry*, **273** (6), 3180-3191.

- Ricordy, R., Gensabella, G., Cacci, E. (2002). Impairment of cell cycle progression by aflatoxin B<sub>1</sub> in human cell lines. *Mutagenesis*, **17** (3), 241-249.
- Riganti, C., Aldieri, E., Bergandi, L., Miraglia, E., Costamagna, C., Bosia, A., Ghigo, D. (2003). Nitroarginine methyl ester and canavanine lower intracellular reduced glutathione. *Free Radical Biology & Medicine*, **35** (10), 1210-1216.
- Roberfroid, M. (1995). Toxicology: a science and an art. *Toxicology in Vitro*, **9** (6), 839-844.
- Robertson, J. D., Datta, K., Biswal, S. S., Kehrer, P. (1999). Heat-shock protein 70 antisense oligomers enhance proteasome inhibitor-induced apoptosis. *Biochemistry*, **344** (Part 2), 477-485.
- Roche Diagnostics. (2005). Annexin-V-FLUOS Staining Kit. Catalog Numbers 11 858 777 001 and 11 988 549 001. 1-2.
- Roda, A., Guardigli, M., Pasini, P., Mirasoli, M. (2003). Clinical and diagnostic applications: luminescence immuno- and gene probe assays. Tarbiat Modares University [Website]. Available from: < [http://www.modares.ac.ir/sci/saman\\_h/Pages/applications.htm](http://www.modares.ac.ir/sci/saman_h/Pages/applications.htm) > [Accessed: 26 October 2008, 13.00pm].
- Rojas, E., Lopez, M. C., Valverde, M. (1999). Single cell gel electrophoresis assay: methodology and applications. *Journal of Chromatography*, **722** (1-2), 225-254.
- Rosenthal, G. A. (1977). The biological effects and mode of action of L-canavanine, a structural analogue of L-arginine. *The Quarterly Review of Biology*, **52** (2), 155-178.
- Rosenthal, G. A. (1981). A mechanism of L-canaline toxicity. *Biochemistry*, **114** (2), 301-304.
- Rosenthal, G. A. (1988). The protective action of a higher plant toxic product. *Bioscience*, **38** (2), 104-109.
- Rosenthal, G. A. (1997). L-canaline: a potent antimetabolite and anti-cancer agent from leguminous plants. *Life Sciences*, **60** (19), 1635-1641.

Rosenthal, G. A., Dahlman, D. L. (1991) a. Incorporation of L-canavanine into proteins and the expression of its antimetabolic effects. *Agricultural and Food Chemistry*, **39** (5), 987-990.

Rosenthal, G. A., Dahlman, D. L. (1991) b. Studies of L-canavanine incorporation into insectan lysozyme. *Biological Chemistry*, **266** (24), 15684-15687.

Rosenthal, G.A., Reichhart, J.M., Hoffmann, J.A. (1989). L-canavanine incorporation into vitellogenin and macromolecular conformation. *Biological Chemistry*, **264** (23), 13693-13696.

Roy, A. K. (1968). Effects of aflatoxin B<sub>1</sub> on polysomal profiles and RNA synthesis in rat liver. *Biochimica et Biophysica Acta (BBA) - Nucleic Acids and Protein Synthesis*, **169** (1), 206-211.

Sabbioni, G., Skipper, P. L., Büchi, G., Tannenbaum, S. R. (1987). Isolation and characterization of the major serum albumin adduct formed by aflatoxin B<sub>1</sub> *in vivo* in rats. *Carcinogenesis*, **8** (6), 819-824.

Sajan, M. P., Satav, J. G., Bhattacharya, R. K. (1995). Activity of some respiratory enzymes and cytochrome contents in rat hepatic mitochondria following aflatoxin B<sub>1</sub> administration. *Toxicology Letters*, **80** (1-3), 55-60.

Santoro, M. G. (2000). Heat shock factors and the control of the stress response. *Biochemical Pharmacology*, **59** (1), 55-63.

Sarasin, A., Moulr, Y. (1973). *In vivo* effect of aflatoxin B<sub>1</sub> on protein synthesis in rat liver. *FEBS Letters*, **29** (3), 329-332.

Scaife, J. F. (1971). Aflatoxin B<sub>1</sub>: Cytotoxic mode of action evaluated by mammalian cell cultures. *FEBS Letters*, **12** (3), 143-147.

Schachtele, C. F., Anderson, D. L., Rogers, P. (1968). Mechanism of canavanine death in *Escherichia coli*: Membrane-bound canavanyl-protein and nuclear disruption. *Molecular Biology*, **33** (3), 861-868.

Schatz, G., Manson, T. L. (1974). The biogenesis of mitochondrial proteins. *Annual Reviews in Biochemistry*, **43**, 51-87.

Schoeniger, L. O., Curtis, W., Esnaola, N. F., Beck, S. C., Gardner, T., Buchman, T. G. (1994). Myocardial heat shock gene expression in pigs is dependent on superoxide anion generated at reperfusion. *Shock*, **1** (1), 31-35.

Sharp, F. R., Massa, S. M., Swanson, R. A. (1999). Heat-shock protein protection. *Tins*, **22** (3), 97-99.

Shen, H. M., Ong, C. N., Shi, C. Y. (1995). Involvement of reactive oxygen species in aflatoxin B<sub>1</sub>-induced cell injury in cultured rat hepatocytes. *Toxicology*, **99** (1-2), 115-123.

Shen, H. M., Shi, C. Y., Lee, H. P., Ong, C. N. (1994). Aflatoxin B<sub>1</sub>-induced lipid peroxidation in rat liver. *Toxicology and Applied Pharmacology*, **127** (1), 145-150.

Shen, H. M., Shi, C. Y., Shen, Y., Ong, C. N. (1996). Detection of elevated reactive oxygen species level in cultured rat hepatocytes treated with aflatoxin B<sub>1</sub>. *Free Radical Biology & Medicine*, **21** (2), 139-146.

Shmueli, A., Oren, M. (2007). Mdm2: p53's lifesaver? *Molecular Cell*, **25** (6), 794-795.

Sia, C. (2004). Spotlight on Ethnomedicine: Usability of *Sutherlandia frutescens* in the treatment of diabetes. *The Review of Diabetic Studies*, **1** (3), 145-149.

Sidransky, H., Verney, E., Murty, C. N., Sarma, D. S. R., Reid, M. (1977). Effect of aflatoxin B<sub>1</sub> on hepatic polyribosomes and protein synthesis in the rat. *Chemico-Biological Interactions*, **18** (1), 69-82.

Sies, H. (1999). Glutathione and its role in cellular functions. *Free Radical Biology & Medicine*, **27** (9), 916-921.

Singh, N.P., McCoy, M. T., Tice, R. R., Schneider, E. L. (1988). A simple technique for quantitation of low levels of DNA damage in individual cells. *Experimental Cell Research*, **175** (1), 184-191.

- Slater, A. F. G., Nobel, C. S. I., Orrenius, S. (1995). The role of intracellular oxidants in apoptosis. *Biochimica et Biophysica Acta*, **1271** (1), 59-62.
- Slavotinek, A. M., Biesecker, L. G. (2001). Unfolding the role of chaperones and chaperonins in human disease. *Trends in Genetics*, **17** (9), 528-535.
- Smela, M. E., Currier, S. S., Bailey, E. A., Essigman, J. M. (2001). The chemistry and biology of aflatoxin B<sub>1</sub>: from mutational spectrometry to carcinogenesis. *Carcinogenesis*, **22** (4), 535-545.
- Solary, E., Dubrez, L., Eymin, B. (1996). The role of apoptosis in the pathogenesis and treatment of diseases. *European Respiratory Journal*, **9** (6), 1293-1305.
- Song, Z., Steller, H. (1999). Death by design: mechanism and control of apoptosis. *TCB*, **9** (12), 49-52.
- Souza, M.F., Tome, A.R., Rao, V.S. (1999). Inhibition by the bioflavonoid ternatin of aflatoxin B<sub>1</sub>-induced lipid peroxidation in rat liver. *Pharmacology*, **51** (2), 125-129.
- Sreedhar, A. S., Csermely, P. (2004). Heat shock proteins in the regulation of apoptosis: new strategies in tumor therapy. *Pharmacology & Therapeutics*, **101** (3), 227-257.
- Stander, B.A., Marais, S., Steynberg, T.J., Theron, D., Joubert, F., Albrecht, C., Joubert, A.M. (2007). Influence of *Sutherlandia frutescens* extracts on cell numbers, morphology and gene expression in MCF-7 cells. *Ethnopharmacology*, **112** (2), 312-318.
- Steenkamp, V., Gouws, M.C. (2006). Cytotoxicity of six South African medicinal plant extracts used in the treatment of cancer. *South African Journal of Botany*, **72** (4), 630-633.
- Stewart, R. K., Serabjit-Singh, C. J., Massey, T. E. (1996). Glutathione S-transferase-catalysed conjugation of bioactivated aflatoxin B<sub>1</sub> in rabbit lung and liver. *Toxicology and Applied Pharmacology*, **140** (2), 499-507.
- Steyn, P. S. (1995). Mycotoxins, general view, chemistry and structure. *Toxicology Letters*, **82-83**, 843-851.

Swaffar, D. S., Ang, C. Y., Desai, P. B., Rosenthal, G. A. (1994). Inhibition of the growth of human pancreatic cancer cells by the arginine antimetabolite L-canavanine. *Cancer Research*, **54** (23), 6045-6048.

Tai, J., Cheung, S., Chan, E., Hasman, D. (2004). *In vitro* culture studies of *Sutherlandia frutescens* on human tumor cell lines. *Ethnopharmacology*, **93** (1), 9-19.

Thomas, D. A., Rosenthal, G. A. (1987). Toxicity and pharmacokinetics of the nonprotein amino acid L-canavanine in the rat. *Toxicology and Applied Pharmacology*, **91** (3), 395-405.

Thomas, D. A., Rosenthal, G. A., Gold, D. V., Dickey, K. (1980). Growth inhibition of a rat colon tumor by L-canavanine. *Cancer Research*, **46** (6), 2898-2903.

Thomson, J. A. (2008). Thompson Lab [Website]. Available from: <<http://ink.primat.wisc.edu/~thomson/protocol.html>> [Accessed: 27 October 2008, 14.45pm].

Törnqvist, M., Fred, C., Haglund, J., Helleberg, H., Paulsson, B., Rydberg, P. (2002). Protein adducts: quantitative and qualitative aspects of their formation, analysis and applications. *Journal of Chromatography B*, **778** (1), 279-308.

Towner, R. A., Mason, R. P., Reinke, L. A. (2002). *In vivo* detection of aflatoxin-induced lipid free radicals in rat bile. *Biochimica et Biophysica Acta*, **1573** (1), 55-62.

Towner, R. A., Qian, S. Y., Kadiiska, M. B., Mason, R. P. (2003). *In vivo* identification of aflatoxin B<sub>1</sub>-induced free radicals in rat bile. *Free Radical Biology & Medicine*, **35** (10), 1330-1340.

Ubagai, T., Tansho, S., Ito, T., Ono, Y. (2008). Influences of aflatoxin B<sub>1</sub> on reactive oxygen species generation and chemotaxis of human polymorphonuclear leukocytes. *Toxicology in vitro*, **22** (14), 1115-1120.

Uhl, M., Helma, C., Knasmuller, S. (2000). Evaluation of the single cell gel electrophoresis assay with human hepatoma (Hep G2) cells. *Mutation Research*, **468** (2), 213-225.

- Van Ness, K. P., McHugh, T. E., Bammler, T. K., Eaton, D. L. (1998). Identification of amino acid residues essential for high aflatoxin B<sub>1</sub>-8,9-epoxide conjugation activity in alpha class glutathione S-transferases through site-directed mutagenesis. *Toxicology and Applied Pharmacology*, **152** (1), 166-174.
- Van Vleet, T. R., Watterson, T. L., Klein, P. J., Coulombe, R. A. (2006). Aflatoxin B<sub>1</sub> alters the expression of p53 in cytochrome P450-expressing human lung Cells. *Toxicological Sciences*, **89** (2), 399-407.
- van Wyk, B. E. (2008). A broad review of commercially important southern African medicinal plants. *Ethnopharmacology*, **119** (3), 342-355.
- van Wyk, B. E., Albrecht, C. (2008). A review of the taxonomy, ethnobotany, chemistry and pharmacology of *Sutherlandia frutescens* (Fabaceae). *Ethnopharmacology*, **119** (3), 620-629.
- Verma, A. K., Pal, A. K., Manush, S. M., Das, T., Dalvi, R. S., Chandrachoodan, P. P., Ravi, P. M., Apte, S. K. (2007). Persistent sub-lethal chlorine exposure augments temperature induced immunosuppression in *Cyprinus carpio* advanced fingerlings. *Fish & Shellfish Immunology*, **22** (5), 547-555.
- Wagner, G., Unterreiner, A. M. (1981). Inhibition of rat liver aminoacyl-tRNA synthetases in vitro after acute and chronic aflatoxin B<sub>1</sub> administration *in vivo*. *Chemico-Biological Interactions*, **37** (1-2), 233-244.
- Wagner, G., Unterreiner, A. M. (1982). Synthesis of transfer RNA in rat liver after acute and chronic aflatoxin B<sub>1</sub> administration. *Chemico-Biological Interactions*, **41** (3), 353-360.
- Wagner, L., Drews, J. (1965). The effect of aflatoxin B<sub>1</sub> on RNA synthesis and breakdown in normal and regenerating rat liver. *European Journal of Cancer*, **6** (6), 465-476.
- Wang, J., Groopman, J. D. (1999). DNA damage by mycotoxins. *Mutation Research*, **424** (1-2), 167-181.



- Wang, M., Li, B., Wang, C., Chen, Y., Zuo, Z. (2008). The concentration-dependent induction of cell death by trimethyltin chloride in rat liver epithelial IAR20 cells. *Toxicology in Vitro*, **22** (5), 1136-1142.
- Weber, H., Huhns, S., Jonas, L., Sparmann, G., Bastian, M., Schuff-Werner, P. (2007). Hydrogen peroxide-induced activation of defense mechanisms against oxidative stress in rat pancreatic acinar AR42J cells. *Free Radical Biology and Medicine*, **42** (6), 830-841.
- White, N. S., Errington, R. J. (2005). Fluorescence techniques for drug delivery research: theory and practice. *Advanced Drug Delivery Reviews*, **57** (1), 17-42.
- Wild, C. P., Hasegawa, R., Barraud, L., Chutimataewin, S., Chapot, B., Ito, N., Montesano, R. (1996). Aflatoxin-albumin adducts: a basis for comparative carcinogenesis between animals and humans. *Cancer Epidemiology, Biomarkers & Prevention*, **5** (3), 179-189.
- Wilkie, D. (1970). Selective inhibition of mitochondrial synthesis in *Saccharomyces cerevisiae* by canavanine. *Molecular Biology*, **47** (1), 107-113.
- Wilson, K., Walker, J. (eds.) (2005). *Principles and Techniques of Biochemistry and Molecular Biology*. 6<sup>th</sup> edition. Cambridge: Cambridge University Press. 143-145, 457-458, 475.
- Winston, R. A., Bosmann, H. B. (1971). Protein and glycoprotein synthesis in rat liver mitochondria and rat intraneural mitochondria and protein synthesis in rat liver microsomes in the presence of L-canavanine. *Chemical-Biological Interactions*, **3** (2), 131-139.
- Worthen, D.R., Chien, L., Tsuboi, C.P., Mu, X.Y., Bartik, M.M. Crooks, P. A. (1998). L-canavanine modulates cellular growth, chemosensitivity and P-glycoprotein substrate accumulation in cultured human tumor cell lines. *Cancer Letters*, **132** (1-2), 229-239.
- Yerlikaya, A. (2004). Polyamines and S-adenosylmethionine decarboxylase. *Turkish Journal of Biochemistry*, **29** (2), 208-214.
- Yoneyama, M., Sharma, R. P., Elsner, Y. Y. (1987). Effects of mycotoxins in cultured kidney cells: Cytotoxicity of aflatoxin B<sub>1</sub> in Madin-Darby and primary fetal bovine kidney cells. *Ecotoxicology and Environmental Safety*, **13** (2), 174-184.

Yu, F. L., Bender, W., Geronimo, I. H. (1988). The binding of aflatoxin B<sub>1</sub> to rat liver nuclear proteins and its effect on DNA-dependent RNA synthesis. *Carcinogenesis*, **19** (4), 533-540.

Yu, J., Zhang, L. (2005). The transcriptional targets of p53 in apoptosis control. *Biochemical and Biophysical Research Communications*, **331** (3), 851-858.

Yu, Z., Yang, X., Wang, K. (2006). Metal ions induced heat shock protein response by elevating superoxide anion level in HeLa cells transformed by HSE-SEAP reporter gene. *Toxicology*, **223** (1-2), 1-8.

Zeimet, A. G. (2003). Refolding mutant p53: a simple way to resolve a complex problem? *DDT*, **8** (14), 620.

Zhang, Q., Zhao, X. H., Wang, Z. J. (2008). Flavones and flavonols exert cytotoxic effects on a human oesophageal adenocarcinoma cell line (OE33) by causing G2/M arrest and inducing apoptosis. *Food and Chemical Toxicology*, **46** (6), 2042-2053.

Zimmermann, K. C., Bonzon, C., Green, D. R. (2001). The machinery of programmed cell death. *Pharmacology & Therapeutics*, **92** (1), 57-70.

Zourgui, L., Golli, E. E., Bouaziz, C., Bacha, H., Hassen, W. (2008). Cactus (*Opuntia ficus-indica*) cladodes prevent oxidative damage induced by the mycotoxin zearalenone in *Balb/C* mice. *Food and Chemical Toxicology*, **46** (5), 1817-1824.

## APPENDIX

### Appendix 1

**Table A1: Components present in EMEM.**

| Component   | Concentration (mg/l) |
|---|----------------------|
| <b>Inorganic salts</b>                              |                      |
| CaCl <sub>2</sub> .2H <sub>2</sub> O                | 186.00               |
| KCl   | 400.00               |
| KH <sub>2</sub> PO <sub>4</sub>                     | 60.00                |
| MgSO <sub>4</sub> .7H <sub>2</sub> O                | 200.00               |
| NaCl  | 8 000.00             |
| NaHCO <sub>3</sub>                                  | 350.00               |
| Na <sub>2</sub> HPO <sub>4</sub> .7H <sub>2</sub> O | 90.00                |
| <b>Other components</b>                             |                      |
| Glucose   | 1 000.00             |
| Phenol red  | 20.00                |
| <b>Amino acids</b>                                  |                      |
| L-Arginine-HCl                                      | 126.40               |
| L-Cysteine  | 24.00                |
| L-Histidine-HCl.H <sub>2</sub> O                    | 42.00                |
| L-Isoleucine  | 52.40                |
| L-Leucine   | 52.40                |
| L-Lysine-HCl  | 73.00                |
| L-Methionine  | 15.00                |
| L-Phenylalanine                                     | 33.00                |
| L-Threonine   | 47.60                |
| L-Tryptophan  | 10.20                |
| L-Tyrosine  | 36.20                |
| L-Valine  | 46.80                |
| <b>Vitamins</b>                                     |                      |
| D-Capantothenate                                    | 1.00                 |
| Choline chloride                                    | 1.00                 |
| Folic acid  | 1.00                 |
| i-Inositol  | 2.00                 |
| Nicotinamide  | 1.00                 |
| Pyridoxine  | 1.00                 |
| Riboflavin  | 0.10                 |
| Thaimine-HCl  | 1.00                 |

## Appendix 2

**Table A2: Absorbance's and concentrations of standards.**

| ABS BSA (1) | ABS BSA (2) | Average ABS BSA | BSA (mg/ml) | ABS   |
|-------------|-------------|-----------------|-------------|-------|
| 0.188       | 0.173       | 0.181           | 0.0         | 0.000 |
| 0.342       | 0.492       | 0.417           | 0.2         | 0.237 |
| 0.846       | 0.789       | 0.818           | 0.4         | 0.637 |
| 1.038       | 1.034       | 1.036           | 0.6         | 0.856 |
| 1.223       | 1.196       | 1.210           | 0.8         | 1.029 |
| 1.490       | 1.388       | 1.439           | 1.0         | 1.259 |

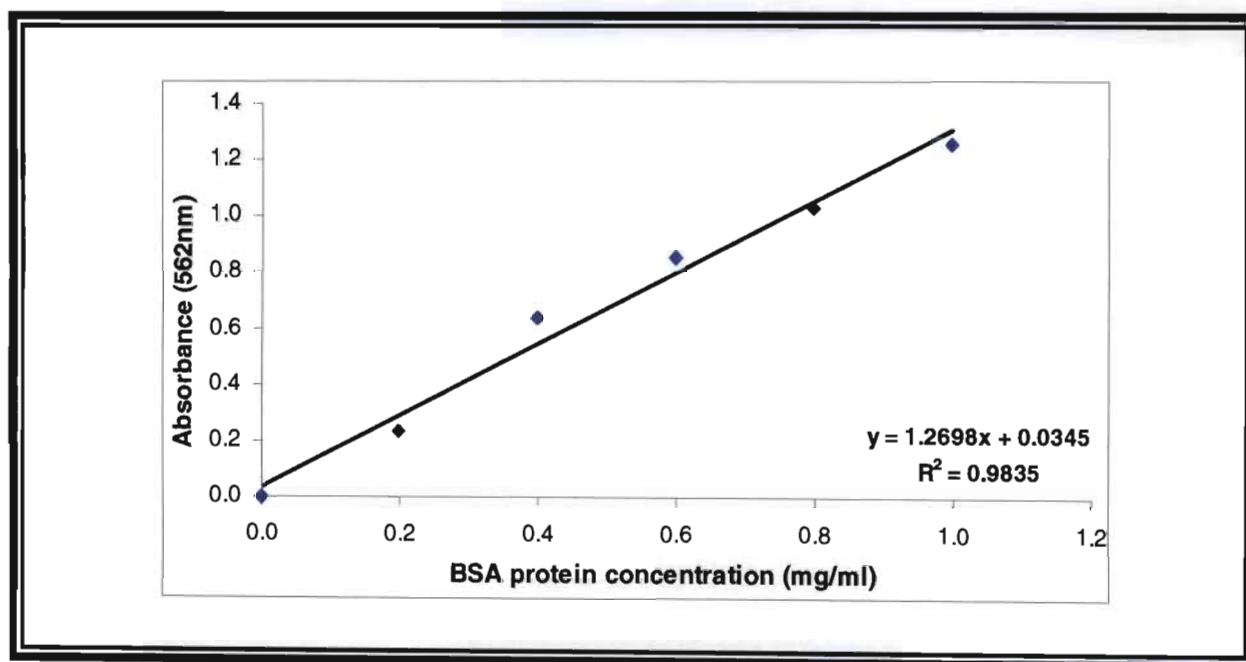


**Figure A1: BSA protein concentration versus average absorbance.**

Figure A1 (values obtained from Table A2) was constructed as a standard curve. The equation defining the curve ( $y = 1.2698x + 0.9835$ ) was used to determine the protein concentration of each sample (Table A3).

**Table A3: Absorbance's and concentrations of samples.**

| Sample                 | ABS (1) | ABS (2) | Avg ABS | Sample (mg/ml) |
|------------------------|---------|---------|---------|----------------|
| Control                | 2.216   | 2.370   | 2.293   | 1.8            |
| SF                     | 1.895   | 1.955   | 1.925   | 1.5            |
| L-can                  | 2.125   | 1.949   | 2.037   | 1.6            |
| AFB <sub>1</sub>       | 2.034   | 2.144   | 2.089   | 1.6            |
| SF-AFB <sub>1</sub>    | 1.683   | 1.817   | 1.750   | 1.4            |
| L-can-AFB <sub>1</sub> | 2.266   | 2.064   | 2.165   | 1.7            |

**Table A4: Standardisation of proteins to 1mg/ml (200µl) using storage buffer.**

| Sample                 | Sample (mg/ml) | Sample (µl) | SB (µl) |
|------------------------|----------------|-------------|---------|
| Control                | 1.8            | 112         | 88      |
| SF                     | 1.5            | 134         | 66      |
| L-can                  | 1.6            | 127         | 73      |
| AFB <sub>1</sub>       | 1.6            | 124         | 76      |
| SF-AFB <sub>1</sub>    | 1.4            | 148         | 52      |
| L-can-AFB <sub>1</sub> | 1.7            | 119         | 81      |

## PRESENTATIONS AND PAPERS

### Presentations

Pillay, E., Phulukdaree, A., Giandhari, J., Chetty, V., Chetty, A. The possible cytoprotective effects of *Sutherlandia frutescens* on mycotoxin-treated rats. Pfizer College of Health Sciences Young Scientists Research Symposium, UKZN (Westville), October 2007.

### Papers

A scientific paper titled “The effects of L-canavanine and aflatoxin B<sub>1</sub> in HepG<sub>2</sub> cells” is currently in progress and will shortly be submitted to *Toxicology in Vitro*.